The *WWOX* Gene: Investigation of its Function and its Role in Ovarian Tumourigenesis

Charlie Gourley

PhD Thesis

University of Edinburgh

2004

EX BIBL. UNIV. EDINBURGH

Declaration

I declare that this thesis has been composed entirely by myself and that this is my own work except where I have indicated the contribution of others.

October 2004

Acknowledgements

I would like to thank the Imperial Cancer Research Fund and then (following the merger with the Cancer Research Campaign) Cancer Research UK, for funding my three years of research in the form of a Clinical Research Fellowship.

I would very much like to thank my two PhD supervisors, Professor Hani Gabra and Professor John Smyth for their advice and staunch support throughout my PhD. Before his departure to London, Prof Gabra provided excellent supervision, his optimism a terrific support when things were going badly and his direction helpful when things were going well. Prof Smyth has helped me immensely by supporting my fellowship at the outset and since the departure of Prof. Gabra by offering essential assistance that has allowed the continuation of our work on the *WWOX* gene.

I would also like to thank the rest of the *WWOX* group. Karen Taylor made all the pcDNA3.1 and pEF6 constructs for transfection into the cell lines, performed the microarray work and offered much useful practical advice. Diane Scott collected all the ovarian tumour samples from theatre and made most of the RNA and some of the cDNA for the human ovarian tumour and cell line studies of *WWOX* expression. Adam Paige made considerable intellectual contributions to my work and also performed most of the tissue culture for the *WWOX* induction work. I would also like to thank Nicola-Jane Francis, an undergraduate student who helped in the early stages of the human ovarian tumour study and Syvia Rye, who ensured the integrity of the clinical data for the study.

Others who provided useful practical advice about specific components of the project include Grant Sellar, Simon Langdon, Jane Sewell, Euan Stronach, Larry Hayward, Sylvie Guichard, Janet MacPherson and Genevieve Rabiasz.

I would like to thank the staff of the biomedical research facility for performing my in vivo experiments.

Thanks also to my parents who made this possible by their support through seven years of higher education and to my fantastic wife Kathryn who facilitates my work incredibly, without a grumble.

October 2004

Abstract

WWOX is a putative tumour suppressor gene. Although this statement is supported by the identification of homozygous deletions and high frequency allelic loss in a variety of human tumours, the role of the gene in human tumourigenesis is still unknown. In particular, no *in vitro* phenotype has been identified for *WWOX*. The reconstitution of *WWOX* in the PEO1 ovarian cancer cell line (homozygously deleted for most of the coding region) resulted in the abolition of tumourigenicity in nude mice. *In vitro* studies revealed that exogenous *WWOX* expression decreased the ability of PEO1 cells to migrate towards fibronectin. Preliminary data also suggested that *WWOX*-transfected PEO1 cells had a decreased ability to attach to matrigel and fibronectin. In a panel of 71 human ovarian tumours, 2 tumours expressing no full-length *WWOX* mRNA (isoform 1) were identified. The level of *WWOX* isoform 1 expression in the ovarian tumour panel was significantly lower than that of 13 normal human ovaries ($p<0.0001$). In addition, the expression of the *WWOX* Δ6-8 transcript (isoform 4) was associated with high grade ($p=0.006$), advanced stage ($p=0.012$) ovarian cancer. However, the expression of *WWOX* isoform 4 was also identified in 9 out of 13 normal ovaries. The data presented support the role of *WWOX* as a tumour suppressor in ovarian cancer and suggest that it plays a role in the prevention of cell migration and attachment to extracellular matrix components.

List of Abbreviations

ACTION	Adjuvant Chemotherapy in Ovarian Neoplasm
BAC	Bacterial Artificial Chromosome
BFA	brefeldin A
bp	base pairs
BSA	bovine serum albumin
C	centigrade
cDNA	complementary deoxyribonucleic acid
CFS	common fragile site
CI	confidence interval
cm	centimetre
CMV	cytomegalovirus
CSF	colony stimulating factor
dATP	deoxyadenosine triphosphate
dCTP	deoxycytidine triphosphate
DFS	disease-free survival
dGTP	deoxyguanosine triphosphate
DMEM	Dulbecco's modified minimal essential medium
DMSO	dimethyl sulphoxide
DNA	deoxyribonucleic acid
dNTP	deoxynucleotide triphosphate
dsDNA	double stranded DNA
dTTP	deoxythymidine triphosphate
dUTP	deoxyuridine triphosphate
ECM	extracellular matrix
EDTA	ethylene di-amine tetra-acetic acid
EST	expressed sequence tag
FACS	fluorescence activated cell sorter
FCS	fetal calf serum
FIGO	International Federation of Obstetrics and Gynaecology
FISH	fluorescent in-situ hybridisation
g	grams
GFP	green fluorescent protein
GOG	Gynecologic Oncology Group
HOV	human ovarian tumour
HPLC	high performace liquid chromatography
HR	hazards ratio
ICON	International Collaborative Ovarian Neoplasm
IL-1	interleukin 1
iu	international units
Kb	kilobases
kD	kilodaltons
L-Broth	Luria Broth
LOH	loss of heterozygosity

LPA	lysophosphatidic acid
LRP	lung resistance protein
M	Molar
Mb	megabases
MDR	multidrug resistance
min	minutes
ml	millilitres
MMP	matrix metallo-proteinase
mRNA	messenger RNA
MRP	MDR-associated protein involved in glutathione conjugate transport
MTT	3-[4,5-Dimethylthiazol-2-yl]-2,5-Diphenyltetrazolium bromide
NLS	nuclear localisation signal
nm	nanometre
OD	optical density
ORF	open reading frame
OS	overall survival
PAGE	polyacrylamide gel electroporesis
PBS	phosphate buffered saline
PCR	polymerase chain reaction
PSORT	Prediction of Protein Sorting Signals and Localisation Sites in Amino Acid Sequences
5' RACE	rapid amplification of cDNA ends
RFS	recurrence free survival
RNA	ribonucleic acid
RNAse	ribonuclease
rpm	revolutions per minute
RPMI	Roswell Park Memorial Institute
RT-PCR	reverse-transcription PCR
s,sec	seconds
SDS	sodium dodecyl sulphate
SNP	single nucleotide polymorphism
ssDNA	single stranded DNA
TE	Tris/EDTA
TGF	Transforming Growth Factor
TNF	Tumour Necrosis Factor
TSG	tumour suppressor gene
UTR	untranslated region
UV	ultraviolet
VEGF	Vascular Endothelial Growth Factor
wt	wild type
YAC	Yeast Artificial Chromosome
µl	microlitre
µm	micrometre

List of Figures

List of Tables

Contents

1. INTRODUCTION

1.1 Epithelial ovarian cancer: epidemiology and aetiology

1.1.1 Ovarian cancer epidemiology

Ovarian carcinoma is the second most common cause of gynaecological cancer in the developed world. It has the highest mortality of all gynaecological cancers, being responsible for 5% of all cancer female deaths. It is the 4th most common cause of cancer death in women [1]. In the USA there are 25000 new diagnoses of ovarian cancer per year [2]. In the UK there are 6000 new diagnoses and 4500 deaths [3]. The risk of developing ovarian cancer in a woman's lifetime is 1 in 70 [4]. The incidence increases with age and reaches a peak between the ages of 70 and 74.

Advances in surgery and chemotherapy have improved survival from this disease over the past 30 years but 70-80% of women still present with advanced disease and the overall 5-year survival rate is less than 50% [1].

1.1.2 Ovarian cancer aetiology

At least 90% of ovarian cancers occur in patients with no family history of the disease, suggesting that environmental factors have a strong effect upon ovarian cancer risk. This is also suggested by the sharp increase in incidence in Japanese women who emigrate from Japan to the USA [5].

Endocrine factors are thought to play a role in the development of ovarian cancer [6]. High levels of gonadotrophins in early menopause [6,7], factors associated with excessive androgenic stimulation of ovarian epithelial cells [7] and exposure to fertility drugs or hormone replacement therapy [8,9] have all been implicated as increasing the risk of ovarian cancer. Also, multiparity and use of the oral

contraceptive pill have been noted to decrease the risk of ovarian cancer [10]. These findings led to the 'incessant ovulation hypothesis' and the 'gonadotrophin stimulation hypothesis' [7]. The former hypothesis suggests that ovarian cancer arises as a result of repeated proliferative repair cycles of damaged ovarian epithelium following ovulation. This trauma results in the formation of stromal epithelial clefts and inclusion cysts. The cumulative genetic damage predisposes to carcinogenesis. The 'gonadotrophin stimulation hypothesis' proposes that hormonal stimulation of ovarian epithelial cells on the ovarian surface or within inclusion cysts may play a role in ovarian cancer development. There is also evidence that ovarian cancer risk may be increased by factors associated with excess androgen stimulation of ovarian epithelial cells and decreased by factors related to greater progesterone stimulation [7].

Other factors proposed to have a role in ovarian cancer aetiology include increased saturated fat intake [10].

1.2 Epithelial ovarian cancer: pathogenesis and histology

1.2.1 Pathogenesis of epithelial ovarian cancer

The common epithelial ovarian tumours constitute 60% of all ovarian neoplasms and 80 to 90% of ovarian malignancies. These arise from the surface epithelium or from inclusion cysts that are formed during ovulation. The remaining tumours arise from germ or stromal cells. As a result of its embryological origin, malignancies arising from the ovarian surface epithelium can resemble a variety of tissues of Mullerian

origin including the fallopian tube (serous carcinomas), the endocervix (mucinous tumours), the endometrium (endometrioid tumours) and the endometrial glands that occur in pregnancy (clear cell tumours).

Malignant cells are shed from the ovarian surface and they can spread in the peritoneal fluid to any intra-peritoneal surface. Ovarian cancer often attaches to and grows in the omentum. Lymphatic spread may be via the infundibulopelvic ligament to para-aortic and para-caval lymph nodes, through the broad ligament to the external iliac, obturator and hypergastric lymph nodes, or more rarely, via the round ligament to the inguinal lymph nodes.

1.2.2 Histology of ovarian cancer

There are three main subgroups of ovarian carcinoma: epithelial (accounts for 80-90%), stromal and germ cell. Stromal and germ cell tumours are separate entities that will not be considered here. Epithelial ovarian neoplasms can be divided into three subtypes: benign, low malignant potential (borderline) and malignant. Benign epithelial tumours occur in younger women (20-60 years), are often large, are frequently cystic and almost always have a serous or mucinous histology. Ovarian borderline tumours constitute about 15% of epithelial ovarian neoplasms and have a much better prognosis than frankly malignant lesions [4]. They affect an older age-group than the benign ovarian neoplasms but a younger age group than malignant epithelial tumours. Sixty percent of these tumours have a serous histology, 34% are mucinous and the rest are of endometrioid, clear cell, Brenner or mixed epithelial types. Histologically, borderline tumours have epithelial papillae with atypical cell clusters, cellular stratification, nuclear atypia and increased mitotic activity but are

differentiated from invasive tumours mainly because they do not show the same pattern of invasion.

Malignant epithelial ovarian tumours can differentiate into a variety of mullerian-type tissues: serous, mucinous, endometrioid and clear cell (in decreasing order of frequency). The World Health Organisation Classification of malignant epithelial ovarian tumours is shown in table 1.1. Histological tumour type has prognostic significance in so much as clear cell histology has a worse prognosis and is thought to require more aggressive adjuvant treatment in the setting of early disease than the other histological subtypes.

Histological grade is classified from 1 (low grade) to 3 (high grade) and is based on cytological detail and the degree to which a tumour forms papillary structures or glands (i.e. the degree of differentiation). Again, histological grade is felt to be prognostically important when deciding on adjuvant chemotherapy in early stage disease.

Table 1.1: World Health Organisation Classification of Common Malignant Epithelial Ovarian Tumours

Malignant serous tumour
Adenocarcinoma, papillary adenocarcinoma, papillary cystadenocarcinoma
Surface papillary carcinoma
Malignant adenofibroma, cystadenofibroma
Malignant mucinous tumour
Adenocarcinoma, cystadenocarcinoma
Malignant adenofibroma, cystadenofibroma
Malignant endometrioid tumour
Carcinoma
Adenocarcinoma
Adenoacanthoma
Malignant adenofibroma, cystadenofibroma
Endometrioid stromal sarcoma
Mesodermal (Mullerian) mixed tumour: homologous and heterologous
Clear cell (mesonephroid) tumour, malignant
Carcinoma and adenocarcinoma
Brenner tumour, malignant
Mixed epithelial tumour, malignant
Undifferentiated carcinoma
Unclassified

1.3 Epithelial ovarian cancer: clinical management

1.3.1 Staging of ovarian cancer

Full staging of ovarian cancer requires a laparotomy via a vertical midline incision and a total abdominal hysterectomy, bilateral salpingo-oophorectomy and omentectomy. Patients with apparent early disease should have peritoneal lavage for cytological examination. Para-aortic and pelvic lymph node sampling should also be performed. According to the extent of microscopic disease the patient can be staged using the FIGO (Fédération Internationale de Gynécologie et d'Obstétric) system (table 1.2). This then allows a decision to be made on the optimal systemic therapy that should be offered to the patient.

Table 1.2: FIGO staging system for epithelial ovarian cancer

FIGO stage		Description
I		Limited to ovaries
	Ia	Limited to one ovary, capsule intact, no tumour on ovarian surface No malignant cells in ascites or peritoneal washings
	Ib	Limited to both ovaries, capsule intact, no tumour on ovarian surface No malignant cells in ascites or peritoneal washings
	Ic	Limited to one or both ovaries but with either: capsular rupture, tumour on ovarian surface or malignant cells in ascites or peritoneal washings
II		Tumour extends into pelvis but not beyond it
	IIa	Extension and/or implants on uterus and /or fallopian tubes No malignant cells in ascites or peritoneal washings
	IIb	Extension to other pelvic tissue No malignant cells in ascites or peritoneal washings
	IIc	Pelvic extension (2a or 2b) with malignant cells in ascites or peritoneal washings
III		Microscopically confirmed peritoneal metastases outside the pelvis and/or regional lymph node metastases
	IIIa	Microscopic peritoneal metastases beyond the pelvis
	IIIb	Macroscopic peritoneal metastases beyond the pelvis, 2cm or less in greatest dimension
	IIIc	Peritoneal metastases beyond the pelvis, more then 2cm in greatest dimension and/or regional lymph node metastases
IV		Distant metastases (excludes peritoneal metastases)

1.3.2 Role of surgery in management of epithelial ovarian cancer

Removal of the malignancy in its entirety is the optimal treatment for ovarian cancer, but only 20-30% of patients present with disease that is limited to the ovaries or resectable pelvic organs. Most present with advanced disease that cannot be

removed in its entirety. Optimal debulking surgery is defined as removal of the majority of macroscopic disease, leaving residual disease nodules of less than 1 or 2cm (depending on the study). In the setting of advanced disease, studies have shown that optimal debulking significantly improves survival [11]. Advanced ovarian cancer patients who have more than 2cm of residual disease have a median survival of only 12-16 months compared to 40-45 months if the residual disease is less than 2cm [12]. Although progression-free and overall survival are improved in all advanced disease groups by chemotherapy, the greatest impact is in optimally debulked patients [13].

1.3.3 Role of chemotherapy in early stage ovarian cancer

Stage I ovarian cancer patients have disease that is confined to the ovary (although there may be malignant cells in ascites or peritoneal washings taken at the time of surgery). Therefore some of these patients will be cured by surgery alone and do not necessarily require chemotherapy. However, this is a heterogeneous group of patients and it is important not to miss the high-risk patients who have minimal disease and may potentially be cured by chemotherapy administered immediately after surgery.

Stage II ovarian cancer has extended beyond the ovary but has not extended beyond the pelvis and has no regional lymph node metastases. Stage II ovarian cancer, is not now considered to be 'early disease' by many gynaecological oncologists but it has been included in this group in the relevant trials (many of which were initiated in the early 1990s) so it will be considered in this section.

Thirty percent of patients with epithelial ovarian cancer present with disease that is localised to the pelvic organs (FIGO stages I and II). The ten-year survival of these patients is 50-70%, which is better than that for patients presenting with advanced disease (15-25%) but is still unsatisfactory. Until 2003, the only randomised trials investigating adjuvant chemotherapy in early-stage ovarian cancer were small and did not take into account the extent of surgical staging [14-16].

Data from two large randomised controlled trials in this setting was provided by the International Collaborative Ovarian Neoplasm Trial 1 (ICON1) [17] and Adjuvant ChemoTherapy In Ovarian Neoplasm (ACTION) [18] studies, the full results of which were reported both separately and when the trials were analysed in combination [19] in the Journal of the National Cancer Institute in 2003. These studies randomised early-stage ovarian cancer patients into chemotherapy and no chemotherapy arms.

There were important differences between the trials in terms of stage of disease that was eligible and surgical recommendations. At first glance, the outcomes of the trials appear similar. When they were analysed in combination [19] there was a better overall survival (OS) for patients in the chemotherapy arm (82% versus 74%; p=0.008). Recurrence-free survival (RFS) was also better for the patients in the adjuvant chemotherapy arm (76% versus 65%; p=0.001).

When the ICON 1 study was analysed independently [17] a similar result was obtained. The women who received adjuvant chemotherapy had a better overall survival (hazard ratio [HR] of 0.66, 95% confidence interval [CI] =0.45-0.97; p=0.03) and recurrence-free survival (HR=0.65, 95% CI= 0.46-0.91; p=0.01). The investigators in this trial concluded that platinum-based adjuvant chemotherapy

improved survival and delayed recurrence in patients with early-stage ovarian cancer. As the majority of the centres in this trial used single-agent carboplatinum, they recommended the use of this as adjuvant treatment of early-stage ovarian cancer.

When the ACTION study was analysed independently [18], it flagged up what may be an important issue when considering the results of these studies. In this study there was no statistically significant difference in overall survival between the two trial arms. Recurrence-free survival was however significantly improved in the adjuvant chemotherapy arm (HR=0.63, 95% CI=0.43-0.92; p=0.02). Only about one third of the patients in this study had been optimally staged (despite a determined effort to maximise this). Among patients in the observation arm, optimal staging was associated with a statistically significant improvement in overall and recurrence-free survival (HR=2.31 [95% CI= 1.08-49.6]; p=0.03 and HR=1.82 [95% CI=1.02-3.24]; p=0.04 respectively) suggesting that the optimally staged group had better risk disease than the suboptimally staged group. No such association was observed in the chemotherapy arm. In the non-optimally staged patients, adjuvant chemotherapy was associated with a statistically significant improvement in overall and recurrence-free survival (HR=1.75 [95% CI= 1.04-2.95]; p=0.03 and HR=1.78 [95% CI=1.15-2.77]; p=0.009 respectively). In the optimally staged patients no benefit from adjuvant chemotherapy was seen. Thus, the poor prognosis of the non-optimally staged patients could be corrected by administering adjuvant chemotherapy. The suggestion from this study is that the non-optimally staged group may have more to gain from adjuvant chemotherapy because it contains occult stage III patients and the chemotherapy may work predominantly by affecting small volume or microscopic tumour implants or metastases that were unnoticed at the time of surgical staging.

Indeed, it has been shown that incompletely staged ovarian carcinoma harbours occult stage III disease in 20-25% of patients [20-22]. It may also be that the optimally staged subgroup is too small to show a significant difference. In addition, the completeness of surgical staging was found to be an independent prognostic factor.

The main conclusion that can be drawn from the ACTION trial is that complete surgical staging of early-stage ovarian cancer is extremely important. Despite the fact that, in this trial, strict guidelines were set for optimal surgical staging, only one third of patients were optimally staged. The problem is that early ovarian cancer often mimics a benign ovarian cyst clinically, so the surgery is performed by clinicians who are less aware of the requirements for optimal staging of ovarian cancer (including lymph node biopsy). As regards adjuvant chemotherapy, the ACTION trial would suggest that its use in early-stage ovarian cancer is mainly effective in patients with occult residual disease, according to the subgroup analysis. This conclusion could also explain the findings of the ICON1 trial and the results of the combined analysis of the ICON1 and ACTION trials.

Considering the two trials, the most valid conclusions may be firstly that optimal surgical staging is very desirable (if at all possible) and secondly that if optimal surgical staging is not possible then patients with early stage ovarian cancer should be offered adjuvant chemotherapy as there is evidence for statistically significant benefits in terms of overall and progression-free survival in this group (perhaps by virtue of the presence of patients with occult stage III disease in the group). Thus, it seems that there is a role for adjuvant chemotherapy in some of the patients that we currently define as early stage ovarian cancer but we are still unable to identify those

patients who stand to benefit. Perhaps the use of molecular markers, gene expression profiles or proteomics will facilitate this. Further randomised trials are required to clarify this area of controversy but until then local opinion will determine what constitutes 'high risk' for early stage ovarian cancer patients.

1.3.4 Role of chemotherapy in the treatment of advanced stage ovarian cancer

Several meta-analyses published in the 1990s [23-25] clarified the roles of cisplatinum, carboplatinum and doxorubicin in the treatment of advanced ovarian cancer. The main controversy has been regarding whether the addition of paclitaxel to platinum-containing chemotherapy is beneficial in this setting. There have been 4 large [26-29] trials comparing these regimens but they have delivered conflicting results. The first trial reported was the GOG-111 (Gynaecology Oncology Group) trial [26] which randomised 410 patients to either paclitaxel and cisplatin or cyclophospamide and cisplatin. The former group were strongly favoured in terms of overall survival, with a hazards ratio of 0.61 (95% CI 0.47-0.79). Following this a European-Canadian Intergroup trial (OV10) [28] performed the same randomisation in 680 patients and confirmed the findings of GOG-111. The cisplatinum-paclitaxel group were favoured in terms of overall response (59% versus 45%), complete clinical response (41% versus 27%), progression-free survival (PFS; 15.5 months versus 11.5 months) and overall survival (35.6months versus 25.8 months). The conclusion drawn from these trials was that cisplatinum and pacltiaxel was the optimal first-line treatment for advanced ovarian carcinoma. However, this conclusion was contradicted by the findings of two other trials, GOG-132 [27] and

ICON3 [29]. In GOG-132, 648 patients were randomised between three arms consisting of single agent paclitaxel, single agent cisplatinum and the same cisplatinum/paclitaxel combination used in GOG-111. Four hundred and twenty-four patients were randomised between the latter two regimens (single-agent paclitaxel was clearly inferior in terms of response rate, complete response rate and median progression-free survival) but the results suggested that there was no benefit for paclitaxel/cisplatinum over single agent cisplatinum. These groups did not significantly differ in response rate (67% in both groups), progression-free survival (16.4 months for cisplatinum alone, 14.1 months for the combination) or overall survival (30.2 months for cisplatinum alone, 26.3 months for the combination.

By far the largest of the 4 studies, ICON3 [29] was reported in the Lancet in 2002. This study compared the carboplatinum/paclitaxel combination to either carboplatinum alone or a combination of cyclophosphamide, adriamycin and cisplatinum (CAP) in 2074 patients. Median progression-free survival and overall survival were not significantly different between the arms of the study. There was also no clear evidence that paclitaxel plus carboplatin was more or less effective than control in any subgroup for either overall survival or progression-free survival. Therefore this study concluded that single-agent carboplatin, CAP and carboplatin/paclitaxel are all safe and show similar effectiveness up to 5 years as first line treatments for women requiring chemotherapy for ovarian cancer. Of the treatments, single-agent carboplatinum had the best toxicity profile. Possible reasons for the differences between the findings of these four randomised controlled trials are: differences in the extent of cross-over to the taxane-based treatment in the control group; differences in the patient entry criteria for the trial and differences in

the treatment administered in the research or control groups. In particular, the combination of cisplatinum with cyclophosphamide as given in GOG-111 and OV10 may well have been an inferior control arm to the optimum dose single-agent platinum used in GOG-132 and ICON3 [30]. This does not mean that paclitaxel does not have a role in ovarian cancer chemotherapy. Indeed, many patients in the control arm of ICON3 received it when they relapsed. Rather, we need to find the optimal patient group and time in the disease course for its administration.

Equivalence of cisplatin and carboplatin from meta-analyses plus concerns about neurotoxicity of the cisplatinum/paclitaxel combination led many countries to use carboplatinum plus paclitaxel as the routine treatment for these women. Preliminary results from three randomised trials [31-33] comparing paclitaxel plus carboplatinum with paclitaxel plus cisplatin suggest that they are very similar in terms of progression-free and overall survival but with decreased neurotoxicity for the former combination.

1.3.5 Chemotherapy for relapsed ovarian cancer

Patients whose disease progresses on first-line therapy or who relapse within 3 months of treatment are considered to be platinum refractory. Patients who respond to primary treatment but relapse within 6 months are considered platinum-resistant. Patients who relapse more than 6 months after completion of initial therapy are platinum-sensitive. At the time of relapse, platinum-sensitive patients should be re-challenged with platinum. Platinum-refractory patients, platinum-resistant patients or patients who have been platinum-sensitive but whose disease has become platinum-resistant should be treated with paclitaxel (if this was not used first-line). If

they have already been treated with paclitaxel, they should be considered for treatment with topotecan, liposomal doxorubicin, or etoposide. The response rate in this setting is between 7 and 33% [34]. There is little evidence for patient benefit from third line treatment or beyond.

1.4 Epithelial ovarian cancer: molecular biology

Much progress has been made in the identification of the molecular basis for hereditary ovarian cancer but this accounts for only 5-10% of all ovarian cancer and less is known about the molecular biology of the sporadic form of the disease. The BRCA1 and BRCA2 genes have been well studied because they are high-penetrance susceptibility alleles. Many other genetic variants in low-penetrance susceptibility alleles may moderately increase the risk of ovarian cancer. These genetic variants may be much more common in the population than high-penetrance gene mutations and therefore may make a greater contribution to ovarian cancer in the population than mutations in high-risk groups. However, genetic heterogeneity makes these alleles difficult to identify.

1.4.1 Hereditary ovarian cancer

The proportion of ovarian cancers that are hereditary is among the highest for common adult cancer [35]. Previously, hereditary ovarian cancer was descriptively categorised into three clinical syndromes: hereditary breast and ovarian cancer syndrome; hereditary-site specific ovarian cancer syndrome and hereditary non-polyposis colon cancer syndrome (HNPCC). With the possible exception of the

latter syndrome it is now more useful to characterise hereditary ovarian cancer as an autosomal dominant disorder of specific gene mutations.

1.4.2 BRCA1 and BRCA2 genes

The BRCA1 and BRCA2 genes account for most cases of hereditary ovarian cancer. BRCA1 is located at chromosome 17q21 and BRCA2 is located at chromosome 13q12-13. The hereditary breast and ovarian cancer syndrome caused by mutations of these genes is inherited in an autosomal dominant fashion, with variable degrees of penetrance. Mutations in BRCA1 confer a 15-45% lifetime risk of ovarian cancer [36] and a 50-85% lifetime risk of breast cancer. BRCA2 mutations confer a lower (10-20%) lifetime risk of ovarian cancer but a similar lifetime risk of breast cancer. Both protein products have a role in genomic stability. More than five hundred different mutations have been reported in the BRCA1 gene and more than three hundred have been reported in the BRCA2 gene. The position of the BRCA1 or BRCA2 mutation within the coding region of the gene may influence the risk of breast or ovarian cancer. Amongst BRCA2 mutation carriers, the risk of ovarian cancer is greatest for women who have mutations within the ovarian cluster region. These individuals have a 1.9-fold increased risk of ovarian cancer and a decreased risk of breast cancer [37]. Among BRCA1 mutation carriers, if the mutation is in the 5' two-thirds of the gene, the relative proportion of breast cancer to ovarian cancer is higher [38].

1.4.3 Hereditary non-polyposis colon cancer syndrome (HNPCC)

HNPCC is caused by mutations in mismatch repair (MMR) genes such as hMLH1, hMSH2, hMSH6, PMS1 and PMS2 [39]. Female mutation carriers have an increased risk of colorectal and endometrial cancer, often of early onset. They are also at increased risk for ovarian, gastric, urologic tract, small bowel, hepatobiliary and brain tumours [40]. Mismatch repair gene defects in ovarian cancers have been shown to increase their platinum resistance [41-44].

1.4.4 Sporadic ovarian cancer

BRCA1 and BRCA2 mutations are infrequent in sporadic forms of ovarian cancer. There is however accumulating evidence that despite a paucity of somatic mutations, the expression of BRCA1 is frequently decreased in sporadic tumours. Hypermethylation of the BRCA1 promoter or altered activity of BRCA1 upstream transcription factors may contribute to this [45]. Genetic alterations in other tumour suppressor genes and oncogenes are found at higher frequency in the sporadic form of the disease.

1.4.5 Clonal origin of ovarian cancer

Microsatellite instability studies and studies of X chromosome inactivation comparing molecular features of bilateral ovarian cancer and metastases suggest that these cancers are clonal in origin [46]. Loss of heterozygosity (LOH), K-ras and p53 mutation analyses suggest that borderline or benign ovarian lesions are not precursors of epithelial ovarian cancer. There is some evidence, however, that

invasive tumours may have the same clonal origin as neighbouring benign-appearing cysts [47] and that endometrioid and clear cell ovarian cancers have the same clonal origin as adjacent endometriosis [48].

1.4.6 Tumour suppressor genes in sporadic ovarian cancer

Unlike most epithelia, division of normal ovarian surface epithelial cells gives rise to two daughter cells with equal growth potential [49]. This means that mutated tumour suppressor genes (TSGs) can more easily sustain a 'second hit' and play a role in the development of ovarian cancer. The obvious examples of this are BRCA1, BRCA2 and p53. As stated above BRCA1 and BRCA2 are infrequently mutated in sporadic ovarian cancer. Alterations in p53, however, are the commonest genetic mutation identified in sporadic ovarian cancer so far.

Genetic alterations in p53 are present in 50% of advanced stage tumours [4]. The frequency of p53 mutations increases with increasing stage of disease (58% in stage III/IV ovarian cancer and 37% in stage I/II disease [50]). Mutations or over-expression of p53 (suggestive of mutant p53) are most frequently found in ovarian cancers of serous histology. Functional, wild-type p53 is required for ovarian cancer sensitivity to a variety of chemotherapeutic drugs and radiation *in vitro*. This is discussed in section 1.4.8.

Some of the other putative tumour suppressor genes in ovarian cancer are *GPC3*, *NOEY 2*, *OVCA1*, *DOC2* [46], *OPCML* [51] and *WWOX* [52,53]. Widespread loss of heterozygosity (LOH) in ovarian cancer suggests that there may be a number of undiscovered TSGs that are inactivated during ovarian carcinogenesis.

1.4.7 Oncogenes and growth factors in ovarian cancer

A common feature of all cancers is the central role that signal transduction pathways appear to play in the malignant phenotype. The mitogen-activated protein kinase (MAPK) and phosphatidylinositol 3-kinase (PI3K) pathways are examples of two pathways that send diverse signals to the cell controlling proliferation, survival and cell growth. Up-regulation or constitutive activation of any members of these pathways (from the extracellular ligand to the intranuclear transcription factor) can result in development of a more oncogenic phenotype.

Tanaka et al [54] showed that TGFβ1 activated two different src-dependent signal transduction pathways (Src-MAPK-PI3K-NF-KappaB-dependent and Src-MAPK-AP-1-dependent) to bring about TGFβ1-dependent urokinase plasminogen activator (uPA) upregulation and promotion of human ovarian tumour cell invasion.

Hongo et al [55] transfected a dominant-negative variant of the type 1 insulin-like growth factor receptor (IGF-1R) into CaOV3 human ovarian cancer cells resulting in inhibition of tumourigenicity *in vivo* and inhibition of anchorage-independent growth *in vitro*. Also, when the purified dominant-negative IGF-1R recombinant protein (designated 486/STOP) was injected into nude mice implanted with wild-type CaOV3 cells, tumourigenicity was inhibited. These findings suggest a role for this growth factor receptor in ovarian tumourigenesis.

Sewell et al [56] showed that the epidermal growth factor (EGF) receptor-specific tyrosine kinase inhibitor ZD 1839 prevented transforming growth factor-alpha (TGFα)-stimulated growth of 4 ovarian cell lines (PE01, PE04, SKOV-3, OVCAR-5) that expressed the epidermal growth factor receptor. TGFα-stimulated phosphorylation of the epidermal growth factor receptor and downstream

components of the MAP kinase and PI-3 kinase signalling cascades were also inhibited. This data adds weight to the view that the EGF receptor may be important in ovarian carcinogenesis and may be a suitable therapeutic target.

A related receptor that may also be a therapeutic target is the heparin-binding EGF-like growth factor (HB-EGF) receptor. Expression of this receptor was shown to be significantly increased in cancer tissues and in patients' ascitic fluid [57]. Exogenous expression of the gene also increased the tumourigenicity in nude mice of SKOV-3 and RMG-1 ovarian cancer cells.

Matei et al [58] showed that imatinib mesylate (Gleevec), another tyrosine kinase inhibitor suppressed *in vitro* growth of primary ovarian cultures in a platelet-derived growth factor (PDGF) receptor alpha-specific fashion, suggesting that stimulation of this receptor may contribute to the proliferation of ovarian cancer cells.

The vascular endothelial growth factor (VEGF) is thought to play a central role in tumour angiogenesis. Expression of VEGF was shown to be significantly higher in ovarian tumours compared to benign lesions ($p<0.001$) in a study of patient material [59]. VEGF protein expression was also significantly associated with poor survival in this cohort of ovarian cancer patients.

The role of growth factors, growth factor receptors, tyrosine kinases and other signal transduction molecules is central to the malignant phenotype. The challenge is to use this information with a view to aquiring new, perhaps individualised therapies. The use of Gleevec in chronic myeloid leukaemia and gastro-intestinal stromal tumours was the first example of such a therapy and its efficacy in these settings provides hope that small molecule inhibitors can be developed for other malignancies, including ovarian cancer.

1.4.8 Mechanisms of drug resistance in ovarian cancer

Despite being a very chemosensitive tumour with high initial clinical response rates to single agent platinum (cisplatin or carboplatin) or combination carboplatin/paclitaxel therapy, ovarian cancer usually relapses, often with chemoresistant disease. Clinical drug resistance can be due to inadequate drug exposure for pharmacokinetic reasons: the dose administered may be too small; the bioavailability of the drug may be insufficient or the delivery of the drug to the site of the cancer may be inadequate. It is assumed that following intravenous administration of recommended doses of platinum or taxanes that the vast majority of patients will receive a dose of cytotoxic agent to their tumour that is limited only be the tolerance of their other bodily systems. The real challenge in ovarian cancer is to identify the mechanisms responsible for resistance at the level of the cancer cell with a view to targeting these (or creating cytotoxic agents unaffected by these mechanisms) in an effort to improve therapy. The main cellular alterations that result in drug resistance in ovarian cancer are: decreased cellular drug influx; increased cellular drug efflux; mutation of drug targets and apoptotic evasion/cell cycle effects.

a) Decreased cellular drug influx

Andrews et al [60] demonstrated that cisplatin accumulation in the 2008 human ovarian cancer cell line could be interrupted by blocking the Na^+, K^+ ATPase with ouabain and that cisplatin accumulation was partly Na^+ dependent. In another study performed in 2008 ovarian cancer cells, Jekunen et al [61] showed that cellular uptake of a cisplatin analogue in cisplatin-resistant 2008 cells was only 25% of that

in cisplatin-sensitive 2008 cells. This was, however, not the only cause of resistance as DNA intrastrand adduct formation (the cytotoxic effect of cisplatin) was reduced even further in the cisplatin-resistant 2008 cells to 11% of that in the cisplatin-sensitive cells. Katano et al [62] used 3 pairs of human ovarian cancer cell lines, each consisting of a sensitive parental line and a stably cisplatin-resistant subline derived by *in vitro* selection. They showed that accumulation of cisplatin in the resistant sublines ranged from 23 to 55% of the sensitive cells of each pair. The changes in uptake were paralleled by similar changes in copper uptake suggesting that cisplatin may enter and exit the cell via transporters that normally mediate copper homeostasis. The role of decreased platinum influx in cisplatin-resistant ovarian cancer in the clinical setting is unknown.

In a highly paclitaxel-resistant derivative of the CABA1 ovarian cancer cell line, paclitaxel influx was significantly reduced and delayed compared to parental cells [63]. There were no changes in cell surface expression of MRP1 (multidrug-resistance-associated protein 1), MRP2 or P-glycoprotein in these cells.

b) Increased cellular drug efflux

Increased efflux of hydrophobic drugs from the cancer cell can be brought about by upregulation of adenosine triphosphate (ATP)-dependent efflux pumps such as P-glycoprotein and multidrug-resistance-associated protein (MRP) which are encoded by the ABC group of genes. This phenomenon is known as multidrug resistance (MDR).

Baekelandt et al [64] showed that 47% of a cohort of stage 3 ovarian cancer patients expressed P-glycoprotein (by immunohistochemistry) prior to chemotherapy

exposure. P-glycoprotein expression correlated with unfavourable prognostic factors such as advanced age, presence of ascites and larger residual disease deposits after primary surgery. The high frequency of expression prior to cytotoxic drug exposure suggests that it is not necessarily an adaptation to chemotherapy exposure although quantitation of expression before and after chemotherapy would determine if upregulation had occurred. Regardless of the mechanism of induction, the P-glycoprotein-negative cases responded significantly better to combination chemotherapy with cisplatin and epirubicin ($p<0.001$) and in the multivariate survival analysis P-glycoprotein expression was an independent predictor of both overall ($p=0.045$) and progression-free ($p=0.006$) survival. These findings suggest it would be a suitable target in patients treated with this regime (which would no longer be regarded as the standard of care). Brinkhuis et al [65] investigated the prognostic value of P-glycoprotein and a number of MDR-related proteins in advanced ovarian cancer. In the multivariate analysis, the MDR-related protein LRP (lung resistance protein) was the only such factor whose expression was of independent prognostic value. Also, in a study of 54 patients with advanced ovarian cancer (a subset of 23 of whom underwent 'second-look' surgery) expression of P-glycoprotein was not associated with chemoresistance [66] although the study was too small to rule out the possibility that such an association exists. A further study by the same group [67] revealed significantly increased expression of LRP and MRP in the epithelial component of ovarian cancers compared to the epithelial component of normal ovaries. There was, however, no correlation between expression of either of these molecules and chemosensitivity. In one study, Yokoyama et al [68] demonstrated that MRP expression at time of initial surgery was an independent prognostic factor

for chemotherapy resistance. The 5-year disease-free survival rate was 26% for patients with MRP-positive tumours and 75.2% for those with MRP-negative tumours. Therefore on the basis of the *in vitro* data, it is debatable whether P-glycoprotein plays a role in chemoresistance in ovarian cancer (in terms of platinum-resistance at least). There are individual studies that suggest a role for LRP and MRP although the data is conflicting.

In view of the unclear *in vitro* data for the role of P-glycoprotein, it is perhaps unsurprising that Valspodar (PSC 833, an MDR modulator) has shown minimal efficacy in overcoming resistance in pre-treated ovarian cancer patients [69,70].

c) Mutation of drug targets

The classical example of mutation of a drug target in ovarian cancer is the paclitaxel resistance caused by β-tubulin mutation at its target site [71,72]. There is also evidence of paclitaxel resistance in ovarian cell lines secondary to α-tubulin mutation [73]. (It is worth noting however that many microtubule mutations that result in paclitaxel-resistance do not affect binding to the microtubule. Mutations that cause a decrease in microtubule stability, for example, result in paclitaxel resistance [74]).

As cisplatin causes cancer cell death by the formation of intrastrand and interstrand DNA adducts (mainly the former) and does not possess such a specific drug target, cisplatin resistance is less likely to be mediated in this fashion.

d) Apoptotic evasion / cell cycle effects

The above forms of drug resistance affect the ability of a drug to interact with its target. Drug resistance in cancer, however, is often oncogenic when the drug is able to interact with its target but downstream pathways of apoptosis or cell cycle arrest are blocked. The cancer cell can therefore continue to proliferate unchecked, resulting in the propagation of unrepaired DNA to daughter cells with the increased propensity to aquire more mutations and develop a more malignant phenotype (i.e. the cell develops genomic instability).

In response to DNA damage, the normal cellular response is either to invoke cell cycle arrest at the G_1/S, S or G_2/M checkpoints (allowing time to repair the insult) or to undergo apoptotic cell death. In terms of chemosensitivity to DNA damaging agents in cancer in general, experimental models suggest that there may be a critical balance between cell cycle arrest and apoptosis [75]. If the former is favoured then this may allow DNA repair, survival of the cell and drug resistance. Data relating to oncogenic resistance, specifically in ovarian cancer, will now be considered.

Exposure of ovarian cancer cells to cisplatin results in the up-regulation of pro-apoptotic factors such as p53, Bax and Fas [76] and down-regulation of anti-apoptotic cell-survival factors such as Xiap (X-linked inhibitor of apoptosis protein) and Akt [77]. The desired effect of this is cancer cell death by apoptosis. Cisplatin resistance of some ovarian cancer cells has been shown to be due to an unfavourable expression profile of pro-apoptotic and anti-apoptotic factors following cisplatin exposure.

p53 is central to the response to cellular damage. It has a plethora of functions but prevents propagation of mutations to daughter cells by either initiating cell cycle

arrest (activating DNA repair genes and factors such as $p21^{Waf1/Cip1}$, leading to G1 and G2 arrest) or triggering the cell to undergo apoptosis. While p53 mutations in ovarian cancer have been shown to cause cisplatin resistance [78], they are also associated with an increased sensitivity to paclitaxel therapy [79].

Fas is a death receptor belonging to the tumour necrosis factor superfamily. Stimulation of this receptor leads to activation of initiation caspases such as caspase 8 followed by activation of execution caspases such as caspases -3 and -7. Schneiderman et al [76] demonstrated that cisplatin induced Fas and Fas ligand expression and apoptosis in the cisplatin-sensitive A2780 and OV2008 ovarian cancer cell lines. In the cisplatin-resistant derivatives of these cell lines, although cisplatin upregulated Fas, it failed to induce Fas ligand or apoptosis. This suggests that failure to up-regulate Fas may be partly responsible for chemoresistance in these cells although the mechanism responsible for this remains unclear.

Xiap is an anti-apoptotic factor which inhibits caspase-9, caspase -3 and caspase-7. Li et al [77] demonstrated that cisplatin causes down-regulation of Xiap in chemosensitive human ovarian surface epithelial (HOSE) cells but not in their chemoresistant counterparts. Transfection of platinum-sensitive HOSE cells with Xiap sense cDNA resulted in a decrease in the ability of cisplatin to induce apoptosis in these cells. Sasaki et al [80] used antisense to down-regulate Xiap in C13*, A2780S (wild-type p53), A2780-cp (mutant p53) and SKOV3 (null p53) ovarian cancer cell lines. They showed that Xiap down-regulation induced apoptosis in the p53 wild-type cells but not in the mutated or null cells. Xiap down-regulation in this fashion caused caspase-3 activation, caspase-mediated MDM2 processing and p53 accumulation. Adenoviral transfection of p53 into the p53-mutated or null cells

significantly increased the pro-apoptotic effect of Xiap antisense expression. These findings show the effect that p53 status has on the role of Xiap in cisplatin-induced apoptosis. More recently, Xiap overexpression has been shown to inhibit FAK cleavage and apoptosis in cisplatin exposed OV2008 ovarian cancer cells [81], suggesting that this component of integrin-mediated signal transduction may be involved in the contribution of Xiap to cisplatin resistance.

Components of the phosphatidyl inositol-3-kinase/AKT signalling pathway are frequently altered in human cancer. Activated Akt modulates the function of numerous substrates involved in the regulation of cell survival, cell cycle progression and cellular growth. Akt is a serine/threonine kinase which exists in 3 separate isoforms (AKT1, AKT2 and AKT3). Yuan et al [82] demonstrated that constitutively active AKT2 renders cisplatin-sensitive A2780S ovarian cancer cells resistant to cisplatin whereas dominant negative AKT2 sensitises A2780S and cisplatin-resistant A2780CP cells to cisplatin induced apoptosis. This inhibitory effect of AKT2 on apoptosis is mediated by the phosphorylation of ASK1 and the inhibition of its kinase activity. This, in turn, blocks activation of JNK and p38 and inhibits the conversion of Bax (a pro-apoptotic factor) to its active form. Fraser et al [83] showed that both Xiap and Akt can modulate cisplatin sensitivity individually but that Xiap requires Akt for its full function. They also demonstrated that the effect of dominant negative Akt to sensitize ovarian cancer cells to cisplatin only occurs in the presence of functional p53. In OV2008 ovarian cancer cells, but not in their chemoresistant counterpart (C13*), cisplatin was shown to increase p53, decrease Xiap and induce apoptosis. However, all of these features could be returned to C13* cells by transfection of dominant negative Akt.

Therefore, p53, Xiap and Akt2 are all important, functionally related factors in deciding whether cisplatin-exposed ovarian cancer cells will undergo apoptosis. The ability for a cancer cell to engage apoptotic pathways following cisplatin-induced DNA damage now appears to be crucial in determining its platinum-sensitivity. There is accumulating evidence that the mismatch repair pathway in general [41,84-86] and the MLH1 gene in particular may be key factors in this process.

Brown et al [42] demonstrated that 9 out of 10 independent cisplatin-resistant derivatives of the A2780 cell line show loss of expression (at the protein level) of the hMLH1 and hPMS2 subunits of the MutLα-mismatch repair complex. At the RNA level this was shown to be the result of loss of expression of hMLH1. They also showed an increase in ovarian tumours negative for hMLH1 (at the protein level) at second-look laparotomy after platinum and cyclophosphamide-containing chemotherapy (36% vs 10%). This approached statistical significance ($p=0.059$) and suggests that loss of hMLH1 expression may be a mechanism of acquired platinum resistance. The cisplatin-resistant A2780/cp70 cells showed considerably less G2 arrest than the cisplatin-sensitive parental A2780 cells following exposure to cisplatin (1.3 fold and 9 fold increases in numbers of G2/M phase cells 48 hours after cisplatin exposure respectively). Following cisplatin treatment there is a reduction in A2780 parental cells entering S phase which is not present in the cisplatin-resistant lines. This suggests that the loss of the hMLH1 subunit of the MutLα-mismatch repair complex has resulted in disengagement of the cellular response to cisplatin-induced DNA damage. It was later shown by the same group [44] that the reason for the loss of hMLH1 expression in the cisplatin-resistant A2780 cell lines was hypermethylation of both hMLH1 alleles (compared to just one hMLH1 allele in the

cisplatin-sensitive parent line). In the same study, two of the resistant cell lines were treated with 5-azacytidine (an inhibitor of DNA methylation) resulting in re-expression of hMLH1 and an increase in cisplatin sensitivity. They then went on to demonstrate that 3 out of 24 primary ovarian tumours were hypermethylated at the hMLH1 promoter and did not express hMLH1.

An important feature of the work with hMLH1 is that the *in vitro* associations between hMLH1 promoter methylation, lack of hMLH1 expression and cisplatin resistance are reproduced *in vivo*. Plumb et al [43] showed that reversal of A2780/cp70 (cisplatin-resistant ovarian cancer cell line) MLH1 promoter hypermethylation in tumour-bearing nude mice with the demethylating agent 2'-deoxy-5-azacytidine can restore cisplatin sensitivity *in vivo*. Taking the clinical applicability of this one step further, Gifford et al [87] assessed the methylation status of the hMLH1 CpG islands in the plasma of ovarian cancer patients before carboplatin/taxane chemotherapy and then again at the time of relapse. They found a 25% increase in methylation at relapse which significantly predicted poor overall survival for these patients. Importantly, rather than concentrating on tumour characteristics at diagnosis (relevant to intrinsic drug resistance) this method allows analysis of cancer cell subpopulations that have become more apparent following drug exposure (i.e. acquired drug resistance).

In a study of 134 patients with epithelial ovarian cancer (98.5% of whom had received chemotherapy), Bali et al [88] investigated the expression levels of key proteins involved in regulating the G1-S-phase progression. They showed that in univariate analysis reduced overall survival was associated with overexpression of cyclin D1 ($p=0.03$) and p53 ($p=0.03$) and reduced expression of $p27^{Kip1}$ ($p=0.05$) and

$p21^{Wap1/Cif1}$ (p=0.02). In multivariate analysis, overexpression of cyclin D1 and combined loss of $p21^{Waf1/Cip1}$ were independent predictors of survival. Expression of cyclins or cyclin-dependent kinases (CDKs) results in progress through cell cycle checkpoints and cell proliferation. CDK inhibitors such as $p21^{Wap1/Cif1}$, $p27^{Kip1}$ and $p16^{Ink4a}$ cause G1 arrest by binding to cyclin-CDK complexes. This study shows that critical cell cycle regulatory proteins can predict the outcome of patients treated with chemotherapy but does not prove a role in drug resistance. Sui et al [89] showed that the frequency of cdk4 expression was increased in malignant compared to benign ovarian tumours and that the frequency of expression of its inhibitor $p16^{Ink4a}$ was decreased in malignant compared to benign ovarian tumours. Although the loss of $p16^{Ink4a}$ expression was associated with high grade tumours, no role in chemosensitivity was suggested. In fact, few studies have addressed the role of specific cell cycle proteins in ovarian cancer chemosensitivity. One interesting study directly addressed the question by transfecting the CDK inhibitor $p21^{Wap1/Cif1}$ into SKOV3 and OVCAR3 ovarian cancer cells [90]. This caused accumulation of cells in G1 and G2 phase, in-keeping with the role of the protein in cell-cycle regulation but was insufficient to totally maintain growth inhibition of the cells. The $p21^{Wap1/Cif1}$-transfected cells were more sensitive to cisplatin-induced apoptosis suggesting that $p21^{Wap1/Cif1}$ increased their cisplatin-resistance. This is in contrast to data in other cancer types which suggests that p21 protects cancer cells from apoptosis [91-94].

1.4.9 Molecules involved in ovarian cancer adhesion, invasion and angiogenesis

CD44 [95,96], E-cadherin [97,98] and β1 [95,96] and β3 [95,96,99] integrins have been demonstrated to play a role in the adhesion of ovarian cancer cells to the peritoneum. Urokinase-type plasminogen activator [100], matrix metalloproteinases (particularly MMP-2 [101,102] and MMP-9 [102,103]) and AP-2α [104] facilitate the invasion and metastases of ovarian cancer cells. VEGF is highly expressed in ovarian tumours [59] and malignant ascites [105]. It has a central role in angiogenesis.

1.5 Common fragile sites and cancer

Fragile sites are non-random points of chromosome breakage that appear under specific cell culture conditions. They are seen as breaks, gaps or decondensations in metaphase chromosomes at conserved locations in mammalian cells. They are traditionally classified as rare or common, although more recently a group, previously known as viral modification sites [106], has been identified and considered as a separate entity.

Rare fragile sites are heritable, occurring in less than 1 in 20 individuals [107]. They are visible under specific tissue culture conditions (allowing further subclassification into folate, distamycin or bromodeoxyuridine sensitive sites) and are associated with expanded repeat sequence which cosegregates with the fragile sites and is shown to flank the fragile site by fluorescent in situ hybridisation (FISH). Of these sites FRAXA and FRAXE are associated with heritable mental retardation and FRA11B has been mapped very close to the deletion breakpoint in Jacobsen syndrome [108].

Common fragile sites (CFSs) in contrast are present in all humans, have been conserved throughout mammalian evolution, are manifest in metaphase chromosomes in cell culture at varying frequencies and are induced by aphidicolin, a DNA polymerase α/δ inhibitor. They have less well characterised sequence requirements and do not appear to involve expansion of repeats.

In 1984, Yunis and Soreng [109] observed a significant association between the cytogenetic location of CFSs and known structural defects in cancer cells. This led to the theory that CFSs (and the genes located at them) may contribute to cancer development or progression. This theory was controversial because it could be argued that only once a cell became a cancer cell did it develop the inherent instability to express the fragile site, resulting in deletions or translocation events that could be seen as structural defects at the cytogenetic level and were in this way associated with cancer. Thus, some investigators felt that induction of the fragile site was secondary to the cancer rather than being a causative step in its development. More recently however, 9 common fragile sites (FRA2G [110], FRA3B [111] [112] [113], FRA16D [114] [115] [17] [116], FRA7G [117] [117], FRA7H [118], FRA6E [119], FRA6F [120], FRA9E [121], FRAXB [122]) have been fully or partially sequenced and characterised. This has resulted in the identification of many genes located within or near the fragile sites and has allowed a more detailed investigation of the role that these genes may play in cancer.

FHIT, located at FRA3B (the most frequently induced CFS in the human genome), was the first identified gene at a CFS [123] and has been the subject of intense investigation since this time. The fragile site is contained within the genomic structure of *FHIT*. Multiple tumour types have been found to have homozygous deletions [124,125], loss of heterozygosity (LOH) [2,123,124,126-131] and aberrant expression of *FHIT* [123,132]

[2,124,125,127-129,133-135]. Functional studies have pointed towards a role as a tumour suppressor gene, and homozygous and heterozygous knock-out mice have been created [136-140]. Gene therapy to replace *FHIT* in the murine knockout mouse has also been conducted [140].

WWOX, located at and spanning FRA16D (the second most commonly expressed human CFS), was more recently identified and, similarly to *FHIT,* exhibits homozygous deletions, LOH and aberrant expression in tumour cells (as discussed in section 1.6.10). In vitro and in vivo functional studies also suggest a role as a suppressor of tumour growth [52].

Seven genes map to >1Mb of fragility in FRA2G and one of them has homology to the LAG1Hs tumour metastasis suppressor genes [110].

Parkin is located within FRA6E [119]. LOH [119], aberrant (exon-skipped) transcripts [119] and decreased expression have all been associated with tumour tissue.

FRA6F contains 10 known genes, with another 9 genes located nearby [120]. One of the genes within the fragile site induces senescence in vitro.

Three genes, *CAV 1*, *CAV 2* and *TESTIN* are located at FRA7G [141], a region that frequently shows LOH in multiple tumour types [142]. Functional studies in a *CAV 1* knockout mouse suggest that it may act as a tumour suppressor [143]. Also the *MET* oncogene is located telomeric to the fragile site and there is evidence of FRA7G being involved in the amplification of this gene in a gastric cancer cell line [144].

FRA7H is a fragile site that shows allelic replication asynchrony [145] but appears to be gene poor [118].

FRA9E contains 36 known genes; 6 of these are downregulated in ovarian tumour tissue or cell lines [121].

FRAXB contains 3 known genes. Loss of expression of one or more of these genes has been identified in tumour tissue [122].

Many of the genes located at these CFSs share the features of tumour suppressor genes: homozygous deletions, loss of heterozygosity, decreased expression in malignant tissue compared to normal tissue and in some cases evidence of functional suppression of the malignant phenotype *in vivo* or *in vitro*. However, evidence of truncating point mutations is scarce and the role of the best-characterised genes (*FHIT*, *WWOX* and *PARKIN*) in carcinogenesis is complicated by the presence of alternate transcripts that are more frequently expressed in malignant tissue.

1.6 The *WWOX* gene: discovery and characterisation

1.6.1 Background to the discovery of the *WWOX* gene

Loss of heterozygosity (LOH) at chromosome 16q was described in ovarian, breast, prostate and other cancers [146-151], raising the possibility that there was a tumour suppressor gene located in this region. Later studies identified 16q23-24 as a region of particularly high allelic loss in pre-invasive breast lesions and prostate cancer [152-155]. Following this, a region at 16q23.2 was found to be homozygously deleted in malignant ovarian ascites using representational difference analysis as part of a search for novel tumour suppressor genes in ovarian cancer [114]. Overlapping homozygous deletions were also found in the colorectal cancer cell line HCT116 and the small cell lung cancer cell line WX330 and a 700kb physical map of this region

was constructed [114]. Homozygous deletions in this region were also identified in the gastric carcinoma cell line AGS [115].

1.6.2 Discovery of the *WWOX* gene

In April 2000, the *WWOX* gene was mapped to 16q23 by researchers at the MD Anderson Cancer Center [156]. Previous work by this group [152,157] had observed a high incidence of LOH at 16q23.3-24.1 in pre-invasive breast cancer lesions, leading them to speculate that there may be a tumour suppressor gene in this region which had an important role in early breast carcinogenesis. On the basis of this, they concentrated on the 16q23.3-24.1 interval, building a yeast artificial chromosome (YAC) and bacterial artificial chromosome (BAC) contig, spanning the D16S518-D16S516 region. Using conventional shotgun sequencing and cDNA isolation, they identified numerous cDNA clones, 35 of which were sequenced. All of the cDNA clones were mapped back to the corresponding BAC DNAs and their sequences were compared with the genomic DNA sequence to identify evidence of exon-intron structure. Only one of the cDNAs showed these features. Two corresponding independent full-length clones were subsequently isolated from a placental cDNA library. These full-length cDNAs showed a consensus sequence of 2264bp and a predicted ORF of 1245bp with a 125 bp-long 5'UTR, a 870bp-long 3'UTR and a polyadenylation signal AATAAA starting at position +2091. The putative start ATG codon was located within a strong Kozak sequence (TCAGCCatgG). An in-frame stop codon was present –30bp from the predicted translation start site, indicating that the whole ORF had been cloned. The gene was named *WWOX* on the basis of the 2 types of functional domains that it encoded (2 WW domains and an oxidoreductase

domain; see sections 1.6.4-1.6.6). The gene spans a region of >1Mb of genomic DNA which encompasses FRA16D [114,115], the second most frequently expressed common fragile site in the human genome [158].

1.6.3 Exonic structure of *WWOX*

Determination of the exon structure and exon-intron boundaries revealed that *WWOX* is composed of 9 exons, ranging in size from 58 to 1060bp [156] (table 1.3). The first exon is located in a CpG island starting at position –660 and extending into the first intron at 292bp from the translation start site. Interestingly, intron 5 and intron 8 are very large (the latter is almost 800kb in size) [159]. These introns contain the sites of 4 translocation breakpoints participating in t(14;16)(q32;q23) translocations in multiple myeloma [159,160]. Consequently, at least one *WWOX* allele is truncated in some cases of multiple myeloma, although perhaps the most pertinent alteration in these cases is the up-regulation of c-maf brought about by the proximation of the oncogene to the immunoglobulin heavy chain promoter.

Table 1.3: *WWOX* exon size (isoform 1; GenBank accession no. AF211943)

Exon	Starting Position in cDNA	Exon Length (bp)
1	1	232
2	233	65
3	298	58
4	356	179
5	535	107
6	642	89
7	731	186
8	917	265
9	1182	1060
6a	642	129
9a	1182	51
10a	1233	33

1.6.4 *WWOX* protein product

The 1245bp *WWOX* open reading frame encodes a 414 amino acid protein product [156] (figure 1.1). It has two regions near the N-terminus which have high homology to WW domain sequences. WW domains bind to polyproline stretches of binding partners in the cell. The first region (amino acids 18-47) shows typical features of a WW domain, with two highly conserved tryptophan and one proline residue. The second region (amino acids 59-88) has one tryptophan replaced by a

tyrosine residue; this is an alternative motif which is seen in other WW domain proteins. The other main region has homology to the steroid dehydrogenase/reductase (SDR) family of proteins. This family of enzymes oxidise or reduce a variety of hydroxy or keto substrates. This domain is synonymously referred to as the SDR domain, the oxidoreductase domain or the alcohol dehydrogenase (ADH) domain. The most conserved features of SDR proteins are the cofactor (GXXXGXG) and substrate (YXXXK) binding sites. The cofactor bound by WWOX is NAD(H) or NADP(H) and this binds to site GANSGIG at positions 131-137 with the potential substrate binding site YNRSK at positions 293-297 (binding sites shown in figure 1.1). Due to the sequence of the substrate-binding site and the presence of a serine residue 12 amino acids upstream of the YNRSK substrate-binding motif, it is thought that a steroid moiety is the most likely substrate. In keeping with this, Northern blot analysis performed in normal human tissues revealed highest expression of WWOX in testis, prostate and ovary, but not in breast [156]. Proteins that bind to WWOX via the WW domains may be involved in steroid-receptor interaction or regulation.

Figure 1.1: WWOX protein product

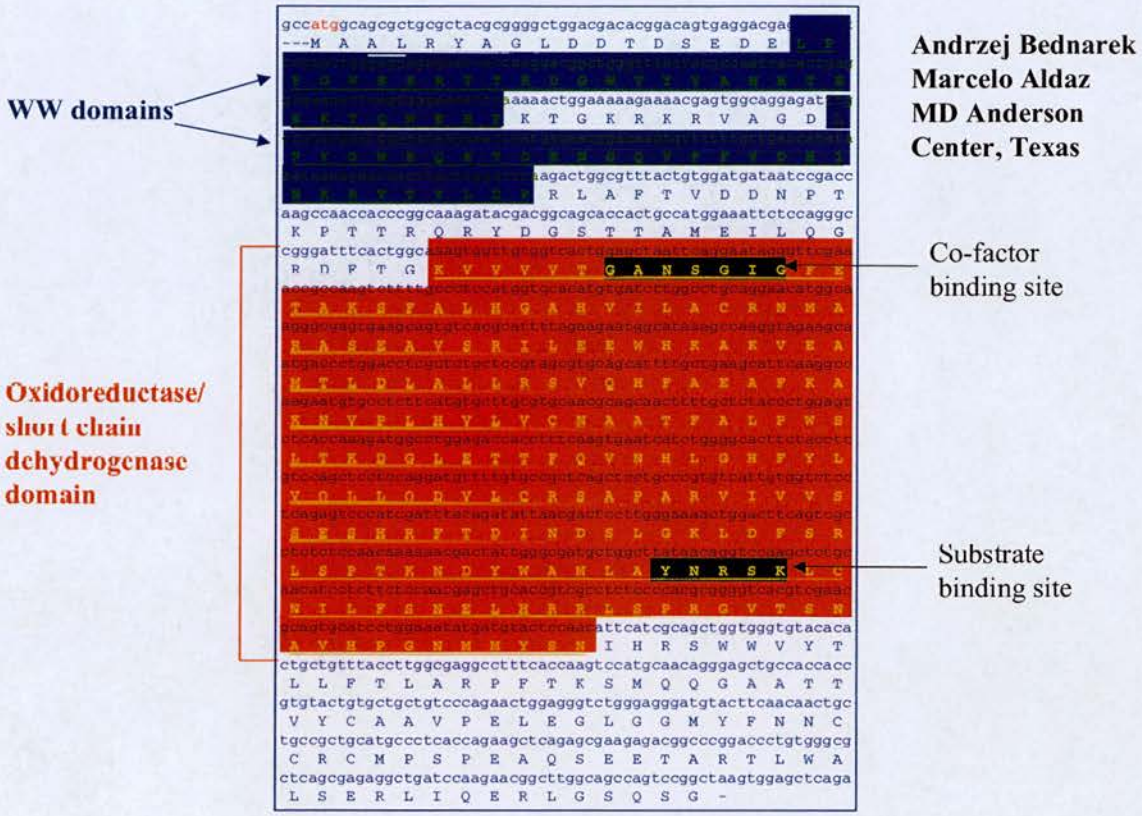

The WWOX protein product showing the domain structure as described by Bednarek et al [156]. The WW domains are highlighted in blue. The alcohol dehydogenase (ADH) or SDR (steroid dehdrogenase/reductase) domain is highlighted in red. The co-factor and substrate binding sites are highlighted in black.

1.6.5 WW domains

These domains are so-called because of a pair of signature tryptophan (W) residues that are 20 to 22 amino acids apart and play a central role in the structure and function of the domain. The whole domain is fairly compact being only 35-45 amino acids long. These domains recognise and bind to polyproline stretches of other

proteins. There are four groups of WW binding domains each with different binding sequence preferences. The major groups are I and II and the minor groups are III and IV. Group I WW domains bind the minimum core consensus PPXY and include such proteins as YAP65, dystrophin and NEDD4. Group II WW domains bind the PPLP motif and include the formin binding proteins and FE65. Group III WW domains bind to polyproline stretches flanked by arginine or lysine and group IV WW domains bind to ligands containing phosphoserine or phosphothreonine residues in their polyproline motifs. An example of a group IV WW domain-containing protein is Pin-1.

Ludes-Meyers et al [159] have found that the first WW domain of WWOX is a group I WW domain as it interacts with the PPXY ligand. The *in vivo* binding partners of the two WW domains have not yet been identified.

1.6.6 SDR domains

Based on structural analysis of human SDRs and comparison across species there are 63 different SDR enzymes in humans which reduces to 58 after elimination of possible isozymes [161]. These 63 SDR enzymes are further subdivided into classical and extended types with 46 and 17 members respectively. The extended type is mostly related to sugar metabolism. WWOX structure is the archetypal representative of one of four separate clusters of SDRs. The other three clusters are represented by Hep27, FVT1 and 17beta-HSD3, but a molecular function has only been ascribed to the latter. The clusters represented by WWOX, Hep27 and FVT1 are all thought to have some link to cancer.

1.6.7 Independent identification of *WWOX* (*FOR*)

Independent identification of the gene also reported alternative mRNA variants with unique 3'-terminal exons [162]. These investigators named the gene *FOR* (fragile site FRA16D oxidoreductase) calling the various isoforms *FOR I, FOR II* and *FOR III*. They had previously performed fluorescent in-situ hybridisation (FISH) using a panel of YAC and BAC DNA subclones to define the minimum DNA sequence spanning FRA16D [115]. Restriction analysis of the subclones and long-range PCR were used to assemble the DNA sequences in a directed manner. GenScan gene prediction analysis performed on their 270kb, FRA16D-spanning sequence identified exon 8 of *WWOX/FOR*. They then performed 5'- RACE (rapid amplification of cDNA ends) using mRNA from normal (HS578BST) and tumour (T47D) breast cells to extend and confirm the sequences of the clusters of Genbank expressed sequence tag (EST) sequences. This allowed them to identify four transcripts, which they named *FOR I-IV*. *FOR I-III* have a common 5' end, indicating a common promoter. The open reading frames encode proteins of 41.2, 46.7 and 21.5kDa respectively with the *FOR III* transcript being truncated for most of the oxidoreductase domain (figure 1.2). Their Northern blot analysis revealed *FOR II* (which corresponds to the full-length *WWOX* identified by Bednarek et al [52]) to be the predominant and ubiquitously expressed transcript. *FOR I* contains exons 1 to 8 of *WWOX/FORII* but it has two smaller 3' exons (9a and 10a) rather than the large exon 9 of *WWOX/FORII*. *FORIII* contains exons 1 to 5 of *WWOX/FORII* and replaces exons 6-9 with exon 6a. *FOR IV* was suggested to exist on the basis of a BLAST search, which revealed ESTs with homology limited to exon 1 of the gene, suggesting that these transcripts may arise from a different promoter and may encode little of the

WWOX/FOR gene product. A complete *FOR IV* transcript has not as yet been identified.

WWOX (the name given by the investigators who identified the gene first) is the name recognised by the HUGO nomenclature committee and, to avoid confusion, the various isoforms have been numbered 1 to 7 in the Genbank database (table 1.4). Only the existence of isoforms 1-4 and 6 are supported by alignment with mRNA. The exonic structure of these isoforms is shown in figure 1.3.

Figure 1.2: Three different isoforms of the WWOX (FOR) gene identified by Reid et al (2000)

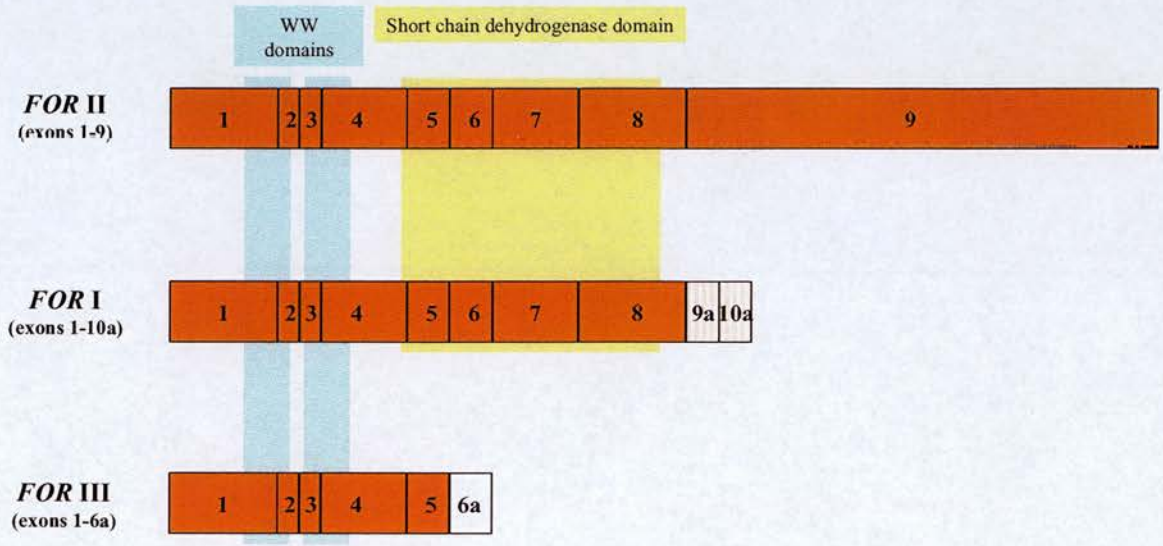

The exonic structure of *FOR I-III*, showing the location of the WW and SDR (steroid dehdrogenase/reductase) domains. Exon numbers are indicated for each transcript. Position of WW domains is indicated by blue bars. Position of SDR domain is indicated by yellow bar. *FOR II* is the wild-type *WWOX* full length transcript. *FOR I* contains exons 9a and 10a rather than the longer exon 9 of the wild-type transcript. *FOR III* contains alternate exon 6a but omits exons 6 to 9 of the wild-type transcript (and most of the SDR domain).

Table 1.4: *WWOX* mRNA Isoforms

WWOX isoform number	Genbank accession number	Transcript encodes	Protein product	Alternative name
1	AF211943	Full-length *WWOX* (the largest isoform)	Predominant form in normal tissues	*FOR* II
2	AF211943, AF227526	A variant with an alternative 3' end to isoform 1	Smaller than isoform 1, with a different C-terminus	*FOR* I
3	AF395124	A variant lacking a 647nt fragment in the middle of the coding region due to deletion of exons 5 to 8	Smaller than isoform 1, deleted SDR domain and subsequent frameshift giving different C-terminus	*WWOX* Δ5–8
4	AF395123	A variant lacking a 540nt fragment in the middle of the coding region due to deletion of exons 6 to 8	Smaller than isoform 1, most of SDR domain deleted	*WWOX* Δ6–8
5	AF211943, AH011068	A variant with an alternative central part compared to the coding region of isoform 1	Smaller than isoform 1, most of SDR domain deleted, different C-terminus	
6	AF211943, AF227528	A variant that is much smaller than isoform 1 with an alternative 3' end	Smaller than isoform 1, most of SDR domain deleted, different C-terminus	*FOR* III
7	AF211943, AF227529	The shortest putative isoform with an alternative 3'end	Lacks part of the first WW domain, all of the second WW domain and all of the SDR domain	*FOR* IV

N.B. Only existence of isoforms 1-4 and 6 are supported by alignment with mRNA

Web address: www.ncbi.nlm.nih.gov/LocusLink/LocRpt.cgi?l=51741

Figure 1.3: Exonic structure of *WWOX* isoforms

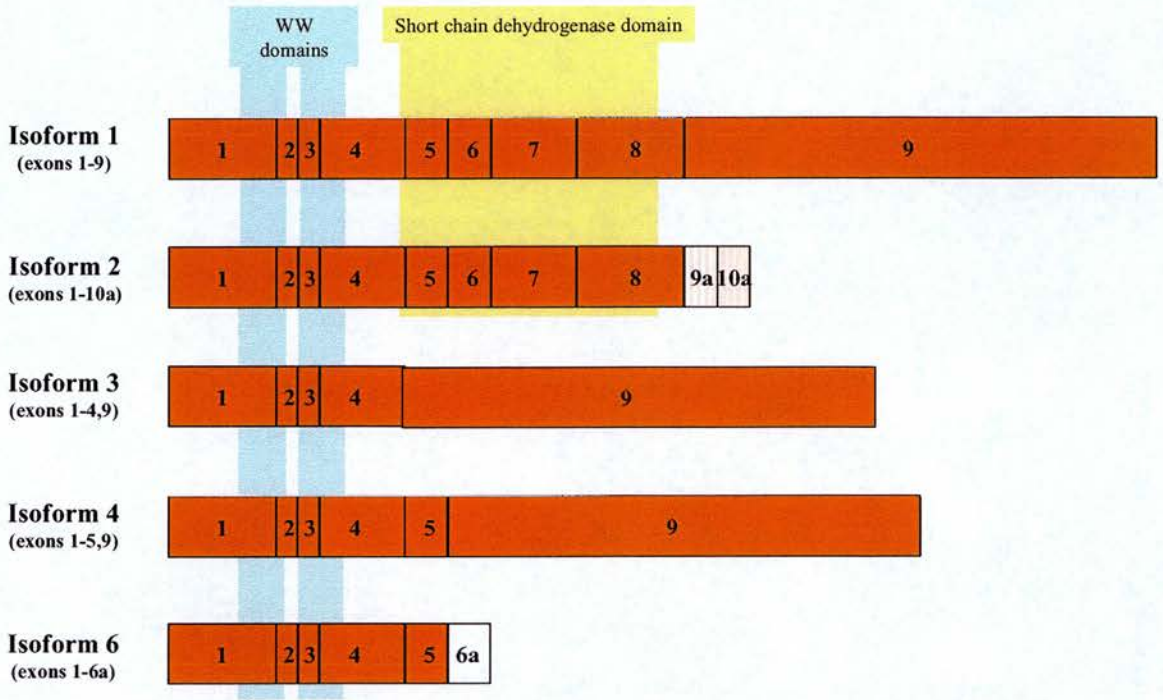

The exonic structure of *WWOX* isoforms 1 to 6, showing the location of the WW and SDR (steroid dehydrogenase/reductase) domains. Exon numbers are indicated for each transcript. Position of WW domains is indicated by blue bars. Position of SDR domain is indicated by yellow bar. Isoform 1 is the wild-type *WWOX* full length transcript. Isoform 2 contains exons 9a and 10a rather than the longer exon 9 of the wild-type transcript. Isoform 3 omits exons 5 to 8 of the wild-type transcript (and most of the SDR domain). Isoform 4 omits exons 6 to 8 of the wild-type transcript (and much of the SDR domain). Isoform 6 contains alternate exon 6a but omits exons 6 to 9 of the wild-type transcript (and most of the SDR domain).

1.6.8 Homozygous deletions identified in *WWOX* coding exons

Homozygous deletions had already been identified at 16q23 in tumour cell lines [114,115] prior to the cloning of *WWOX*. Following the identification of the *WWOX* gene, Paige et al [53] performed PCR amplification of *WWOX* exons in 95 tumour cell lines and found homozygous loss of coding exons in 4 lines (figure 1.4). The PEO4 ovarian cancer cell line (which is derived from the ascites of the same patient as the PEO1 and PEO6 ovarian cancer cell lines [163]) was homozygously deleted for *WWOX* exons 4-8 (causing loss of the SDR domain and a frameshift). The WX330 and NCI-H69 small cell lung cancer cell lines were homozygously deleted for exons 6-8 (causing in-frame loss of most of the SDR domain) and the PANC1 pancreatic cancer cell line showed loss of exons 7-8 (resulting in loss of part of the SDR domain and a frameshift). Reverse transcriptase-polymerase chain reaction (RT-PCR) performed on these cell lines revealed the presence of 'aberrant transcripts' missing the homozygously deleted exons, with no full-length *WWOX* detected. These transcripts were identified only in malignant tissue, which is why they were referred to as aberrant transcripts. As there is some doubt about this, I refer to them as alternate transcripts throughout the rest of the text. As well as causing loss of part, or all, of the SDR domain, these deletions also resulted in loss of the putative mitochondrial localisation signal.

Figure 1.4: Physical map of chromosome 16q23 showing location of exons that are deleted in tumour cell lines

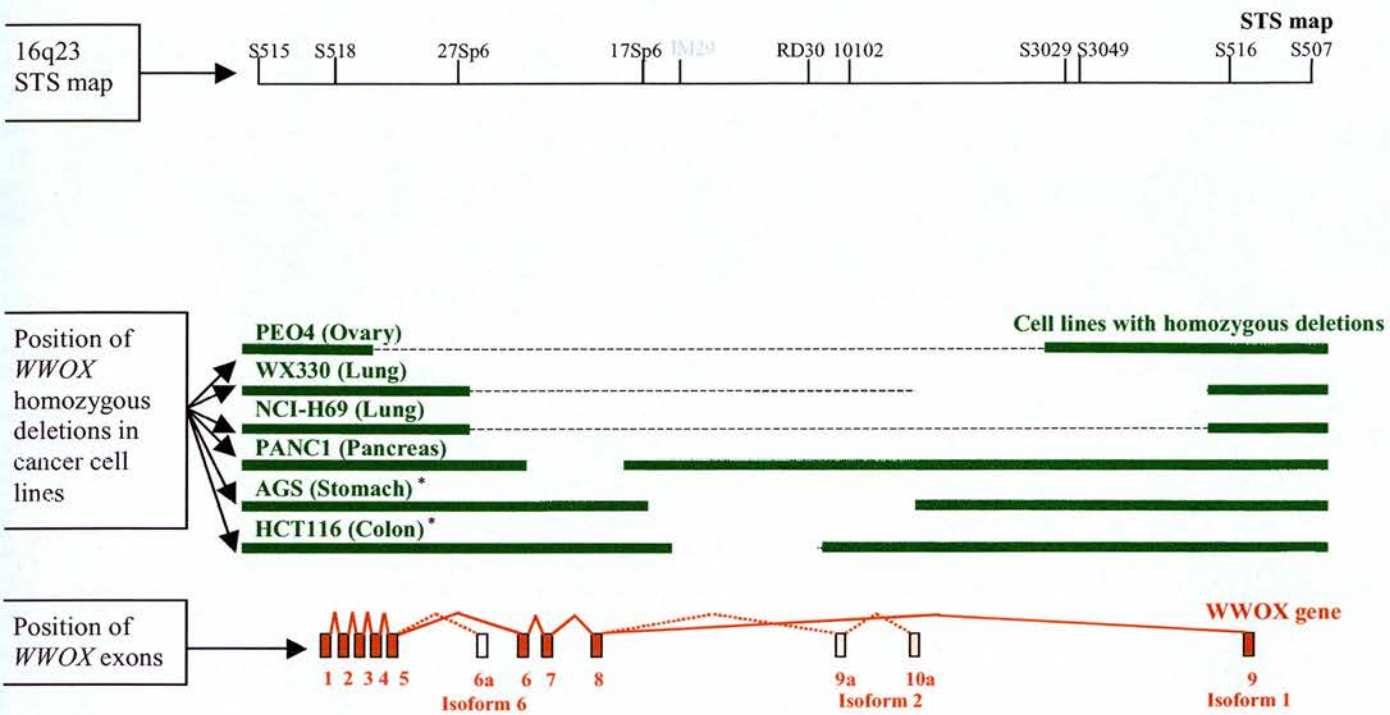

Physical map of chromosome 16q23 showing the location of exons that are deleted in the POE1/PEO4 ovarian cancer cell line series, the WX330 and NCI-H69 small cell lung cancer cell line and the PANC1 pancreatic cancer cell line.

* The deletions in the HCT116 and AGS tumour cell lines are both contained within intron 8 of the *WWOX* gene.

1.6.9 Loss of heterozygosity in the *WWOX* gene

Inactivation of tumour suppressor genes (as classically defined [164]) requires two distinct mutational events in order to knock out both alleles. In sporadic cancers, one allele may be altered by point mutation, deletion, rearrangement or hypermethylation and the other event is often loss of heterozygosity (LOH). As discussed in section

1.6.1, it was the identification of LOH in chromosome 16q [146-151] and then at 16q23-24 [152-155] that raised the possibility that there was a tumour suppressor gene in this region. Following identification of the *WWOX* gene, LOH within the gene itself has been demonstrated in 14 out of 36 (39%) squamous oesophageal cancers [165] and in 10 out of 27 (37%) primary non-small cell lung tumours [166]. In the latter study they noted that LOH was more frequent in squamous cell carcinomas than in lung adenocarcinomas, which may be of significance as the former is more strongly associated with smoking than the latter.

By analogy with the *FHIT* gene (which is located at FRA3B, the most commonly expressed CFS in the human genome), frequent LOH may be significant as there is evidence that *FHIT* can function as a one-hit tumour suppressor gene [167]. It is possible that *WWOX* haploinsufficiency could also have a biological effect.

1.6.10 Features of *WWOX* isoform expression

a) Tissue-specificity of *WWOX* expression

Northern blot analysis of *WWOX* expression pattern in normal human tissues revealed that expression was highest in the testis, prostate and ovary and significantly lower in the other examined tissues (including spleen, thymus, small intestine, peripheral blood leucocytes and breast) [156]. Chang et al [168] found murine *Wox1* mRNA to be ubiquitously expressed in most tissues and organs in the mouse, as determined by RT-PCR.

b) Variable levels of *WWOX* expression in cell lines

When *WWOX* was initially identified, Bednarek et al [156] performed Northern blot analysis on breast cancer cell lines, showing highly variable levels of mRNA expression with some lines producing very little or undetectable transcript. They then proceeded to perform quantitative RT-PCR on these cell lines, confirming that some of these lines (MDA-MB-435, MDA-MB-231, BT549 and T47D) had very low or almost undetectable expression of *WWOX*. Several of these cell lines are highly tumourigenic in nude mice. The highest expresser of *WWOX* (MCF-7), by contrast, is much less tumourigenic in nude mice.

c) Expression of *WWOX* alternate transcripts in tumour tissue

Paige et al [53] performed RT-PCR on 129 cancer cell lines, 31 primary ovarian tumours and normal human ovarian surface epithelial (HOSE) cells, revealing that most of the cell lines and ovarian tumours and all of the HOSE cells expressed the full-length *WWOX* transcript. As well as the full-length transcript, several cell lines and ovarian tumours expressed two additional, smaller products, one of which was sequenced and was found to be a *WWOX* transcript lacking exons 6-8 (Δ6-8) and the other (by size criteria) was thought to be a *WWOX* transcript lacking exon 7 (Δ7). Some of the tumour cell lines expressing these smaller products (e.g. MCF-7) were heterozygous for single nucleotide polymorphisms (SNPs) in exons 6, 7 or 8. This suggested that, in these cell lines at least, the alternate transcripts were generated by RNA processing rather than by hemizygous deletions at the genomic DNA level. No alternate transcripts were detected in normal HOSE cDNA or in a Clonetech® cDNA

panel of 16 normal tissues, suggesting that these smaller isoforms may be cancer-associated.

In a similar study, Bednarek et al [52] performed nested RT-PCR and sequencing of products in tumour cell lines, normal breast samples and breast tumours. This revealed the presence of a Δ6–8 or isoform 4 transcript (missing exons 6-8) in MDA-MB-453, MCF-7, HCT116 and AGS cancer cell lines. It is interesting that HCT116 and AGS which both have homozygous deletions entirely within the exceptionally large intron 8, express this transcript, suggesting that the deletions may have affected RNA processing. A Δ5–8 transcript (omitting exons 5-8) was also identified in KMS11, a multiple myeloma cell line.

As the most frequently identified alternate WWOX transcript in the cell lines (except full-length WWOX) was *WWOX* Δ6–8 , RT-PCR specifically seeking to amplify this transcript (using an exon 5-9 junctional primer) was performed in 53 fresh breast cancer samples and 18 normal breast tissue samples. The Δ6–8 transcript was detected in 17 out of 53 of the cancer specimens (32%) and 0 out of 18 of the normal breast samples [52], again suggesting that this alternate transcript was cancer-specific.

Driouch et al [169] performed competitive RT-PCR on 4 normal breast tissue samples, a pool of 6 normal human breast tissue samples, 9 breast cancer cell lines and 20 human breast tumour samples. Full-length *WWOX* was present in all normals, 8 out of 9 cell lines and 19 out of 20 tumours. The tumour lacking full-length *WWOX* expressed *WWOX* Δ6-8. This tumour had a short interstitial deletion at the end of intron 5 but no exonic deletions, suggesting that the Δ6-8 isoform in this case was the result of a transcriptional event. *WWOX* isoform 4 (Δ6-8) was not

present in any of the normal breast tissue and was present only in one breast cancer cell line (MCF-7). Only one tumour (the one not expressing full-length *WWOX*) expressed significant amounts of this transcript, but what the authors describe as 'minor' amounts were present in other tumours. *WWOX* isoform 6 (FOR III) was not present in the 4 normal breast tumour samples but was present in the normal human breast tissue samples (although apparently at lower levels than in the tumour samples). This isoform was found in 8 out of 9 cell lines and 10 out of 20 tumour samples with high concentrations of these transcripts found in most of these samples. In addition, these investigators analysed two matched normal and tumour pairs. One pair expressed only isoform 1. The other pair expressed isoform 6 in the tumour material but not in the matched normal tissue. The conclusions from these findings were once again that the shorter alternate isoforms may be specific to malignant tissue.

Mori et al [170] had previously reported that the *FHIT*/FRA3B locus was susceptible to damage by environmental carcinogens, such as smoking and alcohol in oesophageal carcinoma. As they wished to investigate whether this might be because fragile site-associated genes in carcinogen-exposed sites were susceptible to mutation they investigated *WWOX* for genetic alterations in 36 Japanese patients with squamous oesophageal carcinomas [165]. They identified one tumour that lacked a full-length *WWOX* transcript and found two tumours that expressed the Δ6-8 transcript as well as the full-length transcript.

In a similar study, Yendamuri et al performed RT-PCR, exonic PCR, mutation and LOH analysis on 27 paired normal and non-small cell lung cancer samples and 8 lung cancer cell lines [166]. Seven out of 27 lung cancers (25.9%) expressed

transcripts with missing exons. Two of these had no normal-sized transcripts. In all cases, corresponding normal tissues showed normal-sized transcripts without alternate transcripts. Five out of 8 lung cancer cell lines expressed transcripts with missing exons. Exonic PCR (from genomic DNA) revealed no homozygous deletions in any of these tumours or cell lines.

An important bone of contention concerning the importance of the alternate transcripts found in these studies is the lack of evidence that they are expressed at the protein level. Immunoblot analysis performed by Ishii et al [171] detected short forms of *WWOX* in haematopoietic malignancies although no indication of the specificity of the antibody is given. In the same study, RNA was pooled from monocytes, granulocytes, T cells, erythroblasts and peripheral blood lymphocytes from four healthy volunteers to characterise *WWOX* and *FHIT* expression in non-tumour cells. There was abundant expression of full-length forms of *WWOX* and *FHIT,* but small amounts of short form transcripts for both genes were found in non-malignant haematopoietic cells.

d) Evidence of *WWOX* knockout in tumour tissue

In a study investigating whether there was a correlation between the expression of the common fragile site genes *FHIT* and *WWOX* in 74 primary haematopoietic neoplasias and 20 leukaemia cell lines, Ishii et al [171] found absent *WWOX* transcripts in 29 primary neoplasias (39%) with alternate transcripts in a further 9 (12%). Similarly absent or alternate isoform expression was found in 11 out of 20 cell lines (55%). The alternate transcripts showed exon-skipping although, unlike in solid tumours, there were examples of partial exonic loss. Interestingly, the

incidence of *WWOX* transcript alteration was higher than that of *FHIT* (15 with no transcripts and 12 with alternate transcripts out of 74 primary neoplasias and 3 out of 20 cell lines with altered expression). Importantly, they used immunoblot analysis to show that the absence of wild-type WWOX protein correlated with the absence of wild-type *WWOX* transcript. All of the cases of *FHIT* alteration also had *WWOX* alteration, suggesting that *WWOX* and *FHIT* genes may be concordantly affected in the progression of haematopoietic disorders. It is possible that the incidence of alteration of expression of the two genes reflects the selective advantage conferred by knockout of either gene alone compared to that conferred by knockout of both genes. One could further speculate that in this setting, *FHIT* alteration only confers a selective advantage if *WWOX* is also knocked out, but the converse may not necessarily be true.

The reason for the absence of *WWOX* expression in a large percentage of these haematological malignancies (as well as the presence of alternate transcripts in a further significant percentage) led Ishii et al to perform DNA blot analysis in 18 cases with altered or absent expression of both the *FHIT* and the *WWOX* gene [171]. The genes were deleted in only 2 of the 18 cases suggesting that some other mechanism of knockout such as small deletions or epigenetic modification may have occurred.

e) *WWOX* promoter methylation / histone deacetylation in tumour cells

Promoter methylation does not appear to be a major mechanism of *WWOX* knockout in breast cancer cell lines as evidenced by a lack of CpG methylation around the translation start codon (-630 to +280) and a lack of significant increase in *WWOX*

expression after treatment of one of the low *WWOX*-expressing breast cancer cell lines (MDA-MB-435) with 5-aza-2'-deoxycytidine (an inhibitor of CpG methylation) [52].

In an effort to explain a high incidence of loss of *WWOX* transcript expression in haematological neoplasias, Ishii et al [171] treated K562 leukaemia cells (which express a low baseline level of *WWOX*) with 5-aza-2'-deoxycytidine and depsipeptide (an inhibitor of deacetylation) with the result that either agent increased the expression of both full-length and short forms of *WWOX*. However in non-malignant 293 control cells, neither agent had any effect on *WWOX* expression, suggesting an epigenetic downregulation of *WWOX* specifically in malignancy.

1.6.11 Lack of mutations in the *WWOX* gene

One of the classical requirements for a gene to be considered as an archetypal tumour suppressor gene is the demonstration of examples of truncating point mutations within the coding region in tumour tissue [164]. So far, there have been few examples of this identified for *WWOX*. Bednarek et al [156] reported no mutation of the gene in a panel of 27 breast cancer cell lines. Paige et al [53] identified no truncating point mutations within the *WWOX* coding region of 95 tumour cell lines, 15 ovarian cancers and 34 colorectal cancers, although several missense alterations were detected. Kuroki et al [165] found only one somatic missense mutation (leucine to proline in codon 291) in 36 squamous oesophageal carcinomas. The site of this mutation is only 2 residues away from the putative active site of the SDR domain so could well affect enzymatic function (figure 1.5). Also, this tumour displayed LOH, suggesting a possible 2-hit Knudson knock-out. Yendamuri et al

[166] found no point mutations in 27 lung tumour samples but one out of 8 lung cancer cell lines (NCI-H23) had a missense mutation resulting in an aspartic acid to asparagine substitution within its putative oxidoreductase domain. Three *WWOX* nucleotide variants were found among a panel of 20 leukaemia cell lines but it was not known whether these were polymorphisms or point mutations [171]. In the same study they were able to find no point mutations or large deletions within the coding exons of 74 primary haematological malignancies.

Figure 1.5: WWOX protein product: location of point mutation (Kuroki et al)

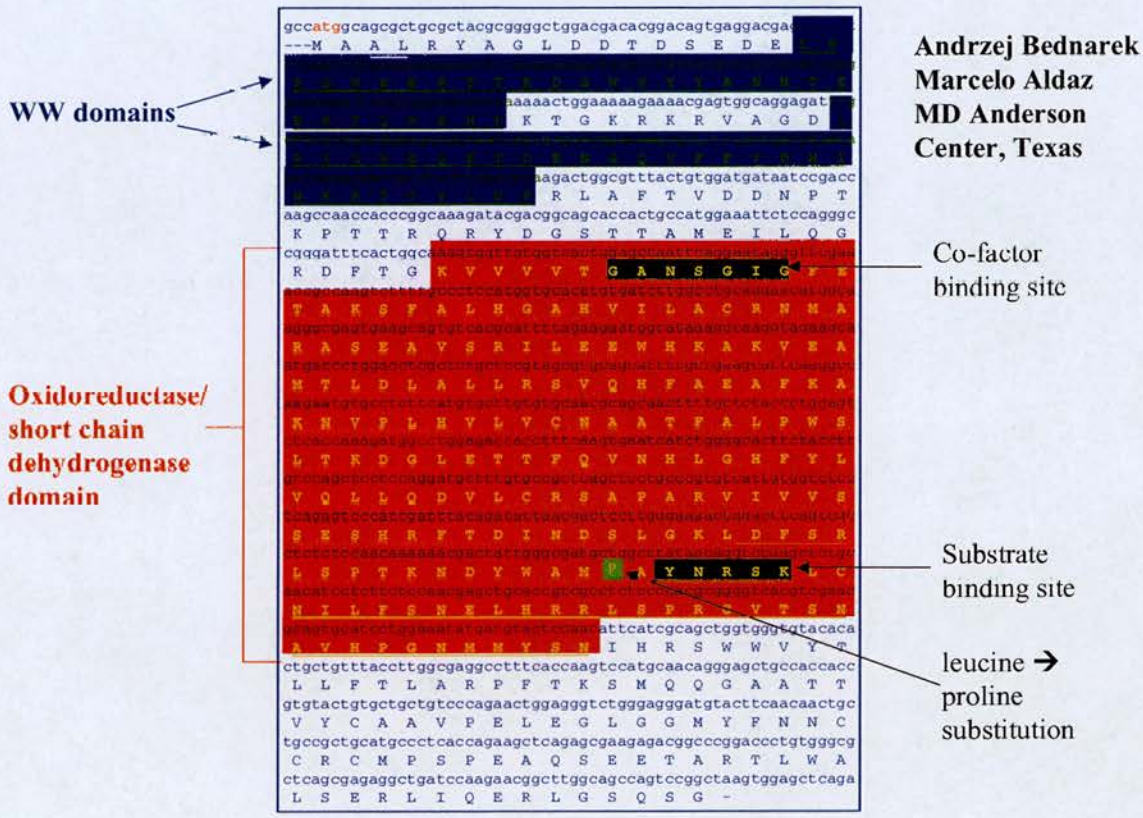

Structure of the WWOX protein showing the position of the proline to leucine substitution identified by Kuroki et al in a squamous oesophageal carcinoma. The WW domains are highlighted in blue. The ADH (alcohol dehydrogenase) or SDR (steroid dehydrogenase/reductase) domain is highlighted in red. The co-factor and substrate binding sites are highlighted in black. The leucine to proline substitution is highlighted in green.

1.6.12 *WWOX* is highly polymorphic

Paige et al [53] performed a SNP analysis on DNA from 95 tumour cell lines, 15 ovarian cancers and 34 colorectal cancers. This revealed that *WWOX* was highly polymorphic (around 1 polymorphism per 100bp). They identified 34 polymorphic bases (16 exonic SNPs and 18 intronic SNPs) in tumour cell lines. Fourteen or these

were also identified in normal individuals and 17 in the blood from cancer patients. Eleven polymorphisms (3 silent and 8 missense) were found in the *WWOX* coding region. Four of these missense polymorphisms were not detected in normal individuals. Of these four, two (Arg-120 → Trp and Arg-314 → His) substitute non-charged or weakly basic amino acid residues for highly basic residues conserved in both mouse and drosophila. Both of these were found as homozygous changes in tumour cell lines, suggesting possible loss of the second allele or reduplication.

1.6.13 *WWOX* phenotypic analysis in breast cancer cells

Bednarek et al [52] took two breast cancer cell lines with very low endogenous *WWOX* expression (MDA-MB-435 and T47D) and transduced them with recombinant retroviruses carrying the *WWOX* cloned cDNA. The *WWOX* transfectants showed no detectable differences in ability to grow in monolayer culture compared to empty vector transfectants but they did demonstrate a dramatically decreased ability to grow in soft agar, for both breast cancer cell lines. The cells expressing ectopic *WWOX* formed fewer and much smaller colonies than control cells transfected with vector alone. These findings suggest that *WWOX* may be a strong suppressor of anchorage-independent growth of breast cancer cell lines T47D and MDA-MB-435.

Following this, they injected the MDA-MB-435/*WWOX* and MDA-MB-435/vector cells into the intramammary fat pads of nude mice. The *WWOX* transfectants had a markedly reduced tumour growth rate and size ($p=0.00001$), strongly supporting the conclusion that *WWOX* is a suppressor of tumour growth.

1.6.14 Intracellular localisation of WWOX protein

Analysis of the WWOX primary amino acid sequence using PSORT (Prediction of Protein Sorting Signals and Localisation Sites in Amino Acid Sequences) algorithm predicted that WWOX had no N-terminal signal peptide and was probably located in the cytoplasm [156].

Using confocal microscopy and colocalisation analysis with an anti-Wox1 antibody in a variety of malignant and non-malignant cell lines Chang et al [168] interpreted the intracellular localisation of mouse Wox1 as being mainly in the mitochondrion, but also with some localisation in the nucleus. The presence of WOX1 in the mitochondrion was further suggested by Western blotting using purified rat liver mitochondria. By expressing successive GFP-WOX1 deletion constructs in COS-7 cells, the mitochondrial targeting sequence was localised within the ADH domain of murine WOX1 (amino acids 209-273) [168]. Constructs lacking this region but containing both WW domains (with the putative nuclear localisation signal between them) were expressed in the nucleus.

A time-course experiment in L929 murine fibroblast cells showed that tumour necrosis factor alpha (TNFα) induced GFP-WOX1 translocation from the mitochondrion to the nucleus [168]. Alteration of the nuclear localisation signal (GKRKRV) to a less hydrophilic sequence (GQGTGV) by site-directed mutagenesis abolished this TNF-induced nuclear translocation. Similarly, no nuclear translocation was seen when a GFP-WOX1adh construct (expressing a GFP-WOX1 ADH domain fusion protein) was transfected into L929 cells and they were treated with TNFα [168].

Bednarek et al [52] performed confocal microscopy on normal breast MCF-10 cells transiently transfected with GFP-WWOX to show that GFP-WWOX fusion protein is localised in distinct perinuclear particles. They used dual colour detection and mitochondrial specific staining to show that GFP-WWOX does not localise within mitochondria. GFP-WWOX did however colocalise with the anti-Golgi K protein antibody (specific for an epitope on the Golgi membrane) suggesting that it is localised within the Golgi complex. This was confirmed by treatment of GFP-WWOX transfected cells with brefeldin A (BFA) resulting in the redistribution of GFP-WWOX diffusely throughout the cytoplasm. (Brefeldin A causes disassembly of the Golgi complex and redistribution of its contents to the cytoplasm). If BFA was removed and the cells were allowed to recover, GFP-WWOX was again seen to localise in the Golgi.

The subcellular localisation of full-length WWOX disagrees sharply between the two studies [52,168]. Possible reasons for this could be: the use of endogenous WOX1 (as localised initially by Chang et al) and exogenous GFP-WWOX (as localised by Bednarek et al); inter-species variation in subcellular location of the protein; expression levels of the proteins in the cells or technical differences in the experimental protocols used. The endogenous/exogenous argument is not favoured because Chang et al [168] also used exogenous GFP-WOX1 constructs and this did not alter their interpretation of the subcellular localisation of WOX1. It would seem unlikely that the human and mouse proteins, which are so closely conserved through evolution have different subcellular locations. Both groups used transient assays to determine the subcellular location of the protein in non-malignant cell lines. The levels of expression could have been different in the cell lines with a possible effect

on protein trafficking. Also the origins of the cell lines were different, with Bednarek et al using normal breast MCF-10 cells and Chang et al using African Green Monkey kidney fibroblast COS-7 cells.

A third study by Watanabe et al [172] localised endogenous WWOX to the mitochondrion (consistent with the results of Chang et al [168]) and also detected a nuclear translocation of the protein under confluent cell culture conditions. Resolution of this area of contention is clearly important for a fuller understanding of the role of WWOX in the cell. If the protein does translocate to the nucleus in vivo, either because of cell contact inhibition (as suggested by Watanabe et al [172]) or exogenous signalling such as TNFα (as suggested by Chang et al [168]) then this translocation may be pivotal to the function of the protein.

GFP-WWOX Δ6–8 and GFP-WWOX Δ5–8 (which lack most of the ADH domain) were both found to localise to the cell nucleus rather than the cytoplasm in the study by Bednarek et al [52]. Chang et al similarly found that constructs lacking the WOX1 ADH domain (inside which they mapped the mitochondrial localisation signal) localised to the nucleus [168] so the studies agree on this.

Therefore the exon-skipped alternate transcripts identified in many tumour samples and tumour cell lines not only lack the catalytic function of the oxidoreductase domain, but their putative protein products also have altered intracellular localisation. These factors may combine to dramatically alter the function of WWOX in the cell. Potentially, different protein partners could bind to the WW domains of WWOX in the nucleus than bind in the cytoplasm. Another possibility is that the shorter exon-skipped forms may compete with wild-type WWOX for its binding partner then transport it to the nucleus.

1.7 Significance of *WWOX* alternate transcripts

WWOX isoform 1 (full-length form) is expressed in normal tissues and in most malignant tissues also. A variety of cancer cell lines harbouring homozygous deletions in the gene have been identified and although some contain exonic deletions e.g. PEO1, PANC1, WX330 and NCI-H69 [53], others such as HCT116 and AGS are homozygously deleted only in intron 8 [53,114,115,162]. It is easy to see how the former group (homozygously deleted exons) could knock out the function of a putative tumour suppressor gene but it is harder to explain how the latter cell lines (deletions in intron 8) could affect the function of the gene. However, both HCT116 and AGS express the alternatively spliced, shorter forms of *WWOX* [53,162]. It is possible that deletions within this huge intron could affect the processing of the *WWOX* mRNA transcript such that production of the shorter isoforms is favoured. This could have one of two effects. Firstly, it could simply result in lower expression of the full-length, enzymatically functional protein product. Secondly, the shorter protein products, if synthesised and functionally active, could act in a dominant negative fashion, competing with full-length WWOX for the binding partner at the WW domains.

The fact that alternatively spliced transcripts have been identified in cells that do not have genomic deletions [52,159] suggests that they can be generated by alternate splicing as well as by exonic deletions. This is also suggested by the demonstration of tumour cell lines that expressed these smaller products (e.g. MCF-7) and were heterozygous for single nucleotide polymorphisms (SNPs) in exons 6, 7 or 8. Thus there are at least two mechanisms by which the shorter forms of *WWOX* can be generated.

It has been suggested that the shorter WWOX isoforms may act in a dominant negative fashion, resulting in the knockout of full-length WWOX function in the cell thereby resulting in tumourigenesis. The finding of these isoforms exclusively in malignant tissue initially and the lack of point mutations in a gene which otherwise seemed to fit the criteria for a tumour suppressor, made this seem like a reasonable proposal. The fact that the alternate transcripts are often expressed at much lower levels than full-length *WWOX* does not preclude such a mechanism. As the isoforms are largely localised to different compartments of the cell (until, for example, an apoptotic signal is received), competition for potential binding partners to the WW domains may not therefore be equal.

It is also possible that *WWOX* alternate transcripts are non-functional mRNAs. Splicing abnormalities occur frequently in cancer e.g. oestrogen receptor alpha [173,174]. If a gene were to be affected by a cancer-induced splicing abnormality, one would imagine that genes with large transcripts such as *WWOX* would be prime candidates. There is evidence that *WWOX* alternate transcripts can produce protein [171,172]. In the former study, however, this was only seen when proteasomal degradation was blocked, suggesting that in some cell types they may be candidates for rapid degradation. It is questionable whether such short-lived protein species could have a significant dominant negative effect in the cell. Also, going somewhat against the dominant negative theory for alternate transcripts is their identification in some normal tissues, albeit at low levels [169,171].

1.8 Wox1 (the murine ortholog of WWOX): discovery of a possible role in p53-mediated apoptosis

1.8.1 Discovery of murine *Wox1* by differential display

Most cancer cells secrete hyaluronidase, which degrades the extra-cellular matrix (ECM) and induces angiogenesis in vivo [175]. Increased hyaluronidase levels are associated with progression, invasion and metastases of a variety of cancers, including breast and ovarian [176-179]. It has been shown that exogenous hyaluronidase can reverse resistance to cytotoxic drugs of cultured cancer cells [180].

Chang et al had previously shown that hyaluronidase increased TNFα–mediated cell death in murine L929 fibroblasts and in the human prostate cancer cell line LN-CaP [181]. Using differential display and cDNA library screening, they identified a cDNA, which was induced by exposure of L929 murine fibroblast cells to hyaluronidase [168]. This cDNA was named *Wox1* and is highly homologous to full-length human *WWOX*, encoding a 414 amino acid protein with two N-terminal WW domains and a C-terminal short-chain ADH domain. A nuclear localisation signal (NLS) was identified between the WW domains (amino acids 50-55) with sequence GKRKRV. They demonstrated by non-reducing sodium dodecylsulphate polyacrylamide gel electrophoresis (SDS-PAGE) that WOX1 is a single chain protein that does not exist as a multimer. A putative caspase recognition site was also identified at amino acid positions 267-270 (DIND). They demonstrated that exposure of L929 cells (whose constitutive expression of *Wox1* mRNA is low) to hyaluronidase resulted in a 150% increase in *Wox1* mRNA, peaking at 8-24 hours

post initiation of exposure. The timing of *Wox1* induction by hyaluronidase correlated with the timing for induction of TNF sensitivity in L929 cells (which requires 8 hours of pre-treatment with hyaluronidase).

1.8.2 WOX1 up-regulates p53 and down-regulates Bcl-2 and Bcl-x_L

Chang et al stably transfected L929 murine fibroblasts with GFP-WOX1 constructs containing various amounts of the WOX1 open reading frame [168]. All constructs enhanced TNF-mediated cytotoxicity compared to GFP controls and the full-length construct induced a greater degree of TNF-mediated cytotoxicity than either the WW or ADH domain construct alone. When the same cells were engineered to express antisense *Wox1* mRNA there was a 65-90% increase in resistance to TNF killing. The authors interpreted these findings as indicating that WOX1 participates in the TNF cytotoxicity pathway.

Western analysis showed that p53 expression was increased by around 200% in L929 cells expressing GFP-WOX1 or GFP-WOX1adh (GFP-ADH domain fusion protein) but not those expressing GFP-WOX1ww (GFP-WW domain fusion protein). Also, the ADH domain (but not the WW domain) significantly decreased the expression of Bcl-2 and Bcl-x_L (both apoptosis inhibitors) by more than 85%. This suggests that part of WOX1's enhancement of TNFα-mediated cytotoxicity is secondary to increased p53 expression and reduced Bcl-2 and Bcl-x_L expression.

Bcl-2 and Bcl-x_L block mitochondrial permeability transition and prevent cytochrome c release from mitochondria. Chang et al speculate that the reduction of Bcl-2 and Bcl-x_L expression caused by WOX1 may result in opening of the

mitochondrial permeability pores and release of apoptogenic proteins from the intermembrane space [168]. This is supported by their finding that over-expression of the ADH domain resulted in cytochrome c release and cell death.

1.8.3 WOX1 mediates apoptosis by two separate pathways

Transient over-expression of full-length *Wox1* in a variety of TNF-resistant cell lines resulted in apoptotic cell death 48 hours post transfection [168]. Similarly, over-expression of the ADH domain or the WW domain alone resulted in apoptosis but over-expression of NLS-mutated *Wox1* did not. This suggested that nuclear translocation is necessary for mediating WW domain-induced cell death. The reason for the ADH domain failing to induce cell death as part of NLS-mutated WOX1 may be that the 3-dimensional conformation of the full-length protein does not allow this to happen. There is a precedent for dehydrogenases mediating cell death as mitochondrial apoptosis inducing factor [182] and CC3 protein [183] have both been shown to induce cell death when they are over-expressed.

The cell death induced by the WW domains is independent of caspases and serine proteases as evidenced by the failure of caspase or serine protease inhibitors to block death of NIH/3T3 cells transiently transfected with constructs expressing the WW domains alone. Thus, enhancement of TNFα-mediated cytotoxicity by WOX1 appears to be mediated by separable nuclear-targetted WW domain and mitochondrial-targetted ADH domain functions, suggesting that WOX1 functions at both cytosolic and nuclear levels.

1.8.4 p53-mediated apoptosis requires WOX1, but not the converse

The death of NIH/3T3 cells transiently expressing the Wox1 domains was increased by cotransfection with p53 [168]. Expression of *Wox1* antisense mRNA in NIH/3T3 or THP-1 cells abolished p53-mediated cell death. These findings suggest some synergy between WOX1 and p53-induced apoptosis. Chang et al used p53-deficient NCI-H1299 cells to show that transient expression of WW or ADH domains could still mediate cell death [168]. They interpreted these findings as suggesting that WOX1-mediated apoptosis is independent of p53, but that p53-mediated apoptosis requires the participation of WOX1.

1.8.5 WOX1 WW domain appears to bind p53 polyproline region

Chang et al [168] use coimmunoprecipitation and yeast two-hybrid analyses to substantiate their claim that WOX1 interacts with p53. Immunoprecipitation of L929 cytosolic lysates with anti-p53 antibodies resulted in coprecipitation of p53 and WOX1. Stimulation of the L929 cells with TNFα resulted in migration of both proteins to the nucleus and disappearance of both proteins from the cytosolic lysates in coimmunoprecipitation studies. These findings suggest that WOX1 and p53 may bind to each other in the cytoplasm and then comigrate to the nucleus on stimulation by TNFα. They interpreted their yeast two-hybrid analyses as showing that the proline-rich region of p53 (amino acids 66-110) physically interacts with the WW domains of WOX1 *in vivo*. This region had previously been shown to be necessary

for p53-mediated apoptosis [184] and Chang et al [168] suggested that binding of WOX1 to this region is essential for p53 apoptosis-inducing activity.

1.9 Relationship between *WWOX* and FRA16D

In 1984 Yunis and Soreng noted that the cytogenetic location of many of the common fragile sites (CFSs) map to regions that are frequently altered or rearranged during cancer development [109]. FRA3B is the most commonly expressed CFS in the human genome and the putative tumour suppressor gene FHIT maps to this region. FRA16D is the second most commonly expressed CFS in the human genome. Prior to the identification of *WWOX*, Krummel et al wished to determine whether the tumour-associated deletions and LOH at 16q23 corresponded at the molecular level with FRA16D [116]. They constructed a Bacterial Artificial Chromosome (BAC) contig that spanned FRA16D as evidenced by the most centromeric clone not hybridising telomeric to the CFS and the most telomeric clone not hybridising centromerically when fluorescent in situ hybridisation (FISH) was performed on metaphases from aphidicolin-treated lymphocytes. This contig extended over greater than 1Mb. This allowed them to show that the 3 markers that exhibited high LOH in multiple solid tumours (D16S504, D16S516 and D16S518) all map within FRA16D. This correlated the molecular position of the fragile site and the region of instability, providing further evidence that the CFS may have a causal role in cancer. Also, t(14q32;16q23) is a translocation estimated to occur in up to 25% of all multiple myelomas [160]. The 4 multiple myeloma breakpoints identified by Chesi et al [160] were all mapped by Krummel et al [116] to within

FRA16D. In the multiple myeloma cell lines from which the 4 breakpoints were cloned, c-maf (which lies telomeric to FRA16D) was up-regulated. This suggests that as well as a possible role in gene disruption in solid malignancy, FRA16D-associated translocations may also be implicated in upregulation of proto-oncogenes.

Krummel et al [185] positioned the mouse ortholog to *WWOX* (*Wox1*) at chromosome band 8E1 in the mouse genome. They then demonstrated that *Wox1* co-localises with Fra8E1, a frequently expressed common fragile site (CFS) in the mouse genome. Furthermore, the sequence from this region, including introns, is highly conserved between human and mouse over at least a 100-kb region. The human *FHIT* gene and its mouse ortholog Fhit were also found to co-localise with FRA3B (the most frequently expressed CFS in humans) and Fra14A2 (a frequently expressed CFS in mice) [186,187] respectively. This suggests that the two most active CFSs share many features, that CFSs and their associated genes may be necessary for cell survival, and that the function of the associated genes may depend upon their localization at the CFS.

1.10 Aims of the project

The three main aims of the PhD project were:

1) To elucidate whether the *WWOX* gene functions as a tumour suppressor in epithelial ovarian cancer
2) To clarify the role of the *WWOX* gene (and its alternate transcripts) in ovarian carcinogenesis
3) To ascribe a phenotype associated with expression of the *WWOX* gene and WWOX protein function

In order to achieve these aims two approaches were employed in parallel. The first approach was to investigate the *WWOX* mRNA isoform expression profile of a panel of human ovarian tumours, normal ovaries and ovarian cancer cell lines. The second approach was to develop a cell line system with a functional *WWOX* pathway and by means of manipulation of *WWOX* expression levels perform functional assays in the search for an *in vitro* phenotype.

2. MATERIALS AND METHODS

2.1 Conventional PCR

2.1.1 PCR blocks

All non-quantitative PCRs were performed on a PTC-225 Peltier Thermal Cycler (MJ Research).

2.1.2 PCR reagents

10 x PCR Reaction Buffer

10 x PCR Reaction Buffer consisted of 100mM Tris, 500mM KCl; pH8.3

50 x dNTP mix

A 50 x mix of the four dNTP's (2'-deoxynucleoside 5'-triphosphates, Amersham Pharmacia) was made up as follows:

40µl of each dNTP (100mM) were mixed together with 240µl of distilled water. This gave a final concentration of 10mM of each dNTP.

The 50 x dNTP mix was stored at –20°C.

0.5µl of this mix was added to each 25µl PCR reaction, giving a final concentration of 200µM each dNTP in each PCR reaction.

Thermus Aquaticus (Taq) DNA polymerase

Standard Taq polymerase was in the form of Pic Taq supplied at a concentration of 5U/µl (supplied by Cancer Research UK). This was stored at –20°C. 0.2µl (1U) was added to each PCR reaction.

Taq Gold® (Applied Biosystems) was a high fidelity hot-start Taq DNA polymerase that was used for amplification of large fragments when this was suboptimal using

standard Pic Taq. This was stored at –20°C. It was supplied at 5U/ml and 0.2µl (1U) was used in each PCR reaction.

Reaction Buffer II

For amplifications using Taq Gold®, the reaction buffer used was that supplied by Applied Biosystems with Taq Gold®, namely reaction Buffer II. Its constituents were identical to our in-house reaction buffer (see above).

2.1.3 Oligonucleotide primers

Primers were chosen using 'Primer 3', a bioinformatics program accessible through the following web site: http://www.broad.mit.edu/cgi-bin/primer/primer3_www.cgi/. The nucleotide sequence for the full-length human *WWOX* transcript (GenBank accession number AF211943) was pasted into the program, the target region requiring amplification was identified and any regions to be excluded were annotated. Limits for maximum 3' stability, primer size (18-27 nucleotides), primer melting temperature (T_M) (55-63°C), primer GC% (20-80%) and maximum 3' and self-complementarity were set. The output was in the form of possible primer options. The best primers for the required PCR were chosen and optimised. Primers for non-quantitative PCR were obtained from the Cancer Research UK Oligonucleotide Synthesis Service.

2.1.4 Treatment of Oligonucleotides

Primers were supplied fully deprotected and dried down. Ethanol precipitation was used to remove the side products of the synthesis. Each oligonucleotide was dissolved in 200µl of distilled water containing 0.3M sodium acetate (pH 5.6) and

10mM magnesium chloride. 600µl of cold 100% ethanol was added and mixed briefly by vortexing. After 30 minutes at –70°C or overnight at –20°C, the mixture was centrifuged for 5mins at 16000g. The supernatant was discarded and the pellet was washed with 500µl 80% cold ethanol. The supernatant was removed carefully, air-dried and the pellet was resuspended in 100µl of distilled water. The concentration of the oligonucleotide was determined spectrophotometrically and the volume adjusted to give a 20µM primer solution. The primers were stored at –20°C. The primer sequences used for non-quantitative PCR are shown in table 2.1 and 2.2.

Table 2.1: Primers and conditions for non-quantitative RT-PCR

Primers	Sequences (5'-3') For/Rev	Mg^{2+}/ Taq[a]	Cycling conditions
γ-*ACTIN* F+R	ATGACAATGCCAGTGGTGCG ATGGCATCGTCACCAACTGG	1.6mM Pic	94°C 30s; 57°C 45s; 72°C 45s; 35 cycles
3' UTR F+R (both in 3'UTR)	GTGGTGGCCTGTTTGAAAGT GGCACAGCAGGAGGTTTAAG	1.6mM Pic	94°C 30s; 65°C 30s; 72°C 30s; 35 cycles TD[b]
E and Z	GAATTCAGGTGCCTCCACAGTCAGCC GAATTCTGTGTGCCCATCCGCTCTG	1.6mM Pic	95°C 30s; 67°C 30s; 72°C 30s; 40 cycles TD
E + WWOX2rev	GAATTCAGGTGCCTCCACAGTCAGCC AGGATCAAGATTTTAGCCGGACTGGCTGCC	1.6mM Pic	95°C 30s; 67°C 30s; 72°C 30s; 40 cycles TD
8F2+Z2 (exon 8 to 9)	ACTATTGGGCGATGCTGGCT CGTTCTTGGATCAGCCTCTC	2.0mM Pic	94°C 30s; 65°C 30s; 72°C 30s; 40 cycles TD
IM19R + BGHrev	CAATGCAGCAAGGAGCAGT TAGAAGGCACAGTCGAGG	2.0mM Pic	94°C 30s; 55°C 30s; 72°C 30s; 35 cycles
8F2+Z2 (exon 8 to 9)	ACTATTGGGCGATGCTGGCT CGTTCTTGGATCAGCCTCTC	2.5mM Gold[a]	95°C 30s; 65°C 30s; 72°C 45s; 40 cycles TD
7F2+8R2 (exon 7 to 8)	CACCAAAGATGGCCTGGA TGGACCTGTTATAAGCCAGCATCG	2.0mM Pic	94°C 30s; 65°C 30s; 72°C 30s; 35 cycles TD
Ex4/4+Z2 (exon 4 to 9)	TTTCACTGGCAAAGTGGTTG CGTTCTTGGATCAGCCTCTC	2.5mM Gold	95°C 30s; 57°C 30s; 72°C 75s; 35 cycles
Ex1/1+CodR (5'UTR-3'UTR)	GAGTTCCTGAGCGAGTGGAC ACTTTCAAACAGGCCACCAC	2.5mM Gold	95°C 30s; 57°C 30s; 72°C 75s; 35 cycles
Δ6-8 F+R (Ex4-Ex5/9 junction)	TTTCACTGGCAAAGTGGTTG GCTCCCTGTTGCCATTCTTC	1.2mM Pic	94°C 30s; 55°C 30s; 72°C 30s; 35 cycles
Ex1/1-Δ6-8R (5'UTR-Ex5/9 junction)	GAGTTCCTGAGCGAGTGGAC GCTCCCTGTTGCCATTCTTC	2.5mM Gold	95°C 30s; 67°C 30s; 72°C 75s; 40 cycles TD
β*ACTIN* F+R	CTACGTCGCCCTGGACTTCGAGC GATGGAGCCGCCGATCCACACGG	2.0mM Pic	94°C 30s; 55°C 30s; 72°C 30s; 35 cycles
Z1+Z2 (both in ex 9)	TACTTCAACAACTGCTGCCG CGTTCTTGGATCAGCCTCTC	2.0mM Pic	94°C 30s; 58°C 30s; 72°C 30s; 35 cycles
LC1 F+R (both in 3'UTR)	GTGGTGGCCTGTTTGAAAGT GAGGGGACCTCAGGCTATTC	2.0mM Pic	94°C 30s; 60°C 30s; 72°C 30s; 35 cycles

Primer sequences, magnesium concentrations, type of Taq DNA polymerase used and cycling conditions for non-quantitative RT-PCRs.

[a]Gold = Taq Gold®, Pic = Pic Taq

[b]TD = annealing temperature decreased by 1°C per PCR cycle for first 10 cycles

Table 2.2: Primers and conditions for PCR on genomic DNA

Primers	Sequences (5'-3') For/Rev	Mg^{2+}/ Taq[a]	Cycling conditions
Neo F+R	GCGATGCCTGCTTGCCGA GAAGGCGATAGAAGGCGA	1.6mM Pic	94°C 30s; 55°C 30s; 72°C 30s; 35 cycles
Blast F+R	ATCAACAGCATCCCCATCTC CAAGATGCCCCTGTTCTCAT	1.6mM Pic	94°C 30s; 55°C 30s; 72°C 30s; 35 cycles
Exon 1F+R	GGAGACTGGATTTCAGCTTC CCCTGGACCCTTTTCCCT	1.6mM Pic	94°C 30s; 65°C 30s; 72°C 30s; 35 cycles TD[b]
Exon 2F+R	GTCCTCTTTCTCCTTCTTCC CAATAACCTGTCACCTCTCT	1.6mM Pic	94°C 30s; 55°C 30s; 72°C 30s; 35 cycles
Exon 3F+R	GTCTTTACTTCTCCCTGGCACC GCGGGGAAAATAGAAGAATA	1.6mM Pic	94°C 30s; 56°C 30s; 72°C 30s; 35 cycles
Exon 4F+R	CTTTCTCTTTTGGGCAGC GCAGTCCCAAAGATAAATAAC	1.6mM Pic	94°C 30s; 58°C 30s; 72°C 30s; 35 cycles
Exon 5F+R	AGGACTCTACCCCACAAC ACACACTCCACTGAAATC	2.0mM Pic	94°C 30s; 68°C 30s; 72°C 30s; 40 cycles TD
Exon 6F+R	ATTAAACAGGGGAATTCCGAC TCTCCCAATTGTGTTCATCTG	1.6mM Pic	94°C 30s; 63°C 30s; 72°C 30s; 35 cycles TD
Exon 6aF+R	TAGGAGGTGTTGGAAGAAGG CACCTGAAGAGTCGTAAAGC	1.6mM Pic	94°C 30s; 56°C 30s; 72°C 30s; 35 cycles
Exon 7F+R2	ACATCCATGGATCCCGAAG TGATTCACTTGAAAGGTGGTCT	1.6mM Pic	94°C 30s; 55°C 30s; 72°C 30s; 40 cycles
Exon 7F2+R	CACCAAAGATGGCCTGGA TGGTATGAGAAAGGGGATAAGTG	1.6mM Pic	94°C 30s; 65°C 30s; 72°C 30s; 35 cycles TD
Exon 8F+R	TGCACCCAGCATTCCTTAGATTTCC ACCAGACTCATGCCCGCAAG	1.6mM Pic	94°C 30s; 65°C 30s; 72°C 30s; 35 cycles TD
Exon 9F+R	GACGCCATCTCATCACTCC TTTACTTTCAAACGGCCACC	1.6mM Pic	94°C 30s; 65°C 30s; 72°C 30s; 40 cycles TD

Primer sequences, magnesium concentrations, type of Taq DNA polymerase used and cycling conditions exon-specific PCRs on genomic DNA.
Pic = Pic Taq
[b]TD = annealing temperature decreased by 1°C per PCR cycle for first 10 cycles

2.1.5 PCR conditions

Non-quantitative PCRs were performed using Pic Taq, or if the target fragment was long and difficult to amplify, Taq Gold® was used. The amount of each PCR reagent added to each Pic Taq PCR reaction is shown in table 2.3 and the amount added to each Taq Gold® PCR reaction is shown in table 2.4. 2µl of sample

genomic DNA or cDNA was used in each PCR, giving a total volume of 25µl for each PCR. Each PCR was optimised for the primer pair used. The optimal magnesium concentrations, cycling conditions and Taq polymerase enzyme for each primer pair is shown in tables 2.1 and 2.2. Each PCR was initiated with a denaturation step at 94 or 95°C (90s for Pic Taq, 12mins for Taq Gold to activate the enzyme), followed by primer-specific cycling conditions and finished with a 3min elongation step at 72°C.

Table 2.3: Pic Taq PCR reaction mix

Component	**Stock Concentration**	**Volume (µl) in one reaction**	**Actual final concentration**
dNTPs	10mM (50x)	0.5	200µM
Reaction Buffer	10x	2.5	1x
$MgCl_2$	25mM	2.0/1.6	2.0/1.6mM
Forward primer	20µM	1.0	0.8µM
Reverse Primer	20µM	1.0	0.8µM
Pic Taq	5U/ml	0.2	1U total
Distilled water		15.8/16.2	
Total Volume		**23µl**	

Table 2.4: Taq Gold® PCR reaction mix

Component	Stock Concentration	Volume (µl) in one reaction	Actual final concentration
dNTPs	10mM (50x)	0.5	200µM
Reaction Buffer II	10x	2.5	1x
$MgCl_2$	25mM	2.5	2.5mM
Forward primer	20µM	0.25	0.2µM
Reverse Primer	20µM	0.25	0.2µM
Taq Gold®	5U/ml	0.2	1U total
Distilled water		16.8	
Total Volume		**23µl**	

2.1.6 Checking of PCR products by agarose gel electrophoresis

TBE

10 x TBE stock was made up as follows:

108g Tris Base, 55g Boric Acid, 40ml 0.5M EDTA pH 8.0 were mixed (using a magnetic stirrer) with 500ml of sterile distilled water until they had dissolved. The volume was then made up to 1litre with sterile distilled water and autoclaved. This was stored at room temperature.

1 x TBE was made up from the 10 x TBE stock when required using distilled water.

Agarose Gels

0.8g of general purpose agarose were added to 40ml of 1xTBE to make up 40ml of 2% agarose. Weights of agarose and volumes of 1xTBE were adjusted according to the percentage and volumes of agarose gel required.

Loading buffer

6 x loading buffer consisted of 0.25% bromophenol blue and 40% weight by volume sucrose in water. It was made up as follows:

4g sucrose, 0.025g bromophenol blue and 6ml 10 x TBE were made up to 10mls with sterile distilled water.

DNA ladder

A 1kb DNA ladder was obtained from Invitrogen and run as a size marker in agarose gels.

PCR products were mixed with loading buffer and loaded onto general purpose 1-2% agarose containing ethidium. The gel was run at 60-100mV in 1xTBE. To confirm product sizes, a 1kb DNA ladder was also run. The products were visualised under ultra-violet light.

2.1.7 Purification of PCR products

PCR products were purified using the QIAquick® PCR Purification Kit (Qiagen). This protocol is designed to purify single-stranded or double-stranded DNA fragments from PCR and other enzymatic reactions. It allows 100bp to 10kb DNA fragments to be purified from primers, nucleotides, polymerases and salts.

Five volumes of Buffer PB were added to one volume of the PCR reaction and mixed. To bind the DNA, the sample was applied to the QIAquick® column and centrifuged at 16000g for 60s. The flow-through was discarded, 0.75ml of Buffer PE (to wash the DNA) was added and the column was centrifuged for another minute at 16000g. The flow-through was discarded and the column was centrifuged for a further minute at 16000g. The column was placed in a clean microfuge tube. To elute the DNA, 50µl of sterile distilled water or elution buffer was added to the centre of the membrane and the column was centrifuged for a minute at 16000g.

2.2 Engineering of constructs for transfection

Most of the plasmid constructs used for the transfection work presented in this thesis were prepared by Karen Taylor prior to the start of my PhD and I gratefully acknowledge her help.

2.2.1 Media and additives

All media was sterilised by autoclaving before use.

L-Broth

2.46g magnesium sulphate, 10g Bacto-tryptone, 5g yeast extract and 10g sodium chloride per litre of distilled water.

L-agar

15g agar added per litre of L-Broth

Ampicillin

Ampicillin (Sigma) was prepared in a sterile fashion to give a stock solution with a concentration of 50mg/ml. This was stored at -20°C. Ampicillin was added to the bacterial culture media to give a final concentration of 50μg/ml in order to select for bacteria transformed with plasmids carrying the ampicillin resistance.

2.2.2 Bacterial strains

Plasmids were propagated in One Shot® TOP 10 Chemically Competent Cells (Invitrogen).

2.2.3 Plasmids

Two plasmids were used for transfecting *WWOX* sense and antisense constructs into human cancer cell lines.

pcDNA3.1/V5-His-TOPO® (Invitrogen) is a 5523bp mammalian expression vector that carries a geneticin resistance marker. It drives expression of the cloned insert from a CMV promoter. A map of this vector is shown in figure 2.1.

pEF6/V5-His-TOPO® (Invitrogen) is a 5840bp mammalian expression vector that carries a blasticidin resistance marker. Expression of the cloned insert is driven from an EF-1α promoter. A map of pEF6/V5-His-TOPO® is shown in figure 2.2.

Figure 2.1: Map of pcDNA3.1/V5-His-TOPO®

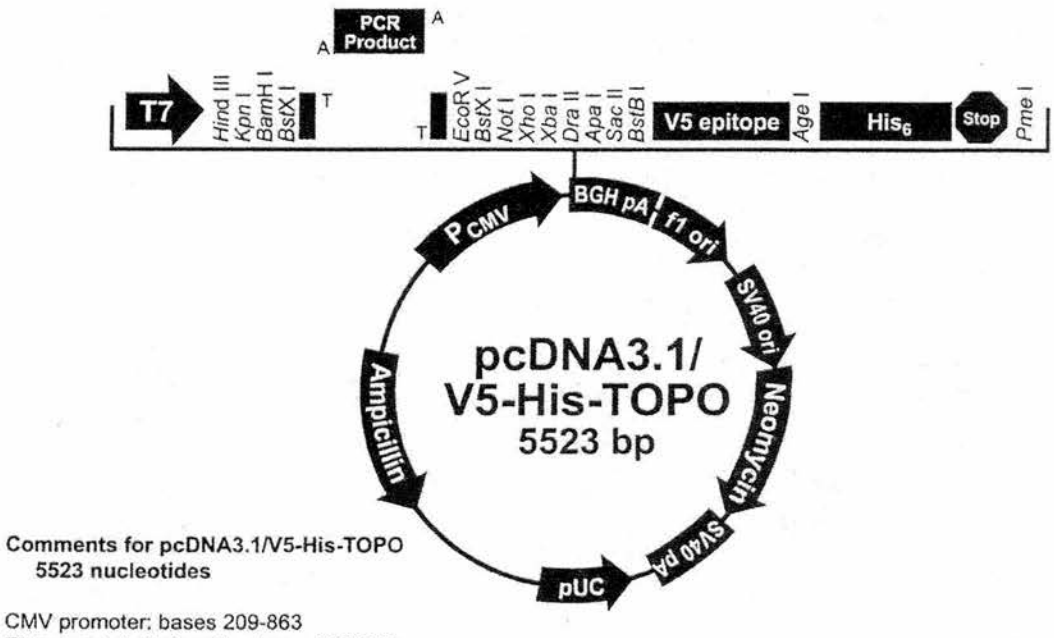

Comments for pcDNA3.1/V5-His-TOPO
5523 nucleotides

CMV promoter: bases 209-863
T7 promoter/priming site: bases 863-882
Multiple cloning site: bases 902-1019
TOPO® Cloning site: 953-954
V5 epitope: bases 1020-1061
Polyhistidine tag: bases 1071-1088
BGH reverse priming site: bases 1111-1128
BGH polyadenylation signal: bases 1110-1324
f1 origin of replication: bases 1387-1800
SV40 promoter and origin: bases 1865-2190
Neomycin resistance gene: bases 2226-3020
SV40 polyadenylation signal: bases 3039-3277
pUC origin: bases 3709-4382
Ampicillin resistance gene: bases 4527-5387

Map of pcDNA3.1/V5-His-TOPO® (Invitrogen) showing promoter, cloning site, restriction sites and sites of antibiotic resistance genes. pcDNA3.1/V5-His-TOPO® is a 5523bp mammalian expression vector that carries a geneticin resistance marker. It drives expression of the cloned insert from a CMV promoter. Figure taken from the manual supplied with the product.

Figure 2.2: Map of pEF6/V5-His-TOPO®

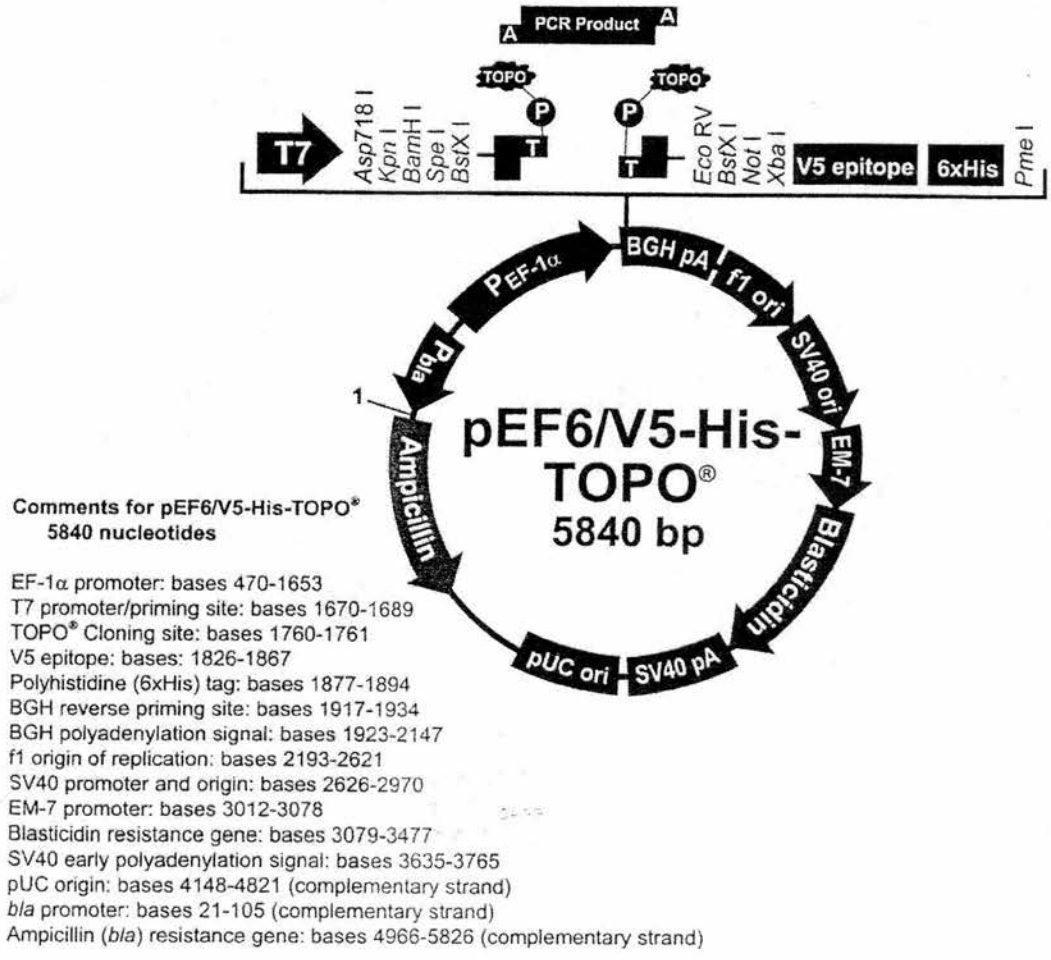

Comments for pEF6/V5-His-TOPO®
5840 nucleotides

EF-1α promoter: bases 470-1653
T7 promoter/priming site: bases 1670-1689
TOPO® Cloning site: bases 1760-1761
V5 epitope: bases: 1826-1867
Polyhistidine (6xHis) tag: bases 1877-1894
BGH reverse priming site: bases 1917-1934
BGH polyadenylation signal: bases 1923-2147
f1 origin of replication: bases 2193-2621
SV40 promoter and origin: bases 2626-2970
EM-7 promoter: bases 3012-3078
Blasticidin resistance gene: bases 3079-3477
SV40 early polyadenylation signal: bases 3635-3765
pUC origin: bases 4148-4821 (complementary strand)
bla promoter: bases 21-105 (complementary strand)
Ampicillin (*bla*) resistance gene: bases 4966-5826 (complementary strand)

Map of pEF6/V5-His-TOPO® (Invitrogen) showing promoter, cloning site, restriction sites and sites of antibiotic resistance genes. pEF6/V5-His-TOPO® is a 5840bp mammalian expression vector that carries a blasticidin resistance marker. Expression of the cloned insert is driven from an EF-1α promoter. Figure taken from the manual supplied with the product.

2.2.4 Constructs

An insert designed to express a transcript complementary to part of full-length *WWOX* 3'UTR was cloned into pcDNA3.1. It was envisaged that when transfected into cells this antisense construct would target endogenous *WWOX* transcripts, resulting in clones with decreased *WWOX* expression. These constructs were labelled 'A'. For ease, the resultant transfected clonal cell lines were labelled A1, A2, A3.

A second insert designed to express a transcript complementary to the full-length *WWOX* open reading frame (ORF) was cloned into pEF6. It was envisaged that when transfected into cells this antisense construct would also target endogenous *WWOX* transcripts. These constructs were labelled 'D'.

A third insert designed to express a transcript homologous to the full-length *WWOX* ORF (without the 3'UTR region targeted by the antisense construct cloned into pcDNA3.1) was cloned into pEF6. It was envisaged that when transfected into cells this sense construct would result in high-level exogenous expression of *WWOX*. These constructs were labelled 'H'.

The strategy of using expression vectors with different antibiotic resistance markers was chosen to allow the possible replacement of *WWOX* in a cell after it had been knocked out by an antisense construct targeting the 3'UTR, which could facilitate the identification of a phenotype for *WWOX*.

2.2.5 TOPO® cloning reaction and bacterial transformation

The inserts were cloned into both the pcDNA3.1/V5-His-TOPO® and the pEF6/V5-His-TOPO® cloning vectors which provide an efficient, one-step cloning strategy for direct insertion of Taq polymerase-amplified PCR products. Primers used to make the A insert (see section 2.2.4) were 3'UTR F and 3'UTR R (for primer sequences see table 2.1). The 'D' construct was made using primers E and Z. The 'H' construct was made using primers E and WWOX2rev. In each case, the PCR product was purified using the QIAquick® PCR Purification Kit (Qiagen) (see section 2.6.6). 0.5-4µl of PCR products was added to 1µl of the TOPO® vector in a salt solution with a final concentration of 200mM sodium chloride and 10mM magnesium chloride. The reactants were mixed gently and incubated for 10 minutes at room temperature, then placed on ice.

The TOPO® cloning reaction was performed by taking 2µl of the TOPO® cloning reaction and adding it to 50µl One Shot® TOP 10 Chemically Competent Cells (Invitrogen). This mixture was incubated on ice for 30 minutes. The cells were heat-shocked for 30s at 42°C without shaking, then immediately transferred to ice. 250µl of SOC medium (supplied with the chemically competent cell kit) was added and the tube was shaken horizontally (200rpm) at 37°C for 1 hour. 25-200µl from each transformation were spread on a pre-warmed selective L-agar plate and incubated overnight at 37°C. Colonies were then picked the following day and grown in 5ml of L-Broth (containing ampicillin) overnight. PCR was performed on 2µl of L-Broth for each colony to identify the presence of insert. For the *WWOX* sense (H) and full-length antisense (D) transfectants the primers used were 7F2 and 8R2. For the 3' antisense construct (A) the primers used were 3'UTR F and R. The primer sequences

and PCR conditions are shown in table 2.3. For the colonies that contained insert on the basis of PCR, DNA was prepared using the QIAGEN Qiaprep® Spin Miniprep Kit according to manufacturers guidelines. An EcoR1 restriction digest was perfomed (to release the insert) and the products were run on a 0.8% agarose gel to determine the size of the insert. Those colonies with correctly sized inserts were then sequenced for identity.

2.2.6 Sequencing of cloned inserts

2µl of plasmid DNA was used to sequence the entire cloned insert. To the 2µl of plasmid DNA was added 4µl ABI Prism® Big Dye, 1µl sequencing primer (3.2µM stock) and water to a final volume of 20µl. The following hot-start sequencing programme was run: 96°C hold for 30s, 50°C hold for 15s, 60°C hold for 4mins for 24 cycles, then 4°C hold.

For each sequencing reaction a 1.5ml microfuge tube was prepared containing 2µl 3M sodium acetate (pH 4.6), 0.5µl pellet paint and 50µl of 100% ethanol. The contents of each tube were vortexed and left at room temperature for at least 30mins to precipitate the extension products. The tubes were then centrifuged for 20mins at 16000g at 4°C. The supernatant was aspirated and discarded. The pellets were rinsed by the addition of 250µl of 70% ethanol and a brief vortex. The tubes were centrifuged for 5mins at 16000g at 4°C. The ethanol was removed using a fine tip pastette and the pellets allowed to dry briefly at room temperature. The precipitated sequences were run on an ABI 377 DNA sequencer (Agnes Gallacher, Medical Research Council, Human Genetics Unit).

2.3 Human cancer cell line culture

2.3.1 Media and additives

RPMI

RPMI 1640 medium (+L-glutamine) was obtained from GIBCO (Invitrogen Corporation).

DMEM

Dulbecco's Modified Eagle Medium (with sodium pyruvate with 100mg/l glucose) was obtained from GIBCO (Invitrogen Corporation).

Foetal calf serum (FCS)

Foetal calf serum was obtained from Harlan Sera-Lab Ltd.

Penicillin and Streptomycin

Penicillin and Streptomycin were obtained from GIBCO (Invitrogen). They were aliquoted at concentrations of 10000U/ml and 10000µg/ml respectively. These were added to tissue culture medium at a 1:100 dilution.

RPMI/10% FCS/P+S

55ml of FCS were added to 500ml of RPMI under sterile conditions. Penicillin and streptomycin (P+S) were also added to the media at final concentrations of 100U/ml and 100µg/ml respectively. Media was stored at 4°C when not being used and was heated to 37°C prior to use.

DMEM/10% FCS/P+S

55ml of FCS were added to 500ml of DMEM under sterile conditions. Penicillin and streptomycin were also added to the media. Media was stored at 4°C when not being used and was heated to 37°C prior to use.

Acid-inactivated fetal calf serum

Protease activity can inhibit cellular invasion so acid-inactivated FCS was used in invasion assays. To do this a 100ml bottle of heat inactivated foetal calf serum was heated to 37°C in a water bath, concentrated hydrochloric acid was added until the pH reached 3.0, the incubation was continued for a further 3 hours, the pH was brought back to 7.4 using concentrated sodium hydroxide and the serum was then 0.22μm filtered.

Geneticin

Geneticin (50mg/ml) was obtained from GIBCO BRL. It was stored at 4°C, protected from light. It was added to media to give a final concentration that depended upon the cell line (table 2.6).

Blasticidin S, Hydrochloride

Blasticidin S, Hydrochloride was obtained from ICN Biomedicals. It was diluted in sterile distilled water to give a stock solution at a concentration of 1mg/ml that was stored at -20°C. It was added to media to give a final concentration that depended upon the cell line (table 2.5).

Hygromycin B

Hygromycin B (50mg/ml) was obtained from Roche. It was stored at 4°C, protected from light. It was added to media to give a final concentration that depended upon the cell line (table 2.5).

Freeze Mix

Freeze mix was composed of 10% dimethyl sulfoxide (DMSO) in FCS.

Table 2.5: Antibiotic concentrations used for cell line culture

Cell Line	Requires	Blasticidin (µg/ml)	Geneticin (µg/ml)	Hygromycin (µg/ml)
A2780 HC2	hyg	2	100	75
HCT116	n/a	3	400	
HCT116 cl 4	n/a	3	400	
OAW42 hyg1	hyg	1	100	75
PEO1	n/a	3	300	
PEO1 hyg1.6	hyg	3	300	50

2.3.2 Maintenance of cell lines

All human tissue culture was carried out in a class II tissue culture hood (laminar flow) using sterile plasticware and autoclaved glassware. Sterile technique was employed at all times. Cell lines were maintained on RPMI/10% FCS/P+S or DMEM/10%FCS/P+S. Cells were cultured in humidified incubators at 37°C, 5% CO_2. Harvesting of cells was performed by removal of media, washing with phosphate-buffered saline (PBS) and incubation at 37°C for 5 to 10mins with a minimal amount of trypsin. 6ml of serum-containing media was then added (to

neutralise trypsin), the cells were recovered to a sterile universal container and the mixture of media and cells were centrifuged at 522g for 5mins. The media was then poured off and the cells were ready for further manipulation.

After recovery from liquid nitrogen, prior to freezing down and regularly during culturing each cell line was tested for the presence of mycoplasma. 5ml of media containing some shed cells was collected after 48-72 hours of incubation and the sample was sent for routine testing to Cell Production, Cancer Research UK, Clare Hall Laboratories, South Mimms.

2.3.3 Tumour cell lines

The HCT116 human colorectal cancer cell line and the PEO1, A2780 and OAW42 human ovarian cancer cell lines were transfected with the *WWOX* sense and antisense constructs.

HCT116 [188] is a colorectal cancer cell line that has a homozygous deletion within intron 8 of *WWOX* but still expresses a full-length transcript as well as a number of smaller transcripts [53]. The clonal line (HCT116 clone 4) used for the *WWOX* sense and antisense transfections was derived by Dr. Larry Hayward (Edinburgh Cancer Research Centre) by diluting the parent line to unicellularity and expanding out the clone.

The PEO1 cell line was derived from the ascites of an ovarian cancer patient [163]. It is homozygously deleted for *WWOX* exons 4-8 [53] and expresses a small transcript containing exons 1,2,3 and 9. Clonality for this line was achieved by transfecting the parent line with a hygromycin resistance vector then positively

selecting for growth. These cells were maintained in media containing 50μg/ml hygromycin.

A2780 is a human ovarian cancer cell line [189,190]. The clonal line used for the *WWOX* transfections was derived by initially transfecting the parent line with a hygromycin resistance vector then positively selecting for growth. These cells were maintained in media containing 75μg/ml hygromycin. This cell line was transfected with the construct expressing the *WWOX* sense transcript.

OAW42 is a human ovarian cancer cell line [191]. The clonal line used for the *WWOX* transfections was derived by initially transfecting the parent line with a hygromycin resistance vector then positively selecting for growth. These cells were maintained in media containing 75μg/ml hygromycin.

RNA from a panel of cancer cell lines was used for the quantitative analysis of WWOX isoform expression (table 2.6). This RNA was extracted from cultured cells by Diane Scott.

The wild-type (wt), p53-null, p21-null and Bax-null HCT116 isogenic colorectal cancer cell lines were obtained from the laboratory of Prof Bert Vogelstein.

Table 2.6: Cell lines used for quantification of *WWOX* isoforms (listed according to tissue of origin)

Tissue of Origin					
Ovary	**Colon**	**Lymphocyte**	**Breast**	**Prostate**	**Lung**
OVCAR3	HT115	FATO	T47D	DU145	NX002
CaOV3	HCT15	K562	ZR75.1	LN CAP	
OAW42	HRT18	HBL	MDA MB231	PC3	
PEA1	HT29	JURKAT	MCF7		
SKOV3	SW48	HL60			
A2780cis	HCT116				
PEA2	LOV0				
PEO14					
HELA					
OVCAR5					
59M					
A2780ad					
41M					
A2780					
OVCAR4					
PEO16					
PEO23					

2.3.4 Storage of cell lines in liquid nitrogen

Cells were grown in $75cm^3$ or $175cm^3$ tissue culture flasks until they were 70% confluent. They were washed with sterile PBS, a minimal volume of trypsin was added and the cells were incubated at 37°C for 5-10 minutes. The cells were recovered by the addition of 6ml of serum-containing tissue culture medium which was then removed using a pipette and placed into a universal container. The cells were then spun at 522g for 5 minutes to pellet and the RPMI/trypsin discarded. The

cell pellet was resuspended in freeze mix and aliquoted into freezing vials (Corning) in 1 ml volumes. The freezing vial was stored at -70°C overnight, then transferred to liquid nitrogen (-180°C to -175°C) for long-term storage.

2.3.5 Recovery of cell lines from liquid nitrogen

Recovery of the cells was performed by rapid thawing of the vial in a beaker of water at 37°C, followed by two washes in media and seeding into flasks.

2.3.6 Counting cells using the haemocytometer

When specific numbers of cells were required for an experiment, they were in general counted using a haemocytometer, which allows discrimination of viable and non-viable cells. Cells were harvested and washed as required for the purposes of the experiment in question. On occasion (if cell numbers were large) a 1 in 10 or a 1in 20 dilution was performed for the purposes of counting cells. A cover slip was adhered to the surface of a clean haemocytometer. Using a pastette, a suspension of the cells to be counted was applied to one half of the haemocytometer, under the cover-slip. Under the microscope, the number of cells in each quadrant of that half of the haemocytometer (16 smaller squares) was counted. This was performed for all 4 quadrants and the average count for a quadrant was calculated. This number, x, multiplied by 10000, gave the number of cells per ml of original suspension. Using simple proportion, the volume of cell suspension required to give a particular number of cells could then be calculated.

2.3.7 Determination of antibiotic sensitivities of individual cell lines

In order to determine the sensitivity of the cell lines used in the transfection experiments (HCT116, PEO1, A2780 and OAW42) to the antibiotic resistances (geneticin and blasticidin) on the vectors carrying the *WWOX* sense and antisense inserts, kill curves were performed prior to each transfection.

The cell lines were cultured in $75cm^3$ flasks until in log phase, then subcultured into 24-well plates. Cell numbers per well varied according to the cell line (from 1.5×10^3 per well for OAW42 to 1.2×10^4 per well for A2780). Estimates of the number of cells to use per well were obtained from Dr. Larry Hayward, Dr. Jane Sewell and Mr. Peter Mullen, who were familiar with the use of these cell lines. In order to allow a baseline count and three formally counted time-points, at least four 24-well plates were set up for each cell line with each antibiotic. The first column of each 24 well-plate was left blank. Cells from the $75cm^3$ flasks were harvested, washed and counted with a haemocytometer, so that a dilution with the correct number of cells per millilitre could be made. The cells in 1ml of growth medium were added to the 24-well plates and incubated at 37°C for 24 hours. The following day a baseline cell count was performed for one 24-well plate using the coulter-counter. For the other 24-well plates, the growth medium was removed and replaced with media containing a concentration range of selective antibiotics. The 2^{nd} column of wells had no antibiotic and the following 4 columns had antibiotic of progressively increasing concentrations. For geneticin, the first 4 antibiotic concentrations tested were 50, 100, 150 and 200µg/ml. For blasticidin, the first 4 antibiotic concentrations tested were 0.5, 1.0, 1.5 and 2.0µg/ml. The effect of the antibiotic was monitored by

counting the cells at regular intervals using the coulter-counter and by direct visualisation of the cells. Complete cell death at 5-7 days post exposure was considered to be optimal for transfection purposes.

The geneticin and blasticidin concentrations used for the cell lines involved in the transfection experiments are shown in table 2.7.

Table 2.7: Geneticin and blasticidin concentrations used in transfections

Cell Line	Geneticin Concentration (µg/µl)	Blasticidin Concentration (µg/µl)
HCT116 cl4	400	3
PEO1 hyg 1.6	300	3
A2780 HC2	100	2
OAW42 hyg1	100	1

2.3.8 Stable transfection of plasmid DNA into cell lines

Transfections were performed using linear rather than circular DNA to minimise the possibility of interrupting the insert during integration into the mammalian genome. The plasmid was prepared, linearised, gel purified and ethanol precipitated as described in section 2.2 (above).

At least two transfections events were performed for each plasmid construct to ensure that truly independent clones were obtained. Transfections were performed using the Effectene® Transfection Reagent Kit (Qiagen).

Adherent cells were grown to 70% confluence, then 5-20 x 10^5 cells (depending on the cell type) were seeded into a 100mm Petri dish in 10ml of growth medium containing serum and appropriate antibiotics. The cells were cultured in humidified incubators at 37°C, 5% CO_2. When the cells were in log phase the transfection was performed. 1µg of linearised plasmid DNA (dissolved in 5µl TE) was added to 145µl of buffer EC and 8µl of enhancer and briefly vortexed. The mixture was incubated at 25°C for 5mins and briefly centrifuged. 25µl of Effectene® Transfection Reagent was added to the DNA-Enhancer mixture. This was mixed by vortexing for 10s and the mixture was incubated for a further 10mins at 25°C to allow complex formation. The transfection complexes were removed from the reaction tube and placed in a universal with a further 3ml of growth medium. This mixture was pipetted up and down twice before being added drop-wise onto the cells in the 100mm Petri dishes (which were swirled during addition of the transfection complexes). The cells were then cultured at 37°C, 5% CO_2 in a humidified incubator. For each plasmid transfection (whether vector-only or vector containing insert) 2 separate Petri dishes containing cells were transfected with the plasmid, a further Petri dish was exposed to buffer and enhancer (but no plasmid) and a further Petri dish containing cells was not exposed to any of the transfection reagents. The cells were then cultured for a further 48 hours, before subculturing each Petri dish into 5 Petri dishes. The cells were then incubated for a further 24 hours before exposing them to antibiotic selection.

The cells were cultured in selective media until no live cells were visible in the control dish that was not exposed to transfection reagents and until sizeable colonies were visible in the Petri dishes containing the plasmid transfections.

2.3.9 Picking of resistant clones

Colonies were identified with the naked eye and their location marked on the undersurface of the dish with a marker. The degree of isolation of each colony was checked under the microscope. Each petri dish was washed with PBS and one drop of trypsin was placed on the colony. Five seconds were allowed to elapse before the colony was aspirated with a fine pastette and deposited into one well of a 24-well tray containing 1ml of tissue culture medium containing selection. The contents of the well were pipetted up and down to break up the colony.

The cells were progressed through 24-well trays, 6-well trays, $25cm^3$ tissue culture flasks into $75cm^3$ tissue culture flasks. Cells from $25cm^3$ flasks were used to obtain RNA and the contents of one $75cm^3$ flask were frozen down in 3 freezing vials to allow long-term storage of the cells in liquid nitrogen.

2.4 DNA preparation

2.4.1 Tumour cell lines

Tumour cell lines were grown in culture until log phase and harvested as described earlier. DNA extraction was performed using the QIAamp® DNA Mini Kit (Qiagen). The washed cells were suspended in a final volume of 200µl PBS in a 1.5ml microcentrifuge tube. 20µl Proteinase K and 200µl Buffer AL were added to the sample which was mixed by pulse-vortexing for 15s. The sample was incubated at 56°C for 10min and the microcentrifuge tube was briefly centrifuged. 200µl ethanol was added to the sample, which was then mixed by pulse-vortexing for 15s

and briefly centrifuged. The mixture was applied to a QIAamp spin column and centrifuged at 10000g for 1min. The column was washed firstly with 500µl of Buffer AW1 (centrifuged for 1min at 10000g) and secondly with 500µl of Buffer AW2 (centrifuged for 3min at 16000g). 200µl Buffer AE was added to the column, which was spun at 10000g for 1 min to elute the DNA. The concentration of the DNA was estimated by spectrophotometry (section 2.4.3) and stored at -20°C.

2.4.2 Clinical material

Primary ovarian tumour material and non-malignant tissues were obtained from patients undergoing gynaecological surgery in Lothian University Hospitals NHS Trust, Scotland, UK. This material was gathered by Diane Scott and her help with this is gratefully acknowledged. Institutional ethical approval for this work was granted by the Lothian University National Health Service Trust Medicine/Clinical Oncology Research Ethics Subcommittee. Tissue samples were excised, transferred on ice for section then transferred into liquid nitrogen. All the patient samples were anonymised during laboratory investigation but were given human ovary (HOV) numbers as unique identifiers in order to allow matching of clinical and laboratory data.

One section of tissue was transferred to a freezing vial and dismembranated prior to storage in liquid nitrogen. This vial was used for DNA extraction.

DNA was extracted from clinical samples using the Nucleon® Genomic DNA Extraction Kit (Soft Tissue) supplied by Tepnel Life Sciences plc.

Dismembranated frozen tissue was taken from liquid nitrogen storage and weighed. 2.5ml of Reagent A was added for each 0.25g of tissue. Following centrifugation at 1300g for 10 mins, the supernatant was discarded without disturbing the cell pellet. 0.5ml of Reagent B/0.25g of tissue was added to the pellet and the solution briefly vortexed to resuspend the pellet. The suspension was then transferred to a polypropylene tube and RNase I was added to a final concentration of 400ng/ml. The suspension was then incubated at 37°C for 30mins. Following this, 150µl of sodium perchlorate was added for each 0.25g of tissue. The suspension was mixed by inverting 7 times to emulsify the phases. 150µl of Nucleon® Resin was added for each 0.25g of tissue. This was rotary mixed for 5 mins and centrifuged at 350g for 1min for samples of <0.25g or at 1300g for 3 mins with samples >0.25g. Without disturbing the Nucleon® Resin layer, the upper phase was transferred to a clean polypropylene tube. Two volumes of cold absolute ethanol were added to precipitate the DNA and the tube was inverted several times. The DNA was removed from the tube using a glass hook, was allowed to air-dry and was then placed into a microfuge containing TE. The OD_{260} of the DNA solution was then determined spectrophotometrically (section 2.4.3).

2.4.3 Quantification of DNA/RNA by spectrophotometry

1-5µl of nucleic acid was diluted in distilled water to a final volume of 1000µl. The absorbance of this dilution was read using a spectrophotometer at wavelengths of 260nm (OD_{260}) and 280nm (OD_{280}). An OD_{260} of 1.0 is equivalent to a dsDNA (double-stranded DNA) concentration of 50µg/ml, a ssDNA (single-stranded DNA) concentration of 33µg/ml and an RNA concentration of 40µg/ml allowing simple

proportional calculations to determine the DNA or RNA concentration of the sample. For DNA and RNA, the OD_{280} to OD_{260} ratio indicates the purity of the sample with a ratio of 1.8 being optimal for DNA and a ratio of 1.8 to 2.0 being optimal for RNA. A ratio of less than 1.8 indicates considerable protein contamination.

2.5 RNA preparation

2.5.1 Cell lines

Cultured cells were grown to 70% confluence in a $25cm^3$ tissue culture flask and the tissue culture medium was discarded. RNA was then prepared using the Absolutely RNA® RT-PCR Miniprep Kit (Stratagene). 600µl of lysis buffer was added to 4.2µl of β-mercaptoethanol in a labelled 1.5ml microcentrifuge tube and the mixture was pulse-vortexed. The mixture was added to the $25cm^3$ tissue culture flask, spread evenly over the surface and run back and forth over the surface of the flask. The cell lysate was then returned to the microcentrifuge tube, which was vortexed to homogenize the lysate. Up to 700µl of homogenate was transferred to a Prefilter Spin Cup seated in a 2ml receptacle tube and centrifuged at 16000g for 5mins. The spin cup was removed and discarded. The filtrate was retained. An equal volume of 70% ethanol was added to the filtrate and the tube was vortexed for 5s. Up to 700µl of the mixture was transferred to a Fibre-Matrix Spin Cup, seated in a fresh 2ml receptacle tube and centrifuged at 16000g for 60s. The filtrate was discarded and the spin-cup retained. For samples homogenised in >350µl of lysis buffer, the last 2 steps were repeated. For all steps up to this the RNA was protected from RNases by

the presence of guanidine thiocyanate. All further steps were performed in an RNase-free hood. 600µl of Low-Salt Wash Buffer was added to the tube, which was centrifuged at 16000g for 60s. The filtrate was discarded and the tube was centrifuged for a further 2mins. The DNase solution containing 45U DNase I in 55µl buffer was added directly onto the fiber matrix inside the spin cup and the sample was incubated at 37°C for 15mins in an air incubator. After incubation, 600µl of High-Salt Wash Buffer was added and the tube was centrifuged at 16000g for 60s. The filtrate was discarded and the spin cup retained. Next, 600µl of Low-Salt Wash Buffer was added and the tube was centrifuged at 16000g for 60s. The filtrate was discarded and the spin cup was retained. Following this 300µl of Low-Salt Wash Buffer was added and the tube was centrifuged at 16000g for 2mins to dry the fibre-matrix. The filtrate was discarded and the spin cup was placed in a clean 1.5ml microcentrifuge tube. 60µl of Elution Buffer was placed directly onto the centre of the fibre matrix inside the spin cup and the tube was incubated for 2mins at room temperature. The tube was then centrifuged at 16000g for 60s to elute the RNA.

5µl of RNA was taken immediately for quantification by spectrophotometry and the remainder stored at –70°C.

2.5.2 Clinical material

Sections used for RNA preparation had not previously been freeze-thawed. RNA was prepared using the Absolutely RNA RT-PCR Miniprep Kit (Stratagene) and a dismembranator. The sample was retrieved from liquid nitrogen into a weighed freezing vial on dry ice. Using a sterile scalpel, the sample was cut into fragments on a Petri dish on dry ice to give 25-30mg aliquots. They were placed into numbered

freezing vials and reweighed. Steel balls were washed in 50% neutricon®/distilled water, then distilled water, then ethanol. One steel ball was then placed in each tube. 600µl of Lysis Buffer and 4.2µl of β–mercaptoethanol were added to each tube and the sample was dismembranated for 1min at 1800Hz. Using a pastette, the solution was transferred into a clean 1.5ml microfuge tube. The sample at this stage could be stored at –70°C for use at a later date if required. Otherwise, isolation of RNA was similar to that for cell line RNA from the cell lysate step onwards, except that the published protocol required optimisation for tissue samples because the DNaseI treatment step was not satisfactory for removing contaminating DNA in all cases.

A further 600µl of cell lysis buffer was added to the homogenate and the microfuge tube was vortexed. Thus, a total volume of 1.2-1.6 ml was present in the microfuge tube. This was run down two columns instead of one to prevent the capacity of the column for removing all contaminating DNA from being overcome. Up to 700µl of homogenate was transferred to each of two Prefilter Spin Cups seated in 2ml receptacle tubes. The tubes were centrifuged at 16000g for 5mins. The spin cups were removed and discarded. The filtrates were retained. An equal volume of 70% ethanol was added to each filtrate and the tubes were vortexed for 5s. For each tube, up to 700µl of the mixture was transferred to a Fibre-Matrix Spin Cup seated in a fresh 2ml receptacle tube in a fresh receptacle tube and this was centrifuged at 16000g for 60s. The filtrates were discarded and the spin-cups were retained. For all steps up to this the RNA was protected from RNases by the presence of guanidine thiocyanate. All further steps were performed in an RNase-free hood. 600µl of Low-Salt Wash Buffer was added to each tube and they were centrifuged at 16000g for 60s. The filtrate was discarded and the tubes were centrifuged for a further

2mins. The DNase solution was prepared by gently mixing 50µl of DNase Digestion Buffer with 15 µl of reconstituted RNase-Free DNase I for each column. The DNase solution was added directly onto the fiber matrix inside each spin cup and the samples were incubated at 37°C for 15mins in an air incubator. After incubation, 600µl of High-Salt Wash Buffer was added to each tube and they were centrifuged at 16000g for 60s. The filtrates were discarded and the spin cup was retained. Next, 600µl of Low-Salt Wash Buffer was added to each tube and they were centrifuged at 16000g for 60s. The filtrates were discarded and the spin cups were retained. Following this 300µl of Low-Salt Wash Buffer was added to each tube and they were centrifuged at 16000g for 2mins to dry the fibre-matrix. The filtrates were discarded and the spin cups were placed in a clean 1.5ml microcentrifuge tube. 60µl of Elution Buffer was placed directly onto the centre of the fibre matrix inside the spin cup and the tubes were incubated for 2mins at room temperature. The tubes were then centrifuged at 16000g for 60s to elute the RNA.

5ul of RNA was taken immediately from each sample for quantification by spectrophotometry (see below). The rest was stored at –70°C.

2.6 Preparation of first strand cDNA

First strand cDNA was synthesised using the 1st Strand cDNA Synthesis Kit for RT-PCR (AMV), obtained from Roche. Using this method AMV reverse transcriptase synthesised the new cDNA strand from the 3'-end of the poly(A) mRNA, the reaction having been primed by Oligo-p$(dT)_{15}$.

1µg of RNA was used for each 1st strand cDNA synthesis of 20µl. Two 1µg aliquots of RNA were prepared for each sample to allow for a positive (+ve RT) and a control (-ve RT) reaction. For each set of aliquots a mastermix of reagents was prepared to include 2µl 10x Reaction Buffer (100mM Tris, 500mM KCl; pH8.3), 4µl 25mM Mg Cl_2, 2µl Deoxynucleotide Mix (dATP, dCTP, dTTP, dGTP; 10mM each), 2µl Oligo-$p(dT)_{15}$ Primer (0.8µg/µl) and 1µl RNase inhibitor. To the first strand cDNA synthesis reaction, 0.8µl of AMV reverse transcriptase was added. The samples were briefly vortexed then briefly centrifuged before being placed in a PCR block (PTC-225 Peltier Thermal Cycler, MJ Research). The samples were heated on the block at 25°C for 10mins, 42°C for 60mins, followed by 5mins incubation at 99°C to denature the AMV reverse transcriptase and then removed to ice

2µl of each first strand cDNA product (+ve and –ve RT reactions) was aliquoted off for a PCR using γ-*ACTIN* primers (section 2.1) and the rest was aliquoted into the desired volumes and stored at –70°C.

2.7 Quantitative RT-PCR

Quantitative PCR was performed initially using a Light-cycler® (Idaho Technologies) and subsequently using a Rotorgene® 2000 (Corbett Research).

2.7.1 Quantitative RT-PCR using the Light-cycler®

The Lightcycler® was a quantitative PCR machine that had 24 slots for PCR reactions contained within glass capillaries (although in practice only 22 were usable). It had a heating block that rotated once per cycle, allowing the incorporated

fluorescence of each sample to be determined once per cycle. The PCR reactions each contained SYBR Green, a stain that fluoresces when it binds to dsDNA. The level of fluorescence is negligible at the beginning of the PCR reaction but, as the exponential production of dsDNA occurs, the fluorescence rises off the baseline, becomes detectable and continues to rise (figure 2.3). The number of cycles required for there to be a significant rise in fluorescence off the baseline is proportional to the concentration of the target DNA sequence in the original reaction mixture. Therefore, by the use of standards of known DNA target copy number, a standard curve can be produced (figure 2.4) which allows extrapolation from the number of PCR cycles that produce a rise in fluorescence to the initial copy number in the unknown samples (figure 2.5).

Figure 2.3: Change in fluorescence as a real-time PCR progresses

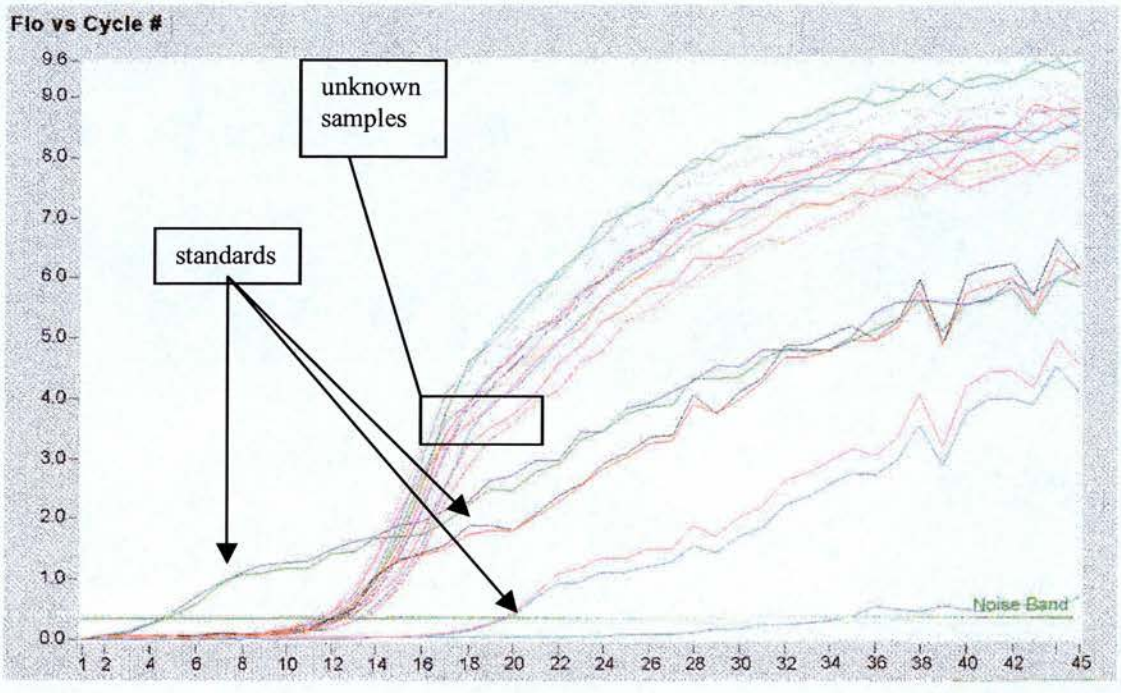

fluorescence

cycle number

Rise in fluorescence as a real-ime PCR progresses on the Lightcycler®. PCRs were performed using *ACTIN* or *WWOX* specific primers, cell line cDNA as a template and SYBR green as a fluorophore. Fluorescence is plotted against cycle number. Pairs of standards cut the noise band at 4, 12.5 and 19 cycles of PCR. On the basis of this a standard curve can be generated (fig 2.5) and quantitation of unknown samples can be conducted (fig 2.6).

Figure 2.4: A standard curve

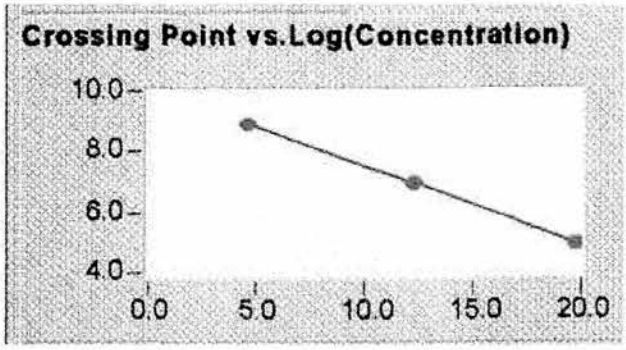

Standard curve generated from a Lightcycler® PCR run. PCRs were performed using *ACTIN* or *WWOX* specific primers, cell line cDNA as a template and SYBR green as a fluorophore. The point where the standards cross the noise band (in terms of numbers of cycles) is plotted against the log of the concentration of the target in the starting sample. This allows extrapolation of the point that unknown samples cross the noise band to give the concentration of the target fragment in that unknown sample at the start of the reaction.

Figure 2.5: Lightcycler® quantification of unknown samples

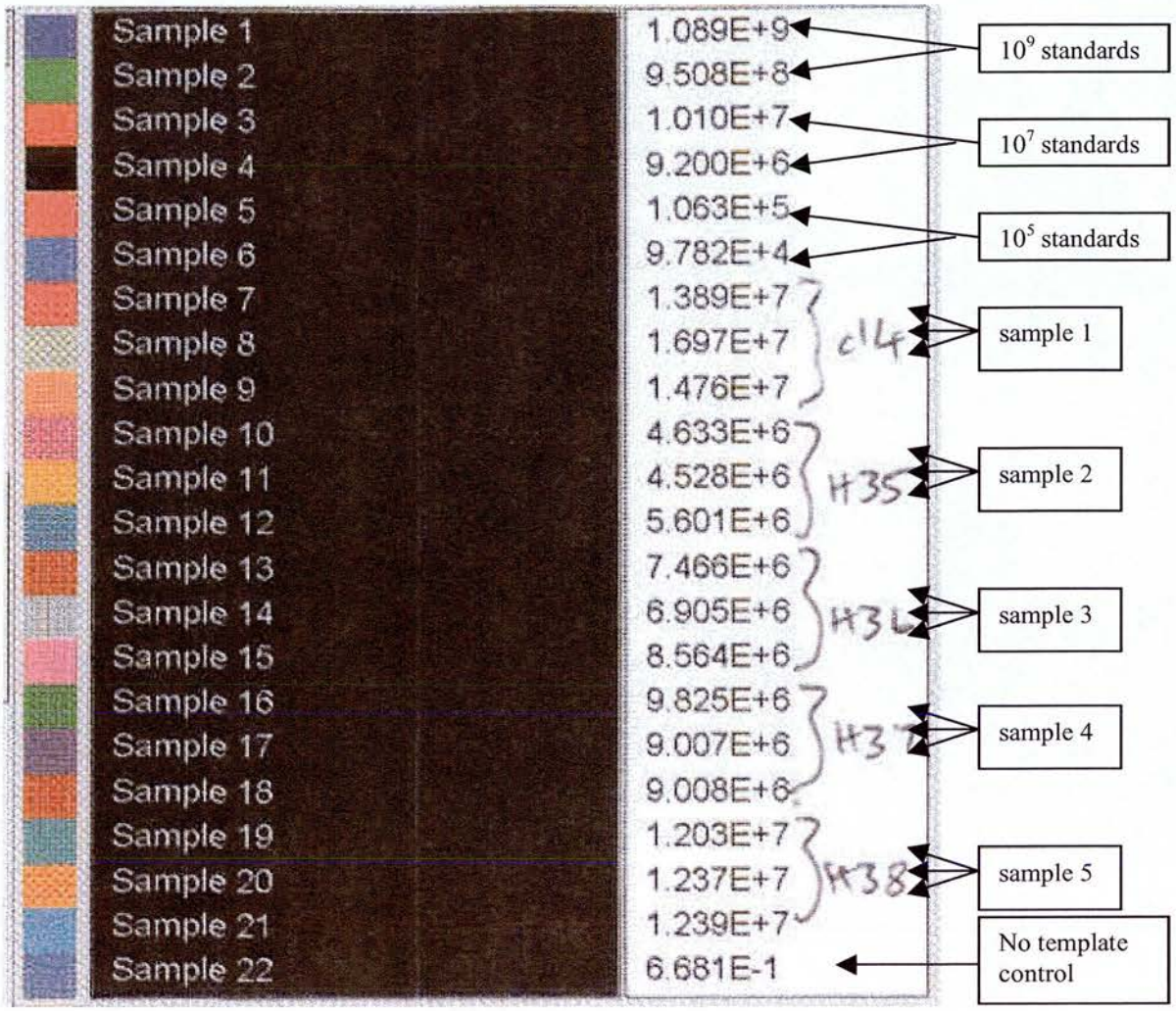

Quantification of target DNA copy number in unknown samples using the Lightcycler® by extrapolation from a standard curve. PCRs were performed using *ACTIN* or *WWOX* specific primers, cell line cDNA as a template and SYBR green as a fluorophore. Samples 1 to 6 are the standards of designated concentration (in duplicate). Sample 22 is the NTC. Samples 7 to 21 are the samples of unknown concentration (in triplicate).

Standards (amplified DNA with known gene copy number) at three different concentrations, each in duplicate, were put in the first 6 slots of the machine.

Typical copy numbers for these standards were either 10^9, 10^7 and 10^5 or 10^7, 10^5 and 10^3 depending on the abundance of the gene in the cell line being investigated. Every effort was made to ensure that the copy number of the unknown samples was contained within the extent of the standard curve. One no template control (NTC) was included in each run. The main interest was in the level of gene expression in transfectants compared to the parent line. Cell line cDNA was used and for each cell line (whether parent or transfectant) the reactions were performed in triplicate. The parent line was included in each run to allow comparability between runs without relying entirely on the exact reproducibility of the standard curve. The average copy number of each triplicate was used for quantitation analysis. In order to correct for any differences in the amount of RNA used in each first strand reaction or for differences in the efficiency of the first strand reactions, quantification of a housekeeping gene (in this case β-*ACTIN*) was performed and the expression level of the gene of interest (in most cases *WWOX*) in each cell line was corrected for the expression level of β-*ACTIN*.

The output from the Lightcycler®, as well as including the fluorescence of each sample after each cycle of the PCR, also included a melt curve which was created by slowly increasing the temperature of each tube from 70°C to 95°C at the end of the PCR reaction (figure 2.6). This allowed the determination of the melt temperature for all the double-stranded DNA molecules in the PCR products and helped in distinguishing primer dimer from desired PCR products.

Figure 2.6: Example of melt curves generated by the Lightcycler®

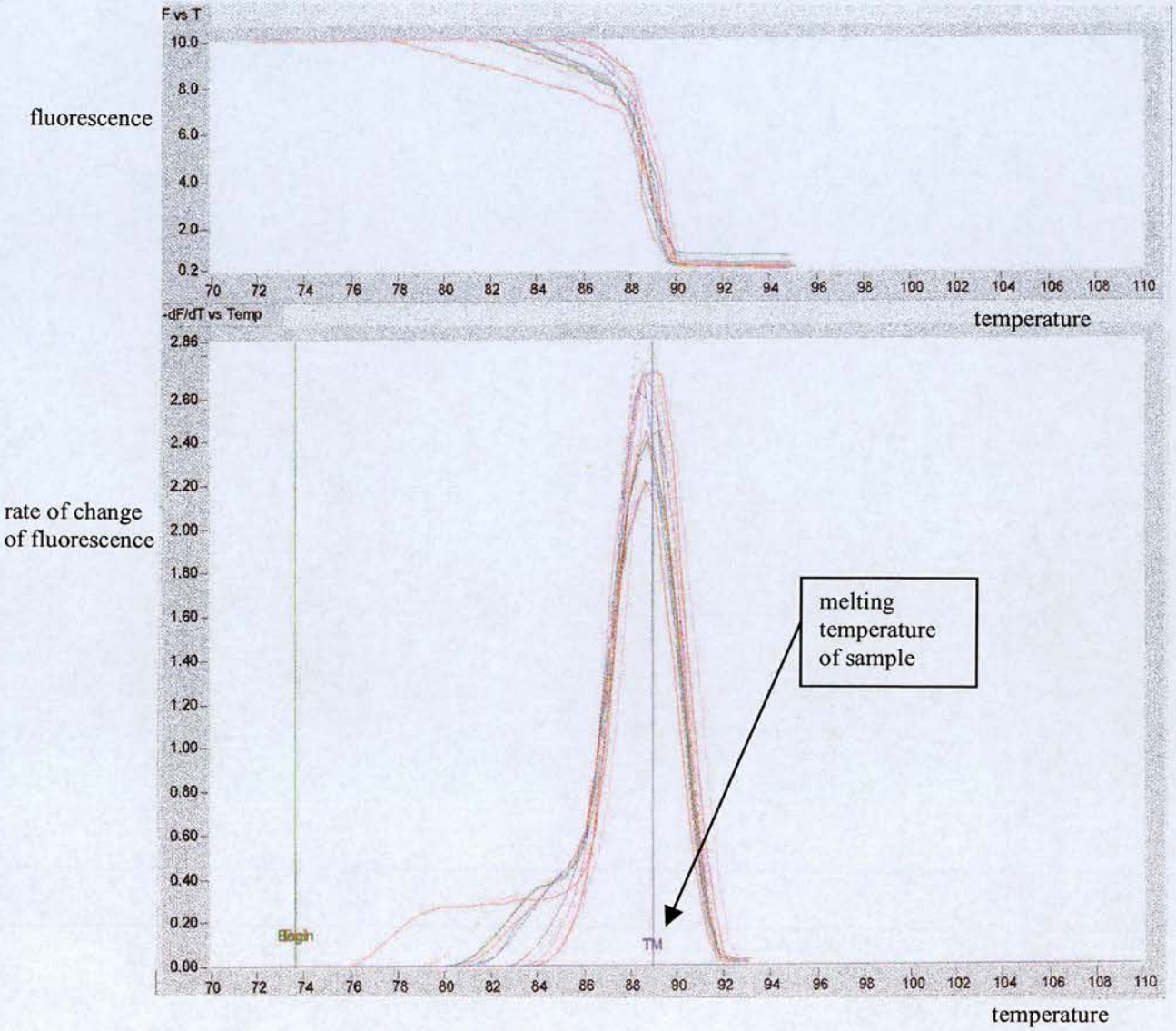

Melt curves generated by the light cycler. PCRs were performed using *ACTIN* or *WWOX* specific primers, cell line cDNA as a template and SYBR green as a fluorophore. Melt curves were produced by slowly increasing the temperature of each tube from 70°C to 95°C at the end of the PCR reaction. This allowed the determination of the melt temperature for all the double-stranded DNA molecules in the PCR products and helped in distinguishing primer dimer from desired PCR products. Fluorescence was plotted against temperature (top graph) and rate of change of fluorescence was plotted against temperature (bottom graph).

2.7.2 Lightcycler® reagents

2x PCR Mastermix

2x Taq based Glass Capillary Master Mix 2mM $MgCl_2$ (Biogene) was used for all Lightcycler® PCR reactions. This contained Taq DNA polymerase, reaction buffer, magnesium chloride (to give a final concentration of 2.0mM) and dNTPs. The Mastermix was stored at –20°C.

SYBR Green I

SYBR Green I (Biogene) was used in all Lightcycler® PCR reactions. This was stored at –20°C, protected from light. A 1 in 10 stock solution was made up by adding 45µl of TE to 5µl of SYBR Green I. This was mixed and stored at -20°C, protected from light. A 1 in 1000 working solution was made up by adding 3µl of the 1 in 10 stock to 297µl of TE. This was dated and stored at -20°C, protected from light.

HPLC-purified primers

HPLC purified PCR primers, obtained from Imperial Cancer Research Fund (subsequently Cancer Research UK) Oligonucleotide Synthesis Service were found to give optimal results and were subsequently used for all quantitative RT-PCR. They were stored at –20°C at a stock concentration of 200mM.

2.7.3 Lightcycler® primers

Primers were chosen using Primer 3 (as for non-quantitative PCR, above). For quantitative real-time PCR, maximum 3' and self-complementarity were kept to an absolute minimum. The primer sequences used for quantitative RT-PCR on the lightcycler® are shown in table 2.8.

Table 2.8: Lightcycler® PCR primers and conditions

PCR	Primers	Sequences (5'-3') For/Rev	$[Mg^{2+}]$/ Taq[a]	Cycling conditions
Quantitative real time RT-PCR using Lightcycler®	β*ACTIN* F+R	CTACGTCGCCCTGGACTTCGAGC GATGGAGCCGCCGATCCACACGG	2xMM	95°C 0s (20°C/s); 56°C 2s (20°C/s); 72°C 15s (5°C/s); 85°C 2s (20°C/s) ACQUIRE; 45 cycles
	Z1+Z2 (both in ex 9)	TACTTCAACAACTGCTGCCG CGTTCTTGGATCAGCCTCTC	2xMM	95°C 0s (20°C/s); 58°C 2s (20°C/s); 72°C 15s (5°C/s); 85°C 2s (20°C/s) ACQUIRE; 45 cycles
	LC1 F+R (both in 3'UTR)	GTGGTGGCCTGTTTGAAAGT GAGGGGACCTCAGGCTATTC	2xMM	95°C 0s (20°C/s); 59°C 2s (20°C/s); 72°C 15s (5°C/s); 78°C 2s (20°C/s) ACQUIRE; 45 cycles

Primer sequences, magnesium concentrations, type of Taq DNA polymerase used and cycling conditions quantitative real time RT-PCR performed on the lightcycler®.

[a]2x MM = 2x Taq based Glass Capillary Master Mix 2mM Mg (Biogene)

2.7.4 Generation of standards for the Lightcycler®

Conventional PCR was performed (primer sequences and PCR conditions in table 2.1) to generate amplified DNA for the required target sequences that was then used to create DNA standards of known copy number. For example, in the case of β-*ACTIN*, a conventional PCR was performed to generate amplified β-*ACTIN* DNA. The template for this PCR was cell line cDNA, usually from HCT116 clone 4. The PCR products were checked by running on a 2% agarose gel and then purified using the QIAquick® PCR Purification Protocol (section 2.1.7). The purified DNA was then quantified spectrophotometrically. On the basis of the OD_{260} of the sample and the size of the amplified fragment, it was possible to calculate the number of copies of the target per µl. On the basis of this, a stock solution containing 10^{10} copies per µl was made up. This was stored at –20°C and used to make up the standards for each run. Dilutions of the 10^{10} stock were made fresh each day. Dilutions used as

standards in the runs contained 10^9, 10^7 and 10^5 or 10^7, 10^5 and 10^3 copies per µl (depending on the abundance of the gene in the cell line being investigated). As 1µl of standard was used for each PCR reaction, this meant that construction of a standard curve with Ct values (number of cycles prior to significant amplification) against starting target copy number was straightforward.

2.7.5 Lightcycler® conditions

As the lightcycler® used a silicon-based PCR methodology, optimisation of PCR conditions on the non-quantitative block was not found to be useful. Optimisation of Lightcycler® conditions involved trying a variety of magnesium concentrations (in some cases generating a magnesium curve), various annealing temperatures and primer concentrations and adding linearised plasmid DNA to the reaction mix in an attempt in the first instance to achieve a clean melt curve with a single peak of dsDNA product. For this reason, initial runs were conducted with a low fluorescence acquisition temperature (e.g. 72°C). Once the melting temperature for the double-stranded DNA product was known, the cycling acquisition temperature was set just below this. One of the main problems encountered was the generation of primer dimers during the PCR. These were seen as PCR products that had low melting temperatures in the melt curve. Attempts to minimise this involved decreasing the primer concentration, decreasing the magnesium concentration, increasing or (paradoxically) decreasing the annealing temperatures of the reaction and adding linearised plasmid DNA. Once conditions were found that generated a satisfactory melt curve, the ability of the conditions to generate a good standard curve with a low error ($<1x10^{-3}$) was tested. The fluorescence plot generally rose slowly with the

number of PCR cycles, until a critical level was reached, after which the gradient of the plot increased rapidly. The noise band (figure 2.7) was the horizontal line parallel to the x-axis, the intersection of which by the fluorescence plot gave the Ct value for each standard or sample. This was set so that all standards and samples had entered the phase of rapidly increasing fluorescence (figure 2.7). The Ct values of the standards were used to create a standard curve. The copy number in the samples was calculated by extrapolation from this standard curve.

Figure 2.7: Setting the noise band

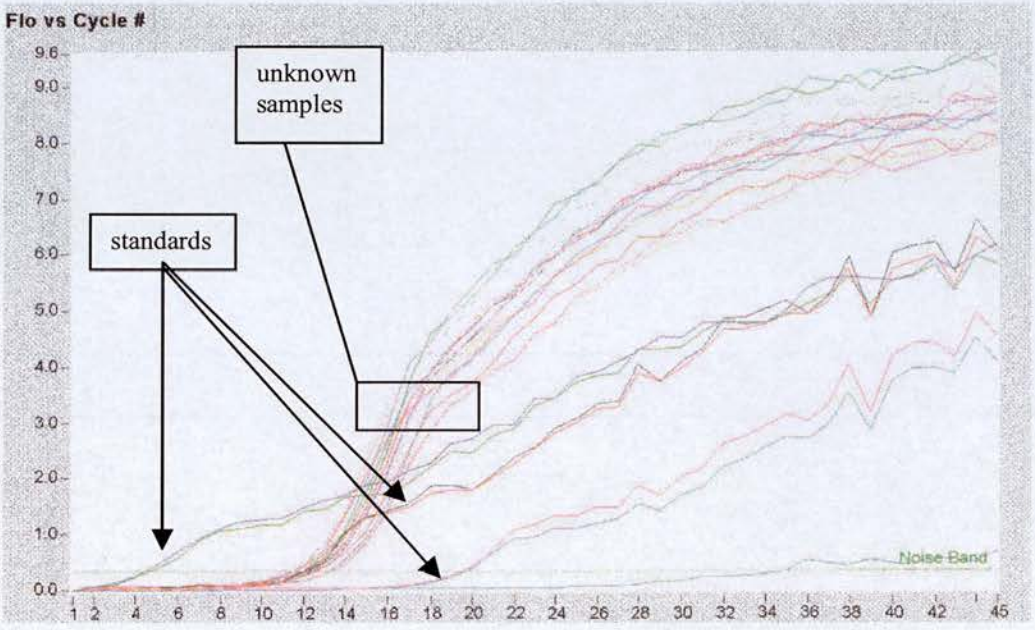

Demonstration of how the noise band is set. PCRs were performed using *ACTIN* or *WWOX* specific primers, cell line cDNA as a template and SYBR green as a fluorophore. The noise band (green horizontal line) was set at a level where the fluorescence of all the samples was rising rapidly off the baseline (all standards and samples had entered the phase of rapidly increasing fluorescence). The intersection of the noise band by the fluorescence plot gave the Ct value for each standard or sample. The Ct values of the standards were used to create a standard curve. The copy number in the samples was calculated by extrapolation from this standard curve.

The best conditions for a house-keeping gene were achieved for a β-actin primer pair. The best results were obtained with high performance liquid chromatography (HPLC) cleaned oligonucleotides. For full-length *WWOX*, a new primer pair, Z1/Z2 with a PCR product of 101bp was used. This gave reproducible results with good melt curves (figure 2.8 and 2.9) and a satisfactory standard curve (figure 2.10). The presence of a single gene product as suggested by the melt curve was confirmed by running the PCR products on a 2% agarose gel (figure 2.11). This PCR primer pair targeted exon 9 of the *WWOX* gene, so was used for quantifying endogenous *WWOX* expression in untransfected cell lines, vector controls and 3' antisense (A/B) transfectants and for quantifying total *WWOX* expression in sense (H) transfectants. However, they were unsuitable for quantifying *WWOX* expression in full-length antisense (D) transfectants (which expressed an antisense molecule targeting the whole open reading frame) as they would amplify from the antisense molecule itself. Therefore a second *WWOX*-specific primer pair, LC1F/R, which targeted a region of the 3'UTR was optimised for the Lightcycler®. This primer pair was used for quantifying endogenous *WWOX* expression in untransfected cell lines, vector controls, full-length sense (H) transfectants and full-length antisense (D) transfectants. They were unsuitable for quantifying total *WWOX* expression in full-length sense (H) transfectants or for quantifying WWOX expression in 3'antisense (A/B) transfectants.

Figure 2.8: Melt curves for 10^5-10^9 standards for Z1/Z2 Lightcycler® PCR

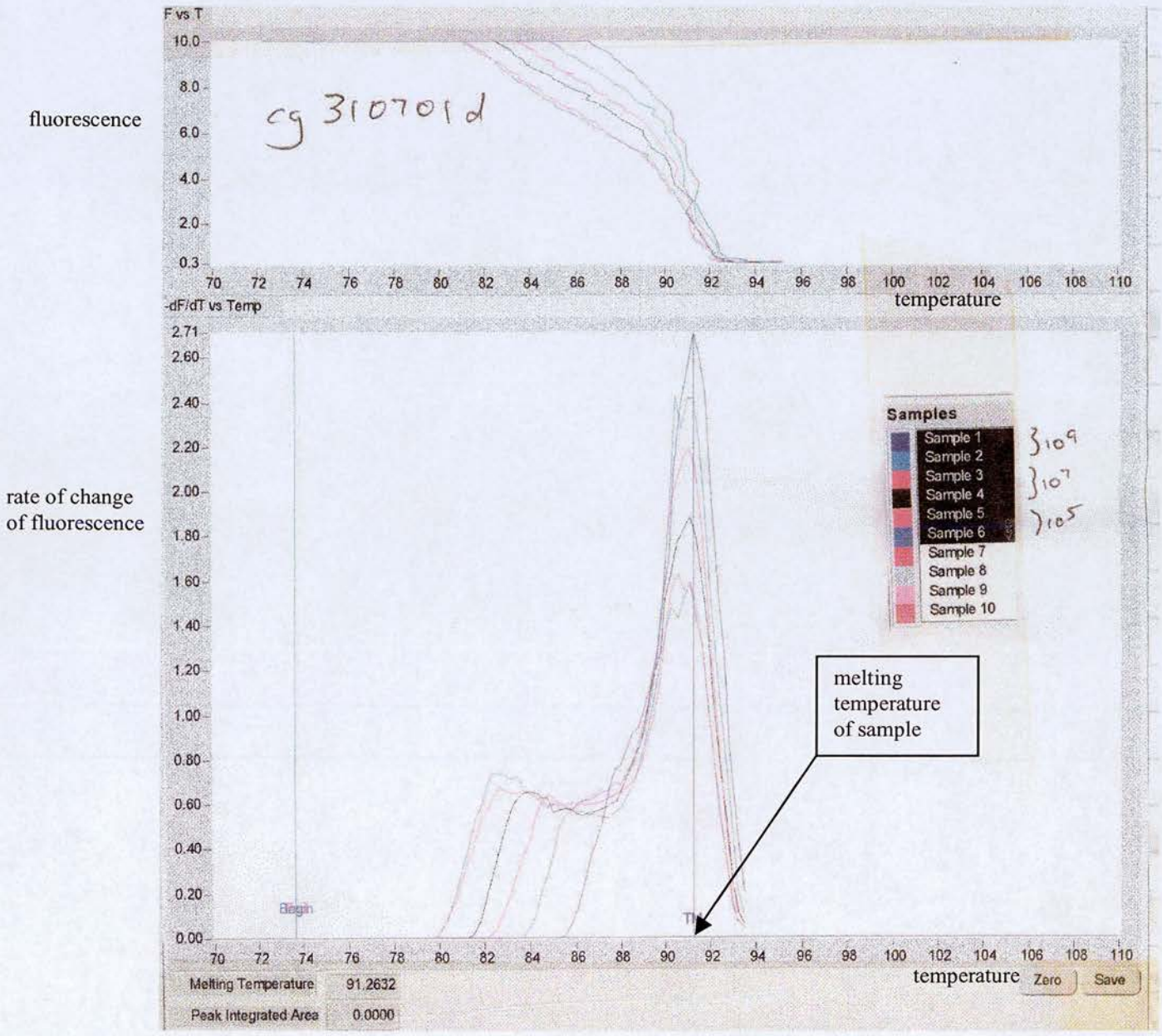

Melt curves produced following the Lightcycler® PCR using Z1 and Z2 primers with various dilutions of amplified *WWOX* DNA as the PCR template. Melt curves shown here are from the reactions of the 10^5, 10^7 and 10^9 standards. Note the single peak in the lower curve for all the samples indicating a single dsDNA product.

Figure 2.9: Melt curves for 10^9 and 10^3 standards as well as NTC for Z1/Z2 Lightcycler® PCR

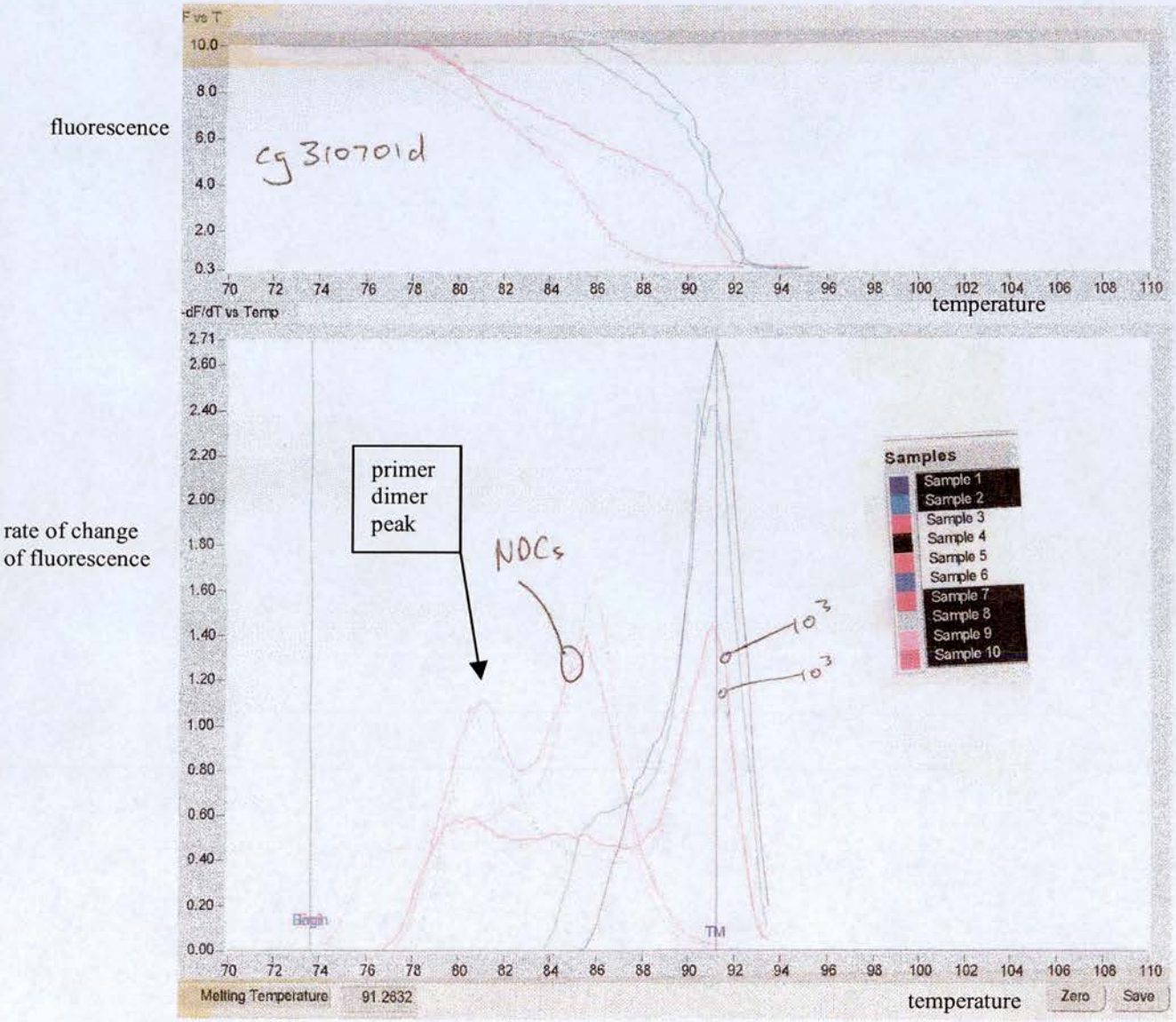

Melt curves produced following the Lightcycler® PCR using Z1 and Z2 primers with various dilutions of amplified *WWOX* DNA as the PCR template. Melt curves shown here are from the reactions of the 10^3 and 10^9 standards. Single peak to melt curve for 10^9 standards for Z1/Z2 Lightcycler® PCR. Primer dimer only in no template controls (NTC). One of the 10^3 standards contains only double-stranded product, the other contains mostly double-stranded product but also some primer dimer.

Figure 2.10: Standard curve for Z1/Z2 Lightcycler® PCR

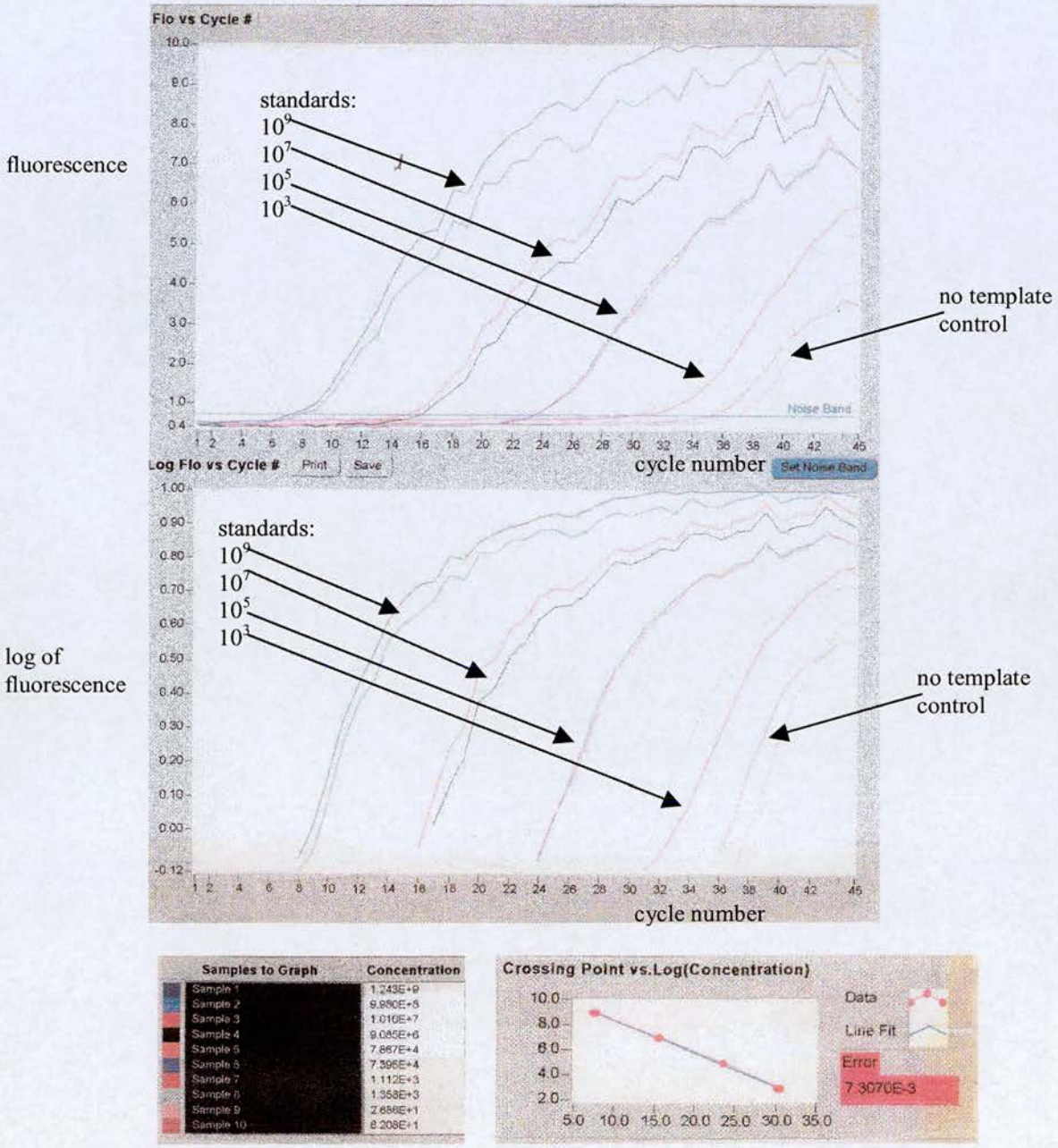

Quantitation facility of the Lightcycler® being used to set up a standard curve for the PCR using the Z1 and Z2 primers with various dilutions of amplified *WWOX* DNA as the PCR template. The noise band is set above the level of 'take-off' of fluorescence for all the standards (top section of the figure). The samples come up in pairs: 10^9 standards first, then 10^7 standards, then 10^5 standards, then 10^3 standards. The last 2 samples to start to fluoresce are the NTC (no template controls) and this is due to primer dimer formation (seen in the melt curve, figure 2.9). The Lightcycler® performs the quantitation analysis (bottom left) and generates a standard curve (bottom right).

Figure 2.11: PCR products from the Z1/Z2 Lightcycler® standard curve

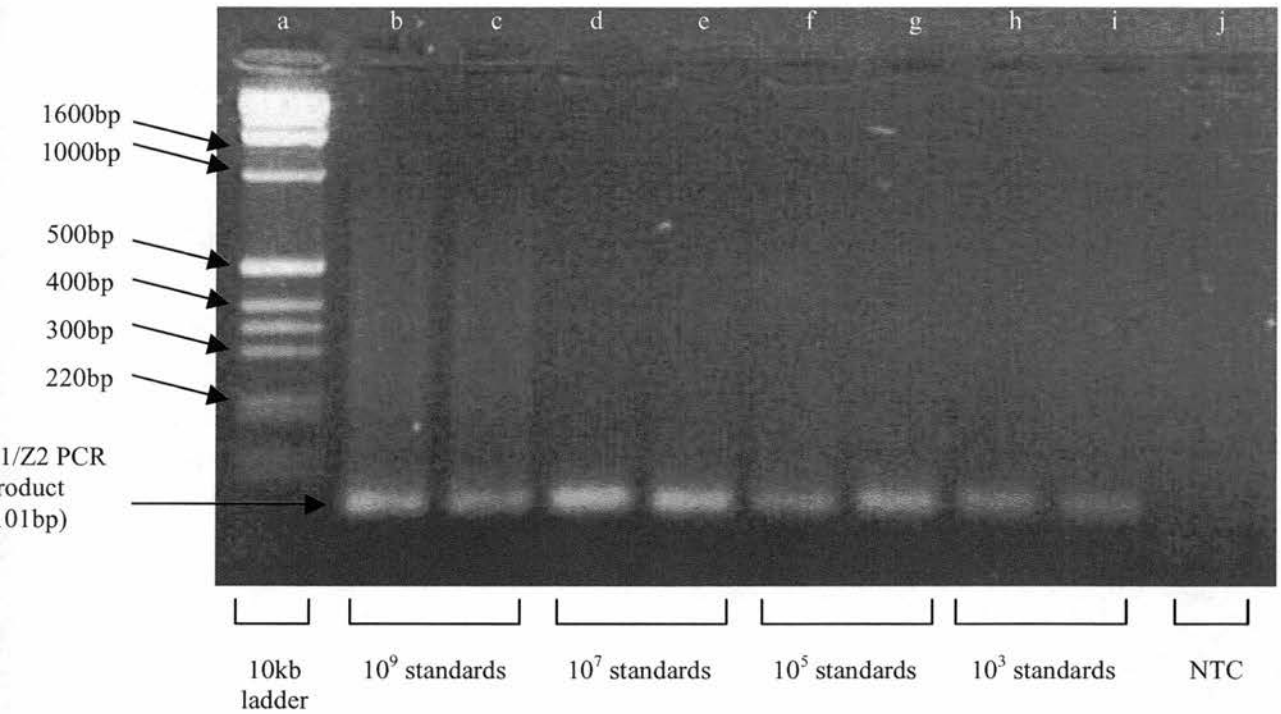

PCR products following the Lightcycler® PCR using Z1 and Z2 primers with various dilutions of amplified *WWOX* DNA as the PCR template. Lane a: 1kb ladder. Lanes b+c: 10^9 standards. Lanes d+e: 10^7 standards. Lanes f+g: 10^5 standards. Lanes h+i: 10^3 standards. Lane j: NTC

The reaction mix for all optimised Lightcycler® reactions is shown in table 2.9. The reactants were added to a 500µl eppendorf tube with 1µl of sample to give a total volume of 10µl. The tube was then briefly vortexed and centrifuged. 5µl from each eppendorf was aliquoted into a labelled glass capillary (Biogene). The glass capillaries were briefly centrifuged and then placed in the Lightcycler® and the reaction was commenced.

All optimised Lightcycler® reactions started with a 95°C denaturation step (temperature ramp 20°C/s), followed by 45 cycles of PCR (cycling conditions shown

in table 2.8) and finished with a melt curve formed by continuous fluorescence acquisition as the temperature of the PCR products was raised from 72°C to 95°C (temperature ramp 0.1°C/s).

Table 2.9: Lightcycler® PCR reaction mix

Component	Stock Concentration	Volume (µl) per reaction	Actual final concentration
Taq Mastermix	2x	5	1x
$MgCl_2$	25mM	0.8/0.6[a]	4mM[b]
SYBR Green	1:1000	0.25-0.50[c]	1:40000 to 1:20000
Forward primer	20µM	0.125-0.250[d]	0.25µM to 0.5µM
Reverse Primer	20µM	0.125-0.250[d]	0.25µM to 0.5µM
Distilled water		variable	
Total Volume		**9µl**	

[a]0.8µl of magnesium added to the standards, but only 0.6µl added to the samples, to account for magnesium coming through from the first strand reaction in the latter.

[b]The final concentration of $MgCl_2$ is 4mM, half provided from the mastermix and half in the form of added magnesium.

[c]0.25µl of SYBR Green was used in the Z1/Z2 PCRs. 0.5µl of SYBR Green was used in the β–*ACTIN* and LC1 PCRs.

[d]0.125µl of each primer was used for the LC1 PCRs. 0.25µl of each primer was used for the β–*ACTIN* and Z1/Z2 PCRs.

2.7.6 Quantitative RT-PCR using the Rotorgene®

The Rotorgene® 2000 is a real-time PCR machine which works on similar principals to the Lightcycler®. It detects the fluorescence of PCR reactants/products after every cycle of the reaction, allowing the use of fluorescent stains such as SYBR Green to determine the relative or absolute amounts of target in the starting sample (depending upon the standard curve used). It differed from the Lightcycler® in that it was a polypropylene tube-based system and allowed higher throughput, with a higher capacity rotor.

Although all the quantitative RT-PCR performed in this project was interested in relative gene expression (e.g. expression in transfectant cell lines versus controls or expression in ovarian tumours versus normal ovaries), the Lightcycler® protocol attempted absolute quantification because the standards were of known copy number. The only concern with this was that the template in the standards (amplified DNA) was not the same as that in the samples (first strand cDNA). This was acceptable for two reasons. Firstly, the standard curve was a reference for the samples to be compared to. As long as it was reproducible between runs, whether it was a true representation of the actual copy number in the samples or not did not matter for the analysis. Secondly, all the RT-PCRs contained an internal control that was present in every run being compared (e.g. the HCT116 parent line was present in all the runs screening HCT116 transfectants for *WWOX* expression). All quantitation was normalised to this internal control so the final expression was represented as a percentage of the level of expression in the parent line and not as an absolute copy number.

However, in the quantitative RT-PCR performed on the Rotorgene®, no attempt was made to perform absolute quantitation at all. The standards that were used were more comparable to the samples in that they were all first strand cDNA. A cell line that expressed the gene of interest at adequate copy number was chosen, RNA and first strand cDNA were generated and serial dilutions of this were used to manufacture a standard curve (with the dilutions given nominal values e.g. 1, 0.25, 0.0625, 0.015625). Again, every effort was made to ensure that the amplification of the unknown samples occurred at a PCR cycle number that was covered by the standard curve. At least 3 no template controls were included in each run. All standards were run in triplicate and all samples were run in quadruplicate. An internal control sample was included in all PCR runs to be compared. Quantification was performed by averaging the expression (compared to the standard) for the quadruplicate for both the gene of interest and β-*ACTIN*, dividing the former by the latter and presenting the expression as a percentage of the internal control.

Like the Lightcycler®, the Rotorgene® generated a melt curve profile of the PCR products once the PCR was completed. The polypropylene tube format of the Rotorgene® system allowed setting up to be performed on ice, meaning that Hot Start Taq DNA polymerase could be used. As a result of this, far fewer problems with primer dimer formation were encountered with this machine.

2.7.7 Rotorgene® reagents

2 x SYBR Green PCR Master Mix

2 x SYBR Green PCR Master Mix was obtained from Applied Biosystems. It contained SYBR Green I dye, AmpliTaq Gold® DNA polymerase, dNTPs with dUTP, a passive buffer and optimised buffer components.

2.7.8 Rotorgene® Primers

Primers were again chosen using Primer 3 (as for non-quantitative PCR, section 2.1). Again, maximum 3' and self-complementarity were kept to an absolute minimum. Primer sequences are shown in table 2.10. The concentration of primers used for each reaction is given in section 2.7.10.

2.7.9 Generation of standards for the Rotorgene®

A cell line that expressed adequate amounts of the gene of interest was chosen (e.g. HCT116, A2780, MCF7). Large amounts (e.g. 250µl) of first strand cDNA were prepared (as described in section 2.6) for the cell line chosen, effectiveness of the first strand reactions were checked, the products were pooled, vortexed, then split into 5µl aliquots to avoid compromising the target cDNA and stored at –70°C. Rotorgene® runs that were being compared were always performed with standards produced from the same first strand reaction.

Table 2.10: Rotorgene® PCR primers and conditions

PCR	Primers	Sequences (5'-3') For/Rev	$[Mg^{2+}]$ / Taq[a]	Cycling conditions
Quantitative real time RT-PCR	β*ACTIN* F+R	CTACGTCGCCCTGGACTTCGAGC GATGGAGCCGCCGATCCACACGG	SYBR	95°C 15s; 57°C 60s; 85°C 15s (aquire); 40 cycles
	8F2+Z2 (exon 8 to 9)	ACTATTGGGCGATGCTGGCT CGTTCTTGGATCAGCCTCTC	SYBR	95°C 30s; 67°C 30s; 72°C 45s; 85°C 15s (aquire); 45 cycles TD
	Δ6-8 F4+R2 (ex4 to 5/9 junct)	GGTTGTGGTCACTGGAGCTAA CAGCTCCCTGTTGCCATTC	SYBR	95°C 15s; 67°C 60s; 78°C 15s (aquire); 45 cycles TD

Table x: Primer sequences, magnesium concentrations, type of Taq DNA polymerase used and cycling conditions for quantitative real time RT-PCR performed on the Rotorgene®.

[a]SYBR = 2xSYBR Green PCR Mastermix (containing $MgCl_2$).

[b]TD = annealing temperature decreased by 1°C per PCR cycle for first 10 cycles

2.7.10 Rotorgene® conditions

20µl reactions were performed in quadruplicate using 0.2 to 1µl first strand cDNA per reaction, 2 x SYBR Green PCR Master Mix (Applied Biosystems). Reactions were performed in triplicate for the standards and in quadruplicate for the samples. Fluorescence was detected using the FAM channel (source 470nm; detector 510nm). Final concentration of β-*ACTIN* primers was 200nM each, of *WWOX* isoform 1 specific primers was 400nM each and of *WWOX* isoform 4 specific primers was 200nM (forward) and 50nM (reverse). The PCR conditions for the 3 reactions all included a 15 minute Taq activation step at 95°C before cycling and a 4 minute step at 72°C and a melt curve post-cycling. The cycling conditions and primer sequences are given in table 2.10. Specificity for isoform 4 was obtained by designing the reverse primer across the junction of exon 5 and exon 9. Previous studies have used a similar reverse primer and found no cross-amplification from isoform 1 (full-length) cDNA [52]. A mispriming control was included in all isoform 4-specific

PCRs to ensure that amplification detected could not be due to mispriming from isoform 1. This control was derived by transfecting an isoform 1-overexpressing plasmid into PEO1 cells, which express no endogenous isoform 1 or isoform 4. Expression levels were extrapolated from a standard curve (that was included in every run) and corrected for β-*ACTIN* expression. The standard curve was made up of at least 4 sequential dilutions of a cell line cDNA known to express the WWOX isoform being quantified. Selected products were run on a 2% agarose gel to confirm band size and identity of the sequences were validated.

2.8 Quantitation of *WWOX* transcript levels in transfected cell lines

Transfected cell lines were cultured in $25cm^3$ flasks until they were 70% confluent. Media was removed from the flasks and 600µl lysis buffer and 4.2µl of β–mercaptoethanol were added. This cell lysate could be stored at –70°C until other samples were ready so that the RNA could be prepared in batches. RNA was prepared as previously described using the Absolutely RNA® RT-PCR Kit (Stratagene) and cDNA was prepared using the AMV First Strand cDNA Kit (Roche). The levels of *ACTIN*-corrected *WWOX* expression were then quantified using the Lightcycler®. This was a screening exercise to identify transfectants that may be useful in phenotypic assays. All transfectants that were taken forward for extensive phenotypic work had their *WWOX* expression verified through multiple real-time PCR reactions.

2.9 Quantification of *WWOX* transcript levels in cell lines exposed to hyaluronidase and TNFα

Hyaluronidase-exposure of HCT116 and PEO1 cells was performed by Dr. A Paige and I gratefully acknowledge his help. Quantification of *WWOX* levels in mRNA from the exposed cells was performed by myself.

Hyaluronidase

Each vial of hyaluronidase was prepared as follows:

20ml of PBS was added to a universal. 6.67µl of 30% Bovine Serum Albumin (BSA, Sigma A-9576) was added to the universal and mixed, giving a 0.01% solution. The solution was passed through a 20µm filter into a sterile universal. 16.35ml of this solution was added to a vial of 327 U of hyaluronidase (Sigma) to give a 2000u/ml solution.

Two $175cm^3$ flasks of tissue culture cells were used for each cell line to be investigated. The media was decanted, the cells washed in PBS and trypsinised in the usual fashion. The cells were resuspended in 30ml of serum-containing media, dissociated with a pastette and counted on a haemocytometer. The exact cell numbers used depended on the cell line. For HCT116 cells, 1×10^6 cells were sub-cultured into each $25cm^3$ flask. The flasks were labelled as follows: 4hr 0units/ml, 4hr 100units/ml, 4hr 200units/ml, 4hr 400units/ml, 8hr 0units/ml, 8hr 100units/ml, 8hr 200units/ml, 8hr 400units/ml. The flasks were incubated at 37°C, 5% CO_2 for 48 hours. The media was removed from the flasks to be treated with hyaluronidase and 5ml of media containing the appropriate concentration of hyaluronidase was added to

the flask. The cells were then cultured at 37°C, 5% CO_2 for the desired duration of hyaluronidase exposure. Media was removed from the baseline (0hr) flasks and 600µl lysis buffer, 4.2µl of β–mercaptoethanol were added as previously described. The cell lysate was stored at –70°C until RNA extraction was performed (section 2.5.1). The same step was performed for the hyaluronidase-exposed cells, once their duration of exposure was complete. RNA was prepared using the Absolutely RNA® RT-PCR Kit (Stratagene) and cDNA was prepared using the AMV First Strand cDNA Kit (Roche). The levels of *ACTIN*-corrected *WWOX* expression were then quantified using the Lightcycler®.

2.10 Quantification of *WWOX* transcript levels in cell lines exposed to cytotoxic agents

Cytotoxic-exposure of HCT116 cells was performed by Dr. A Paige and I gratefully acknowledge his help. Quantification of *WWOX* levels in mRNA from the exposed cells was performed by myself.

Doxorubicin

Doxorubicin (adriamycin) was obtained from the Western General Hospital Pharmacy, Edinburgh. Stocks of 1mg/ml (1.7mM) doxorubicin were stored at 4°C. 8.2µl of doxorubicin was added to 70ml media to give a 200nM solution.

Oxaliplatin

Oxaliplatin was obtained from Sanofi Synthelabo. 3.525mg of oxaliplatin powder was dissolved in 1.11ml of sterile distilled water, giving a 8mM stock solution. The

solution was stored at –20°C. Oxaliplatin was added to give a final concentration of 8μM.

5-Fluorouracil (5-FU)

5-FU was obtained from Sigma. 2.578mg of 5-FU powder was dissolved in 1.0ml of sterile distilled water, giving a 20mM stock solution, which was stored at –20°C. 70μl of 5-FU was added to 70ml media (giving a 20μM solution).

These *WWOX* induction assays were performed in 6-well plates. The top 3 wells of the plate were used for the p53 normal HCT116 cells and the bottom 3 wells of the plate were used for the p53-null HCT116 cells. One 6-well plate was used for the 24-hour exposure to each drug and another 6-well plate was used for the 48-hour exposure. The first well in each row was the untreated well. The other two wells in each row were the exposed wells (performed in duplicate).

175cm^3 tissue culture flasks of HCT116 cells in log phase were trypsinised and recovered in the usual fashion. The cells were counted on a haemocytometer, plated in serum-containing media at 7.5 x 10^5 cells per well and incubated at 37°C, 5% CO_2 overnight. The following day, the media was removed from the plates and replaced with 5ml of media containing the appropriate drug (concentrations given above) or 5ml of RPMI only in the case of the untreated plates. The plates were then incubated at 37°C, 5% CO_2 for 24 hours or 48 hours respectively and cells collected in lysis buffer for RNA extraction.

2.11 Quantification of *WWOX* isoform levels in a human ovarian tumour panel

2.11.1 Retrieval of human ovarian tumour samples

83 consecutive tumour samples were taken for analysis from the tissue bank described in section 2.4.2. Twelve were excluded before analysis: 3 on histological grounds (primary peritoneal, cystadenoma, pseudomyxoma peritonei); 4 samples were not obtained at the time of primary surgery; extraction of RNA was unsatisfactory in 2 cases; 2 patients had concurrent malignancies at the time of diagnosis and 1 patient had no available clinical information.

13 non-malignant tissue samples were also removed from the tissue bank for analysis. These patients underwent bilateral oophorectomies for suspected malignancy but were found to have various benign histologies such as serous cystadenoma, fibrothecoma, ovarian fibroma, endometriosis and salpingitis. On each occasion, the apparently normal contralateral ovary was used for our analysis.

RNA and first strand cDNA were prepared as described in sections 2.5 and 2.6.

2.11.2 Quantitative RT-PCR

Quantitative RT-PCR to analyse levels of β–*ACTIN*, *WWOX* isoform 1 and *WWOX* isoform 4 expression in the ovarian tumours was carried out on the Rotorgene® as outlined above (section 2.7.6-2.7.10). As a result the *ACTIN*-corrected *WWOX* isoform 1 and isoform 4 expression levels were obtained for the ovarian tumour panel.

2.11.3 Clinical data retrieval

After the laboratory data had been obtained, clinical data for each HOV sample was retrieved using the local Cordite database. Missing clinical data was then retrieved from case notes. Syvia Rye (Cancer Research UK Clinical Trials Office, Western General Hospital, Edinburgh) correlated this information and her help is gratefully acknowledged.

Clinical data retrieved included date of birth, age at diagnosis, date of diagnosis, date of death/date last seen, overall survival, tumour grade, tumour stage, tumour histology, degree of debulking and censor values.

2.11.4 Statistical Methods

Analyses for clinicopathological associations were conducted using Fisher's Exact Test, Mann-Whitney Test and linear regression. These analyses were performed using SPSS Version 10 (SPSS Inc, USA) and the Analyse-it® plug-in (Analyse-it Software Ltd, UK) for Microsoft® Excel. Univariate analysis was performed comparing clinicopathological factors and *WWOX* isoform expression to survival. All parameters found to be significant at the univariate level were included in the multivariate Cox regression analysis (forward stepwise likelihood ratio method; entry probability 0.05; removal probability 0.1). I acknowledge the help of Robert Rush in performing the multivariate Cox regression analysis.

2.12 Quantification of *WWOX* isoform levels in human cancer cell lines

RNA was isolated from a panel of cell lines (methods in section 2.4.1), first strand cDNA manufactured and *β-ACTIN*, *WWOX* isoform 1 and *WWOX* isoform 4 expression quantified using real-time PCR on the Rotorgene® (section 2.7.6-2.7.10). Each gene quantification was performed in quadruplicate in each run. The average expression for each cell line was obtained by taking the average expression from three runs. The standard error of the mean was calculated from the average expression from the three runs. The absolute error was calculated by dividing the standard error of the mean by the mean expression. The actin-corrected *WWOX* expression was calculated for each isoform by dividing the average *WWOX* expression by the average *β-ACTIN* expression. The total final error was obtained by adding together the absolute error for both the *WWOX* and the *β-ACTIN* quantification. This was the error to which the final quantification of actin-corrected *WWOX* expression was subject.

2.13 DNA-FACS (fluorescense activated cell sorting) analysis

Cells for FACS analysis were transferred into a FACS tube, washed in cold PBS and resuspended in 1ml 70% ethanol. They were fixed on ice in 70% ethanol. They were washed once and resuspended in 1ml of PBS. 100µl of 5mg/ml RNaseA and 100µl of 100mg/ml propidium iodide were added and the tube was incubated for 15mins at room temperature in the dark. The cells were than analysed on the flow cytometer (FACSCalibur, Becton Dickinson).

2.14 Growth curves

2.14.1 Set-up

Log phase cultures of parent and transfected cell lines were harvested as previously described, passed 3 times through a 21G needle and seeded in duplicate in 6 well trays for each time point. The number of cells seeded per well was 5 x 10^4 for HCT116 and 1 x10^5 for PEO1.

2.14.2 Counting cells

The cells in growth curve experiments were counted using a coulter-counter (Beckmann Coulter). Twenty-four hours after the cells were plated down, a 'time zero' count was performed. The counts for this and all subsequent time points were performed in the same fashion.

Media was removed from all of the wells in the 6-well tray. The wells were washed with 2ml PBS per well. The PBS was removed in its entirety using a pastette. 0.8ml of trypsin was added to each well and the tray was incubated at 37°C in 5% CO_2 for 5 minutes. Following this 1.2ml of media was added to each well to give a total volume of 2ml. The contents of the well were aspirated 6 times using a 21G needle and 200µl of this cell suspension was added to 9.8ml of 0.9% saline in a coulter counting cuvette. The contents of the cuvette were mixed by inverting 8 times, the cuvette was placed in the coulter counter and 0.5ml of the solution was counted. The settings of the coulter counter (e.g. the size criteria) were dependent on the cell line used.

2.14.3 Analysis

The counts for each cuvette were printed out and were subject to multiplication by a factor of 200 (200µl out of 2ml added to cuvette and 0.5ml out of 10ml actually counted). They were then entered into Excel® (Microsoft®), corrected for the day zero counts and growth curves were produced.

2.15 *In vivo* tumourigenicity assays

Tumourigenicity assays were performed by injecting tumour cells subcutaneously into both flanks of nude mice (one injection per flank). Between 1×10^5 and 1×10^7 cells were used per injection (depending on the cell line). Where possible, ten injections were performed per cell line. Growth of the tumours was then followed until they reached such a size (2cm in maximum dimension) that the mice had to be sacrificed.

2.15.1 Harvesting cells for xenograft experiments

Tumour cells were grown sterilely in tissue-culture. When they were in log phase (30-80% confluent), they were harvested. Media was removed from the tissue-culture flasks, the cells were washed twice with PBS and the cells were trypsinised. The trypsinised cells were resuspended in 7ml standard serum-containing media and transferred to a universal. The cells were centrifuged at 580g for 5minutes. The media was poured off and the cells were resuspended by flicking the universal. 10ml of serum-free media was then added to each universal. (If there was more than one universal for each cell line then they could be pooled during these steps of washing

the cells in serum-free media). This step was repeated another twice so that the cells had been washed three times in serum-free media. Another 10ml of serum-free media was added to each universal, the cells were passed three times through a 21G needle and a 1 in 10 or 1 in 20 dilution of this was made for the purposes of counting the cells. The cells were counted on a haemocytometer and the volume of cell suspension required to give the total number of cells for the required injections was calculated. This volume of cells was placed into a universal and spun at 580g for 5 minutes. The media was discarded and the cells were transferred into a 1.5 ml microfuge tube that had a level marked on it for the total volume required (100µl per injection). If the cells were being injected in purely serum-free medium then the volume was made up to this level with serum-free medium. If the cells were being injected into nude mice with matrigel then they were transferred across from the universal using the required volume of matrigel (half the total volume required) and the remainder of the volume (up to the mark on the microfuge tube) was made up with serum-free media. The cells were immediately transferred on ice to the Cancer Research UK Biomedical Research Facility, Western General Hospital, Edinburgh, where the container with the eppendorfs was put into an isolator container port and sprayed using Alcide ABQ disinfectant and left on cool packs for 30 minutes. The container was then taken into the isolator and the cells were injected subcutaneously, using a sterile 1ml luerlock syringe with a sterile 25G needle, 0.1ml per flank.

2.15.2 Maintenance of animals

The animals were housed in negative pressure isolators in groups of 5 unless there were fewer animals per study group. The procuration of animals, the husbandry and

the experiments conform to the United Kingdom Co-ordinating Committee on Cancer Research (UKCCCR) Guidelines for the Welfare of Animals in Experimental Neoplasia (Second Edition) [192].

2.15.3 Measurement of tumours

The frequency of measurement of tumours depended upon the cell line used. Measurements were taken with callipers between once and twice a week, in two dimensions. When tumours reached 2cm in maximum diameter, the mouse was sacrificed and the experiment terminated.

2.16 Soft agar proliferation assays

These assays were performed in 6-well trays. 2ml of 1% seaplaque agarose (BioWhittaker Medical Applications) was poured into each well and left at 4°C overnight (bottom layer). 5000, 10000 and 20000 PEO1 parent, vector-only and sense (H) transfected cells were plated on top of the bottom layer in 3ml of 0.4% seaplaque agarose containing selective antibiotics and serum (top layer). 1ml of antibiotic and serum-containing media was added over the top layer of agarose the following day. Experiments were performed in duplicate. The cells were cultured for 3 weeks, then counted down a microscope.

2.17 Clonogenicity assays

2.17.1 Preparation of cells

PEO1 parent, vector-only and sense transfected cells were grown in $75cm^3$ or $175cm^3$ flasks. They were trypsinised and recovered in the usual fashion. A 3ml aliquot of each cell suspension was transferred into a separate universal and syringed ten times through a sterile 21G needle. 1ml of this cell suspension was transferred to a separate universal and 19ml of medium was added to this. A cell count was performed on the haemocytometer and a calculation of multiplicity was performed (formula in figure 2.12). A multiplicity of less than 1.05 was required in order for that cell preparation to be used.

Figure 2.12: Formula for the calculation of multiplicity

$$\text{Multiplicity} = \frac{\text{no. of single cells} + 2 \times (\text{no. of doublets}) + 3 \times (\text{no.of triplets}) \text{ etc.}}{\text{no. of single cells} + (\text{no. of doublets}) + (\text{no.of triplets}) \text{ etc.}}$$

2.17.2 Seeding of cells

Cells were plated into Petri dishes with gridded bases. A cell suspension was made up so that the required number of cells for each dish was contained in 4ml of media. The first clonogenicity experiment used 500 and 1000 cells per dish but subsequent experiments used 200 cells per dish. The cell suspension was then added to the required number of dishes using an eppendorf multi-dispenser. If drug was to be

added to the dishes then this was made up in media at twice the final concentration and 4ml of this solution was added to each plate. The cells were then incubated at 37°C in 5% CO_2 for 21 days before being counted. The media was not changed.

2.17.3 Counting of cells

The media was poured off the Petri dishes and the cells were washed twice with PBS. The cells were fixed for 2 minutes in 2ml of 2:1 acetone/methanol. The dishes were washed in tap water and the fixed cells were stained with haematoxylin. The stain was washed off with water and the dishes were allowed to air dry. The number of colonies on each plate was then counted.

2.18 Aggregation Assays

Log phase PEO1 parent, vector control and sense-transfected lines were trypsinised and recovered in serum-containing media. 1 x 10^6 cells were resuspended in 1ml of media and passed through a 21G needle to create a single-cell suspension. Cell suspensions were incubated at 37°C, 5% CO_2. At 0, 15, 30 and 60 minutes aliquots were removed using a wide bore pipette and the number of single cells was counted with a haemocytometer.

2.19 Transwell migration assays

2.19.1 Reagents

Fibronectin, Laminin and Collagen IV

Fibronectin, Laminin and Collagen IV were obtained from Sigma. A 1mg/ml stock solution of each was made up. This was split into 50µl aliquots and stored at –20°C. These extracellular matrix components were diluted to a concentration of 10µg/ml in PBS for the assays.

Bovine Serum Albumin (BSA)

BSA was obtained from Sigma and was made up freshly for each experiment. BSA was 0.22µ-filtered prior to use.

Transwells

Transwell cell culture inserts 6.5mm diameter, 8µm pore size in a polycarbonate membrane were obtained from Costar.

DMSO (dimethyl sulphoxide)

Spectroscopic grade dimethyl sulphoxide was obtained from BDH Laboratory Supplies.

MTT (3-(4,5-dimethylthiazol-2-yl)-2,5-diphenyl tetrazolium bromide)

MTT (3-(4,5-dimethylthiazol-2-yl)-2,5-diphenyl tetrazolium bromide) was obtained from Sigma. It was made up to a concentration of 2mg/ml for the purposes of the MTT assay used in this setting.

2.19.2 Preparation of transwells

400µl of a 10µg/ml solution of the matrix component was added per well to a 24-well tissue culture tray. The transwell cell culture insert was placed into the tissue

culture well so that the underside of the well was in contact with the solution. This allowed the matrix component to become immobilised on the lower surface of the polycarbonate membrane. The transwells were incubated at 37°C for 1 hour. The transwells were then transferred to a 24 well plate containing 400µl 0.1%BSA in PBS for 1 hour at room temperature (blocking step). The under surface of the well insert was washed twice by replacing the BSA with PBS. 400µl of serum-free media was then placed in the lower compartment of the transwell.

2.19.3 Preparation of cells

Cells were cultured in 175cm^3 flasks, trypsinised and recovered in serum-containing media. The cells were washed 3 times in serum-free media, syringed four times using a 21G needle and then counted on a haemocytometer. A cell suspension of the desired concentration was made up so that the number of cells to be aliquoted into the upper compartment of each transwell was contained in 100µl. In general the cells were made up to a concentration of 5 x 10^5 cells per ml and 5 x 10^4 cells were aliquoted per well. The cells were incubated for 84 hours at 37°C, 5% CO_2.

2.19.4 Quantification of migrating and non-migrating cells

The upper chamber of the transwell was washed twice very carefully with PBS and then a further 100µl of PBS was added to this chamber. 10µl and 40µl of 2mg/ml of MTT were added to the top and bottom compartments of the transwell respectively. The plate was wrapped in foil and incubated for 3 hours at 37°C, 5% CO_2. The unreacted MTT was aspirated off from the lower well and pipetted off from the upper well. The crystals were removed from the under surface of the transwell insert

using a cotton bud, the end of which was cut off and placed in an eppendorf containing 1ml of spectroscopic grade DMSO. The eppendorf was vortexed to release and solubilise the crystals. The transwell was placed in a culture well containing 1ml DMSO. The sample was mixed by pipetting the solution up and down several times.

Three x 200µl aliquots of solution per sample were transferred into a 96 well plate and their absorption was read at 570nm using a plate-reader (Biohit). The first column of the 96 well tray contained DMSO only and was used to zero the rest of the readings. Migration was expressed as the ratio of the under surface OD reading relative to the upper surface OD reading.

The experiment was repeated five times, the migration figures were averaged for the cell lines tested and the standard error of the mean was calculated.

2.20 Invasion assays

Invasion assays were conducted with media containing 10% acid-inactivated serum (section 2.3.1). Biocoat® Matrigel® invasion chambers were obtained from BD Biosciences and stored at 4°C. They were allowed to equilibrate with room temperature prior to use. The inserts were rehydrated for 2 hours at room temperature by the addition of 0.5ml of media into the well (surrounding the insert) and 0.25ml of media inside the insert. The media was carefully removed and log phase cells that had been washed twice to remove untreated serum were resuspended in media containing 10% acid-inactivated serum. The cells were passed 4 times through a 21 G needle, counted on the haemocytometer and the concentration of the

cell suspension adjusted to give a cell density of 10^5 cells per ml. 0.75ml of serum-containing media was added to each well in a 24 well tray. The inserts were carefully loaded into the wells and 0.5ml of cell suspension was added inside each insert. The cells were incubated at 37°C, 5% CO_2 for 72 hours then analysed by MTT assay as described for the migration assay (section 2.19.4)

2.21 Attachment Assays

Attachment to matrigel was assessed using matrigel-coated 96 well trays obtained from Biocoat®. Attachment to laminin and fibronectin was assessed using bacteriological-grade 96 well trays obtained from Nunclon®. These wells were prepared by the addition of 100µl of 10µg/ml fibronectin or laminin to each test well followed by 60 minutes incubation at room temperature, careful washing with PBS, blocking with 200µl of 0.1% BSA, a further 1 hour incubation at room temperature and final washing with PBS.

In optimisation assays, 1 x 10^4 to 5 x 10^4 PEO1 cells (washed 3 times in serum-free media) were added to each well. Following this each assay used 5 x10^4 PEO1 cells per well. The cells were incubated at 37°C, 5%CO_2 for the specified duration of the particular experiment, washed carefully then quantified by MTT assay as described for the migration assay (section 2.19.4).

2.22 Western Blotting

Western blotting of the *WWOX*-transfected PEO1 cells was performed by Karen Taylor and I gratefully acknowledge her help. The polyclonal antibody used was a kind gift from Marcelo Aldaz (MD Anderson Cancer Centre, Texas).

Cells grown in monolayer culture were harvested and lysed with lysis buffer supplemented with 1 x Complete protease inhibitors (Roche) and 0.5 mM phenylmethylsulfonyl fluoride. Following incubation on ice for 15 min, the lysate was centrifuged at 16000g for 5 min, and the postnuclear supernatant was harvested and sampled for quantitation of protein concentration, using the BioRad protein reagent. Forty mg of the lysate were then mixed with SDS-PAGE sample buffer, boiled for 5 min, and subjected to electrophoresis in 10% SDS gels under reducing conditions. The separated proteins were electrophoretically transferred to Trans-Blot transfer membrane (BioRad). Blots were incubated with primary anti-WWOX (a polyclonal antibody, raised in rabbit using as antigen a WW-GST fusion protein) or anti-GAPDH (Abcam) antibodies overnight at 4°C. Immunocomplexes were visualized with the BM chemiluminescence detection kit (Roche) using horseradish peroxidase-conjugated secondary antibodies. Quantitative values for WWOX and GAPDH proteins were obtained by densitometric analysis using a gel scanner (UVP Life Sciences) and analyzed by Labworks gel analysis software (UVP Life Sciences). This provided integrated absorbance values.

3. RESULTS: *WWOX* mRNA ISOFORM EXPRESSION PROFILE IN A PANEL OF OVARIAN TUMOURS AND NORMAL OVARIES

3.1 Rationale for investigating the WWOX mRNA isoform expression profile in an ovarian tumour panel

There is controversy surrounding whether the *WWOX* gene can be regarded as a tumour suppressor. As discussed previously (sections 1.6 and 1.7), the fact that the gene is homozygously deleted in a number of tumour cell lines [53], the high incidence of loss of heterozygosity at the *WWOX* locus in a variety of human cancers [165,166], the presence of alternate transcripts predominantly in malignant tissue [52,53,165,166,169,171] and the reduction in tumourigenicity when the gene is transfected into breast cancer cells [52] all support a role as a tumour suppressor. However, the fact that no truncating point mutations have been identified and the lack of a familial cancer syndrome caused by *WWOX* gene mutation have been cited as reasons why it cannot be regarded as a classical tumour suppressor.

WWOX transcripts are found in a variety of malignant tumours and cell lines [52,53,165,166,169,171] but examples of these transcripts in non-malignant tissues are a rare, recent, somewhat understated finding [169,171]. This fact, combined with the finding that most of the alternate transcripts omit the region encoding the alcohol dehydrogenase domain of the protein, have led many investigators to postulate that these transcripts may act in a dominant negative fashion, disrupting the normal (presumed tumour suppressor) role of *WWOX* in the cell. Although a variety of the above studies have investigated *WWOX* isoform expression in specific cancer types, none have looked at ovarian cancer or have investigated the *WWOX* mRNA isoform expression profile in relation to clinical details.

This chapter investigates whether *WWOX* gene expression is down-regulated in a panel of ovarian cancers compared to a panel of normal ovaries. It also examines the

possible role of the *WWOX* alternative transcripts by establishing the mRNA expression profile in the same ovarian tumour and normal ovary panels and by using this information to identify whether there is any association with clinicopathological factors or patient survival.

3.2 Characteristics of the human ovarian tumour panel

Eighty-three consecutive samples in two blocks (one collected from March 1991 to September 1993, the other collected from January 1999 to December 2001) were obtained from the tissue bank held at the University of Edinburgh Cancer Research Centre. Twelve were excluded during the comparison with clinicopathological factors: 3 on histological grounds (primary peritoneal, cystadenoma, pseudomyxoma peritonei); 4 samples were not obtained at the time of primary surgery; extraction of RNA was unsatisfactory in 2 cases; 2 patients had concurrent malignancies at the time of diagnosis and 1 patient had no available clinical information. Tumour characteristics of the remaining 71 tumours are described in table 3.1.

Table 3.1: Characteristics of the human ovarian tumour panel

Tumour Characteristic		Number of Patients
Grade	1	3
	2	16
	3	49
	unknown	3
Stage	I	11
	II	6
	III	41
	IV	10
	unknown	3
Histology	serous papillary	36
	endometrioid	13
	clear cell	10
	mucinous	6
	mixed serous papillary/endometrioid	4
	unknown	2

3.3 Investigation of *WWOX* mRNA isoform expression in an ovarian tumour panel by non-quantitative RT-PCR

3.3.1 PCR across the entire WWOX coding region

Previous attempts at amplifying the whole *WWOX* coding region with conventional Taq DNA polymerase had met with limited success (perhaps due to the size of the PCR product at 1.5kb, perhaps due to sequence characteristics) and required the use of nested PCR in order to get significant amplification [53]. It was considered desirable to avoid this if possible as nested PCR is renowned for the production of spurious products and its use in the early work on the *FHIT* gene was a major source of controversy. Therefore a single round PCR was optimised using the hot-start Taq DNA polymerase Taq Gold®. This worked well on cDNA from A2780 cell lines that had been transfected with *WWOX* expressing constructs. This cDNA was used for the optimisation process (figure 3.1) with *WWOX* isoforms 1 and 4 clearly amplified. Unfortunately, results from PCRs performed using cDNA from human ovarian tumours were less consistent, with many samples providing extremely faint or no amplification (figure 3.2). This may have been related to the quality of the RNA/cDNA used in the reaction as the process of RNA extraction from human ovarian tumours is less efficient than the extraction from cells grown in culture.

Smaller PCR targets were therefore designed in order to characterise the *WWOX* mRNA expression profile in the ovarian tumour panel. Three PCRs were used: a PCR specifically targeting *WWOX* isoform 1 using primers in exon 8 (8F2) and exon 9 (Z2); a PCR specifically targeting *WWOX* isoform 4 by amplifying from exon 4

(Δ6-8 F) to the exon 5/9 boundary (Δ6-8 R) and a PCR spanning the region of deletion using primers in exon 4 (ex 4/4) and exon 9 (Z2).

Figure 3.1: Single round PCR across *WWOX* coding region using cell line cDNA

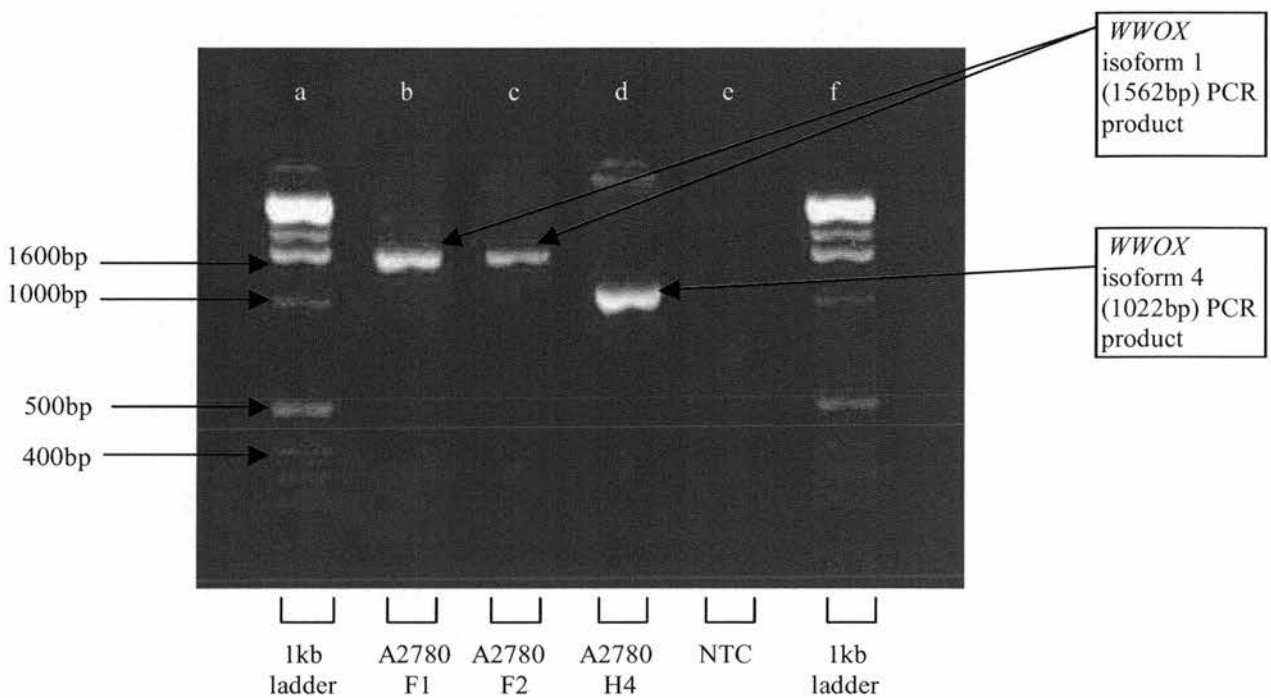

Single round PCR across the *WWOX* coding region using A2780 ovarian cancer cell line cDNA as the template. Lane contents as follows: a 1kb DNA ladder; b A2780 F1 cDNA as template (expresses *WWOX* isoform 1); c A2780 F2 cDNA as template (expresses *WWOX* isoform 1); d A2780 H4 cDNA as template (expresses *WWOX* isoform 4); e no template control (NTC); f 1kb DNA ladder

Figure 3.2: Single round PCR across *WWOX* coding region using tumour cDNA

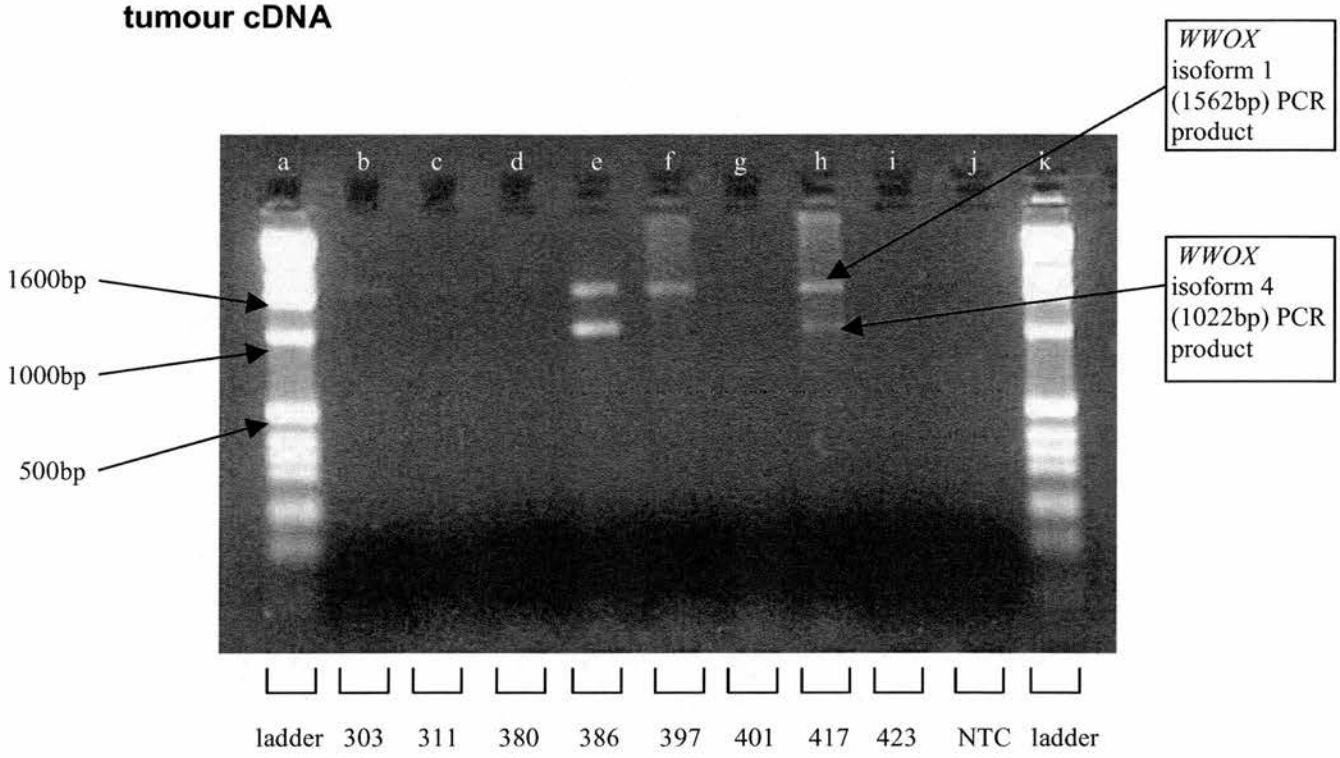

PCR products following single round PCR across the *WWOX* coding region using human ovarian tumour (HOV) cDNA as template. Lane contents as follows: a 1kb DNA ladder; b HOV303; c HOV311; d HOV380; eHOV386; f HOV 397; g HOV 401; h HOV 417; i HOV 423; j no template control (NTC); k 1kb DNA ladder

3.3.2 PCR from exon 8 to exon 9 to specifically detect full-length *WWOX* (isoform 1)

Non-quantitative PCR using Taq Gold® amplifying between exons 8 and 9 (primers 8F2 and Z2) revealed a product for all but two of the human ovarian tumour (HOV) samples (HOV 12 and HOV 104; figure 3.3).

For these two tumours the 8F2/Z2 PCR was repeated another twice without any amplification. The γ-*ACTIN* PCR was repeated, showing that the first strand reaction

had been successful for both of these HOVs (figure 3.4). In case there had been a mutation or small deletion at one of the primer binding sites, PCRs using different primers located in exons 7 and 8 (7F2 and 8R2; figure 3.4) and primers located in exons 4 and 9 (exon 4/4 and Z2; figure 3.4) were performed but no amplification resulted in either the case of HOV 12 or HOV 104. Amplification across the whole open reading frame for theses 2 tumours (using primers exon1/1 and coding R) gave a truncated product for HOV 12 (size around 950bp instead of 1550bp) and no product for HOV 104 (figure 3.4). Exon-specific PCR of genomic DNA revealed that all the exons were present in both cases (figure 3.5).

Figure 3.3: All but two human ovarian tumours expressed *WWOX* isoform 1

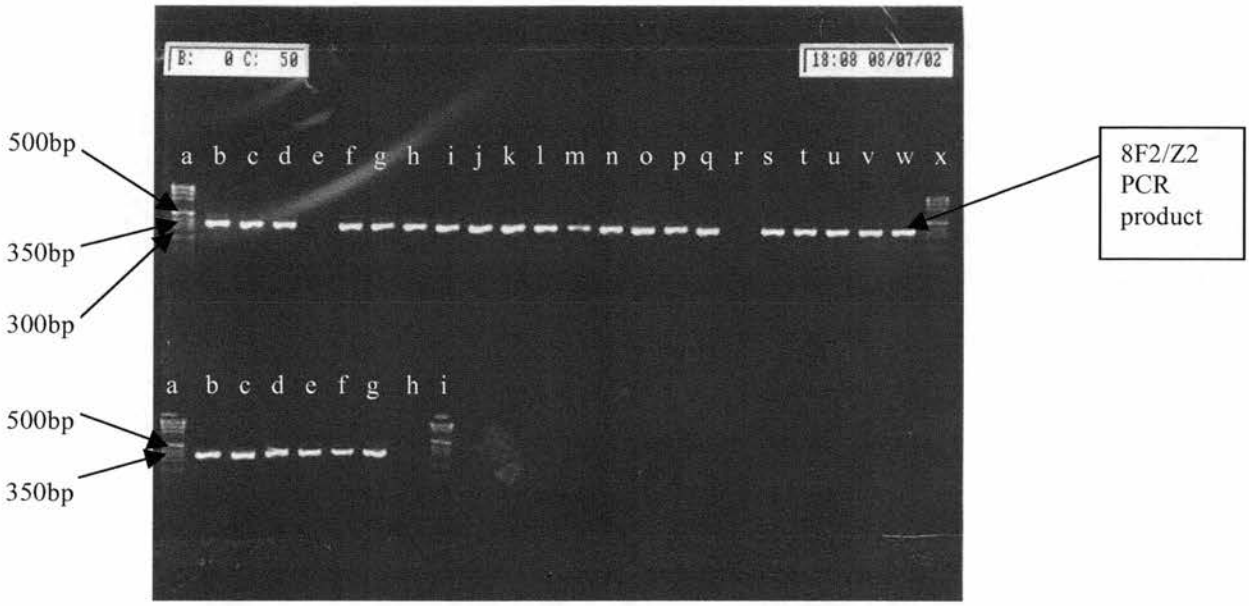

PCR products from the *WWOX* specific 8F2/Z2 PCR (primers in exon 8 and exon 9) performed on first strand cDNA from human ovarian tumours (HOVs). Upper panel lane contents: a 1kb DNA ladder; b HOV5; c HOV8; d HOV9; e HOV12; f HOV14; g HOV21; h HOV53; i HOV58; j HOV60; k HOV69; l HOV76; m HOV77; n HOV80; o HOV88; p HOV92; q HOV98; r HOV104; s HOV170; t HOV179; u HOV180; v HOV183; w HOV188; 1 kb DNA ladder. Lower panel lane contents: a 1kb DNA ladder; b HOV190; c HOV192; d HOV273; e HOV296; f HOV507; g HCT116cl4 cDNA (positive control); h no template control (NTC); i 1kb DNA ladder.

Figure 3.4: PCRs investigating the apparent lack of *WWOX* isoform 1 expression in HOV 12 and HOV 104

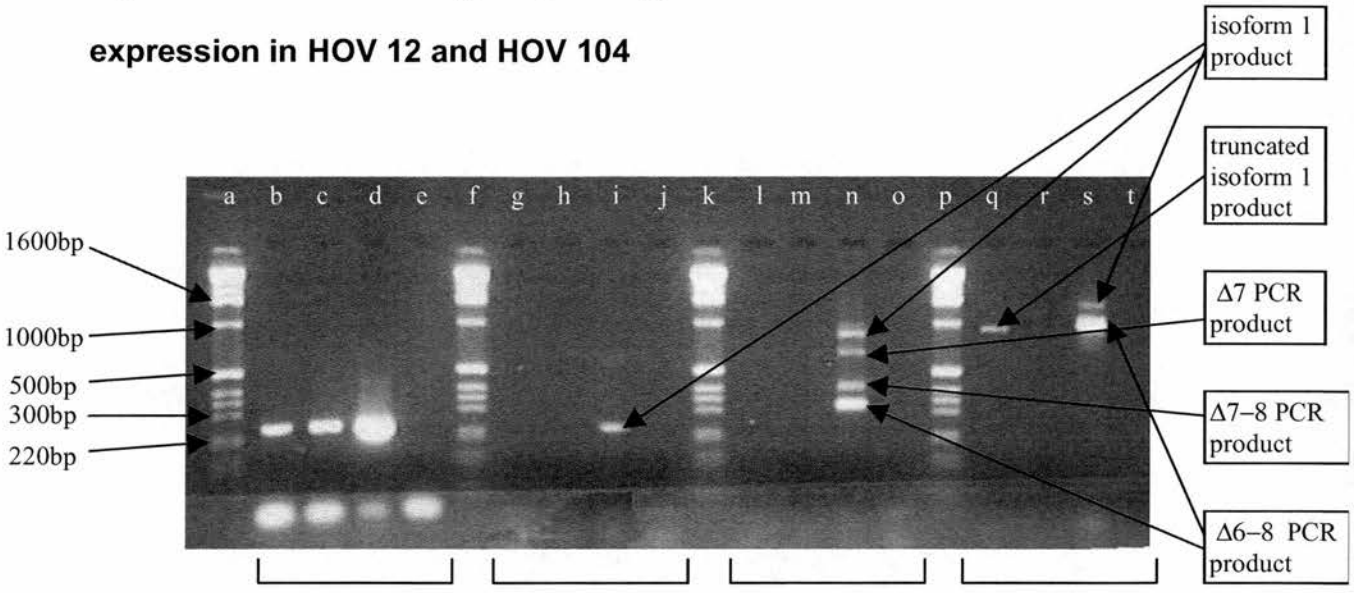

PCRs investigating the apparent lack of *WWOX* isoform 1 expression in HOV 12 and HOV 104. Lanes a, f, k and p contain the 1kb ladder. Lanes b to e contain the products of the γ-*ACTIN* PCR; templates are: b HOV12 cDNA; c HOV 104 cDNA; d HCT116 positive control cDNA; e no template control (NTC). Lanes g to j contain the products of the 7F2/8R2 PCR (primers from exon 7 to exon 8 of *WWOX*); templates are: g HOV12 cDNA; h HOV 104 cDNA; i HCT116 positive control cDNA; j NTC. Lanes l to o contain the products of the exon 4/4 and Z2 PCR (primers from exon 4 to exon 9 of *WWOX*); templates are: l HOV12 cDNA; m HOV 104 cDNA; n HCT116 positive control cDNA; o NTC. Lanes q to t contain the products of the exon 1/1 and coding R PCR; templates are: q HOV12 cDNA; r HOV 104 cDNA; s HCT116 positive control cDNA (primers amplifying across the *WWOX* coding region); t NTC. In lane s, the largest band is amplified from *WWOX* isoform 1, the shorter bright band is from *WWOX* isoform 4.

Figure 3.5: Exon-specific PCR of HOV 12 and HOV 104 genomic DNA

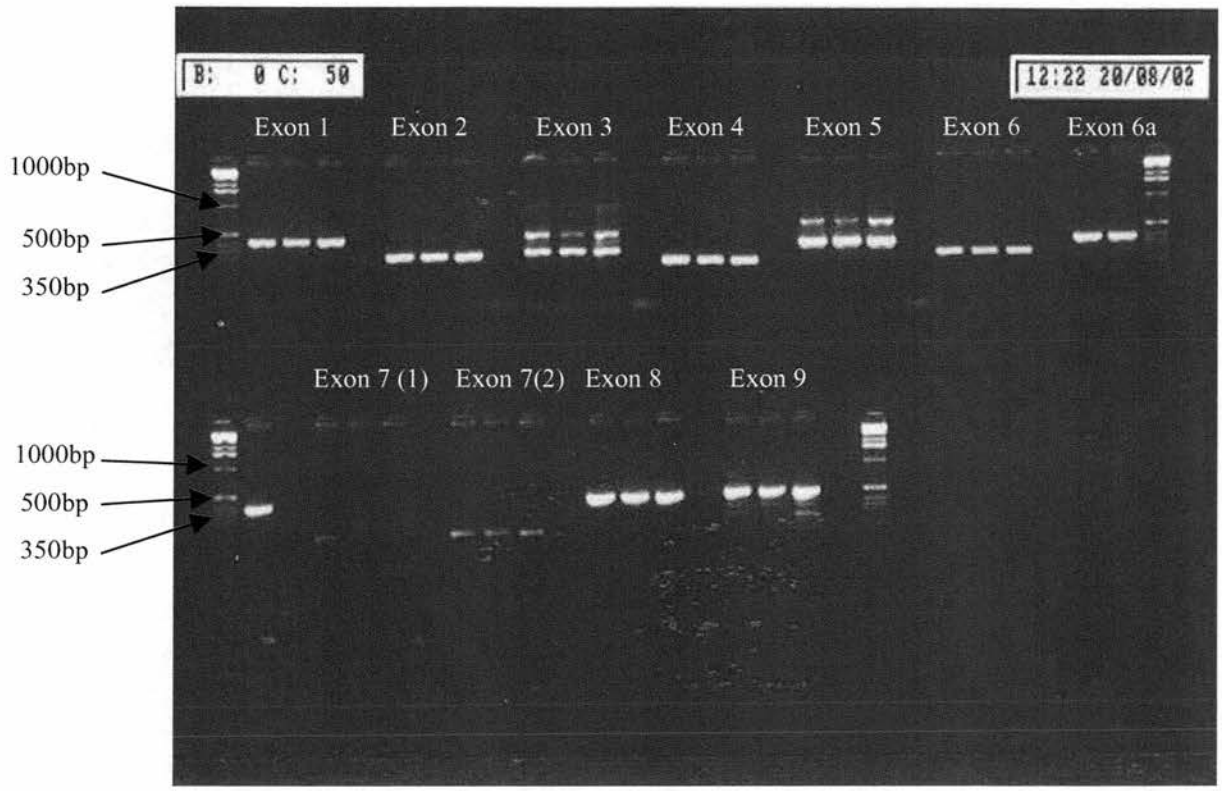

Exon-specific PCR of HOV 12 and HOV 104 genomic DNA. The first and last lane of each panel contain 1kb ladder. Otherwise the exon-specific PCRs are performed in quadruplicates. The template for the first sample in the quadruplicate is HOV12 DNA, for the second sample is HOV 104 DNA and for the third sample is HCT116 DNA (positive control). The final sample in each quadruplicate is the no template control (NTC). The exon being tested is annotated above each quadruplicate on the gel. The first quadruplicate is amplified exon 1, the second is amplified exon 2, the third is amplified exon 3, the fourth is amplified exon 4, the fifth is amplified exon 5, the sixth is amplified exon 6, the seventh is amplified exon 6a, the eighth is amplified exon 7 (primer set 1), the ninth is amplified exon 7 (primer set 2), the tenth is amplified exon 8 and the eleventh is amplified exon 9.

In a final effort to try and amplify a *WWOX* transcript for HOV 104, a nested RT-PCR was performed (using primers exon 1/1 and coding R for the first round and

primers E and Z2 for the second round). Once again no PCR product was obtained for this tumour sample.

In summary, of 71 ovarian tumour samples, 69 expressed full-length *WWOX* (by virtue of the PCR amplification of a target in exons 8 and 9 of the gene). One tumour expressed no *WWOX* transcript at all and another tumour expressed a truncated transcript. Neither of these tumours had large exonic deletions. The tumour (HOV104) expressing no transcript may have undergone epigenetic silencing of the *WWOX* gene, secondary to promoter methylation or histone deacetylation, or may have aquired a large insertion into one of its exons, preventing PCR amplification. The tumour (HOV12) expressing a truncated *WWOX* transcript may have a mutation at a normal splice site, resulting in altered mRNA processing.

3.3.3 PCR to specifically detect isoform 4 (from exon 4 to the exon 5/9 boundary)

Initially, *WWOX* isoform 4-specific amplification was performed using a primer pair known as Δ6-8 F and R. Δ6-8 F was located in *WWOX* exon 4 and Δ6-8 R was located at the junction of exons 5 and 9 in the *WWOX* Δ6-8 (isoform 4) transcript. It had 9 nucleotides in exon 5 and 11 nucleotides in exon 9. As the 9 nucleotides in exon 5 only shared homology with 2 of the 9 most 3' nucleotides of exon 8, it was felt that the potential for mispriming from the full-length transcript was minimal. At this time, no source of isoform 4 without the presence of isoform 1 was available to allow optimal controls for mispriming to be performed but these were generated later in the project. Investigation of isoform 4 expression was initially carried out on the second batch of tumours from the tumour bank (January 1999 to December 2001).

Of these 50 ovarian cancer patients analysable for isoform 4 expression, 21 (42%) expressed isoform 4 on the basis of this PCR. In these patients there was a correlation between isoform 4 expression and stage 3 or 4 disease (p=0.001, 2-tailed Fisher's Exact test; table 3.2) and a trend towards an association with high-grade ovarian cancer (p=0.09, 2-tailed Fisher's Exact test; table 3.3). Stage information was available for 47 patients and grade information was available for 49 patients. Kaplan-Meier analysis also revealed that there was a significant association between expression of the isoform 4 transcript and poor survival (p=0.047; figure 3.6).

Table 3.2: *WWOX* isoform 4 expression and tumour stage

	Tumour stage		TOTAL
	I/II	III/IV	
Isoform 4 expression	0	19	19
No isoform 4 expression	11	17	28
TOTAL	11	36	47

P=0.001, Fisher's Exact test

Table 3.3: *WWOX* isoform 4 expression and tumour grade

	Tumour grade		TOTAL
	1 or 2	3	
Isoform 4 expression	2	19	21
No isoform 4 expression	9	19	28
TOTAL	11	38	49

P=0.087, Fisher's Exact test

Figure 3.6: Kaplan-Meier analysis according to isoform 4 (Δ6-8) transcript expression

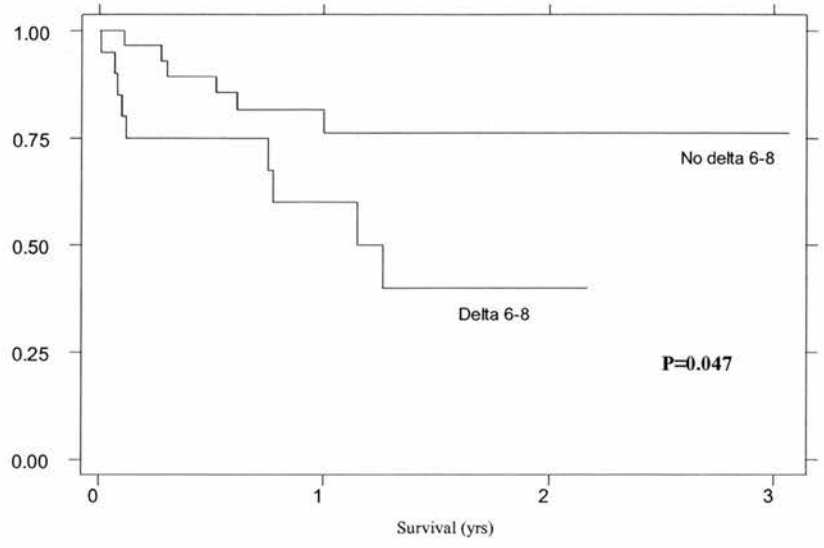

Kaplan-Meier analysis of 50 ovarian cancer patients demonstrating proportion of surviving patients according to *WWOX* delta 6-8 (isoform 4) expression as judged by non-quantitative RT-PCR. Significantly worse survival for patients that expressed *WWOX* delta 6-8 (p=0.047).

As there had been only 15 deaths in this group of tumours (which had been collected between January 1999 and December 2001), it was decided to also analyse the older group of samples from the tumour bank (collected between March 1991 and September 1993) for isoform 4 expression. These patients had longer follow-up and may be more informative with regard to any association between this transcript and survival.

Although the initial data regarding a possible association between isoform 4 expression and adverse clinicopathological features was interesting and exciting, the level of the isoform 4 transcript was extremely low in many of these tumours. It was

not known whether this transcript was genuinely expressed at very low levels in some tumours or whether there was a problem with *WWOX* isoform 1 partially sequestering some of the reverse primer. It was therefore decided to perform an exon-spanning PCR (from exon 4 to exon 9) for the batch of tumours already analysed and also for the older batch of tumours with longer follow-up.

3.3.4 Exon-spanning PCR from exon 4 to exon 9 (detects expression of multiple isoforms)

A PCR spanning exons 4 to 9 (using primers exon 4/4 and Z2) was optimised using Taq Gold®. HCT116 clone 4 cell line cDNA was used to optimise this PCR as it was known to express multiple *WWOX* isoforms [53]. Five bands were amplified (figure 3.7). The largest band is faint and of uncertain origin. On size criteria the other 4 bands correspond to (from largest to smallest) full-length *WWOX*, *WWOX* Δ7 (skipping exon 7), *WWOX* Δ7-8 (skipping exons 7-8) and *WWOX* Δ6-8 (table 3.4).

Figure 3.7: Exon4/4 and Z2 (Taq Gold®) PCR performed on HCT116 cDNA

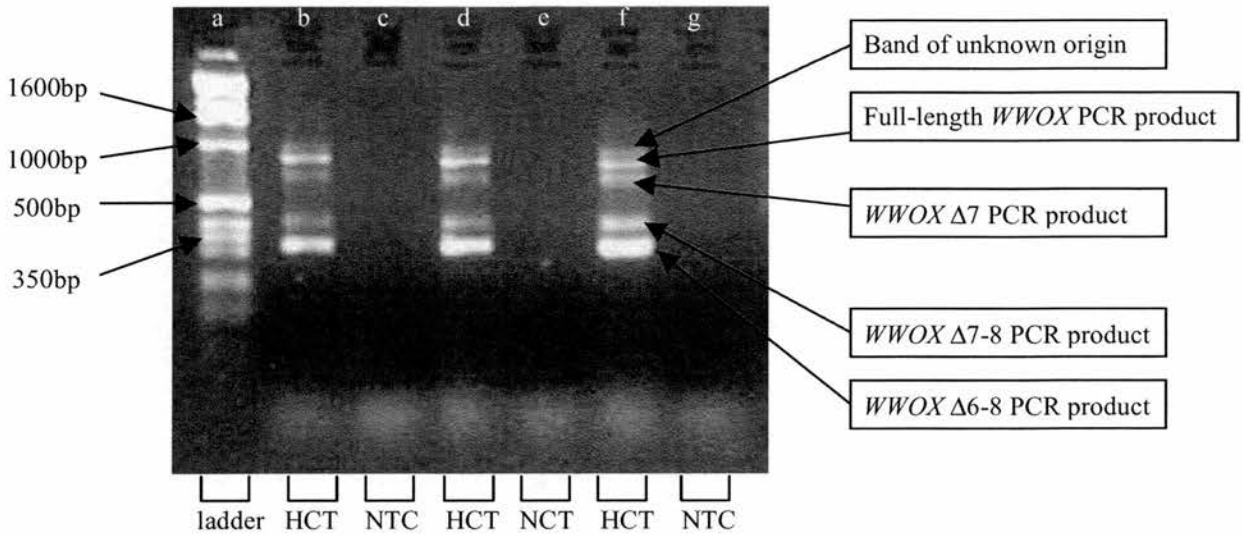

Exon 4/4 and Z2 (Taq Gold®) PCR performed using HCT116 cell line cDNA as template. Lane a contains the 1kb DNA ladder. Lanes b to g contain the PCR products of PCRs performed using Taq gold® and the exon 4/4 and Z2 primers under 3 different sets of PCR conditions. HCT116 cDNA is the template in lanes b, d and f. NTC (no template control) was the template in lanes c, e and g. The largest amplified band is of unknown origin. The second largest band corresponds to full-length *WWOX* (an example was sequenced). The third largest band corresponds to Δ7 (assumed on size criteria; band too faint to sequence). The fourth largest band corresponds to Δ7-8 (assumed on size criteria; band too faint to sequence). The smallest band corresponds to *WWOX* Δ6-8 (an example was sequenced).

Table 3.4: Origins of exon 4/4 and Z2 PCR products

Size of exon 4/4 and Z2 PCR product on agarose gel electrophoresis (bp)	**Origin on size criteria**
950	Unknown
850	Full-length *WWOX* (861bp)
700	*WWOX* Δ7 (664bp)
400	*WWOX* Δ7-8 (410bp)
320	*WWOX* Δ6-8 (321bp)

A preliminary exon-spanning PCR was performed on HOV samples whose isoform 4 status was previously investigated using the Δ6-8 F and R primers (figure 3.8). This showed concordance for isoform 4 detection between the two PCR reactions (table 3.5).

Figure 3.8: Preliminary exon-spanning PCR on selected HOV samples

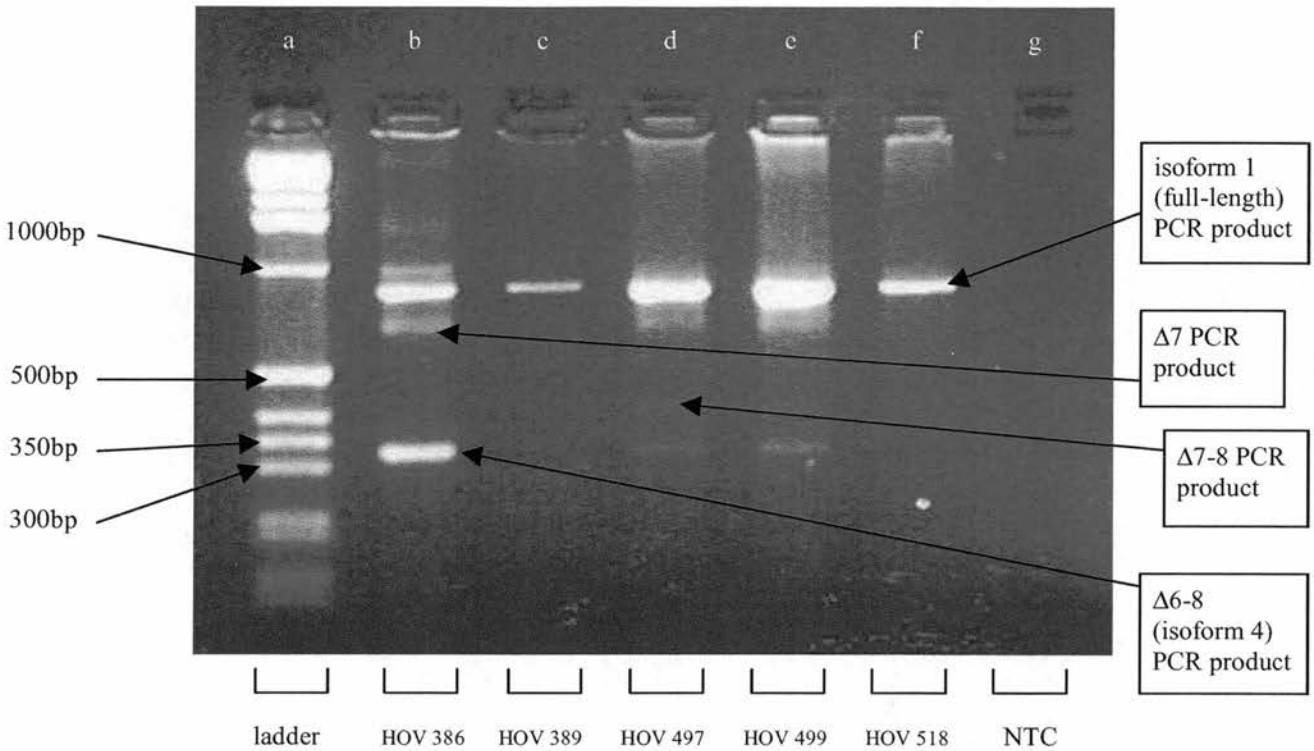

Preliminary exon-spanning PCR on selected human ovarian cancer (HOV) cDNA samples. Lane a contains the 1kb DNA ladder. Lanes b to g contain the PCR products of PCRs performed using Taq gold® and the exon 4/4 and Z2 primers. The templates used were as follows: b HOV386; c HOV389; d HOV497; e HOV499; f HOV518; g no template control (NTC).

Table 3.5: Concordance between isoform 4 detection using exon-spanning (exon4/4 and Z2 primers) and isoform 4-specific (Δ6-8 F and R primers) PCRs

HOV Sample	Isoform 4 status on Δ6-8 F and R PCR	Isoform 4 status on exon 4/4 and Z2 PCR	Other transcripts visible on exon 4/4 and Z2 PCR
386	Strongly positive	Strongly positive	Isoform 1, Δ7
389	Negative	Negative	Isoform 1
497	Faintly positive	Faintly positive	Isoform 1, Δ7-8
499	Positive	Positive	Isoform 1
518	Negative	Negative	Isoform 1

The exon 4/4 and Z2 PCR was performed for 68 tumours in the panel (RNA and cDNA required to be made again for a small number of samples and these were not included in this experiment). A band corresponding to the full-length *WWOX* transcript was identified for all tumours except HOV 12 and HOV 104. Expression of exon-skipped forms (on size criteria) was identified in a number of samples (example of PCR products shown in figure 3.9). The most abundant alternate transcript was isoform 4 (Δ6-8), which was present in 35 (51%) of the tumour samples. The Δ7 transcript was present in 7 (10%) of the tumour samples and the Δ7-8 transcript was present in 5 (7%) of the tumours. Interestingly, the Δ7-8 transcript was only ever found in tumours that also expressed the Δ6-8 transcript, but the Δ7 transcript was present in tumours that expressed no other alternate transcripts

and was never found in the presence of a Δ7-8 transcript. Only 12 tumours (18%) contained transcripts other than isoforms 1 and 4 based on this experimental methodology.

Figure 3.9: PCR products from exon-spanning PCR on HOV samples

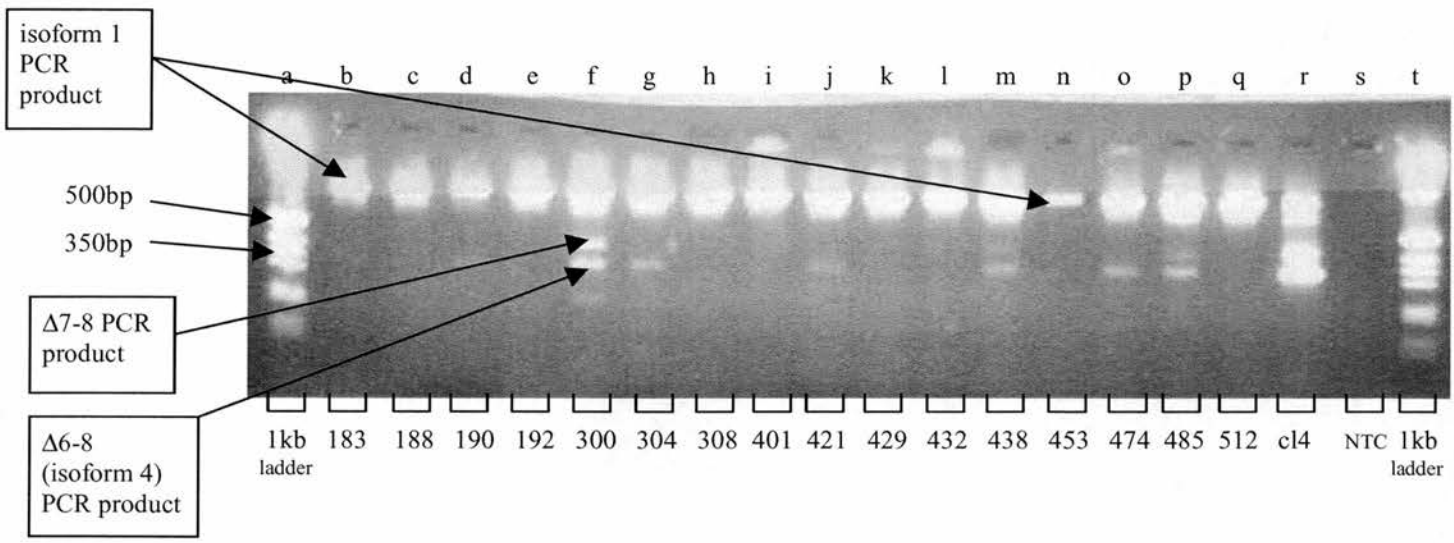

PCR products from exon-spanning PCR on human ovarian cancer (HOV) cDNA samples. Lanes a and t contain a 1kb DNA ladder. Lane r used HCT116 cDNA as template (+ve control). Lane s contains the no template control (NTC). The other lanes contain the PCR products from the exon-spanning PCR performed on a series of HOV cDNA samples (numbers under the lanes represent the HOV numbers). The ultraviolet light exposure has had to be turned up to maximum in order to see some of the faint bands produced by amplification of the alternate transcripts.

The presence of any of these alternate transcripts was significantly associated with high stage (III or IV) ovarian cancer (p=0.02, Fishers Exact Test). The presence of the Δ7 or Δ7-8 transcript was very significantly associated with high stage disease (p=0.0087, Fisher's Exact Test). The presence of the Δ6-8 transcript showed a trend towards an association with high stage disease but this was non-significant (p=0.08).

These findings suggest that there may be some association between the presence of alternate transcripts and high stage disease. As before, the expression of the alternate transcripts in some of the tumours was very low (figure 3.9), raising the question of whether this level of alternate isoform expression was high enough to be of functional significance. As a result of this it was decided to analyse *WWOX* isoform expression in the tumour panel using real-time PCR (section 3.5).

3.4 Investigation of *WWOX* mRNA isoform expression normal ovaries by non-quantitative RT-PCR

Using the 8F2/Z2 PCR, *WWOX* isoform 1 was found to be expressed in 13 out of 13 normal ovary samples.

Using the exon-spanning PCR (primers exon4/4 and Z2), a product corresponding to isoform 1 was obtained in all 13 samples. In addition, 6 of these normal ovaries were also found to express isoform 4 transcripts, again at extremely low levels. One of these normal ovaries that expressed the Δ6-8 isoform also expressed the Δ7-8 isoform. Thus *WWOX* alternate transcripts were expressed in 46% of the normal ovaries on the basis of this assay. On the basis of previous *WWOX* publications stating the lack of alternate transcripts in normal tissue this was a surprising finding. It was felt that the level of expression of the alternate transcripts may be an important issue, so this was investigated using quantitative RT-PCR (section 3.5).

3.5 Investigation of *WWOX* mRNA isoform 1 expression in an ovarian tumour panel and normal ovaries by quantitative RT-PCR

The expression of *WWOX* isoform 1 cDNA in 71 ovarian tumours and 13 normal ovaries was quantified on the Rotorgene® and corrected for the expression of *β-ACTIN*. All quantitation was relative (expression level calculated by extrapolation from a standard curve constructed using aliquots of cell line cDNA that was the same in all runs to be compared).

3.5.1 *WWOX* isoform 1 mRNA expression in the ovarian tumour panel

The relative *WWOX* isoform 1 expression (*WWOX/β-ACTIN*), as determined by quantitative real-time PCR, varied from 0 to 58.7 (median 9.57) in the ovarian tumours (figure 3.10; the two non-expressing tumours, HOV12 and HOV 104 are not shown). This expression was not normally distributed (figure 3.11) with most of the tumours expressing low levels of *WWOX* and a few tumours expressing more than four times the median level of isoform 1.

Figure 3.10: *ACTIN*-corrected *WWOX* isoform 1 expression in the human ovarian tumour panel.

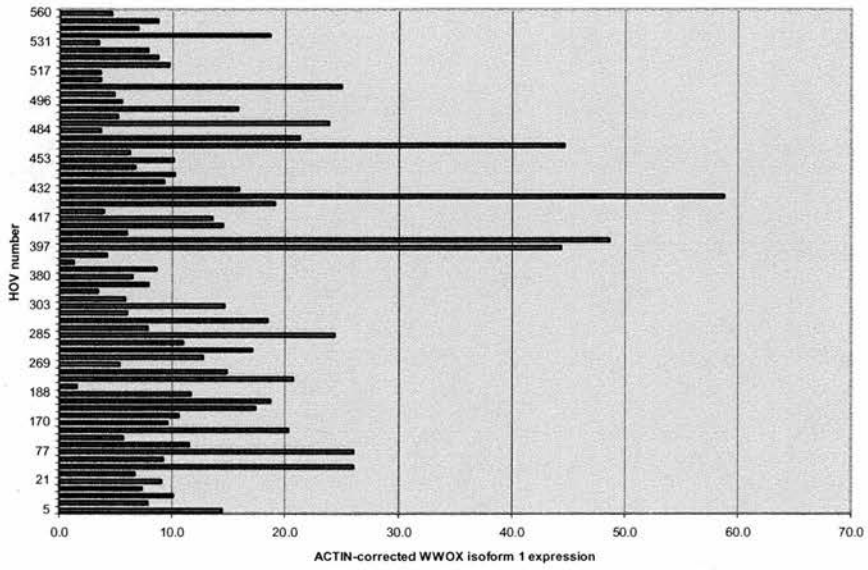

A bar chart illustration of the expression of *WWOX* isoform 1 in ovarian tumour samples with *ACTIN*-corrected *WWOX* isoform 1 expression plotted on the x-axis. The numbers on the y-axis correspond to the human ovarian cancer (HOV) numbers. Therefore each bar corresponds to the *ACTIN*-corrected *WWOX* expression in an individual tumour as measured by quantitative RT-PCR. Each *WWOX* and each *ACTIN* PCR was performed on HOV cDNA and repeated in quadruplicate. Quantification of expression from repeated samples of the same tumour was not possible due to limited tumour material.

Figure 3.11: The *ACTIN*-corrected *WWOX* isoform 1 expression in the human ovarian tumour panel is not normally distributed.

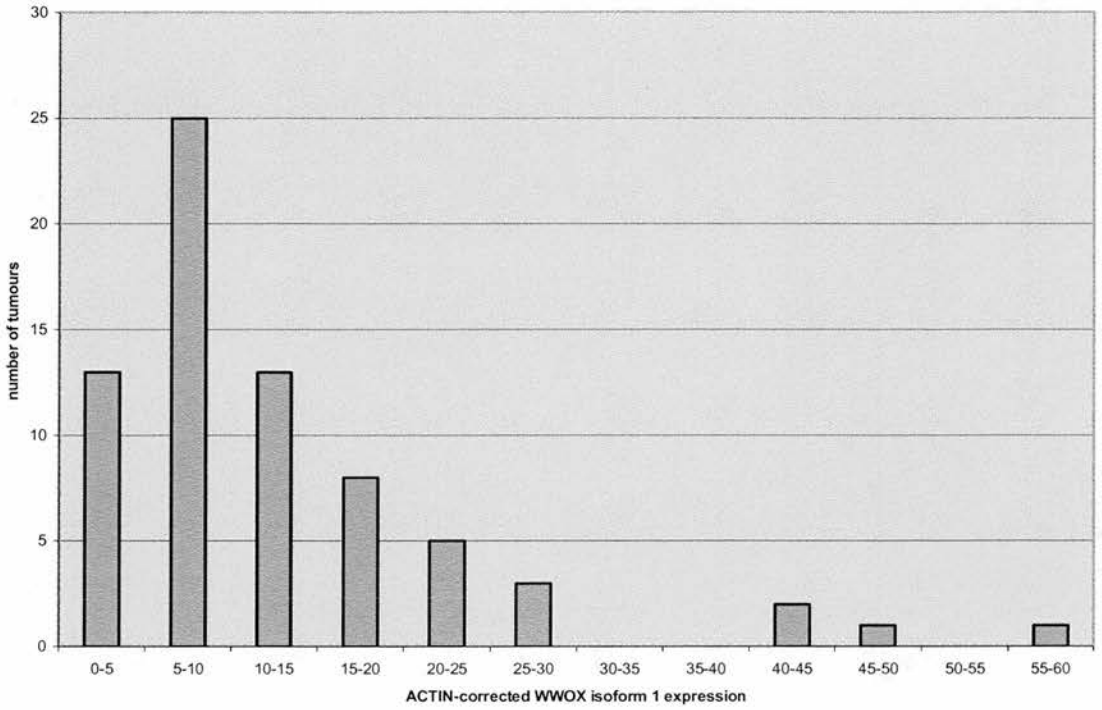

Bar chart showing the distribution of *ACTIN*-corrected *WWOX* isoform 1 expression in human ovarian tumour (HOV) samples. *ACTIN*-corrected *WWOX* isoform 1 expression (as measured by quantitative RT-PCR) is plotted in cohorts on the x-axis. This allows illustration of the spread of expression levels amongst the tumours. There is a non-parametric distribution of *WWOX* expression of these ovarian tumour samples. Each *WWOX* and each *ACTIN* PCR was performed on HOV cDNA and repeated in quadruplicate.

3.5.2 *WWOX* isoform 1 mRNA expression in normal ovaries

The relative *WWOX* isoform 1 expression (*WWOX/β-ACTIN*), as determined by quantitative real-time PCR, varied from 9.3 to 61.6 (median 22.9) in the normal ovarian tissues (figure 3.12). This expression was not normally distributed (figure

3.13) but all the normal ovaries expressed *WWOX* at levels that are higher than the median expression in the ovarian tumours.

Figure 3.12: *ACTIN*-corrected *WWOX* isoform 1 expression in the normal ovaries.

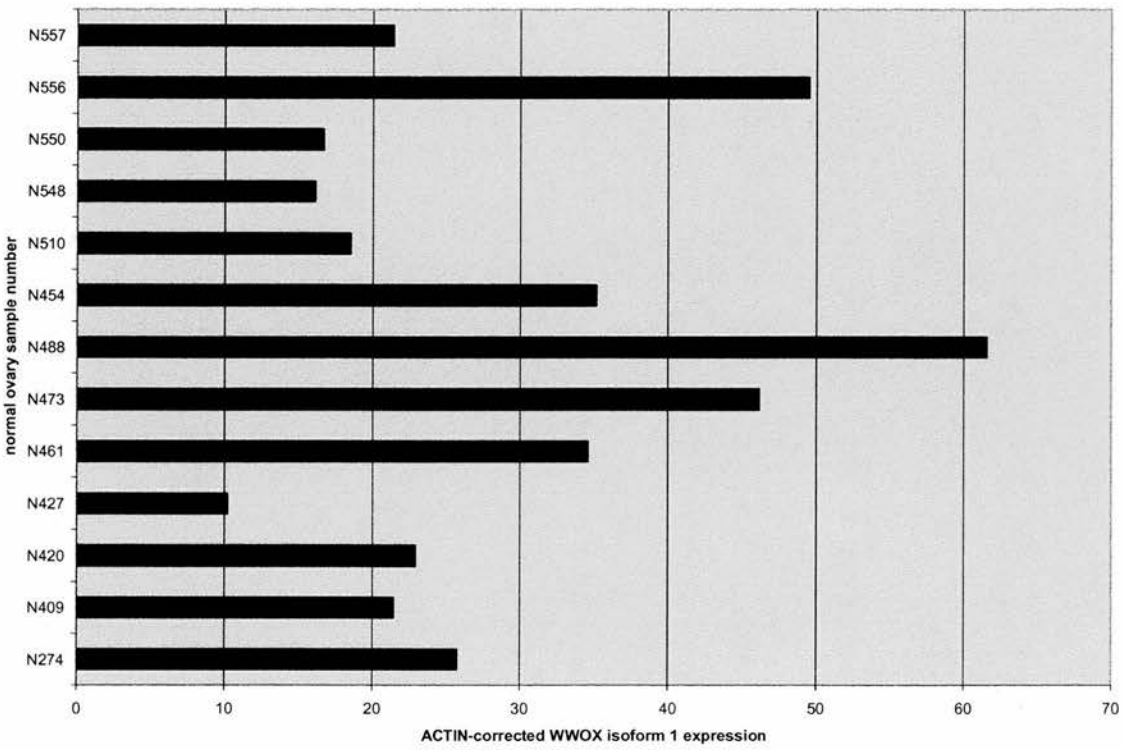

A bar chart illustration of the expression of *WWOX* isoform 1 in 13 normal ovaries with *ACTIN*-corrected *WWOX* isoform 1 expression plotted on the x-axis. The numbers on the y-axis correspond to the number given to the normal ovary sample. Therefore each bar corresponds to the *WWOX* expression in an individual normal ovary as measured by quantitative RT-PCR. Each *WWOX* and each *ACTIN* PCR was performed on normal ovarian cDNA and repeated in quadruplicate. Quantification of expression from repeated samples of the same normal ovary was not possible due to limited normal ovarian material.

Figure 3.13: The *ACTIN*-corrected *WWOX* isoform 1 expression in the normal human ovaries is not normally distributed.

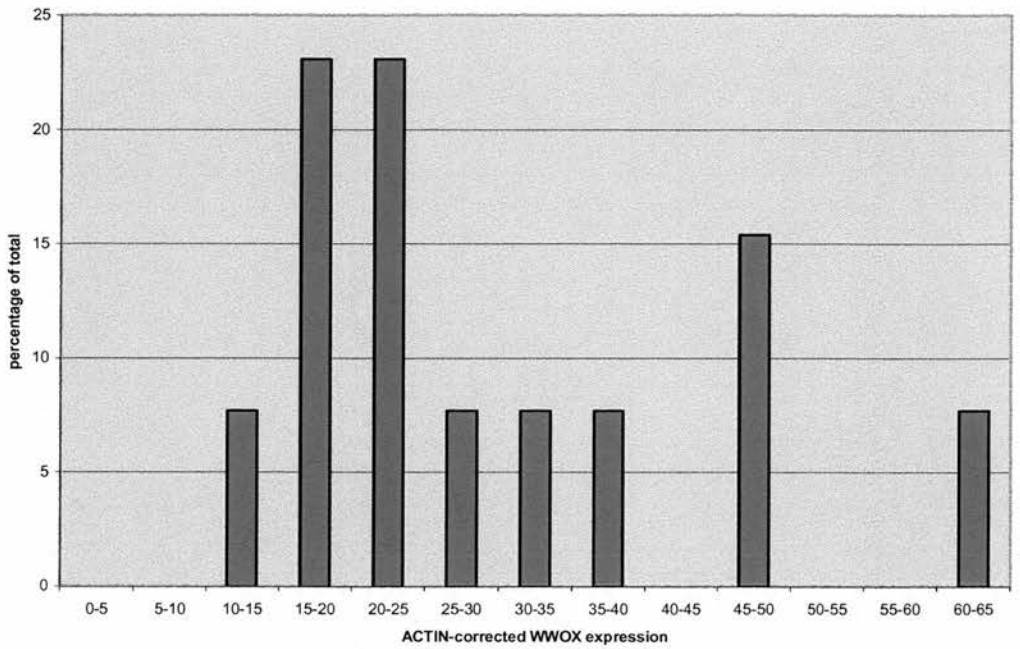

Bar chart showing the distribution of *ACTIN*-corrected *WWOX* isoform 1 expression in normal human ovaries. *ACTIN*-corrected *WWOX* isoform 1 expression is plotted in cohorts on the x-axis. This allows illustration of the spread of expression levels amongst the normal ovaries. There is a non-parametric distribution of *WWOX* expression of these normal ovary samples. Each *WWOX* and each *ACTIN* PCR was performed on normal ovarian cDNA and repeated in quadruplicate.

3.5.3 Comparison of *WWOX* isoform 1 mRNA expression between ovarian tumour and normal ovaries

Neither group of samples had a normal distribution of variant 1 expression (figure 3.14) but the median *WWOX* variant 1 expression was significantly reduced in the ovarian tumours compared to the normal ovarian tissues ($p<0.0001$; Mann-Whitney

test, figure 3.15). Indeed, all the normal ovaries expressed WWOX at a level that was higher than the median expression in the tumours.

Figure 3.14: *ACTIN*-corrected *WWOX* isoform 1 expression in the human ovarian tumours and in the normal ovaries.

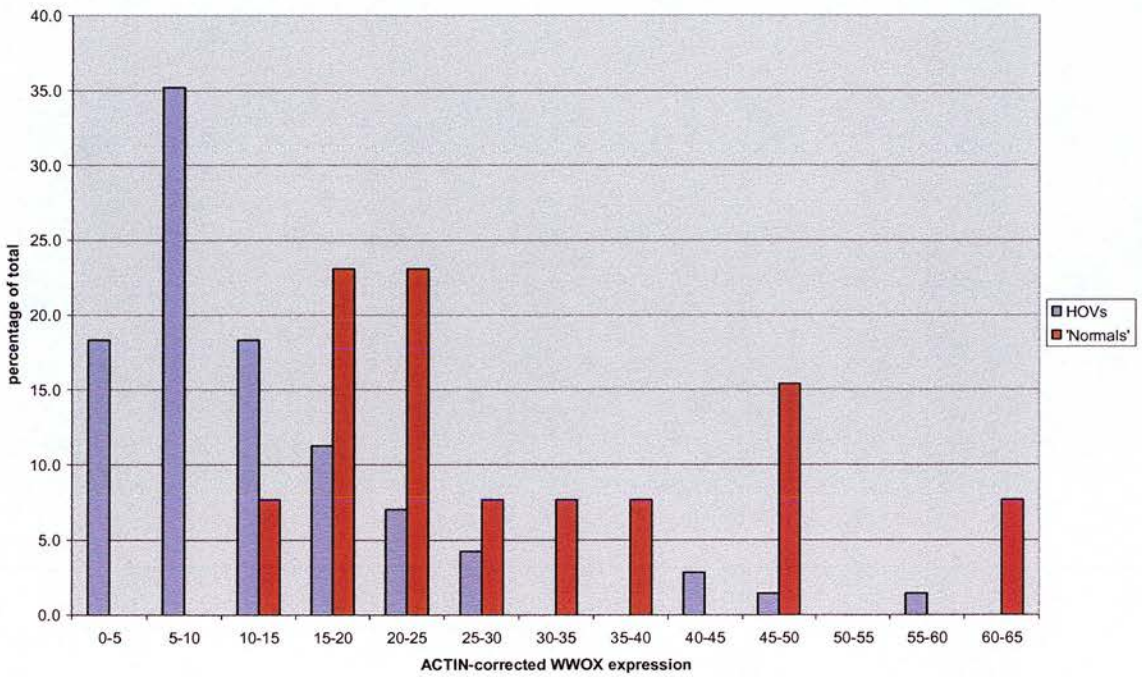

Bar chart showing the distribution of *ACTIN*-corrected *WWOX* isoform 1 expression in human ovarian tumours and in normal ovaries. *ACTIN*-corrected *WWOX* isoform 1 expression is plotted in cohorts on the x-axis. The distribution of expression levels amongst human ovarian tumours (blue) and normal ovaries (red) is illustrated. Each *WWOX* and each *ACTIN* PCR was performed on human ovarian tumour or normal ovarian cDNA and repeated in quadruplicate.

Figure 3.15: *WWOX* isoform 1 expression is significantly decreased in the human ovarian tumours compared to the normal ovaries

n	84			
wwox exp	**n**	**Rank sum**	**Mean rank**	**U**
Normal	13	888.0	68.31	126.0
Hov	71	2682.0	37.77	797.0
Difference between medians	14.509			
95.0% CI	8.815 to 21.635		(normal approximation)	
Mann-Whitney U statistic	126			
2-tailed p	<0.0001	(normal approximation, corrected for ties)		

Mann-Whitney test showing that there is a significant difference between the median *ACTIN*-corrected *WWOX* expression in 71 ovarian tumours compared to the median expression in 13 normal ovaries.

3.6 Investigation of *WWOX* mRNA isoform 4 expression in an ovarian tumour panel by quantitative RT-PCR

The expression of *WWOX* isoform 4 (Δ6-8) cDNA in 71 ovarian tumours and 13 normal ovaries was quantified on the Rotorgene® using primers Δ6-8 F4 (in exon 4) and Δ6-8 R2 (located at the boundary of exon 5 and exon 9, but this time only extending 6 nucleotides into exon 5 and having 13 nucleotides in exon 9 in an attempt to minimise mispriming). As usual, all PCR reactions on the Rotorgene® were performed in quadruplicate.

3.6.1 *WWOX* isoform 4 mRNA expression in the ovarian tumour panel

Expression of *WWOX* isoform 4 was detected in 45 out of 71 (63%) ovarian tumour samples. The expression of isoform 4 was generally low (amplification after 32 to 39 cycles of PCR when 1µl of cDNA sample was used in each case), although the expression in a small number of tumours was an order of magnitude higher than the median for isoform 4-expressing tumours (figure 3.16). By comparison, isoform 1 amplified significantly after 19 to 32 cycles, when 0.2µl of first strand cDNA was used in the PCR.

Figure 3.16: *ACTIN*-corrected *WWOX* isoform 4 expression in the human ovarian tumour panel.

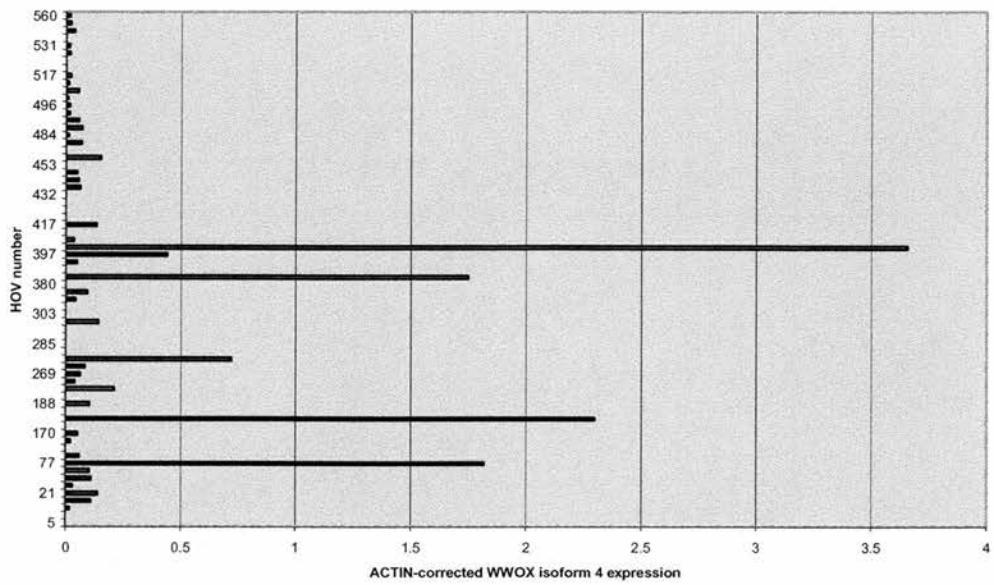

A bar chart illustration of the expression of *WWOX* isoform 4 in the individual ovarian tumours with *ACTIN*-corrected *WWOX* isoform 4 expression plotted on the x-axis. The numbers on the y-axis correspond to the human ovarian tumour (HOV) numbers. Therefore each bar corresponds to the *WWOX* isoform 4 expression in an individual tumour as measured by quantitative RT-PCR. Each *WWOX* isoform 4 and each *ACTIN* PCR was performed on HOV cDNA and was repeated in quadruplicate. Quantification of expression from repeated samples of the same tumour was not possible due to limited tumour material.

3.6.2 *WWOX* isoform 4 mRNA expression in normal ovaries

Expression of *WWOX* isoform 4 was detected in 9 out of 13 (69%) normal ovarian tissue samples. The expression of the isoform 4 transcript was very low (amplification after 36 to 40 cycles, when 1µl of cDNA sample was used in each case). By comparison, isoform 1 amplified significantly after 19 to 32 cycles, when

0.2µl of first strand cDNA was used in the PCR. The reproducibility of the quantitation in these extremely low expressing samples was predictably poor.

3.6.3 Comparison of *WWOX* isoform 4 mRNA expression between ovarian tumours and normal ovaries

Expression of *WWOX* isoform 4 was detected in 45 out of 71 (63%) ovarian tumour samples, and surprisingly in 9 out of 13 (69%) normal ovarian tissue samples. In both normal tissues and in the ovarian tumour samples, the expression of the isoform 4 transcript was generally very low (amplification after 32 to 39 cycles of PCR in the tumours and after 36 to 40 cycles in the normal ovarian tissues, when 1µl of cDNA sample was used in each case). By comparison, isoform 1 amplified significantly after 19 to 32 cycles, when 0.2µl of first strand cDNA was used in the PCR. The relative *WWOX* isoform 4 expression (*WWOX/β-ACTIN*) varied from 0 to 0.33 in the normal ovarian tissues and from 0 to 3.65 in the ovarian tumours, although the reproducibility of the quantitation in the extremely low expressing samples was poor.

3.7 Comparison of *WWOX* mRNA expression profile with clinicopathological factors in ovarian tumours

No correlation was identified between *WWOX* isoform 1 expression level (as tested using this Rotorgene®-based assay) and clinicopathological factors.

There was a significant association between the presence of the isoform 4 transcript (on the basis of the Rotorgene® assay) and high grade ovarian cancer (p= 0.006;

Fisher's Exact Test; table 3.6) for the 66 isoform 1 expressing tumours that had grade information available. The presence of the isoform 4 transcript was also significantly associated with advanced stage disease (p=0.012; Fisher's Exact Test; table 3.7) in the 66 isofom 1 expressing tumours that had stage information available. There was no correlation between expression of isoform 4 and histology of ovarian tumour.

Table 3.6: *WWOX* isoform 4 expression and tumour grade

	Tumour grade		**TOTAL**
	1 or 2	**3**	
Isoform 4 expression	6	37	43
No isoform 4 expression	11	12	23
TOTAL	17	49	66

P=0.006, Fisher's Exact test

Table 3.7: *WWOX* isoform 4 expression and tumour stage

	Tumour stage		**TOTAL**
	I/II	**III/IV**	
Isoform 4 expression	5	37	42
No isoform 4 expression	10	14	24
TOTAL	15	51	66

P=0.012, Fisher's Exact test

3.8 Comparison of *WWOX* mRNA expression profile with patient survival in ovarian tumours

In the 69 ovarian cancer patients assessable for *WWOX* expression, Kaplan-Meier analysis of survival was performed (figures 3.17-3.19). There was no difference in survival between high (*ACTIN*-corrected level >10) and low (*ACTIN*-corrected level <10) *WWOX* isoform 1 expressers (figure 3.17). There was a trend towards worse survival in those patients whose tumours expressed any level of *WWOX* isoform 4 but this did not reach significance (p=0.057; figure 3.18). However, in the patients expressing high levels of isoform 1 (*ACTIN*-corrected level >10), those that expressed isoform 4 had significantly worse survival (p=0.048; figure 3.19) compared with those that did not. In contrast, expression of isoform 4 did not significantly alter the survival in patients expressing low levels of isoform 1 (data not shown).

Analysis of isoform 4 in a multivariate model demonstrated that expression of this isoform was not an independent prognostic variable.

Figure 3.17: Survival according to *WWOX* isoform 1 expression in 69 ovarian cancer patients

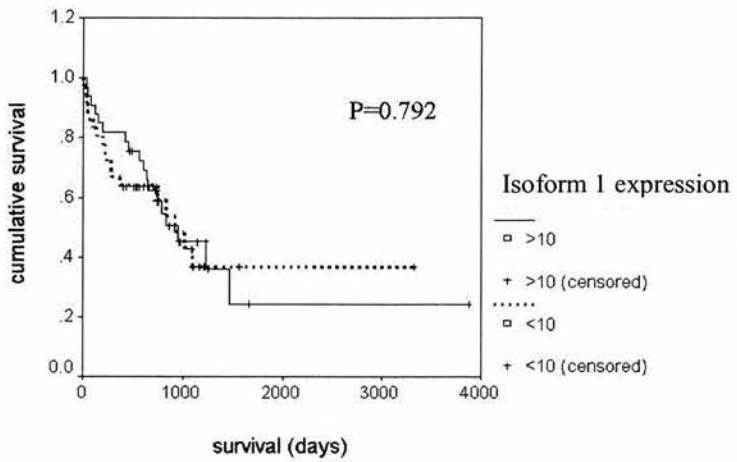

Kaplan-Meier analysis of 69 ovarian cancer patients demonstrating proportion of surviving patients according to *WWOX* isoform 1 expression level as judged by quantitative RT-PCR. The cut-off chosen for this analysis was an *ACTIN*-corrected *WWOX* level of 10 (as the median *ACTIN*-corrected *WWOX* expression in this group was 9.57). No significant difference in survival according to WWOX isoform 1 expression for this group of patients.

Figure 3.18: Survival according to *WWOX* isoform 4 expression in 69 ovarian cancer patients

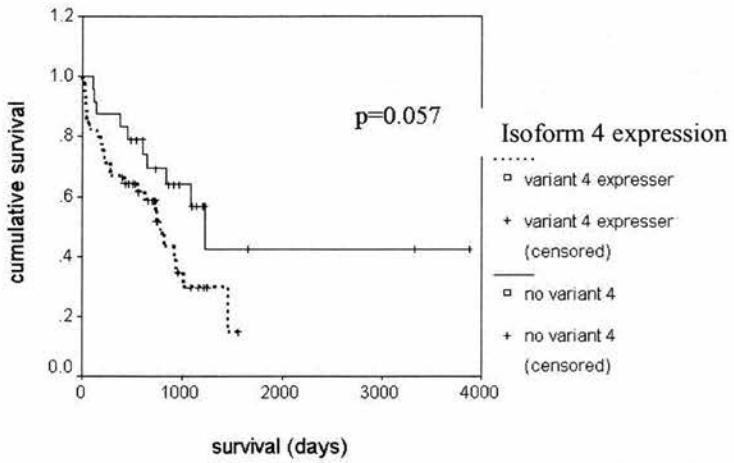

Kaplan-Meier analysis of 69 ovarian cancer patients demonstrating proportion of surviving patients according to *WWOX* isoform 4 expression as judged by quantitative RT-PCR. The survival of patients whose tumours expressed any *WWOX* isoform 4 was compared to those whose tumours expressed no *WWOX* isoform 4. No significant difference in survival according to WWOX isoform 4 expression for this group of patients.

Figure 3.19: Survival according to *WWOX* isoform 4 expression in 33 robust expressers of *WWOX* isoform 1

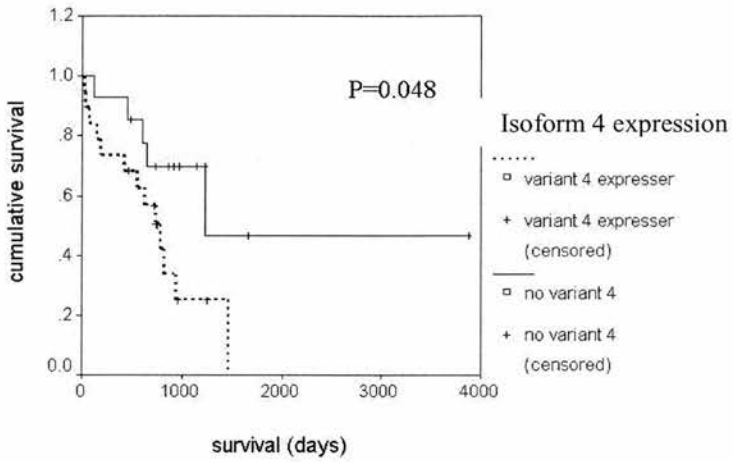

Kaplan-Meier analysis of 33 ovarian cancer patients who expressed high levels of *WWOX* isoform 1 demonstrating proportion of surviving patients according to *WWOX* isoform 4 expression as judged by quantitative RT-PCR. The definition of a high *WWOX* isoform 1 expresser used for this analysis was an *ACTIN*-corrected *WWOX* level of 10 (as the median *ACTIN*-corrected *WWOX* expression in this group was 9.57). The survival of patients whose tumours expressed any *WWOX* isoform 4 was compared to those whose tumours expressed no *WWOX* isoform 4. There was a significant survival difference according to *ACTIN*-corrected *WWOX* isoform 4 expression in patients who expressed high levels of *WWOX* isoform 1 (p=0.048)

3.9 *WWOX* isoform 6 expression

It would have been highly desirable to test for *WWOX* isoform 6 expression in this ovarian cell line panel as it is the other alternate transcript that has been found to be expressed at reasonable frequency in malignant tissue [169]. However, exhaustive attempts to find a consistent, reproducible one round PCR for this isoform of the gene always resulted in the amplification of multiple products. When the conditions

described by Driouch et al [169] to specifically amplify this transcript were used, again multiple products were obtained. Driouch et al performed this reaction as part of a multiplex reaction, which may have altered the dynamics of the reaction compared with the one round PCR tested here. The difficulty in optimising single round PCR conditions was highlighted when a reaction was tested on the Rotorgene®. It gave highly efficient amplification and allowed the generation of an adequate standard curve but the melt curve showed the definite presence of multiple products, although agarose gel electrophoresis suggested that the target product was predominant. Therefore, due to these limitations, this was not pursued further.

3.10 Evaluation of results

Out of 71 ovarian tumour samples, 69 expressed full-length *WWOX*. One tumour expressed no full-length transcript at all and another expressed a truncated transcript. Full-length *WWOX* expression was found to be significantly lower in these 71 epithelial ovarian cancers compared to 13 normal ovaries ($p<0.0001$). These findings support the hypothesis that *WWOX* acts as a tumour suppressor in ovarian cancer and address one of the main aims of the project (to elucidate whether the *WWOX* gene functions as a tumour suppressor in epithelial ovarian cancer). However, this conclusion has to be qualified for two main reasons.

Firstly, a significant problem with comparing gene expression from ovarian tumour samples to normal is choosing a suitable normal tissue. Factors that have to be considered are the cellular content of the normal tissue compared to the tumour tissue, comparability of sample isolation procedures and extent to which gene expression may have been affected by *ex vivo* factors. The tumour component of

epithelial ovarian tumours consists by definition of mainly epithelial cells. There are however a variable number of supporting cell types; stromal cells, endothelial cells etc. Normal ovaries contain only a covering layer of human ovarian epithelium and therefore may be considered a poor comparator. The other option, cultured human ovarian surface epithelial cells, although purely epithelial, will have sustained changes in gene expression as a result of there forced *in vitro* growth and contain no supporting cells. For this reason and so that RNA isolation from tumours and 'normals' could be performed identically it was decided to use normal human ovaries as the comparator although it is recognised that there are inherent problems with this. Secondly, in order to fully characterise gene expression it is optimal for this to be performed at the protein rather than the RNA level. At the time this project was performed the sensitivity of the available antibodies was insufficient to identify alternate transcript expression or even expression of full-length *WWOX* from some tumours or cell lines. It was therefore decided to perform the analysis at the RNA level for reasons of sensitivity.

The analysis of alternate transcript expression revealed that *WWOX* isoform 4 was expressed at low levels in 63% of the ovarian tumour samples. The expression of *WWOX* isoform 4 mRNA was significantly associated with high grade ($p=0.006$) and advanced stage ovarian cancer ($p=0.012$). There was a trend towards adverse survival ($p=0.057$) in patients who expressed this isoform and significantly worse survival ($p=0.048$) in robust isoform 1 expressers who also expressed isoform 4. These findings suggest that in some way the expression of *WWOX* isoform 4 is a poor prognostic factor but do not indicate a mechanism for this. Although it is tempting to propose that these findings suggest a dominant negative mechanism of

action for *WWOX* isoform 4, two facts argue somewhat (although not completely) against this. Firstly, *WWOX* isoform 4 was identified in non-malignant ovarian tissue at a comparable frequency (69%) to the frequency identified in ovarian tumours (63%). Secondly, the level of *WWOX* isoform 4 expression in most of the ovarian tumours (and in all the normal ovaries) was exceedingly low. Although this does not entirely preclude a dominant negative function (as *WWOX* isoform 1 is located in the cytoplasm and *WWOX* isoform 4 is located in the nucleus and competition for binding partners is therefore not equal) it is difficult to imagine that expression at the limit of detection can significantly affect the function of the well-expressed *WWOX* isoform 1. This component of the work addresses one of the main aims of the project (to clarify the role of the *WWOX* alternate transcripts in ovarian cancer). Although it suggests that *WWOX* isoform 4 expression may imply poor prognosis, it does not elucidate whether this is an effect that is directly attributable to *WWOX* isoform 4 or whether the expression of the alternate transcript is a bystander effect in more aggressive tumours whose splicing fidelity is decreased.

4. RESULTS: *WWOX* mRNA ISOFORM EXPRESSION PROFILE IN A PANEL OF HUMAN TUMOUR CELL LINES

4.1 Rationale for investigating the *WWOX* mRNA isoform expression profile in a human tumour cell line panel

The expression of *WWOX* alternate transcripts has been identified in a number of malignant tissues and cancer cell lines (section 1.6.10) [52,53,165,166,169,171]. We wished to establish the pattern of *WWOX* mRNA isoform expression in a panel of human cancer cell lines from a variety of tissues. Specifically, the aims were to identify cell lines expressing:

1) Very low levels of *WWOX* isoform 1 (full-length transcript), suggesting knock-down as these could be transfected with the *WWOX* coding region and used for functional analysis.
2) High levels of *WWOX* isoform 4 (Δ6-8 transcript), suggesting a possible dominant negative mechanism of *WWOX* isoform 1 downregulation that could then be investigated.
3) High levels of expression of both isoform 1 and of alternate transcripts as they would be good candidates for RNA interference based experiments investigating the possible dominant-negative mechanism of action of alternate transcripts.

It was hoped that these findings could be used to create resources that would facilitate the clarification of the role of the *WWOX* alternate transcripts and that would help ascribe a phenotype to the *WWOX* gene.

4.2 Description of human tumour cell line panel

RNA from 37 human tumour cell lines (table 4.1) was analysed for *WWOX* isoform 1 and *WWOX* isoform 4 expression. Cell lines known to be homozygously deleted for *WWOX* exons (PEO4, WX330, NCI-H69 and PANC1) were not included in this analysis. Seventeen ovarian lines, 7 colorectal lines, 5 leukaemia/lymphoma lines, 4 breast lines 3, prostate lines and 1 lung line were investigated.

Table 4.1 Cell lines used for quantification of *WWOX* isoforms (listed according to tissue of origin)

Tissue of Origin					
Ovary	**Colon**	**Lymphocyte**	**Breast**	**Prostate**	**Lung**
OVCAR3	HT115	FATO	T47D	DU145	NX002
CaOV3	HCT15	K562	ZR75.1	LN CAP	
OAW42	HRT18	HBL	MDA MB231	PC3	
PEA1	HT29	JURKAT	MCF7		
SKOV3	SW48	HL60			
A2780cis	HCT116				
PEA2	LOV0				
PEO14					
HELA					
OVCAR5					
59M					
A2780ad					
41M					
A2780					
OVCAR4					
PEO16					
PEO23					

4.3 *WWOX* isoform 1 mRNA expression in the cell line panel

WWOX isoform 1 expression in the cell lines varied over almost 3 orders of magnitude (0.003-2.417, normalised to 41M cell line cDNA; figure 4.1). Cell lines from each tissue of origin demonstrated a wide range of *WWOX* isoform 1 expression, except for the prostate cancer cell lines. Of three prostate cancer cell lines tested, two (PC3 and DU145) expressed extremely low levels of *WWOX* isoform 1. In addition, the expression of this isoform in the CaOV3 ovarian cancer cell line was barely detectable. The MCF-7 and ZR75-1 breast and SW48 colorectal cancer cell lines expressed high levels of *WWOX* isoform 1 compared to the other cell lines.

Figure 4.1 *WWOX* isoform 1 expression (according to tissue of origin) in 37 human cancer cell lines

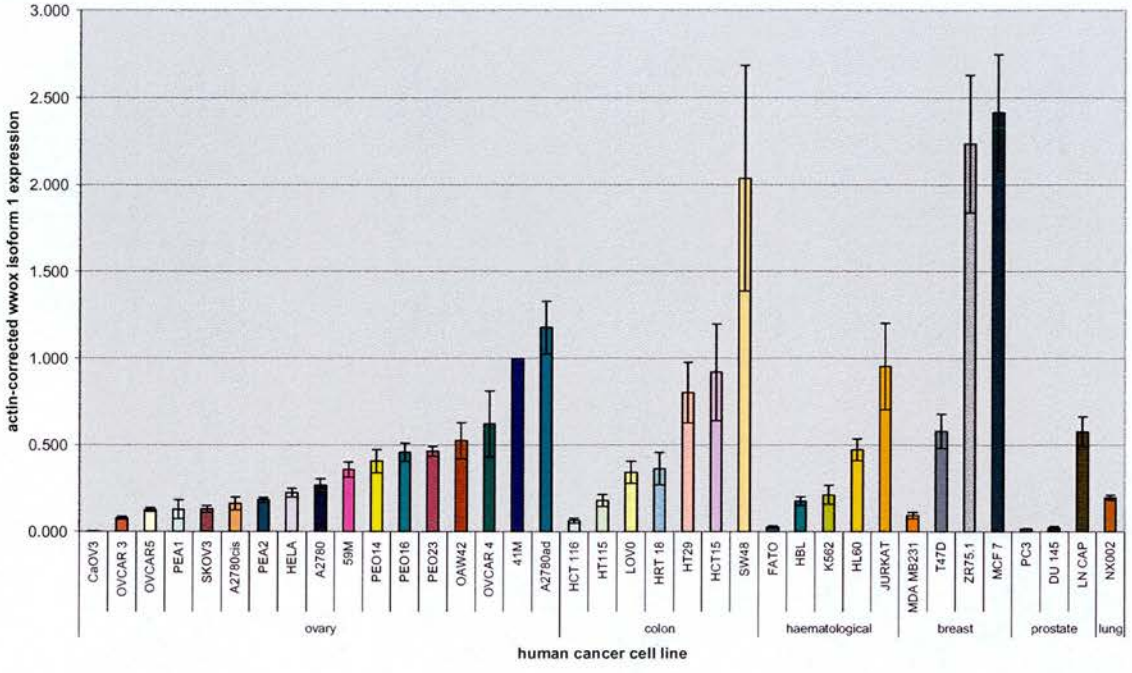

ACTIN-corrected *WWOX* isoform 1 expression in 37 human cancer cell lines, sorted according to tissue of origin. All expression levels were normalised to the expression in the 41M ovarian cancer cell line. Each gene quantification was obtained by performing RT-PCR on cell line cDNA using the Rotorgene®. Each quantification was performed in quadruplicate in each run. The average expression for each cell line was obtained by taking the average expression from three runs. The standard error of the mean was calculated from the average expression from the three runs. The absolute error was calculated by dividing the standard error of the mean by the mean expression. The actin-corrected *WWOX* expression was calculated for each isoform by dividing the average *WWOX* expression by the average *β-ACTIN* expression. The total final error was obtained by adding together the absolute error for both the *WWOX* and the *β-ACTIN* quantification. This was the error to which the final quantification of actin-corrected *WWOX* expression was subject (represented by the error bars in the figure).

4.4 *WWOX* isoform 4 mRNA expression in the cell line panel

WWOX isoform 4 was expressed in 33 out of 37 (89%) human cancer cell lines tested (figure 4.2). Again, there was no association between the tissue of origin and the level of WWOX isoform 4 expression. The HCT116 and LOV0 colorectal and MCF-7 breast cancer cell lines expressed high levels of *WWOX* isoform 4 compared to the other cell lines.

Figure 4.2 *WWOX* isoform 4 expression (according to tissue of origin) in 37 human cancer cell lines

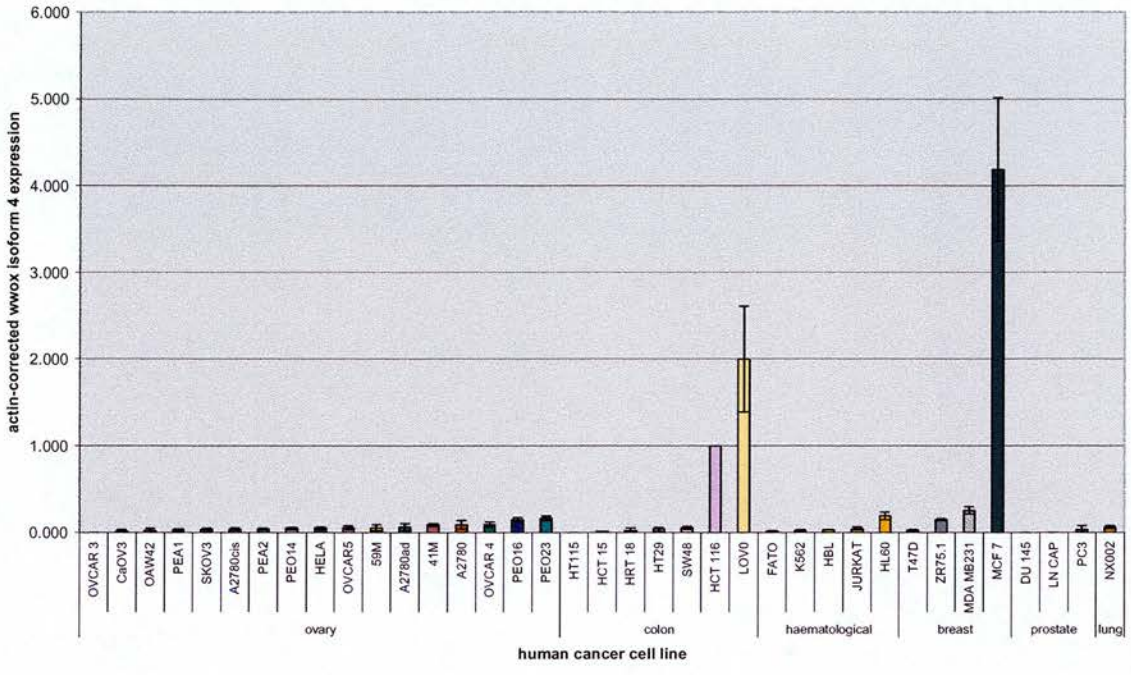

ACTIN-corrected *WWOX* isoform 4 expression in 37 human cancer cell lines, sorted according to tissue of origin. All expression levels were normalised to the expression in the HCT116 colorectal cancer cell line. Each gene quantification was obtained by performing RT-PCR on cell line cDNA using the Rotorgene®. Each quantification was performed in quadruplicate in each run. The average expression for each cell line was obtained by taking the average expression from three runs. The standard error of the mean was calculated from the average expression from the three runs. The absolute error was calculated by dividing the standard error of the mean by the mean expression. The actin-corrected *WWOX* expression was calculated for each isoform by dividing the average *WWOX* expression by the average *β-ACTIN* expression. The total final error was obtained by adding together the absolute error for both the *WWOX* and the *β-ACTIN* quantification. This was the error to which the final quantification of actin-corrected *WWOX* expression was subject (represented by the error bars in the figure).

4.5 Evaluation of results

WWOX isoform 1 expression varied over 3 orders of magnitude in the cell lines tested. The PC3 and DU145 prostate cancer cell lines and the CaOV3 ovarian cancer cell line expressed very low levels of *WWOX* isoform 1. These cell lines would be suitable for investigation of *WWOX* down-regulatory mechanisms and in this sense represent a valuable resource. In addition, the finding of a further ovarian cancer cell line with negligible *WWOX* expression adds support to the hypothesis that *WWOX* may act as a tumour suppressor in ovarian cancer. To prove that the loss of *WWOX* played a role in the malignant phenotype would require for the *WWOX* gene to be re-expressed in these cells and for a change in phenotype (such as a loss of tumourigenicity) to be demonstrated. The finding that 2 out of 3 prostate cancer cell lines expressed very low levels of *WWOX* isoform 1 is also noteworthy because a high incidence of LOH has been identified at the *WWOX* locus in prostate cancer cells [153]. It adds weight to the suggestion that *WWOX* may also act as a tumour suppressor in prostate cancer.

WWOX isoform 4 was expressed in 33 out of 37 (89%) of the cell lines and in 16 out of 17 (94%) of the ovarian cancer cell lines. Although it is tempting to suggest that this represents a high rate of alternate transcript expression, using the same methodology I identified a high frequency of *WWOX* isoform 4 expression in non-malignant ovarian tissue (chapter 3) so the high frequency of expression identified in these cell lines does not allow us to draw any conclusions regarding the role of these alternate transcripts in ovarian cancer. The HCT116 and LOV0 colorectal cancer cell lines and the MCF-7 breast cancer cell line expressed levels of isoform 4 that are almost an order of magnitude higher than any of the other cell lines. Although no

reason for this has been identified, the reason for this expression pattern may become clear as we learn more about the function of the *WWOX* isoforms in the cancer cell. The MCF-7 breast cancer cell line was the highest expresser of both isoform 1 and isoform 4 and would be ideal for RNA interference-based investigation of a possible dominant-negative mechanism of action of *WWOX* isoform 4 (by targeting this isoform for knockout). Although not directly achieving any of the aims of the PhD project, through further investigation the above findings could facilitate the clarification of the role of *WWOX* isoform 4 in ovarian carcinogenesis.

5. RESULTS: INDUCTION OF *WWOX* OCCURS VIA BOTH P53-DEPENDENT AND P53-INDEPENDENT PATHWAYS

5.1 Hyaluronidase-induced *WWOX* mRNA expression in HCT116 cells is p53-dependent

As discussed in section 1.8.1, hyaluronidase is secreted by most cancer cells and induces angiogenesis *in vivo* [175]. Increased hyaluronidase levels are associated with progression, invasion and metastases of a variety of malignancies including ovarian cancer [176-179]. Chang et al showed that hyaluronidase increased TNFα–mediated cell death in murine L929 fibroblasts and in the human prostate cancer cell line LN-CaP [181]. Using differential display and cDNA library screening, Chang et al subsequently identified a cDNA which was induced by exposure of L929 murine fibroblast cells to hyaluronidase [168]. This murine cDNA was named *Wox1* and was highly homologous to full-length human *WWOX*. They demonstrated that exposure of L929 cells (whose constitutive expression of *Wox1* mRNA is low) to hyaluronidase resulted in a 150% increase in *Wox1* mRNA, peaking at 8-24 hours post initiation of exposure. Chang et al [168] also proposed that part of WOX1's enhancement of TNFα–mediated cytotoxicity was secondary to increased p53 expression, that p53-mediated apoptosis required WOX1 and that the WW domain of WOX1 bound to the polyproline region of p53.

In order to determine whether hyaluronidase could induce *WWOX* in our human cancer cell line systems, HCT116 and PEO1 cells were exposed to three doses of hyaluronidase for two different durations, RNA was prepared and the levels of *WWOX* expression were compared to the baseline level of expression. The reason that the HCT116 colorectal cancer cell line was chosen in a mainly ovarian cancer orientated study was the availability of well-characterised isogenic wild-type, p53-null, p21-null and BAX-null derivatives of this cell line.

5.1.1 WWOX mRNA expression in hyaluronidase-exposed p53 normal HCT116 cells

The expression of total *WWOX* mRNA in p53 wild-type (wt) HCT116 cells exposed to 3 doses of hyaluronidase (100, 200 or 400 units/ml) for 4 or 8 hours was quantified using the Lightcycler®. Following 4 hours of exposure, expression of *WWOX* was increased for all doses of hyaluronidase. This was maximal using 200 units/ml hyaluronidase (figure 5.1). After 8 hours exposure, there was no longer any elevation of *WWOX* expression compared to baseline for the cells exposed to 100 units/ml, but the expression in the cells exposed to 200 and 400 units/ml was still elevated (figure 5.1), although starting to decrease. These findings suggest that hyaluronidase induces expression of *WWOX* and that this effect is greater after 4 hours of exposure than after 8 hours of exposure.

Figure 5.1: *WWOX* mRNA expression in wild-type HCT116 cells following 4 and 8 hours of hyaluronidase exposure

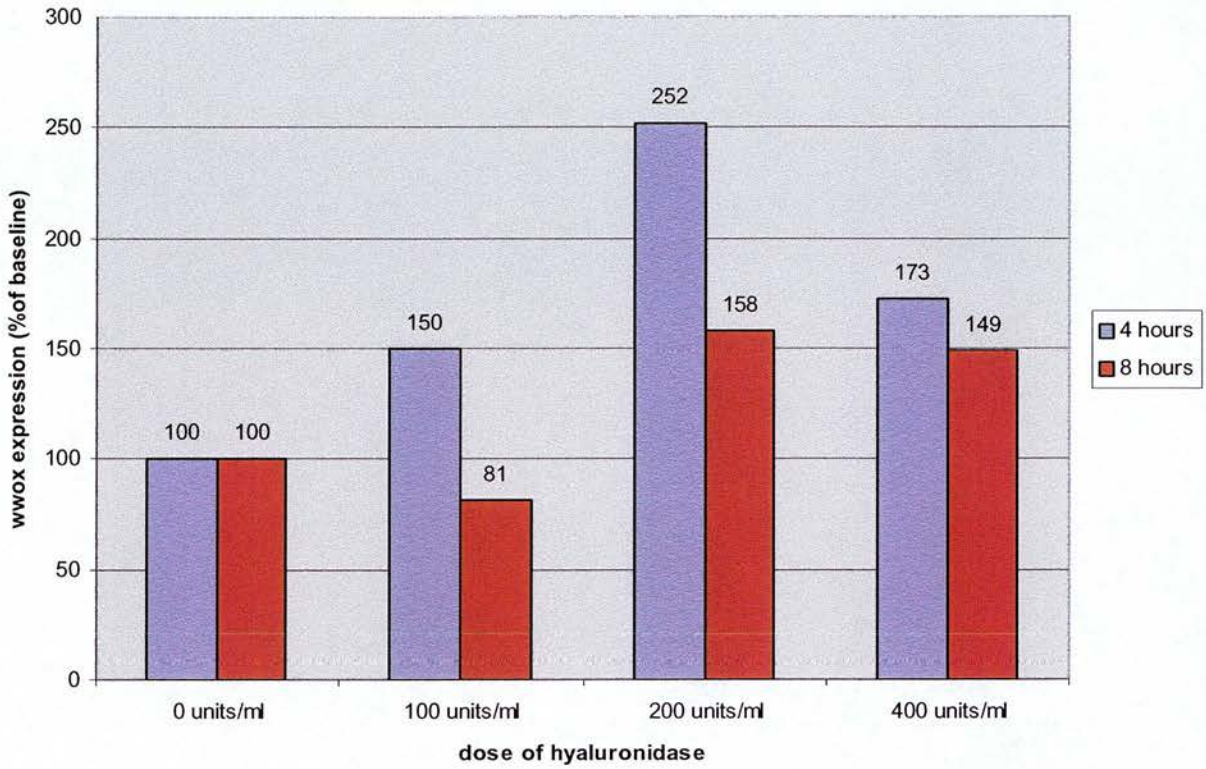

ACTIN-corrected *WWOX* expression following exposure of wild-type HCT116 colorectal cancer cells to 0, 100, 200 and 400units/ml of hyaluronidase for 4 or 8 hours. cDNA was isolated from hyaluronidase-exposed wild-type HCT116 cells and the levels of *WWOX* and β-*ACTIN* gene expression was quantified using the Lightcycler®. This allowed calculation of the *ACTIN*-corrected *WWOX* expression. All values were normalised relative to untreated cells at that timepoint. This experiment was not repeated and the results must be considered as hypothesis generating rather than hypothesis proving.

5.1.2 *WWOX* mRNA expression in hyaluronidase-exposed p53-null HCT116 cells

WWOX levels were also quantified in p53-null HCT116 cells exposed to the same hyaluronidase concentrations (100, 200 or 400 units/ml), again for 4 or 8 hours. No effect on *WWOX* mRNA expression was seen at any dose of hyaluronidase for either duration of exposure (figure 5.2). These data indicate that hyaluronidase induces expression of *WWOX* mRNA in the HCT116 colorectal cancer cell line but not in a p53-null derivative of that line. This suggests that functional p53 may be required for hyaluronidase-induced *WWOX* expression in HCT116 cells.

Figure 5.2: *WWOX* mRNA expression in p53-null HCT116 cells following 4 and 8 hours of hyaluronidase exposure

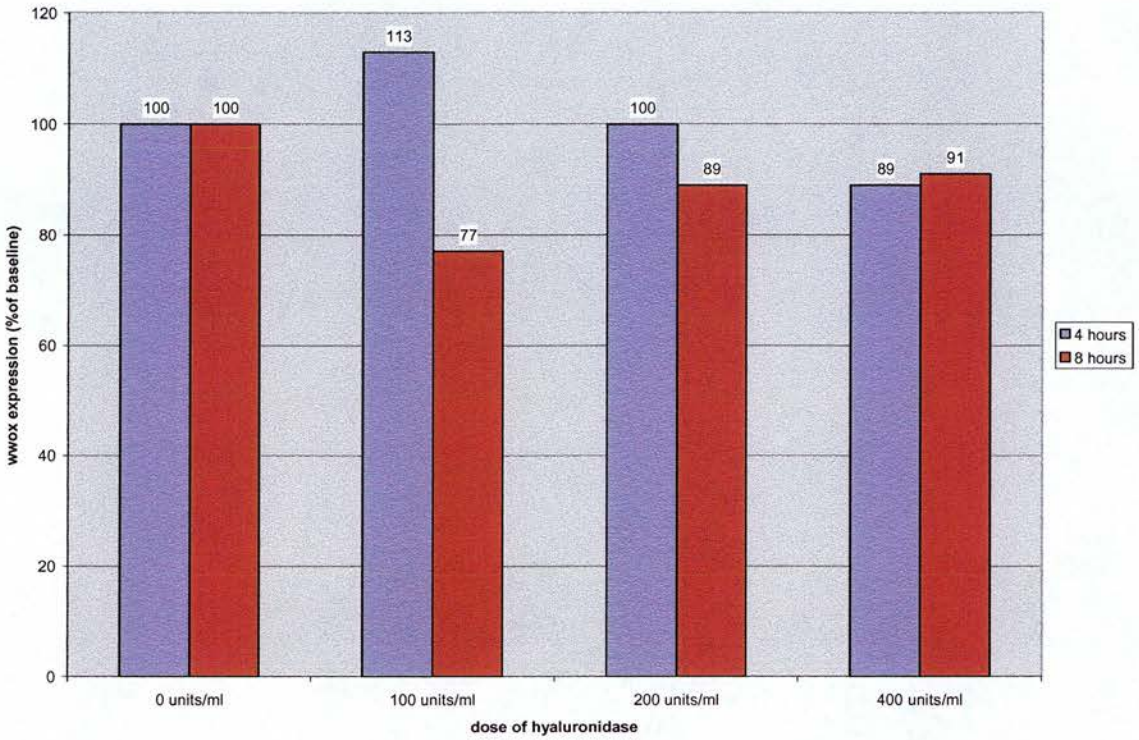

ACTIN-corrected *WWOX* expression following exposure of p53-null HCT116 colorectal cancer cells to 0, 100, 200 and 400units/ml of hyaluronidase for 4 or 8 hours. cDNA was isolated from hyaluronidase-exposed p53-null HCT116 cells and the levels of *WWOX* and β-*ACTIN* gene expression was quantified using the Lightcycler®. This allowed calculation of the *ACTIN*-corrected *WWOX* expression. All values normalised relative to untreated cells at that timepoint. This experiment was not repeated and the results must be considered as hypothesis generating rather than hypothesis proving.

5.2 Hyaluronidase does not induce *WWOX* mRNA expression in PEO1 cells (p53 mutant)

The expression of *WWOX* mRNA in PEO1 cells (which contain a mutant p53) that were exposed to the same 3 doses of hyaluronidase (100, 200 or 400 units/ml) for 4 or 8 hours was also quantified. As with p53-null HCT116 cells no significant effect on *WWOX* mRNA expression was seen at any dose of hyaluronidase for either duration of exposure (figure 5.3). This is consistent with the previous results for HCT116, as PEO1 has mutant p53, and again suggests that *WWOX* induction by hyaluronidase may be p53-dependent.

Figure 5.3: *WWOX* mRNA expression in PEO1 cells following 4 and 8 hours of hyaluronidase exposure

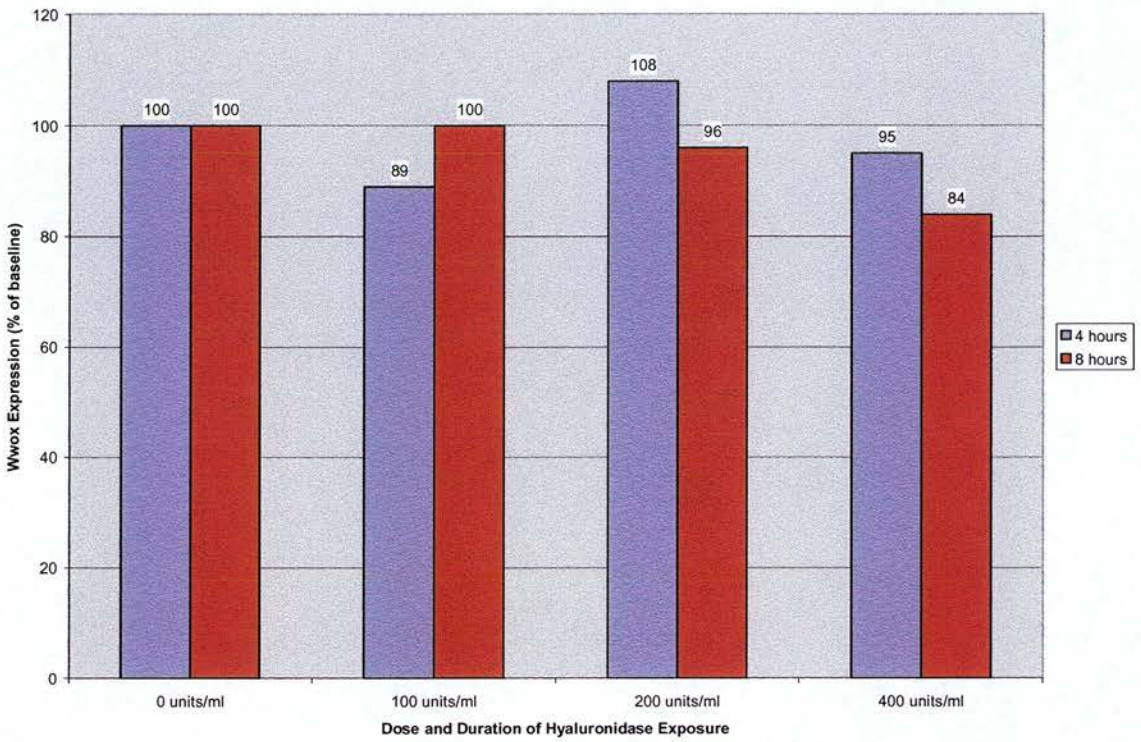

ACTIN-corrected *WWOX* expression following exposure of PEO1 ovarian cancer cells to 0, 100, 200 and 400units/ml of hyaluronidase for 4 or 8 hours. cDNA was isolated from hyaluronidase-exposed PEO1 cells and the levels of *WWOX* and β-*ACTIN* gene expression was quantified using the Lightcycler®. This allowed calculation of the *ACTIN*-corrected *WWOX* expression. All values were normalised relative to untreated cells at that timepoint. This experiment was not repeated and the results must be considered as hypothesis generating rather than hypothesis proving.

5.3 Induction of *WWOX* mRNA expression by cytotoxic agents is partially p53-dependent and partially p53-independent

As *WWOX* induction by hyaluronidase appeared to be p53-dependent, we investigated whether inducers of p53 expression would also induce expression of *WWOX* mRNA. Therefore, the expression of *WWOX* in the wild-type and p53-null variant of the HCT116 colorectal cancer cell line was quantified following exposure to doxorubicin, oxaliplatin and 5-fluorouracil. Doxorubicin is an anthracycline cytotoxic agent that intercalates between DNA base pairs resulting in conformational changes in DNA structure and changes in the activity of topoisomerases. Its complete mechanism of action is not known but it has been shown to increase p53 expression [193]. Oxaliplatin is a platinum-based chemotherapeutic agent that acts through the formation of platinum-DNA adducts, which block DNA replication [46]. It has been shown to induce p53 expression [194]. 5-fluorouracil inhibits thymidylate synthase and is incorporated into nuclear and cytoplasmic RNA, interfering with normal RNA processing and function [46]. It too has been shown to induce expression of p53 in human cancer cell lines [194].

5.3.1 *WWOX* mRNA expression in cytotoxic-exposed p53 normal HCT116 cells

Expression levels of *WWOX* mRNA were quantified in wild-type (wt) HCT116 cells exposed to 200nM doxorubicin, 8μM oxaliplatin or 20μM 5-fluorouracil for 24 or 48

hours. After 24 hours, *WWOX* expression had increased 3-fold in the cells treated with doxorubicin but there was no change in expression in the cells exposed to oxaliplatin or 5-fluorouracil (figure 5.4). After 48 hours exposure, *WWOX* expression in doxorubicin-exposed cells remained 3-fold greater compared to untreated cells. Expression in the 5-fluorouracil-exposed cells was unchanged (figure 5.4) but at this later time point *WWOX* expression in oxaliplatin-exposed cell lines increased to almost 5 times that of the untreated cells.

Figure 5.4: *WWOX* mRNA expression in p53 normal (wild-type) HCT116 cells following 24 and 48 hours of exposure to cytotoxic agents

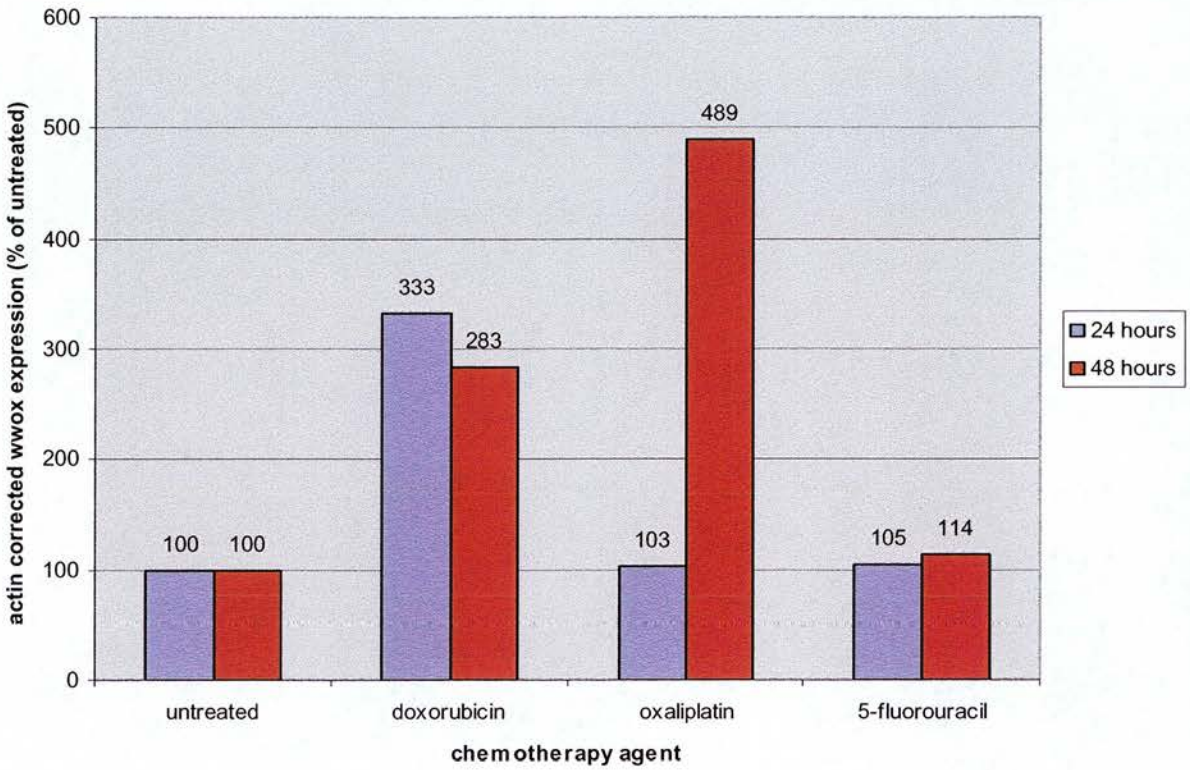

ACTIN-corrected *WWOX* expression following exposure of wild-type HCT116 colorectal cancer cells to doxorubicin, oxaliplatin and 5-fluorouracil for 24 or 48 hours. cDNA was isolated from drug-exposed wild-type HCT116 cells and the levels of *WWOX* and β-*ACTIN* gene expression was quantified using the Lightcycler®. This allowed calculation of the *ACTIN*-corrected *WWOX* expression. All values normalised relative to untreated cells at that timepoint. This experiment was not repeated and the results must be considered as hypothesis generating rather than hypothesis proving.

5.3.2 *WWOX* mRNA expression in cytotoxic-exposed p53-null HCT116 cells

WWOX induction was then tested in p53-null HCT116 cells exposed to the same doses of doxorubicin, oxaliplatin and 5-fluorouracil. Again, the only cells with

induction of *WWOX* after 24 hours (figure 5.5) were those exposed to doxorubicin. The effect was much less than in the p53 wt cells (an increase of only about 50% in expression as opposed to 200% in the p53 wt cells). After 48 hours (figure 5.5), the *WWOX* expression in the doxorubicin-treated cells approached the level seen after 24 hours in the p53 normal cells. Induction after 48 hours of exposure to oxaliplatin was less than 50% of that in the p53 normal line. Again there was no induction in the cells exposed to 5-fluorouracil at either time point.

Figure 5.5: *WWOX* mRNA expression in p53-null HCT116 cells following 24 and 48 hours of exposure to cytotoxic agents

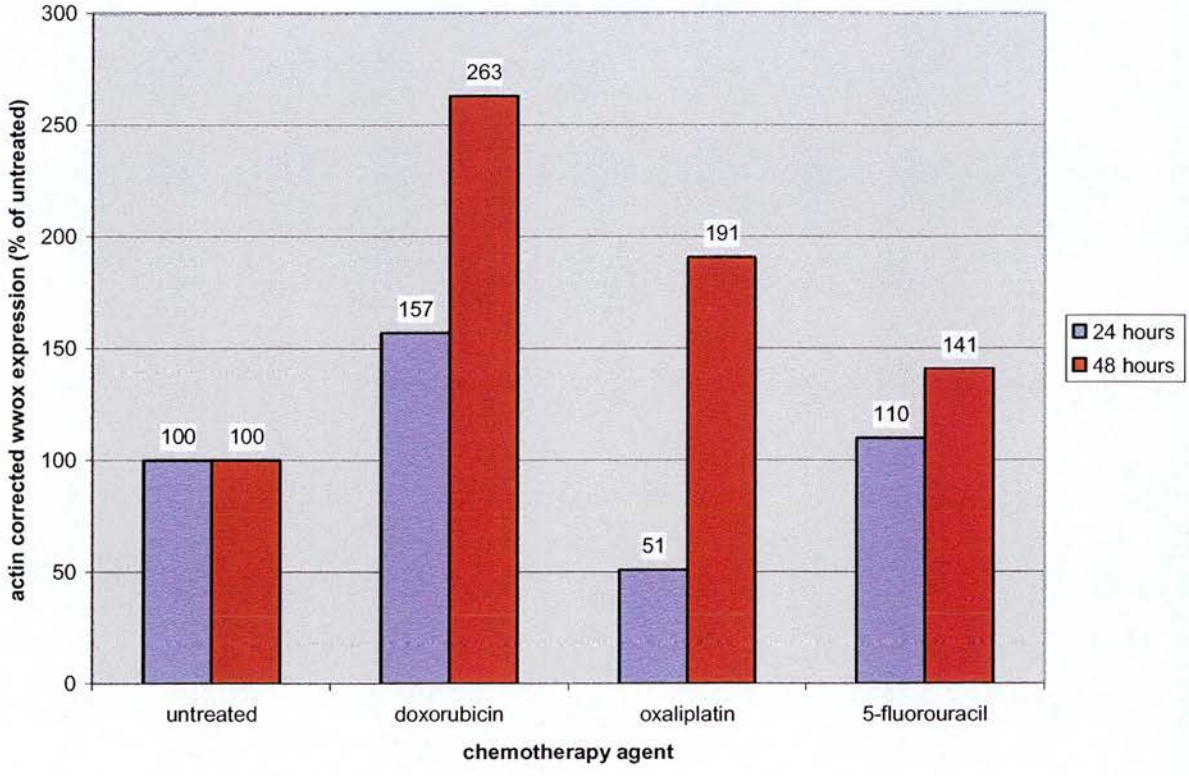

ACTIN-corrected *WWOX* expression following exposure of p53-null HCT116 colorectal cancer cells to doxorubicin, oxaliplatin and 5-fluorouracil for 24 or 48 hours. cDNA was isolated from drug-exposed p53-null HCT116 cells and the levels of *WWOX* and β-*ACTIN* gene expression was quantified using the Lightcycler®. This allowed calculation of the *ACTIN*-corrected *WWOX* expression. All values normalised relative to untreated cells at that timepoint. This experiment was not repeated and the results must be considered as hypothesis generating rather than hypothesis proving.

5.3.3 Comparison of *WWOX* mRNA induction profile in cytotoxic-exposed p53 wt and p53-null HCT116 cells

The profile of *WWOX* induction is different in the p53 normal and p53-null HCT116 colorectal cancer cells (figure 5.6). The response to all agents appears to be blunted in the p53-null cells compared with p53 normal cells. The response to doxorubicin (in terms of *WWOX* induction) reaches almost the same level in the p53-null cells but takes 48 hours rather than 24 hours to do so. The level of induction induced by oxaliplatin at 48 hours in the p53-null cells is less than half that in the p53 wild-type cells. Assuming that the main difference between these cell lines is their p53 status (the p53-null cell line is a derivative of the p53 normal HCT116 line; however, clonal heterogeneity could also be a factor) this suggests that there is both a p53-dependent pathway of *WWOX* induction (that acts early in the case of doxorubicin) and a p53-independent pathway of *WWOX* induction.

Figure 5.6: *WWOX* mRNA induction profile in wild-type and p53-null HCT116 cells following 24 and 48 hours of cytotoxic exposure

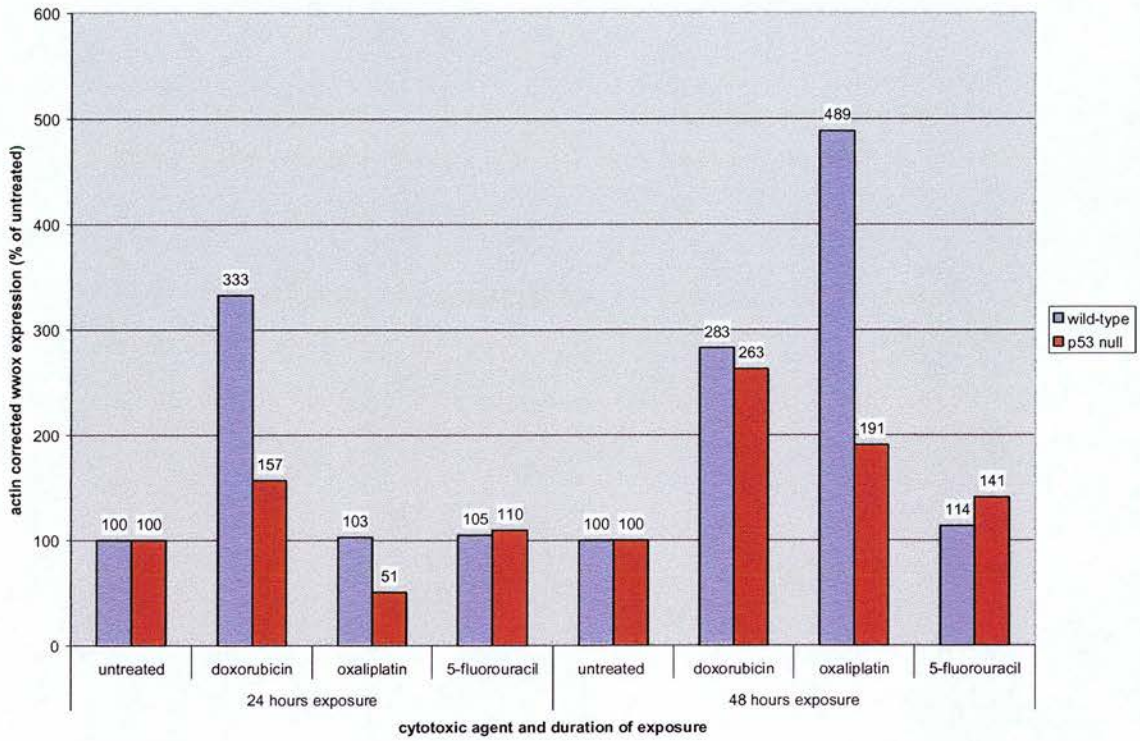

ACTIN-corrected *WWOX* expression following exposure of p53 wild-type and p53-null HCT116 colorectal cancer cells to doxorubicin, oxaliplatin and 5-fluorouracil for 24 or 48 hours. cDNA was isolated from drug-exposed wild-type and p53-null HCT116 cells and the levels of *WWOX* and β-*ACTIN* gene expression was quantified using the Lightcycler®. This allowed calculation of the *ACTIN*-corrected *WWOX* expression. All values normalised relative to untreated cells at that timepoint. This experiment was not repeated and the results must be considered as hypothesis generating rather than hypothesis proving.

5.4 Evaluation of results

The aim of this section of the study was to use the real-time PCR techniques that we had optimised for the *WWOX* gene to determine whether the induction of Wox1 by hyaluronidase demonstrated in L929 murine fibroblasts [168] also occurred for human *WWOX* in human cancer cells. The reason for using the HCT116 colorectal cancer cell line in an ovarian cancer-based project was the availability of well-characterised isogenic wild-type, p53-null, p21-null and BAX-null derivatives of this cell line.

It is important to note that although all drug exposures were performed in duplicate, these experiments were not repeated on separate occasions. This limits the conclusions that can be drawn from the findings and they have to be considered as hypothesis-generating rather than hypothesis-proving.

It was shown that exposure of wild-type HCT116 colorectal cancer cells to hyaluronidase resulted in a maximal *WWOX* induction of 150% (coincidentally the same figure demonstrated by Chang et al [168] in hyaluronidase-exposed L929 murine fibroblasts) but that there was no induction in p53-null HCT116 colorectal cancer cells. This suggests that induction of *WWOX* by hyaluronidase may be p53-dependent. Although an attractive hypothesis (because it would fit with *WWOX* acting as a tumour suppressor) further supporting evidence would be required. In a crude attempt to show that there was no induction in a p53 mutant cell line, the same experiment was repeated in PEO1 ovarian cancer cells. Again there was no induction of *WWOX* but because this was a completely different cell line system, the loss of *WWOX* induction may have been secondary to any number of differences between this cell line and the HCT116 colorectal cancer cell line.

As preliminary evidence suggested that *WWOX* induction may be p53-dependent it was decided to investigate whether induction of p53 using cytotoxic agents would result in *WWOX* up-regulation. It was indeed shown that *WWOX* was induced in wild-type HCT116 colorectal cancer cells following exposure to doxorubicin and oxaliplatin (but not 5-fluorouracil) and that the level of induction in the p53-null HCT116 colorectal cancer cell line was decreased and perhaps also delayed. A serious limitation of this approach, however, is the fact that a variety of alterations in gene expression (not just p53 induction) will occur following exposure of cancer cells to these cytotoxic agents. One could argue that the differences seen in induction between the wild-type and p53-null HCT116 colorectal cancer cell lines is as a direct result of their differing p53 status but inevitably there will be other genetic differences between these supposedly isogenic lines (due to passage since creation of the variants).

Although these experiments provide interesting hypotheses concerning the possible role of p53 in *WWOX* induction, they require to be replicated and to be extended before meaningful conclusions can be drawn. As these experiments are upstream of *WWOX* function and do not directly address the aims of the PhD project (section 1.10) they were not taken forward in the course of this work.

6. RESULTS: MANIPULATION OF *WWOX* EXPRESSION LEVELS IN HUMAN CANCER CELL LINES

6.1 Cell lines and constructs used in *WWOX* transfections

In order to identify a phenotype for the *WWOX* gene, manipulation of *WWOX* expression levels was carried out in the HCT116 colorectal cancer cell line and the PEO1 and A2780 ovarian cancer cell lines.

HCT116 was one of the cell lines found to have a homozygous deletion in the *WWOX* gene, although this transpired to be contained entirely within intron 8. HCT116 expresses full-length *WWOX* (isoform 1), *WWOX* Δ6-8 (isoform 4) as well as probably (on size criteria) exon 7 skipped and exon 7-8 skipped forms of the gene (section 3.3.4). Although HCT116 was a colorectal cancer cell line (as opposed to an ovarian cell line), it was chosen because of evidence suggesting that murine Wox1 was required for p53-mediated apoptosis and that it may physically interact with murine p53 [168]. HCT116 has well characterised wild-type, p53-null, p21-null and Bax-null cell lines that would lend themselves to phenotypic analysis if a functional *WWOX* pathway was found in this cell line.

PEO1 is an ovarian cancer cell line [163] that has homozygous deletions in exon 4-8 of *WWOX* [53]. It expresses a truncated Δ4-8 transcript and no full-length *WWOX*. PEO1 expresses mutant p53.

A2780 is an ovarian cancer cell line that expresses full-length *WWOX* (isoform 1) and *WWOX* Δ6-8 (isoform 4). It expresses wild-type p53.

To investigate the effects of up and downregulated levels of *WWOX*, these cell lines were transfected with the following constructs:

i) 'A' (3' UTR antisense) construct: pcDNA3.1 plasmid containing an insert designed to express a transcript complementary to part of the *WWOX* 3' UTR.

ii) 'D' (full-length antisense) construct: pEF6 plasmid containing an insert designed to express a transcript complementary to the *WWOX* coding region.

iii) 'H' (sense) construct: pEF6 plasmid containing an insert designed to express a transcript identical to the *WWOX* coding region.

iv) 'E' (pcDNA3.1 vector) construct: pcDNA3.1 plasmid with no insert.

v) 'F' (pEF6 vector) construct: pEF6 plasmid with no insert.

For ease of understanding, cells transfected with the 3' UTR construct will be termed 'A' transfectants, those transfected with the full-length antisense construct will be termed 'D' transfectants and those transfected with the sense construct will be termed 'H' transfectants. Cells transfected with the pcDNA3.1 vector alone (no insert) will be termed 'E' transfectants and cells transfected with the pEF6 vector alone will be termed 'F' transfectants.

6.2 Screening of WWOX expression levels in HCT116 antisense transfectants

6.2.1 Screening using conventional PCR

DNA was isolated from HCT116 cells transfected with the construct expressing the antisense transcript targeting the *WWOX* 3'UTR ('A' construct). PCR amplification of the neomycin resistance gene was used to confirm vector incorporation. 22 out of 24 clones were positive for the presence of the vector. RT-PCR was then performed

on these samples using primers 8F2 (in *WWOX* exon 8) and Z2 (in *WWOX* exon 9) to determine levels of *WWOX* expression. Figure 6.1 shows that *WWOX* was still being expressed in these transfectants, indicating that antisense targeting of the 3' UTR did not induce complete knockout of *WWOX*. There was some minor variation in band intensity suggesting that *WWOX* expression was greater in the parent line than in the antisense transfectants, the significance of which was difficult to determine in a saturated PCR.

Figure 6.1: No complete knockout of *WWOX* using the antisense construct targeting the 3'UTR

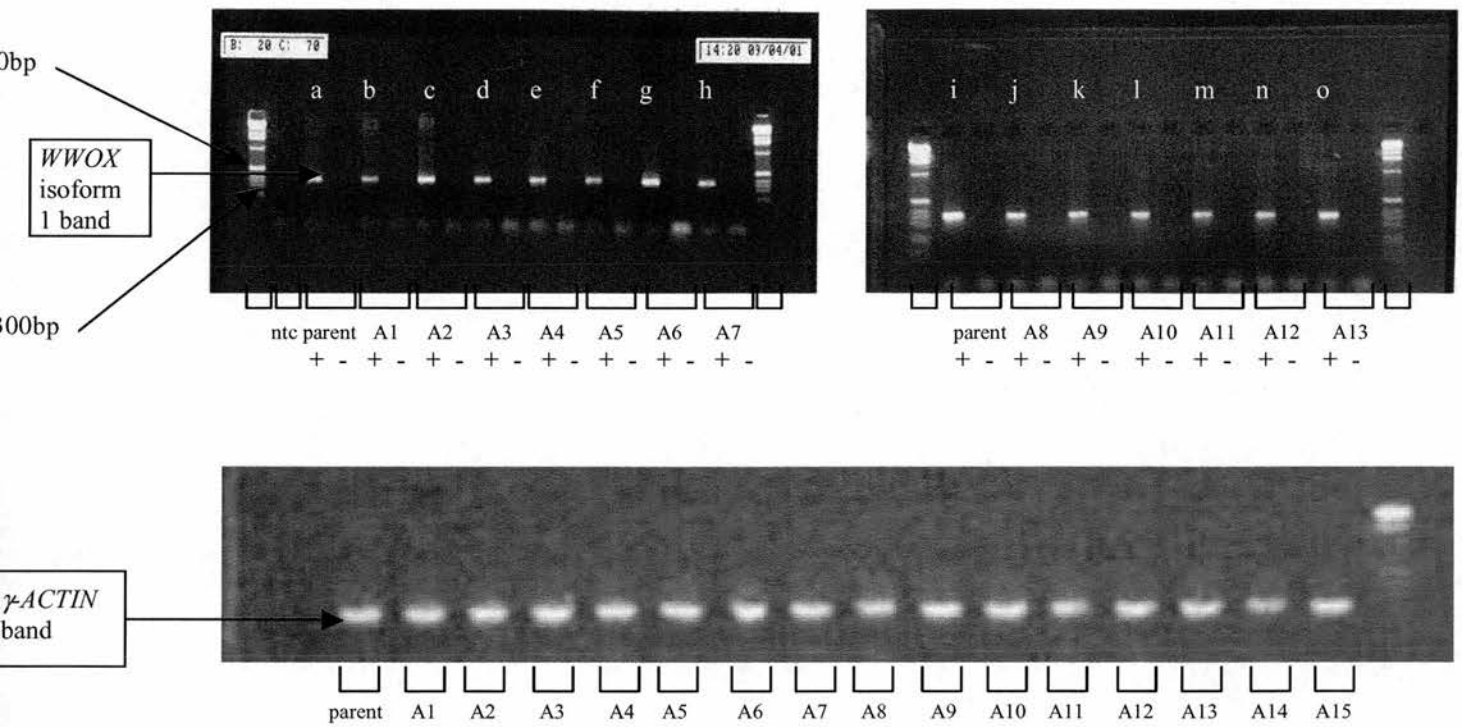

2% agarose gels showing RT-PCR products from *WWOX* specific PCRs (top 2 gels) and *γ-ACTIN* specific PCRs (bottom gel) using cDNA from HCT 116 antisense (A) transfectants as template. The antisense molecule in the A transfectants is directed against the 3'UTR. In the top 2 gels, the first and last lanes contain a 1kb DNA ladder. The other lanes contain PCR products from the *WWOX* specific 8F2/Z2 PCR for alternating postive and negative RT samples. The lane contents are labelled for the positive RT samples as follows: a HCT116 parent line; b HCT116 A1; c HCT116 A2; d HCT116 A3; e HCT116 A4; f HCT116 A5; g HCT116 A6; h HCT116 A7; i HCT116 parent line; j HCT116 A8; k HCT116 A9; l HCT116 A10; m HCT116 A11; n HCT116 A12; o HCT116 A13. There is little difference between the intensity of the *γ-ACTIN* band for the various transfectants and the parent line (which is again the first sample; bottom gel), although the PCRs are saturated.

As none of the transfectants containing the *WWOX* 3'UTR antisense (A) construct showed complete knockout of *WWOX* expression on the basis of RT-PCR, confirmation that the antisense insert of construct A was being expressed was required. RT-PCR was carried out using a forward primer within the *WWOX* 3'UTR (IM19R) and a reverse primer exclusive to a contiguous transcribed region of the vector construct (BGHrev). This revealed that 24 out of 27 of the transfectants expressed the antisense construct.

Incomplete knockout of *WWOX* expression was also seen in HCT116 cells transfected with the full-length antisense (D) construct targeting the WWOX coding region (figure 6.2). Variability in levels of *WWOX* expression was more obvious in this non-quantitative PCR with most of the transfectants apparently expressing *WWOX* at lower levels than the parent line.

The fact that no complete knockout of expression had been achieved was disappointing. However, as the HCT116 cell line does express full-length *WWOX*, it was felt that even partial knockout may allow identification of a phenotype. It was therefore decided to quantify the degree of *WWOX* knockout by quantitative RT-PCR and if it was significant then to proceed to phenotypic assays with these transfectants.

Figure 6.2: Potential partial knockout of *WWOX* expression

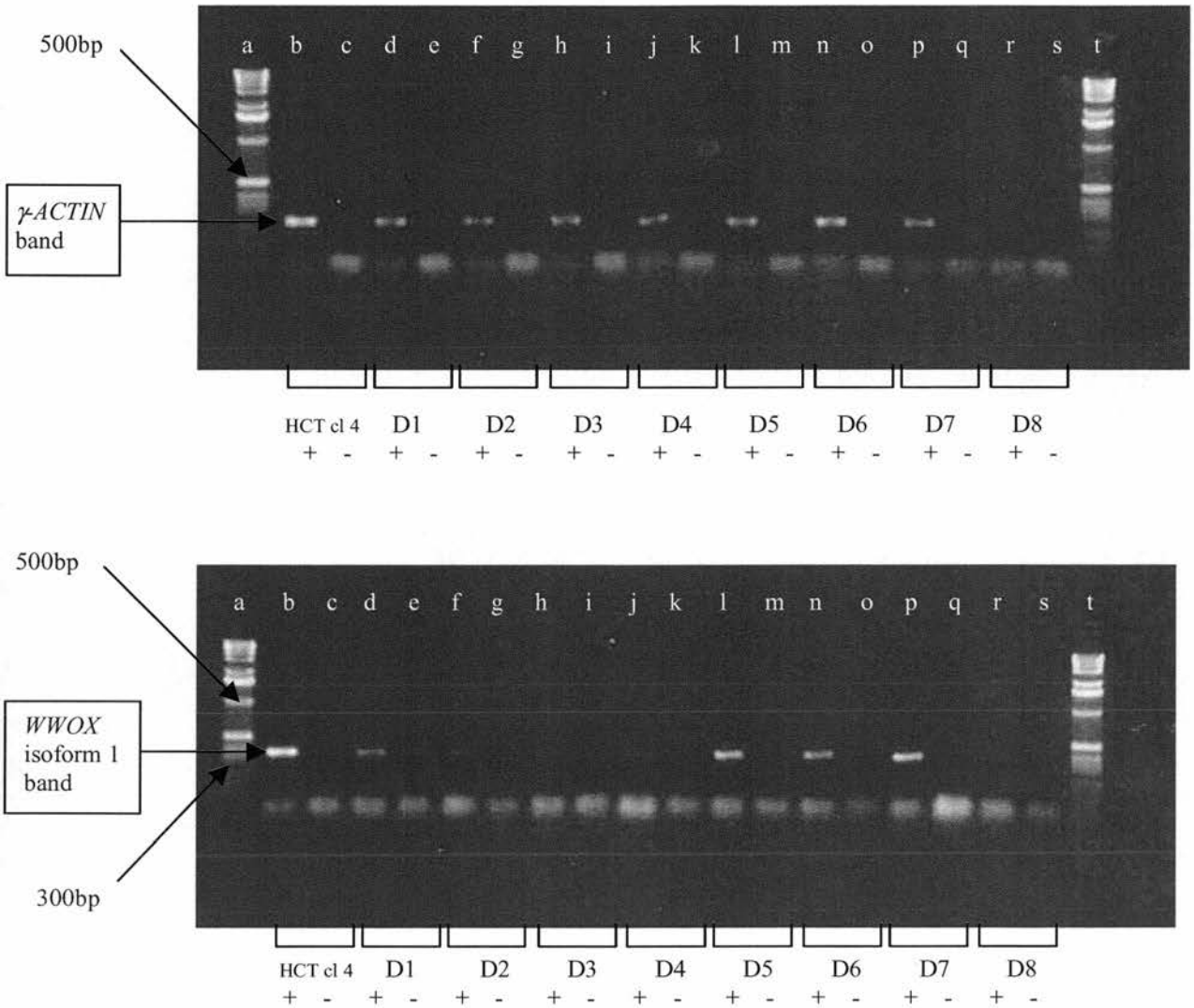

2% agarose gels showing RT-PCR products from *γ-ACTIN* specific PCRs (top gel) and *WWOX* specific PCRs using cDNA from HCT 116 antisense (D) transfectants as template. The antisense molecule in the D transfectants is directed against the whole *WWOX* coding region. The bottom gel shows *WWOX* RT-PCR products from the same cDNA sources. The templates are as follows: lanes c, e, g, i, k, m, o, q and s contain –ve RT template; lane b contains HCT116 clone 4 cDNA; lanes d, f, h, j, l, n, p and r contain cDNA from HCT116 D1-D8 transfected clones respectively. Lanes a and t contain 1kb DNA ladder.

6.2.2 Screening using quantitative RT-PCR

As there was a suggestion from conventional PCR that some of the HCT116 full-length antisense (D) transfectants had reduced *WWOX* expression, these 17 clones and the parent cell line were analysed using real-time PCR on the Lightcycler® (figure 6.3). The LC1F and LC1R primer pair (both located in exon 9) was used to quantify *WWOX* and the expression levels were normalised with respect to *β-ACTIN*.

Figure 6.3: *WWOX* expression in HCT116 antisense (D) transfectants

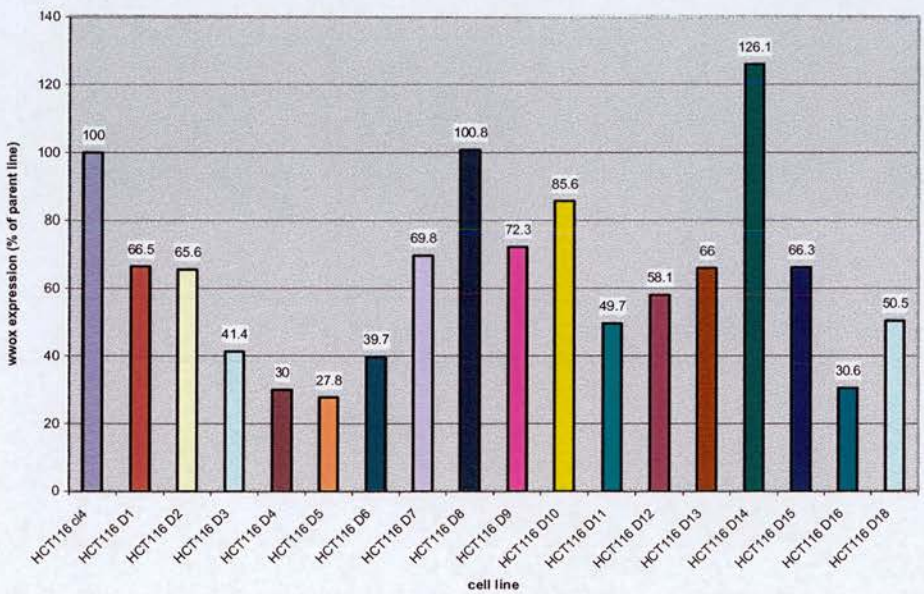

ACTIN-corrected *WWOX* expression in HCT116 antisense (D) transfectants. cDNA was prepared from cultured cells and the levels of *WWOX* and β-*ACTIN* gene expression was quantified in triplicate using the Lightcycler®. This allowed calculation of the *ACTIN*-corrected *WWOX* expression. *WWOX* expression in all the transfectants (D1-16, D18) is expressed as a percentage of the *WWOX* expression in the HCT116 cl4 parent line. This was an initial screening exercise to identify transfected cell lines suitable for phenotypic analysis. Quantification of *WWOX* expression in repeated independent preparations of cDNA for a particular cell line was only performed for cell lines used in phenotypic analyses and is demonstrated in later chapters with resultant error bars inserted.

All but 2 of the transfectant clones (D8 and D14) expressed *WWOX* at between 28% and 86% of the level of the parent line. Although greater *WWOX* knockout would have been desirable for the purposes of phenotypic assays, 3 clones with expression levels of approximately 30% of the parent line (D4, D5 and D16) were selected for phenotypic analysis. The D2 clone with an intermediate level of *WWOX* expression was also used in functional experiments to see if there was any evidence of an intermediate phenotype.

The level of *WWOX* expression in four HCT116 vector-only (F) transfectants was also analysed on the Lightcycler® (figure 6.4) using the same primer pair to ensure that they were suitable controls. They were found to be comparable or expressing slightly higher levels of *WWOX* compared to the parent line. Clones F2 and F4 were used in subsequent phenotypic analysis.

Figure 6.4: *WWOX* expression in HCT116 vector-only (F) transfectants

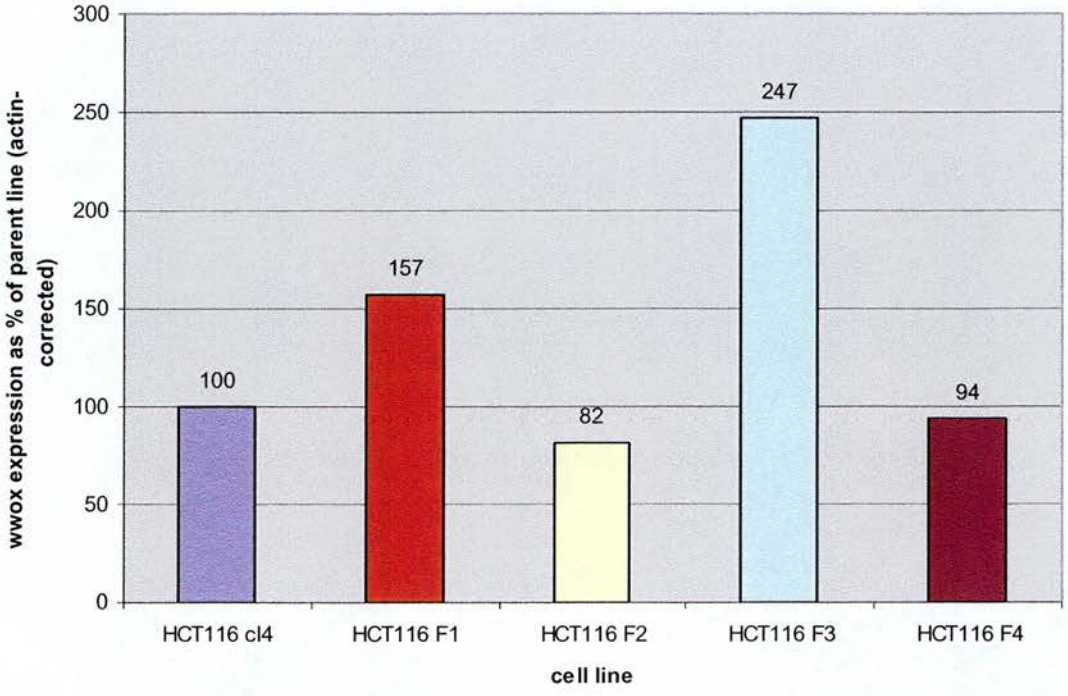

ACTIN-corrected *WWOX* expression in HCT116 vector-only (F) transfectants. cDNA was prepared from cultured cells and the levels of *WWOX* and β-*ACTIN* gene expression was quantified in triplicate using the Lightcycler®. This allowed calculation of the *ACTIN*-corrected *WWOX* expression. *WWOX* expression in all the transfectants (F1-4) is expressed as a percentage of the *WWOX* expression in the HCT116 cl4 parent line. This was an initial screening exercise to identify transfected cell lines suitable for phenotypic analysis. Quantification of *WWOX* expression in repeated independent preparations of cDNA for a particular cell line was only performed for cell lines used in phenotypic analyses and is demonstrated in later chapters with resultant error bars inserted.

6.3 Screening of *WWOX* expression levels in HCT116 sense transfectants

The *WWOX* expression in the parent cell line (HCT116 cl 4) and in 16 sense transfectants (HCT116 H1-8 and HCT116 H31-38) was quantified using the Lightcycler® (figure 6.5). The Z1 and Z2 primer pair (located in exon 9) was used to quantify *WWOX* and the expression levels were corrected for *β-ACTIN*.

The first four clones (H1-4) from the transfection experiment (i.e the first four cell foci to reach a size suitable for transferral to a separate flask) had no upregulation of *WWOX* expression. The next four clones (H5-8) had only minimal upregulation of *WWOX* expression. Some of the slowest growing clones, and the later ones to come through, (H32-36) were found to have the highest level of *WWOX* expression. These latter clones had 7 to 74 fold upregulation of *WWOX* compared to the parent line. Clones H32 to H36 were deemed suitable for further phenotypic analysis.

Figure 6.5: *WWOX* expression in HCT116 sense (H) transfectants

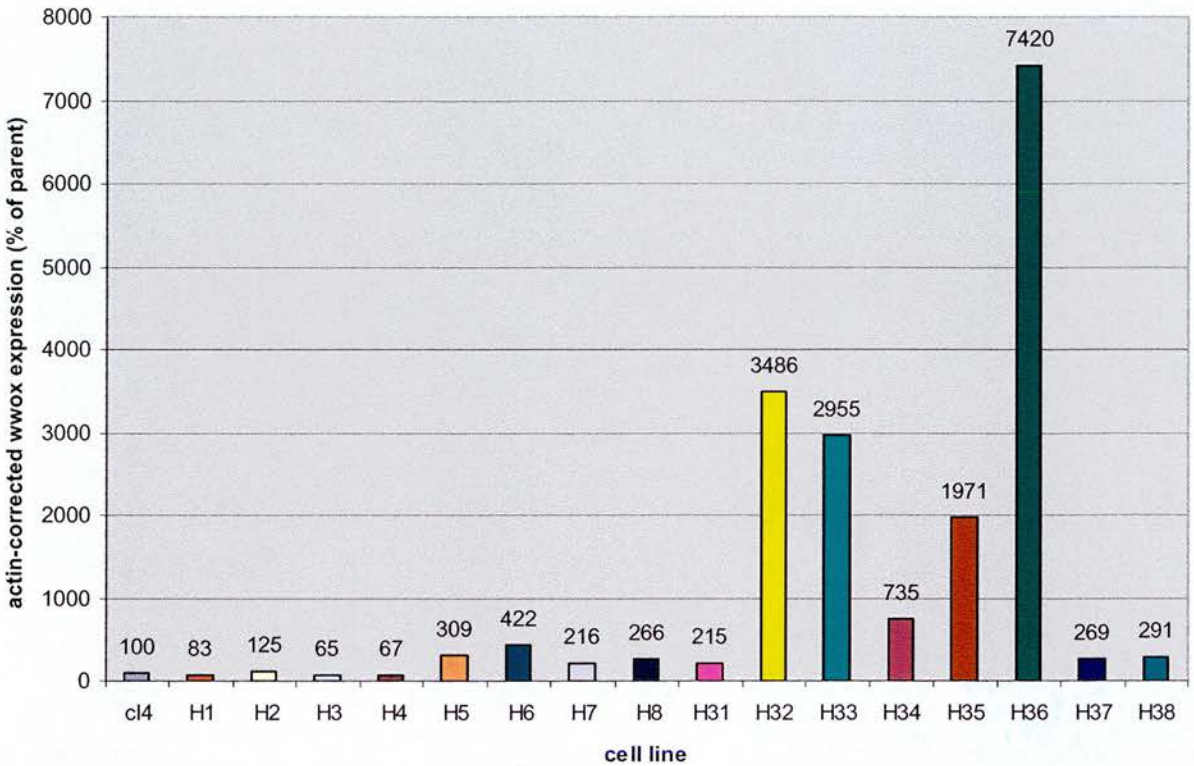

ACTIN-corrected *WWOX* expression in HCT116 sense (H) transfectants. cDNA was prepared from cultured cells and the levels of *WWOX* and β-*ACTIN* gene expression was quantified in triplicate using the Lightcycler®. This allowed calculation of the *ACTIN*-corrected *WWOX* expression. *WWOX* expression in all the sense transfectants (H1-8 and H31-38) is expressed as a percentage of the *WWOX* expression in the HCT116 cl4 parent line. This was an initial screening exercise to identify transfected cell lines suitable for phenotypic analysis. Quantification of *WWOX* expression in repeated independent preparations of cDNA for a particular cell line was only performed for cell lines used in phenotypic analyses and is demonstrated in later chapters with resultant error bars inserted.

6.4 Screening of *WWOX* expression levels in PEO1 antisense transfectants

The *WWOX* expression in the PEO1 hy1.6 parent ovarian cancer cell line and in 9 antisense (D) transfectants (PEO1 D1 and PEO1 D5-12) was quantified using the

Lightcycler® (figure 6.6). Quantification of *WWOX* was performed using the LC1F and LC1R primer pair and the expression levels were corrected for *β-ACTIN*. Clones D6, D7, D8 and D10 showed 55%, 78%, 51% and 37% decreases in *WWOX* expression respectively. As was observed in the HCT116 expression analysis, there were a number of transfects with minimal alteration or even increases in their expression levels.

Again, the level of *WWOX* expression in PEO1 vector-only (F) transfectants was analysed on the Lightcycler® (figure 6.7) using the LC1F and LC1R primer pair to ensure that they were suitable controls. Two of the transfectants (F2 and F4) had comparable *WWOX* expression to the parent line and could be used as control lines in phenotypic assays. The other 4 lines showed increased *WWOX* expression, as had D1 and D5 from the antisense transfection and other vector controls in the HCT116 transfections. Possible explanations for this include clonal heterogeneity of the parent line used for the original transfection and an increase in *WWOX* expression secondary to the integration of the plasmid in the host genome.

Figure 6.6: *WWOX* expression in PEO1 antisense (D) transfectants

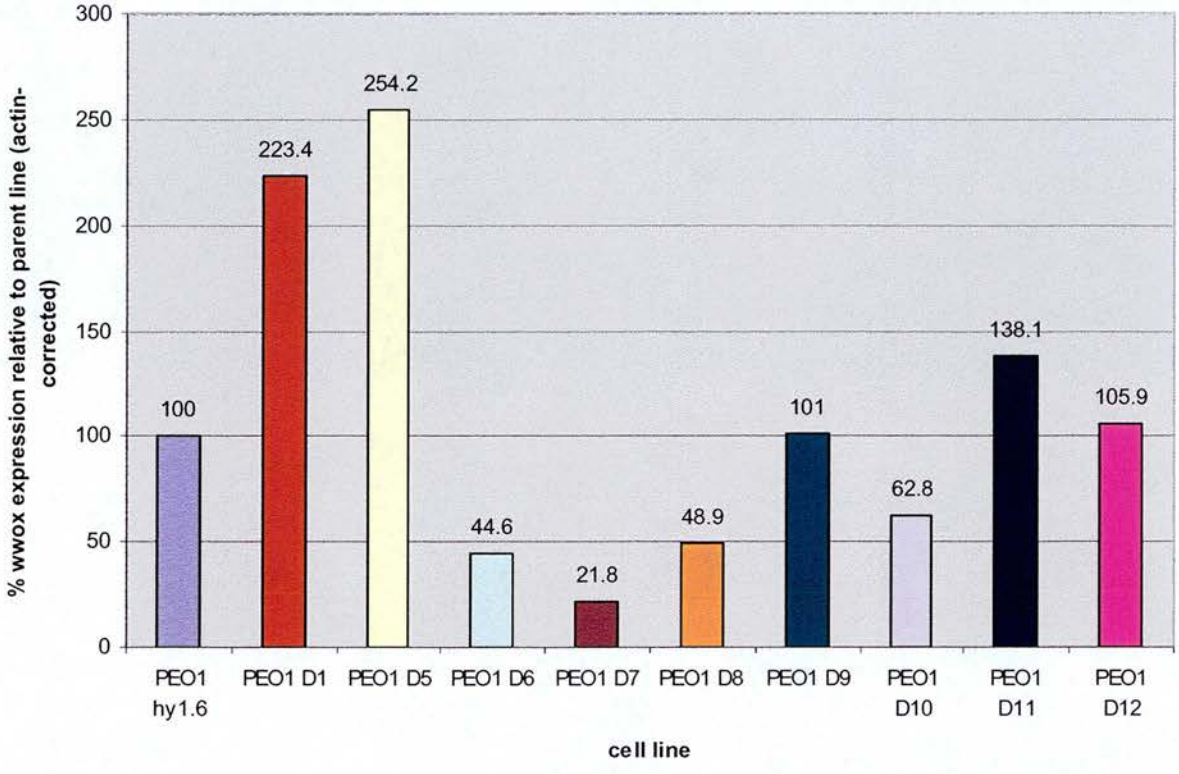

ACTIN-corrected *WWOX* expression in PEO1 antisense (D) transfectants. cDNA was prepared from cultured cells and the levels of *WWOX* and β-*ACTIN* gene expression was quantified in triplicate using the Lightcycler®. This allowed calculation of the *ACTIN*-corrected *WWOX* expression. *WWOX* expression in all the transfectants (D1, D5-12) is expressed as a percentage of the *WWOX* expression in the PEO1 hy1.6 parent line. This was an initial screening exercise to identify transfected cell lines suitable for phenotypic analysis. Quantification of *WWOX* expression in repeated independent preparations of cDNA for a particular cell line was only performed for cell lines used in phenotypic analyses and is demonstrated in later chapters with resultant error bars inserted.

Figure 6.7: *WWOX* expression in PEO1 vector-only (F) transfectants

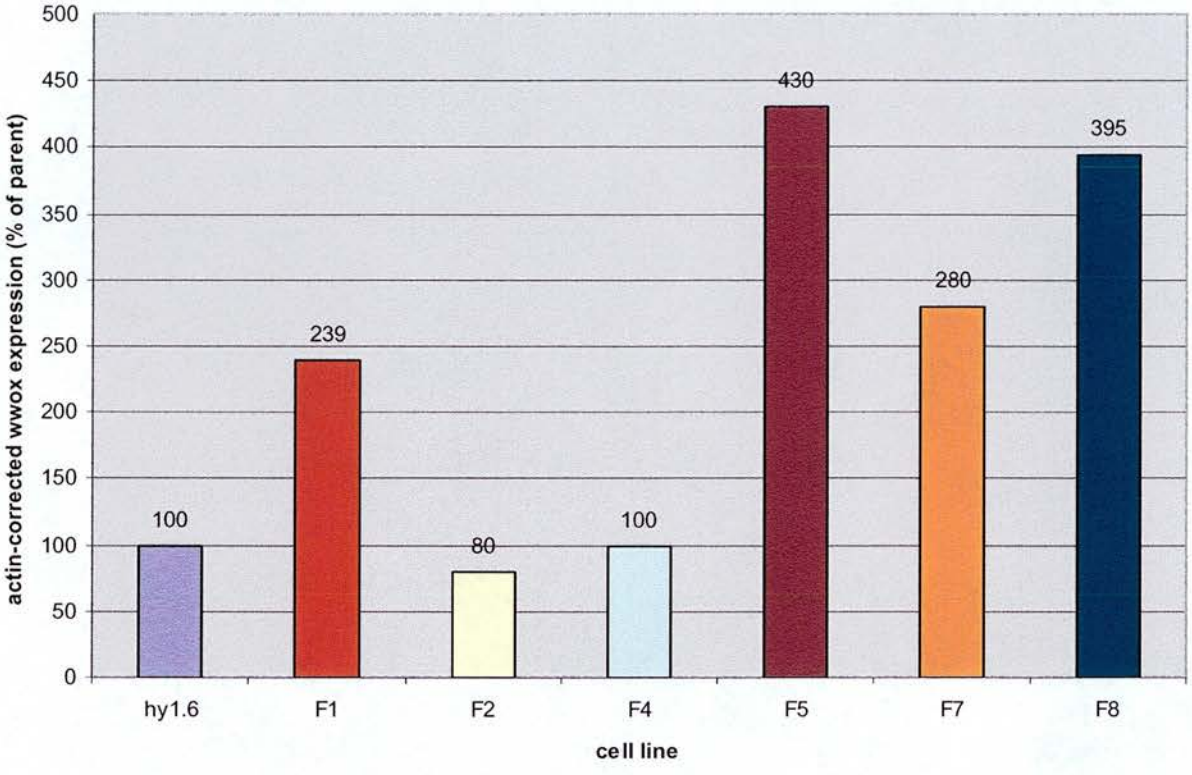

ACTIN-corrected *WWOX* expression in PEO1 vector-only (F) transfectants. cDNA was prepared from cultured cells and the levels of *WWOX* and β-*ACTIN* gene expression was quantified in triplicate using the Lightcycler®. This allowed calculation of the *ACTIN*-corrected *WWOX* expression. *WWOX* expression in all the transfectants is expressed as a percentage of the *WWOX* expression in the PEO1 hy1.6 parent line. This was an initial screening exercise to identify transfected cell lines suitable for phenotypic analysis. Quantification of *WWOX* expression in repeated independent preparations of cDNA for a particular cell line was only performed for cell lines used in phenotypic analyses and is demonstrated in later chapters with resultant error bars inserted.

6.5 Screening of *WWOX* expression levels in PEO1 sense transfectants

As the only *WWOX* transcript present in the PEO1 parent line lacked exons 4-8 (which encode the enzymatic domain of WWOX) it was hoped that this line may be null for WWOX function while still having the rest of its associated functional pathway intact. This would permit reconstitution of the intact pathway and investigation for a functional phenotype by exogenous expression of *WWOX*. The line was therefore transfected with the sense construct encoding the *WWOX* coding region. The level of full-length *WWOX* expression in these cell lines was quantified using the Z1 and Z2 primer pair (located in exon 9) and is shown in figure 6.8 (note the level of *WWOX* expression is plotted on a logarithmic scale).

Figure 6.8: *WWOX* expression in PEO1 sense (H) transfectants (logarithmic scale)

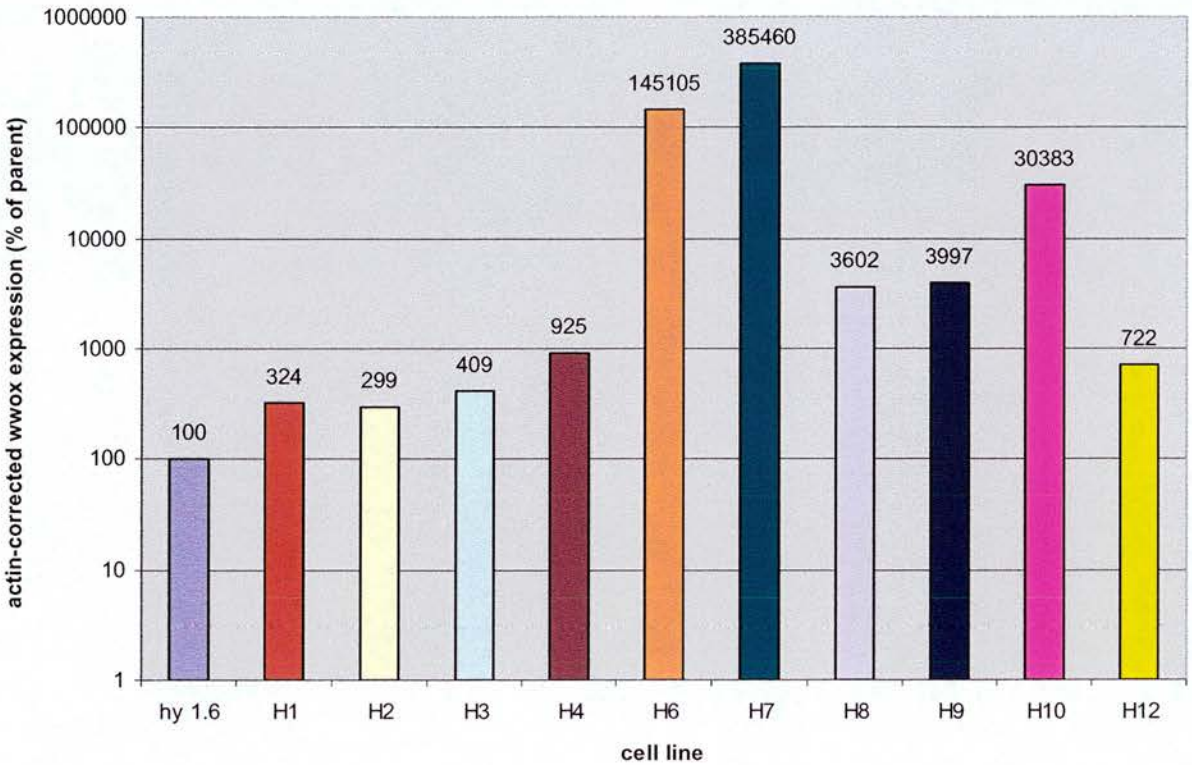

ACTIN-corrected *WWOX* expression in PEO1 sense (H) transfectants. cDNA was prepared from cultured cells and the levels of *WWOX* and β-*ACTIN* gene expression was quantified in triplicate using the Lightcycler®. This allowed calculation of the *ACTIN*-corrected *WWOX* expression. *WWOX* expression in all the transfectants is expressed as a percentage of the *WWOX* expression in the PEO1 hy1.6 parent line. Note that the *WWOX* expression is on a logarithmic scale. This was an initial screening exercise to identify transfected cell lines suitable for phenotypic analysis. Quantification of *WWOX* expression in repeated independent preparations of cDNA for a particular cell line was only performed for cell lines used in phenotypic analyses and is demonstrated in later chapters with resultant error bars inserted.

As previously observed in the HCT116 transfects, the first lines to come through the transfection process had generally lower levels of *WWOX* than the later ones. Lines H4, H6-H10 and H12 expressed full-length *WWOX* at 7 to 3800 times that of the endogenous level of *WWOX* Δ4-8 in the parent line.

To discriminate between endogenous *WWOX* Δ4-8 transcript and exogenous *WWOX*, different primer pairs were used. The LC1F and LC1R primers detect endogenous *WWOX* Δ4-8 transcript only whereas the Z1 and Z2 primer pair detect total (exogenous and endogenous) *WWOX*. Endogenous and total *WWOX* levels are shown in figure 6.9. The difference between these levels represents the level of exogenous *WWOX* transcript in each cell line.

Figure 6.9: Endogenous and total *WWOX* expression in PEO1 sense (H) transfectants

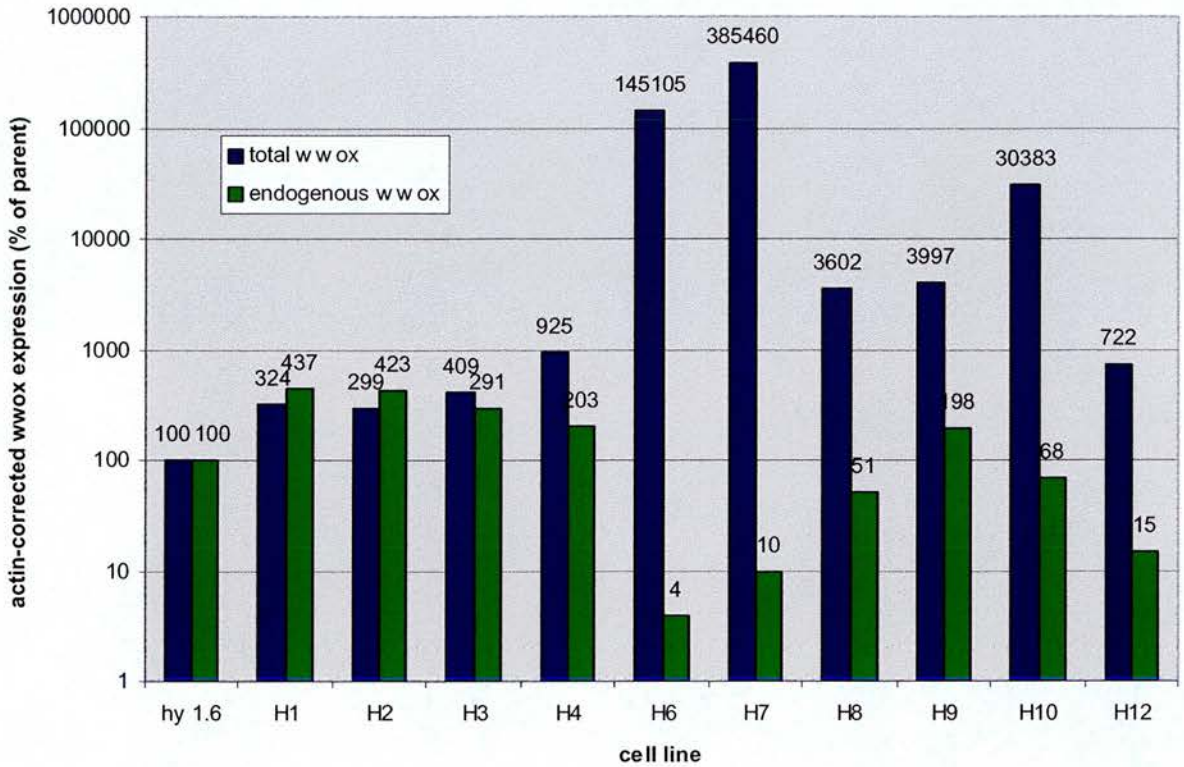

ACTIN-corrected endogenous and total *WWOX* expression in PEO1 sense (H) transfectants. cDNA was prepared from cultured cells and the levels of *WWOX* and β-*ACTIN* gene expression was quantified in triplicate using the Lightcycler®. This allowed calculation of the *ACTIN*-corrected *WWOX* expression. *WWOX* expression in all the transfectants is expressed as a percentage of the *WWOX* expression in the PEO1 hy1.6 parent line. Total *WWOX* expression is shown in blue and endogenous *WWOX* expression is in green. Note that the *WWOX* expression is on a logarithmic scale. This was an initial screening exercise to identify transfected cell lines suitable for phenotypic analysis. Quantification of *WWOX* expression in repeated independent preparations of cDNA for a particular cell line was only performed for cell lines used in phenotypic analyses and is demonstrated in later chapters with resultant error bars inserted.

Figure 6.9 shows that *WWOX* expression in the transfectants H1-3 is almost entirely attributable to endogenous *WWOX*. (This is inkeeping with the finding that PEO1 vector-only controls also seemed to have upregulated *WWOX* expression and suggests that it may have something to do with the transfection/integration process). The other sense transfectants expressed mostly exogenous *WWOX* and in the two most highly expressing clones, H6 and H7 (which were produced as the result of two separate transfection events), the endogenous *WWOX* expression was very low (only 4-10% of the parent line). The H4 to H12 clones were deemed suitable for phenotypic analysis.

6.6 Screening of *WWOX* expression levels in A2780 sense transfectants

The levels of *WWOX* expression were quantified in the A2780 HC2 parent line and in 18 lines that had been transfected with the sense (H) construct (figure 6.10). Three clones (H7, H17 and H20) had highly upregulated levels of *WWOX* (80 to 220 fold upregulated) and would be suitable for phenotypic analysis. The other sense transfectants tended to have lower levels of *WWOX* than the parent line, a feature that was also seen in the vector-only controls (figure 6.11). Quantification of endogenous *WWOX* showed that in these low-expressing sense transfects there was little or no expression of exogenous *WWOX*.

Figure 6.10: *ACTIN*-corrected *WWOX* expression in A2780 sense (H) transfectants

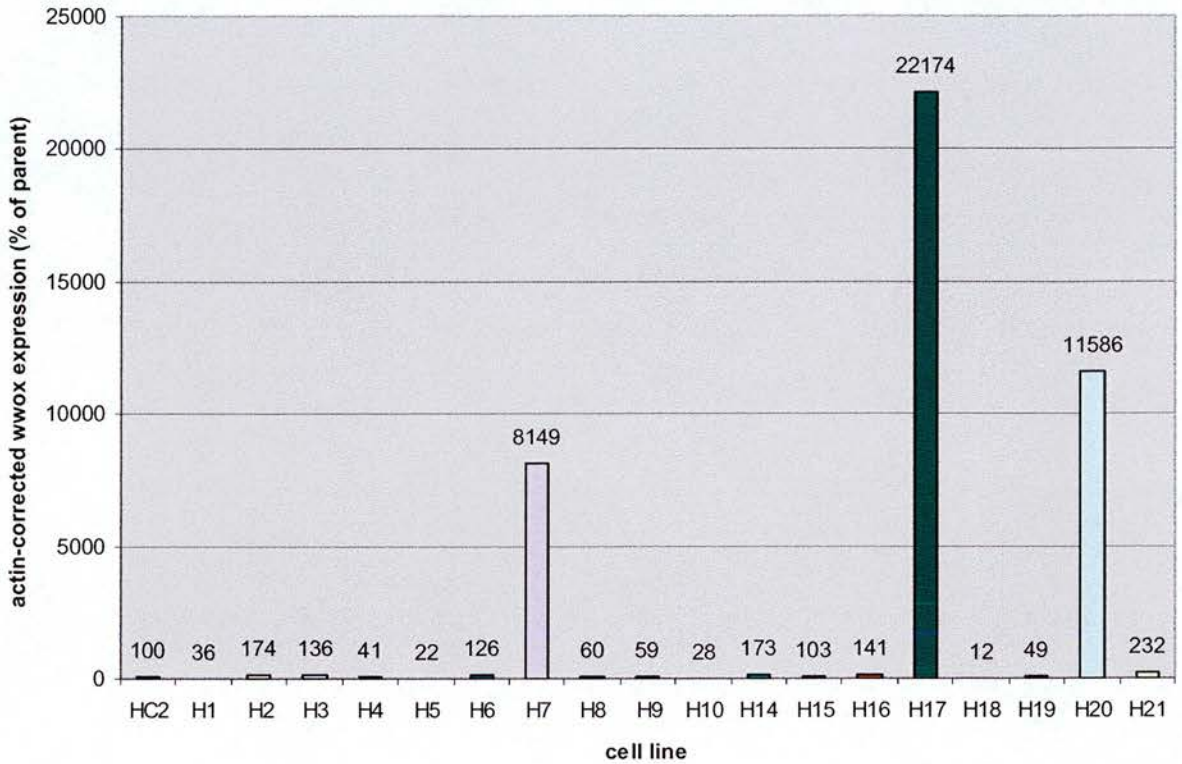

ACTIN-corrected *WWOX* expression in A2780 sense (H) transfectants. cDNA was prepared from cultured cells and the levels of *WWOX* and β-*ACTIN* gene expression was quantified in triplicate using the Lightcycler®. This allowed calculation of the *ACTIN*-corrected *WWOX* expression. *WWOX* expression in all the transfectants is expressed as a percentage of the *WWOX* expression in the A2780 HC2 parent line. This was an initial screening exercise to identify transfected cell lines suitable for phenotypic analysis. Quantification of *WWOX* expression in repeated independent preparations of cDNA for a particular cell line was only performed for cell lines used in phenotypic analyses and is demonstrated in later chapters with resultant error bars inserted.

Figure 6.11: *ACTIN*-corrected *WWOX* expression in A2780 vector-only (F) transfectants

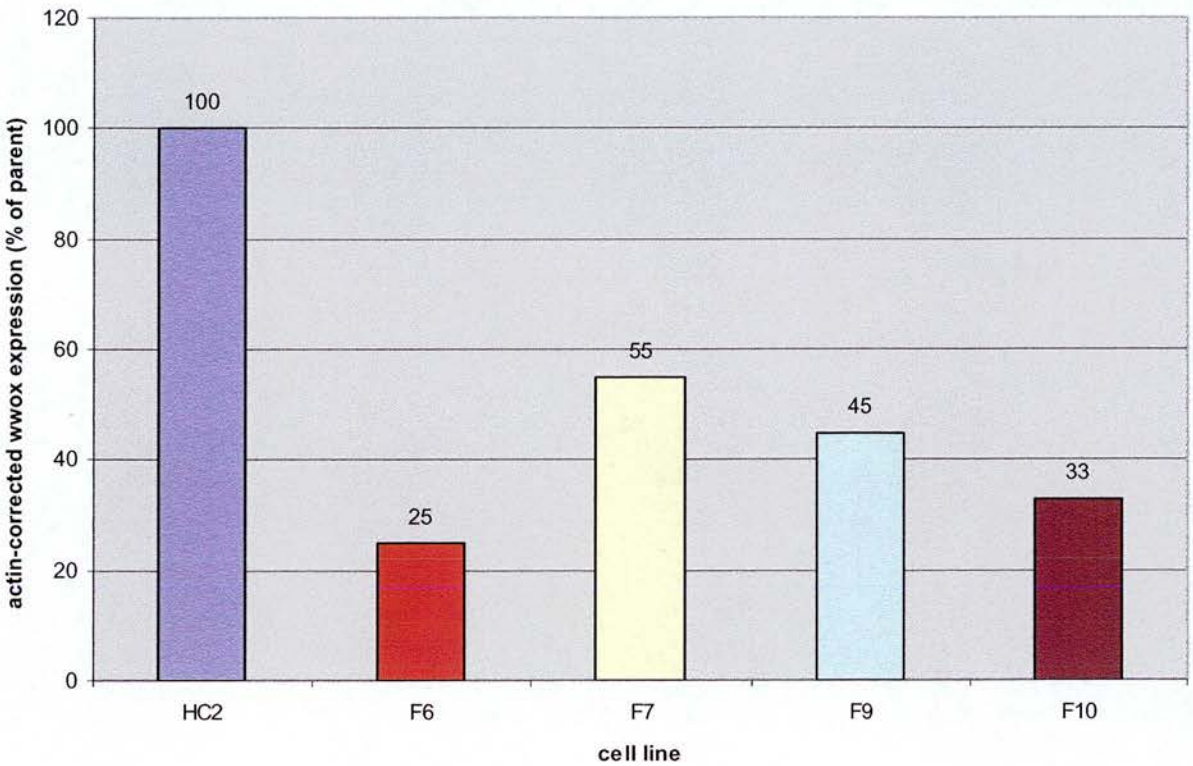

ACTIN-corrected *WWOX* expression in A2780 vector-only (F) transfectants. cDNA was prepared from cultured cells and the levels of *WWOX* and β-*ACTIN* gene expression was quantified in triplicate using the Lightcycler®. This allowed calculation of the *ACTIN*-corrected *WWOX* expression. *WWOX* expression in all the transfectants is expressed as a percentage of the *WWOX* expression in the A2780 HC2 parent line. This was an initial screening exercise to identify transfected cell lines suitable for phenotypic analysis. Quantification of *WWOX* expression in repeated independent preparations of cDNA for a particular cell line was only performed for cell lines used in phenotypic analyses and is demonstrated in later chapters with resultant error bars inserted.

6.7 Evaluation of results

The aim of this section of the study was to identify transfectants of the HCT116 colorectal cancer cell line and the PEO1 and A2780 ovarian cancer cell lines whose level of *WWOX* expression was up-regulated or down-regulated in such a fashion as to facilitate phenotypic analysis. In particular, because the HCT116 colorectal cancer cell line was known to express a number of *WWOX* alternate transcripts it was desirable to achieve down-regulation of *WWOX* in this cell line. The PEO1 ovarian cancer cell line, in contrast, is homozygously deleted for *WWOX* exons 4-8 and therefore expresses only very small amounts of a *WWOX* Δ4-8 transcript. In this cell line the aim was to reconstitute *WWOX* expression (although antisense transfections were also performed in an attempt to create an entirely *WWOX*-null version of the PEO1 cell line).

For the HCT116 colorectal cancer cell line, 3 antisense clones (HCT116 D4, D5 and D16) were identified with expression levels of around 30% of the parent line. A number of clones were identified with more intermediate levels of *WWOX* expression. The justification for using quantitative PCR to select these clones for phenotypic analysis is that it allowed selection of the clones with the greatest reduction in *WWOX* expression. In terms of the HCT116 sense transfectants, a number of significantly upregulated clones (HCT116 H32-36) were identified but these were the clones that grew more slowly after transfection and would not have been selected if quantitative RT-PCR had not been performed.

For the PEO1 ovarian cancer cell line, only 4 clones had down-regulation of *WWOX* and only one of these (PEO1 D7) had expression levels that were less than 30% of the parent line. In terms of the PEO1 sense transfectants, quantitation of *WWOX*

expression levels (both endogenous *WWOX* and total *WWOX*) was particularly useful for selecting clones to be used in phenotypic analysis. In the PEO1 system, for example, the transfection process was associated with some *WWOX* induction as the vector-only controls had increased endogenous (Δ4-8) *WWOX* expression compared to the parent line. The first PEO1 sense clones to grow up following transfection had equivalent endogenous *WWOX* expression to vector-only controls and expressed no exogenous full-length *WWOX*. If these had been used for the subsequent phenotypic analysis then no *WWOX*-specific phenotype would have been identified. Instead, slower-growing sense transfectants with significant expression of exogenous full-length were taken forward for functional assays.

In the case of the sense transfectants of the A2780 ovarian cancer cell line, only 3 out of 18 had significantly up-regulated *WWOX* levels and the use of quantitative RT-PCR allowed identification of these clones.

Therefore, this section of the study was successful in its aim of unambiguously detecting cell lines with suitably manipulated *WWOX* expression levels that could be taken forward and used in functional assays to identify a phenotype for the *WWOX* gene.

7. RESULTS: PHENOTYPIC ANALYSIS OF HCT116 *WWOX* ANTISENSE TRANSFECTANTS

7.1 Rationale for perfoming phenotypic analysis on HCT116 antisense transfectants

As previously discussed (section 6.1), the HCT116 colorectal cancer cell line was used for functional analysis because of the suggestion that murine Wox1 was required for p53-mediated apoptosis and the implication that it physically interacted with murine p53 [168]. Well-characterised wild-type, p53-null, p21-null and Bax-null isogenic HCT116 cell lines were available, so if a functional *WWOX* pathway were found to exist in these cells, the availability of these derivatives would assist the phenotypic analysis.

HCT116 cells express a number of *WWOX* transcripts, so it was decided to analyse the cells with downregulated *WWOX* expression in the first instance. As described in chapter 6, there was little evidence for downregulation of *WWOX* in the cells transfected with the antisense construct targeting the 3' UTR of *WWOX*. On the basis of quantitative RT-PCR, the HCT116 cells transfected with the antisense construct targeting the full *WWOX* coding region did display a variety of levels of *WWOX* mRNA expression (figure 6.3). The most downregulated clones (D4, D5, D16) expressed *WWOX* at 30% of the level of the parent line and their growth was investigated both *in vitro* and *in vivo*. The aim of these experiments was to get an early indication of whether this level of *WWOX* down-regulation was associated with a change in growth characteristics, either *in vitro* or *in vivo* in the HCT116 colorectal cell line system. An alteration in tumourigenicity *in vivo* for instance would then signal the fact firstly that this cell line contained a functional *WWOX* pathway and secondly that a significant degree of *WWOX* downregulation had been achieved.

7.2 Growth of HCT116 antisense transfectants *in vitro*

To determine whether there were any phenotypic effects evident in the most down-regulated antisense transfectants, growth was tested *in vitro* and *in vivo*.

The *in vitro* growth of the HCT116 parent line, two vector only controls (F2 and F4) and three *WWOX* antisense transfectant clones (D2, D4 and D5) was measured. The 3 antisense clones used comprised two of the clones that were most downregulated for *WWOX* expression (D4 and D5) as well as one (D2) that had an intermediate level of *WWOX* expression at 66% of the level in the parent line. No significant difference in growth rate was identified when the antisense clones were compared to the parent line or the vector-only controls (figures 7.1 and 7.2).

Figure 7.1 *In vitro* growth of HCT116 parent line, antisense transfectants and vector-only controls

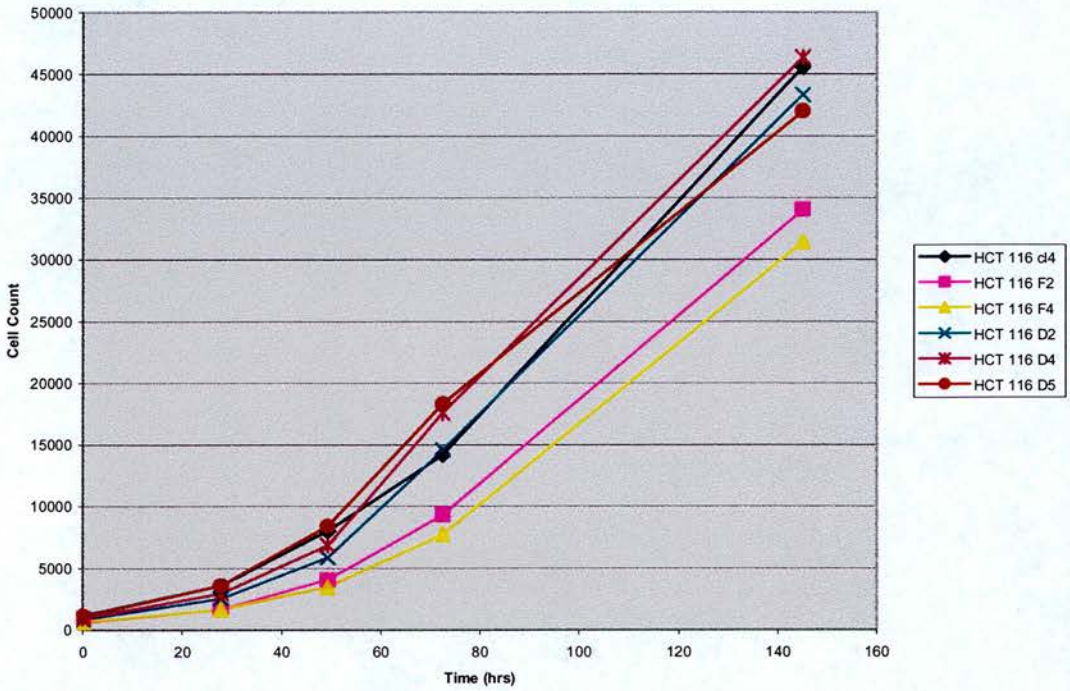

In vitro growth of HCT116 parent line (HCT116 cl4), antisense transfectants (D2, D4 and D5) and vector-only controls (F2 and F4). 5 x 10^4 log phase cells were seeded in duplicate into 6-well trays for each time point and cultured at 37°C, 5% CO_2. At each time point cells were harvested and counted using a coulter-counter.

Figure 7.2 *In vitro* growth of HCT116 parent line, antisense transfectants and vector-only controls (logarithmic scale)

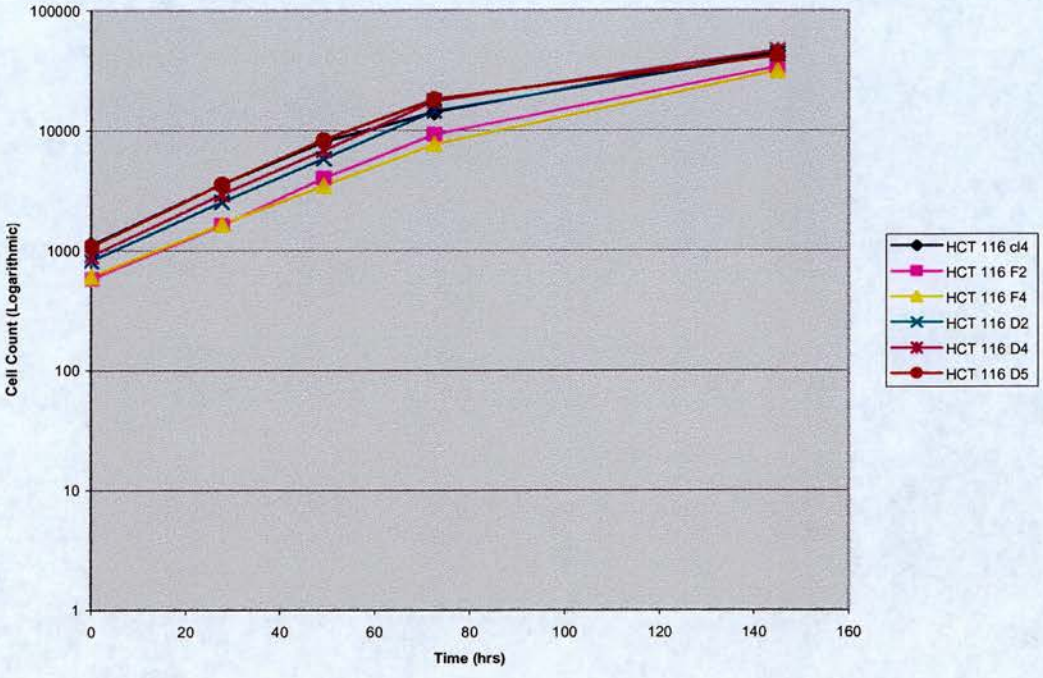

In vitro growth of HCT116 parent line (HCT116 cl4), antisense transfectants (D2, D4 and D5) and vector-only controls (F2 and F4). 5 x 10^4 log phase cells were seeded in duplicate into 6-well trays for each time point and cultured at 37°C, 5% CO_2. At each time point cells were harvested and counted using a coulter-counter. Cell counts are plotted on a logarithmic scale.

7.3 Growth of HCT116 antisense transfectants *in vivo*

The subcutaneous growth in nude mice of the HCT116 parent line, two vector only controls (F2 and F4) and three *WWOX* antisense transfectant clones (D4, D5 and D16) was measured. The 3 antisense clones used were those that were most downregulated for *WWOX* expression. As observed in the *in vitro* growth assay, no significant difference in growth rate was identified when the antisense clones were compared to the parent line or the vector-only controls (figure 7.3).

Figure 7.3 Growth of HCT116 parent line, antisense transfectants and vector-only controls in nude mice

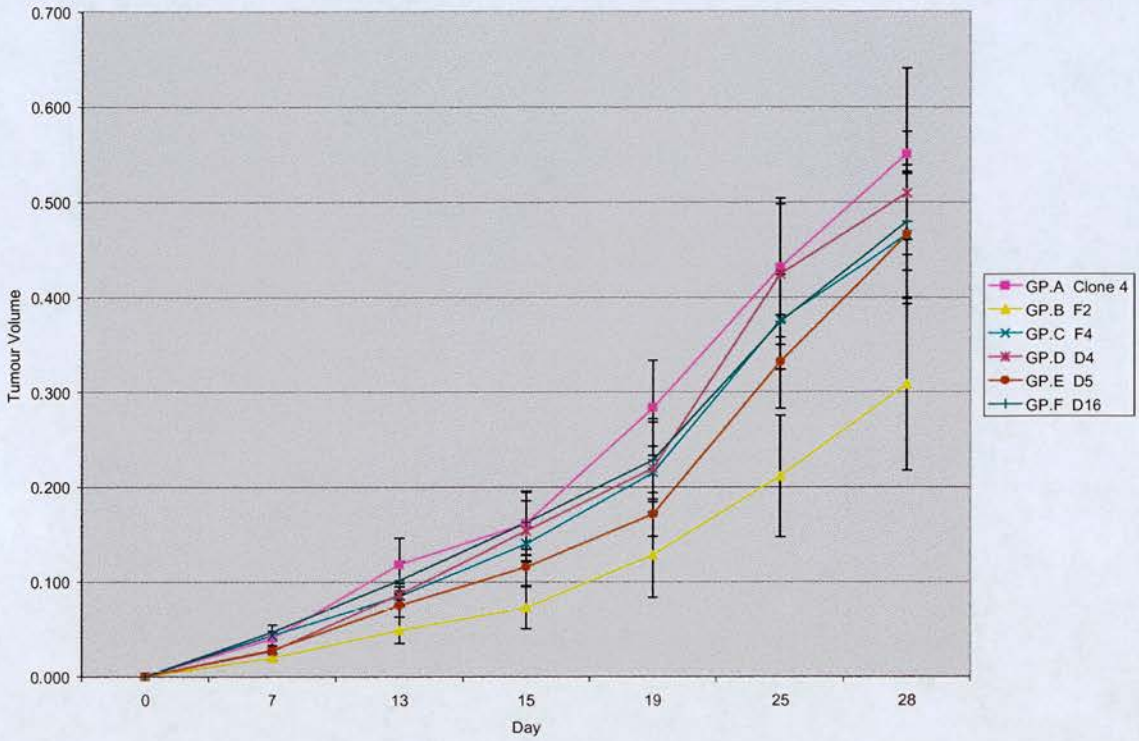

In vivo growth of HCT116 parent line (HCT116 cl4), antisense transfectants (D4, D5 and D16) and vector-only controls (F2 and F4) in nude mice. 5 x 10^6 log phase cells were injected subcutaneously in 100µl serum-free medium into each flank of a nude mouse. Each group consisted of 10 tumours (5 mice). Tumour size was measured twice per week until the tumours reached a size that required the mouse to be sacrificed. The error bars represent the standard deviation of the tumour size for each group.

7.4 Evaluation of results

The aim of these experiments was to get an early indication of whether this level of *WWOX* down-regulation (to 30% of the level in the HCT116 parent line) was associated with a change in growth characteristics, either *in vitro* or *in vivo* in the HCT116 colorectal cell line system. An alteration in tumourigenicity *in vivo* for

instance would then signal the fact firstly that this cell line contained a functional *WWOX* pathway and secondly that a significant degree of *WWOX* downregulation had been achieved.

These experiments identified no significant differences in growth rate *in vitro* or in subcutaneous tumourigenicity *in vivo* for the HCT116 antisense transfectants tested. This does not mean that HCT116 colorectal cells do not have a functional *WWOX* pathway or that the level of *WWOX* downregulation was insufficient to identify a phenotype. Concurrent investigations in the PEO1 cell line system (chapter 8) had identified an *in vivo* phenotype and it made more sense to investigate this fully and then return to the HCT116 colorectal cancer cell line system (if necessary) once the role of the *WWOX* gene had been elucidated in the PEO1 cell line system (which was by this time known to possess a functional *WWOX* pathway). This would avoid the need to perform an exhaustive screen of phenotypic assays in a cell line (HCT116) that may not possess a functional *WWOX* pathway.

Therefore the results reported in this chapter were entirely negative and did not contribute towards the achievement of the aims of the study. Results in the PEO1 cell line system (chapter 8) suggested that this would be the more informative system to use in the first instance.

8. RESULTS: IDENTIFICATION OF *IN VIVO* AND *IN VITRO* PHENOTYPES FOR *WWOX* IN THE PEO1 OVARIAN CANCER CELL LINE

8.1 Rationale for the investigation of the function of WWOX in PEO1 sense transfectants

Until now the only functional data, regarding the role of the *WWOX* gene in tumourigenesis, has been provided by Bednarek et al [52]. They showed that ectopic *WWOX* expression strongly inhibited anchorage-independent growth in soft agar of the MDA-MB-435 and T47D breast cancer cell lines (both of which have a low baseline expression of the *WWOX* gene). They also showed that *WWOX* inhibited the tumourigenicity of MDA-MB-435 breast cancer cells in nude mice. The PEO1 cell line is homozygously deleted for *WWOX* exons 4-8 and as such expresses only a truncated *WWOX* Δ4-8 transcript, which lacks the alcohol dehydrogenase domain of the protein. This makes it a suitable system for testing the phenotypic effects of reconstituting functional *WWOX*. The aims of this component of the study were to establish whether reconstitution of *WWOX* in PEO1 ovarian cancer cells affected subcutaneous tumourigenicity *in vivo*. If this was the case, then an exhaustive search for an *in vitro* phenotype could be conducted.

Additional note:

The PEO1 system was fully characterised for the purposes of these phenotypic assays. This included flow cytometry, which was performed after in vitro growth curves and the first tumourigenicity assay were performed. This revealed that most of the vector-only controls and and some of the sense transfectants had become tetraploid (the parent PEO1 line is diploid). None of these lines were used for any further phenotypic assays. Unfortunately, this left just one suitable, diploid, vector-only control (F9) and also one diploid clone that appeared abnormal down the

microscope, with a lot of dead cells present (F2). As a result it was decided to use, in addition, two polyclonal cell lines containing these vectors (F1p and F2p) to increase the number of vector-only controls. In addition one of the antisense transfectants (D6), which was transfected with the same vector was also used in some of the phenotypic assays

8.2 Confirmation of *WWOX* upregulation in PEO1 sense clones chosen for functional analysis

PEO1 cells were transfected with a sense construct expressing the *WWOX* coding region and also with vector-only controls. *WWOX* expression in these transfects was quantified using the Lightcycler® (section 6.5). A number of transfectants had significantly upregulated *WWOX* levels (clones H4, H6-H10 and H12 were between 7 and 38000-fold upregulated compared to the expression of the endogenous transcript). The RNA used for this screening of clones was obtained while the cells were being expanded following initial transfection. In order to confirm that the expression levels were maintained during functional studies, quantitative RT-PCR was performed on the clones chosen for phenotypic analysis using the Rotorgene® after the cells had been passaged on 2-3 times. The 8F2 and Z2 primer pair (which detects only exogenous *WWOX*) was used for this quantitation. As expected, neither the parent line nor the vector-only controls expressed full-length *WWOX* (figure 8.1). The expression of full-length *WWOX* in the sense transfectants (normalised to H7, the highest expresser) varies from 0.9 to 100% (figures 8.1 and 8.2). In comparison to the initial quantitation, the expression of the H6 clone appears to have fallen (by

around an order of magnitude in comparison to the H7 clone), possibly as a result of the selection of cells with lower *WWOX* expression during cell culture.

Figure 8.1 *WWOX* expression in PEO1 sense (H) and vector-only (F) transfectants

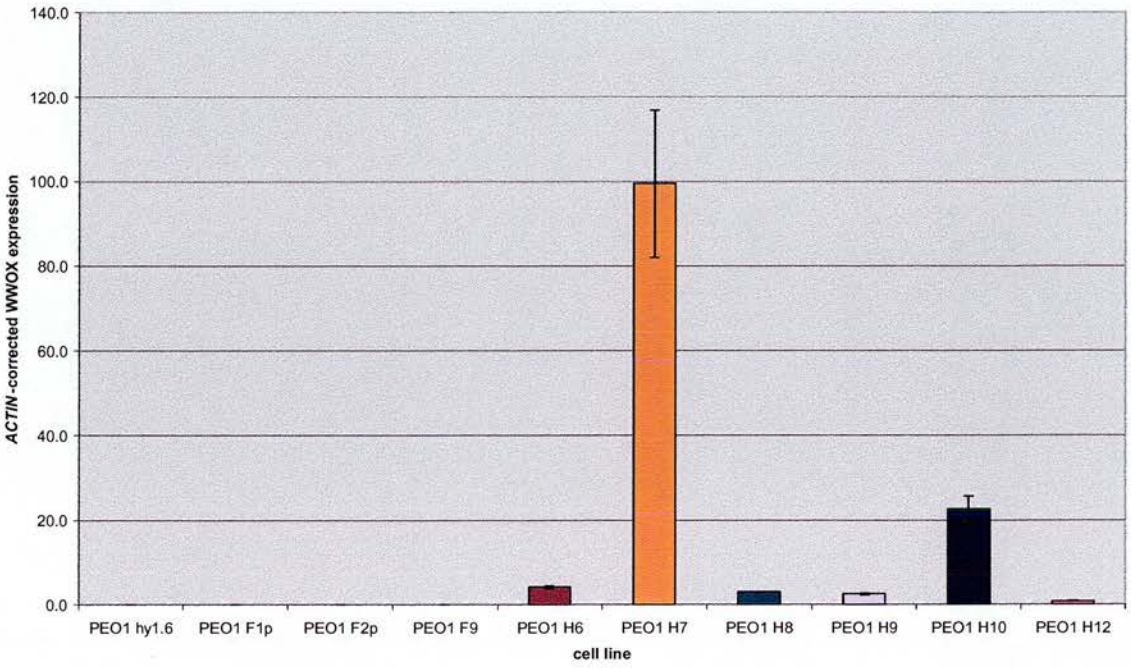

ACTIN-corrected *WWOX* expression in PEO1 parent line (hy 1.6), vector-only (F) and sense (H) transfectants. cDNA was prepared from cultured cells and the levels of *WWOX* and β-*ACTIN* gene expression was quantified in quadruplicate using the Rotorgene®. This allowed calculation of the *ACTIN*-corrected *WWOX* expression. *WWOX* expression in all the transfectants is expressed as a percentage of the expression in the H7 clone. Each gene (*WWOX* and *ACTIN*) quantitation was repeated in quadruplicate on 3 separate occasions and the error bars represent the sum of the fractional error of the *WWOX* and *ACTIN* quantitations.

Figure 8.2 *WWOX* expression in PEO1 sense (H) transfectants (logarithmic scale)

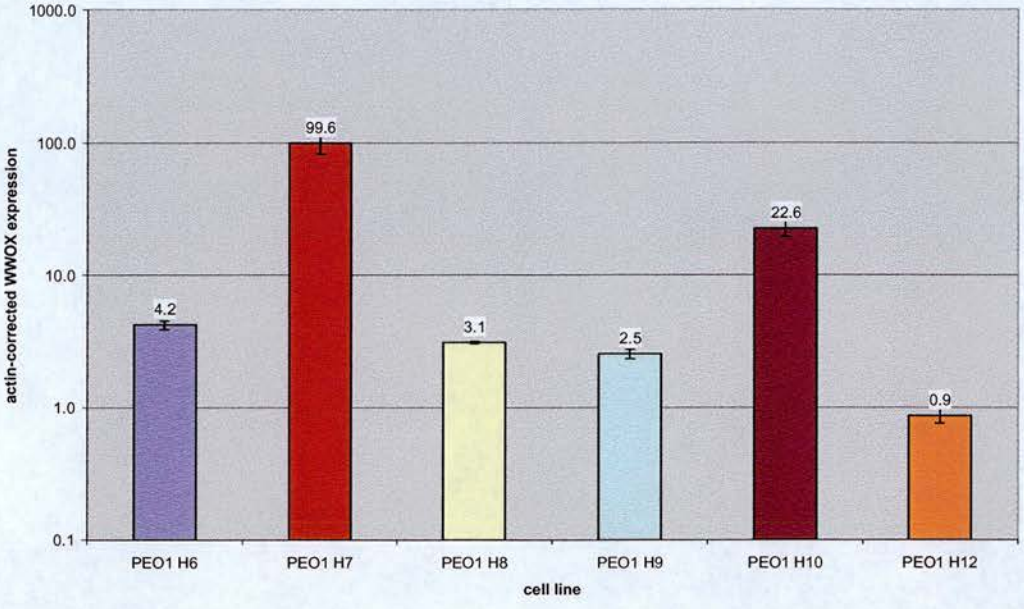

ACTIN-corrected *WWOX* expression in PEO1 sense (H) transfectants. cDNA was prepared from cultured cells and the levels of *WWOX* and β-*ACTIN* gene expression was quantified in quadruplicate using the Rotorgene®. This allowed calculation of the *ACTIN*-corrected *WWOX* expression. *WWOX* expression in all the transfectants is expressed as a percentage of the expression in the H7 clone. Note that *WWOX* expression is on a logarithmic scale. Each gene (*WWOX* and *ACTIN*) quantitation was repeated in quadruplicate on 3 separate occasions and the error bars represent the sum of the fractional error of the *WWOX* and *ACTIN* quantitations.

8.3 Linear correlation between *WWOX* mRNA and protein levels in *WWOX* transfectants used for functional analysis

In order to check that *WWOX* isoform 1 mRNA was translated into protein in the *WWOX* sense transfectants, Western blotting was performed. No *WWOX* expression was detected in 3 vector-transfected controls (data not shown). Western blotting detected translated WWOX protein in 4 out of the 6 sense transfectants (figure 8.3). The two transfectants in which protein was not detected were the lowest expressers of *WWOX* isoform 1 mRNA by real-time PCR (figure 8.2). There was a strong linear correlation between mRNA and protein levels in this transfected cell line system (R^2=0.995; figure 8.4).

Figure 8.3 WWOX protein expression in PEO1 sense transfectants

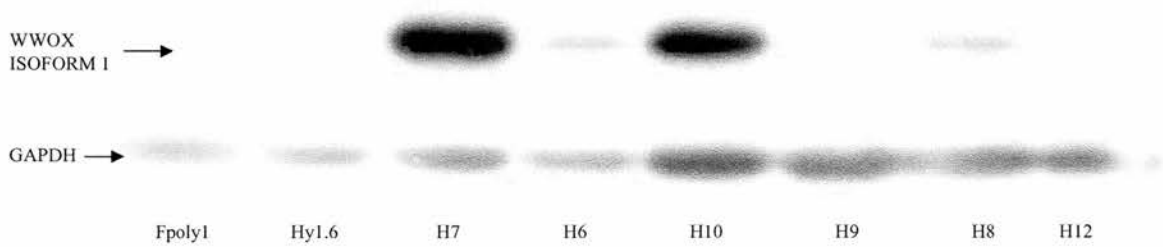

Western blot of PEO1 cell lines: F1p (vector-transfected control); Hy1.6 (untransfected parent cell line); H7, H6, H10, H9, H8, H12 (sense transfectants). Extracts of the cultured cells were Western immunoblotted and analysed using a WWOX-specific antibody. GAPDH was used as an internal control for loading.

Figure 8.4 *WWOX* mRNA plotted against protein in PEO1 sense transfectants

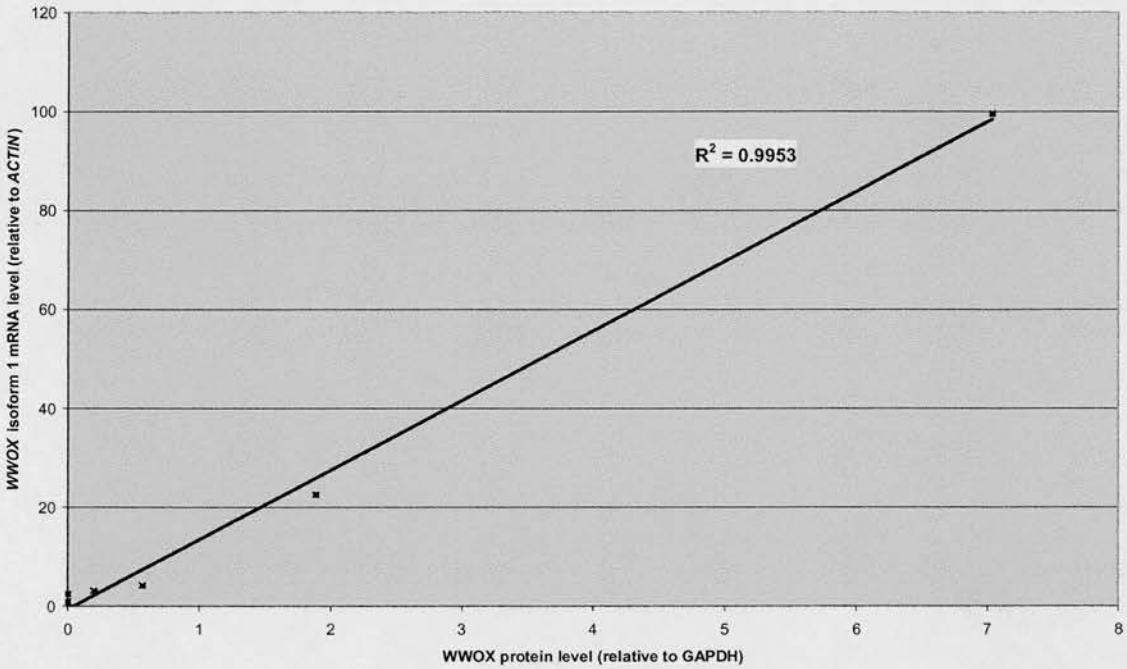

ACTIN-corrected *WWOX* variant 1 mRNA level (as quantified by real-time PCR) plotted against GAPDH-corrected WWOX variant 1 protein level (as quantified by Western blot). For real-time PCR cDNA was prepared from cultured cells and the levels of *WWOX* and β-*ACTIN* gene expression was quantified in quadruplicate using the Rotorgene®. This allowed calculation of the *ACTIN*-corrected *WWOX* expression. For Western blot extracts of the cultured cells were Western immunoblotted and analysed using a WWOX-specific antibody. GAPDH was used as an internal control for loading.

8.4 *WWOX* reconstitution abolishes tumourigenicity of PEO1 cells in nude mice

A preliminary experiment was performed to determine the optimal conditions and cell number for assessing the growth of PEO1 cells following subcutaneous injection into nude mice. Two groups of 5 mice were injected subcutaneously with PEO1

parent cells, using matrigel for injections into one flank and using no matrigel for injections into the contralateral flank. 1 x 10^6 cells per injection were used for the first group of mice (GP.A) and 5 x 10^6 cells per injection for the second group (GP.B). In both groups, the cells injected without matrigel grew best. 5 x 10^6 was the optimal cell injection number on the basis that none of the tumours injected without matrigel in this group failed to grow.

Figure 8.5: Optimisation of PEO1 tumourigenicity protocol

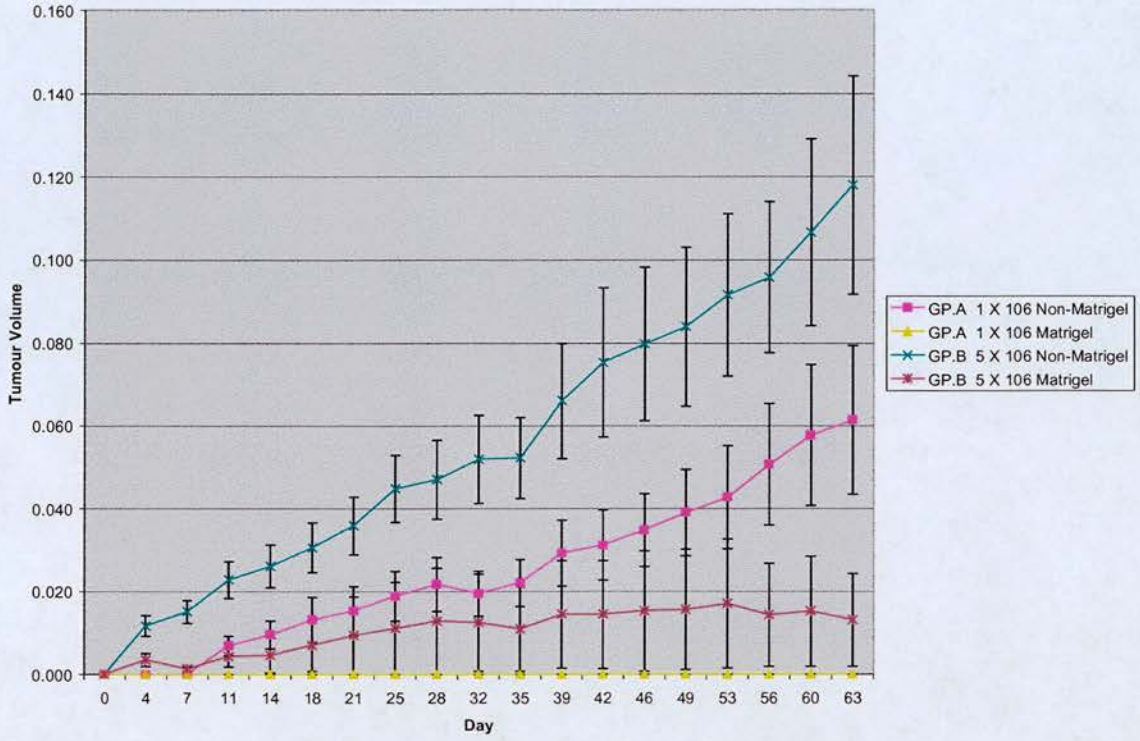

Growth of PEO1 ovarian cancer cells injected subcutaneously into nude mice with or without matrigel. 1 x 10^6 or 5 x 10^6 log phase cells were injected subcutaneously into each flank of a nude mouse. In one flank the cells were injected in 100µl serum free media, in the other flank the cells were injected in 50µl serum free media and 50µl matrigel. Each group consisted of 10 tumours (10 mice). Tumour size was measured twice per week until the tumours reached a size that required the mouse to be sacrificed. The error bars represent the standard deviation of the tumour size for each group.

Following this optimisation protocol, PEO1 parent cells, a vector-only (F) transfectant and 4 *WWOX* sense (H) transfectants were each subcutaneously injected (5 x 10^6 cells per injection) into both flanks of 5 nude mice. The PEO1 parent line and the vector-only control (F9) grew in nude mice but there was no growth of any of the sense transfectants (figure 8.6). This suggested that the expression of *WWOX*

had resulted in the abolition of tumourigenicity in nude mice. There was some variation between the growth rate of the parent line and the vector-only control, which may have been due to clonal heterogeneity. To confirm these findings, the experiment was repeated using further vector-only controls, one of the PEO1 antisense (D) transfectants and two sense transfectants (figure 8.7). This confirmed growth of the parent line, of two vector-only control lines (F1p and F2p) and an antisense transfectant (D6). Once again there was a considerable difference in the growth rate of these clones. As observed previously (figure 8.6), there was no growth of either of the sense transfectants (PEO1 H6 and H7). Therefore, the expression of exogenous *WWOX* in a PEO1 cell line system resulted in the abolition of tumourigenicity in nude mice.

Figure 8.6 Tumourigenicity of PEO1 parent line and transfected cells in nude mice (first series)

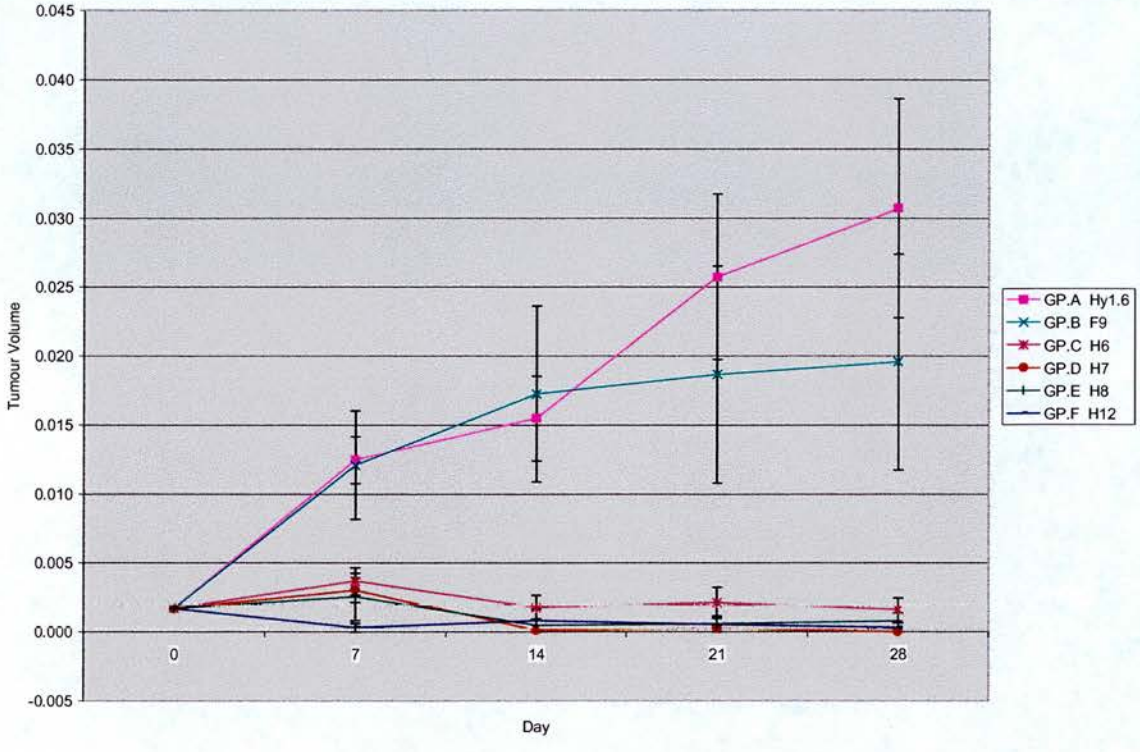

Growth of PEO1 parent cells (hy1.6), vector-only control (F9) and sense transfectants (H6, H7, H8, H12) injected subcutaneously into nude mice. 5 x 10^6 log phase cells were injected subcutaneously in 100µl serum-free medium into each flank of a nude mouse. Each group consisted of 10 tumours (5 mice). Tumour size was measured twice per week until the tumours reached a size that required the mouse to be sacrificed. The error bars represent the standard deviation of the tumour size for each group.

Figure 8.7 Tumourigenicity of PEO1 parent line and transfected cells in nude mice (second series)

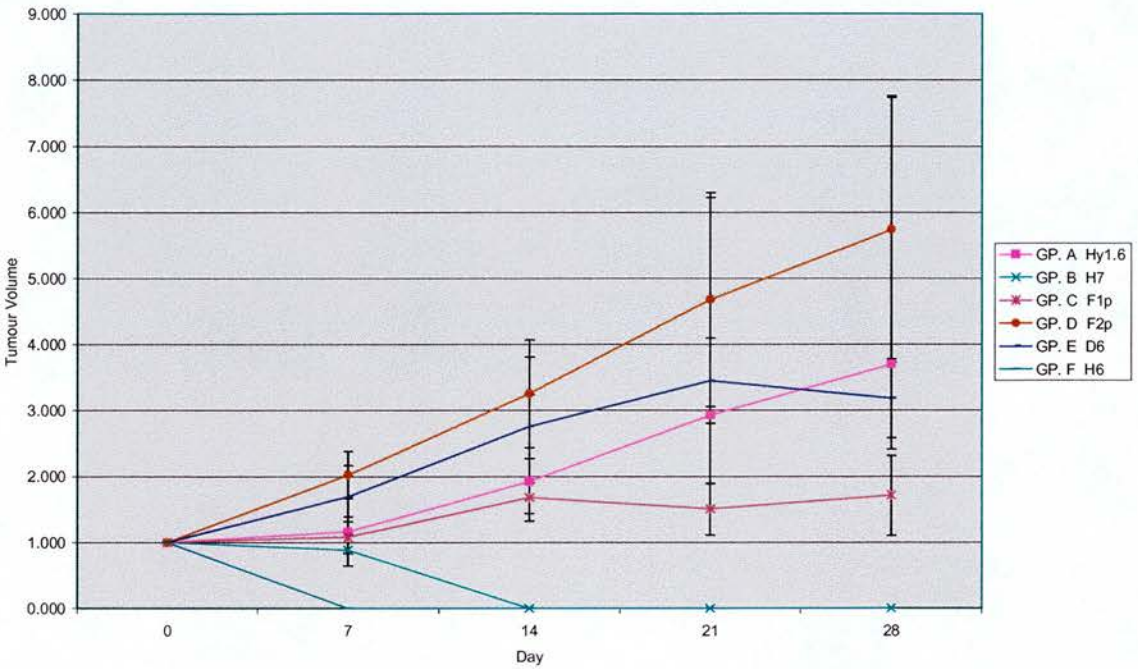

Growth of PEO1 parent cells (hy 1.6), vector-only controls (F1p and F2p), antisense (D6) and sense (H6 and H7) transfectants injected subcutaneously into nude mice. 5 x 10^6 log phase cells were injected subcutaneously in 100µl serum-free medium into each flank of a nude mouse. Each group consisted of 10 tumours (5 mice). Tumour size was measured twice per week until the tumours reached a size that required the mouse to be sacrificed. The error bars represent the standard deviation of the tumour size for each group.

8.5 Demonstration of an in vitro phenotype for the *WWOX* gene

The finding that exogenous *WWOX* expression abolished tumourigenicity in nude mice suggested that there was a functional WWOX pathway in PEO1 cells.

Therefore phenotypic assays were conducted in this cell line system in order to determine an *in vitro* phenotype for *WWOX*.

8.5.1 *In vitro* growth curves

Growth rate of PEO1 sense transfectants was not significantly different to that of the parent line and vector-only controls (figures 8.8 and 8.9).

Figure 8.8 *In vitro* growth of PEO1 parent line, vector-only controls and sense transfectants

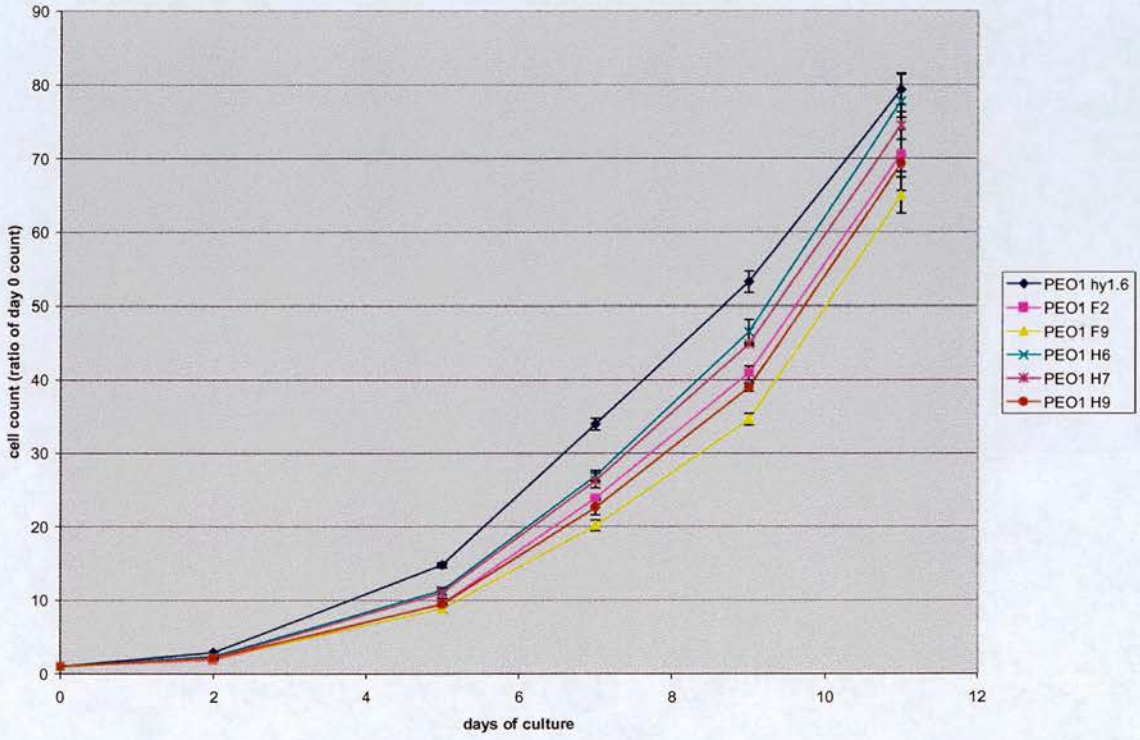

Growth rate of PEO1 parent line (hy 1.6), vector-only controls (F2 and F9) and sense transfectants (H6, H7 and H9) *in vitro*. 1 x 10^5 log phase cells were seeded in duplicate into 6-well trays for each time point and cultured at 37°C, 5% CO_2. At each time point cells were harvested and counted using a coulter-counter. Growth curves were repeated three times and the error bars indicate the standard error of the mean.

Figure 8.9 *In vitro* growth of PEO1 parent line, vector-only controls and sense transfectants (logarithmic scale)

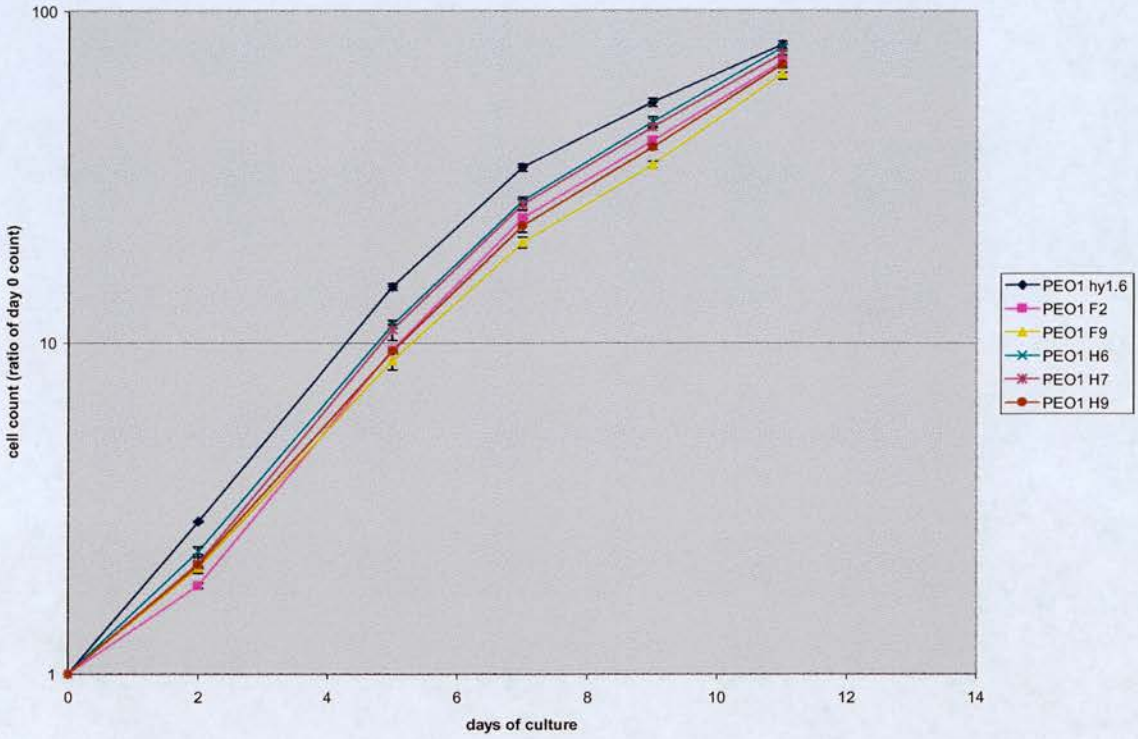

Growth rate of PEO1 parent line (hy 1.6), vector-only controls (F2 and F9) and sense transfectants (H6, H7 and H9) *in vitro*. 1 x 10^5 log phase cells were seeded in duplicate into 6-well trays for each time point and cultured at 37°C, 5% CO_2. At each time point cells were harvested and counted using a coulter-counter. Growth curves were repeated three times and the error bars indicate the standard error of the mean. The cell counts are plotted on a logarithmic scale.

8.5.2 Agarose growth curves

Bednarek et al [52], working with breast cancer cell lines, also failed to identify a difference in growth rate (*in vitro*) between *WWOX* transfected cells and controls. They did, however, find a difference in the rate of anchorage –independent growth in soft agar. Consequently, the possible anchorage-independent growth phenotype associated with *WWOX* was examined in the *WWOX*-transfected PEO1 cell line series. Therefore 5000 cells were seeded per well in 6-well trays. Following 28 days

of incubation, colonies of tumour cells were counted manually down the microscope. No apparent difference was observed in the number of colonies between the cell lines examined in this assay (figure 8.10).

Figure 8.10 Soft agar clonogenicity of PEO1 parent line, vector-only controls and sense transfectants

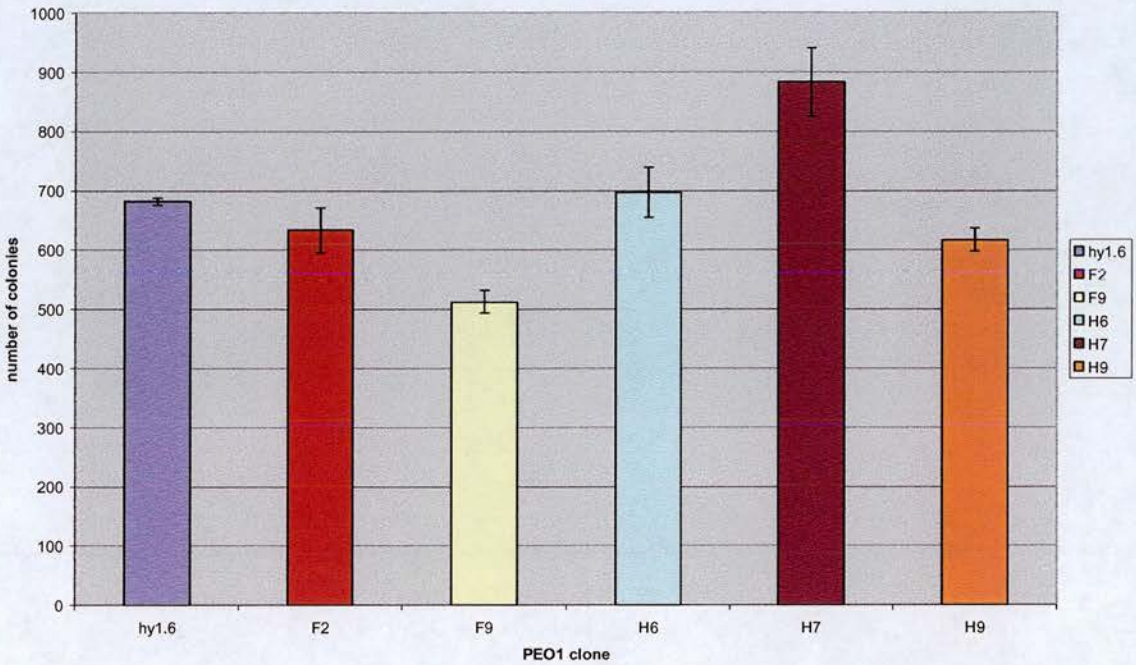

Soft agar clonogenicity of PEO1 parent line (hy 1.6), vector-only controls (F2 and F9) and sense transfectants (H6, H7 and H9). 5000 log phase cells were seeded in 3ml of 0.4% seaplaque agarose on top of a layer of 2ml of 1% seaplaque agarose. The cells were incubated at 37°C, 5% CO_2 and the number of PEO1 colonies counted after 28 days incubation. 5000 cells plated per well at the outset. The experiment was repeated three times and the error bars represent the standard error of the mean.

8.5.3 Clonogenicity

The colony-forming efficiency of cells in the PEO1 series was assessed by performing clonogenicity assays. In the first instance cells were plated at low density (1000 cells per well) in media without cytotoxic agents and the numbers of colony-forming units was counted after 21 days (figure 8.11). One of the vector-only controls (F9) had a lower colony-forming efficiency than the other lines but there was no significant difference between the *WWOX* sense transfectants and the parent line or the other vector-only control. The experiment was repeated (plating 200 cells per well) adding cisplatinum to the medium (0.008μM-1μM). There was again no difference in the colony-forming efficiency of the sense-transfected lines compared to controls for a given concentration of cisplatinum (figure 8.12). Only the highest dose of cisplatinum (1μM) had a significant effect on colony-forming efficiency. The results for this dose are expanded in figure 8.13.

Figure 8.11 Colony-forming efficiency of the PEO1 series in the absence of cytotoxic agents

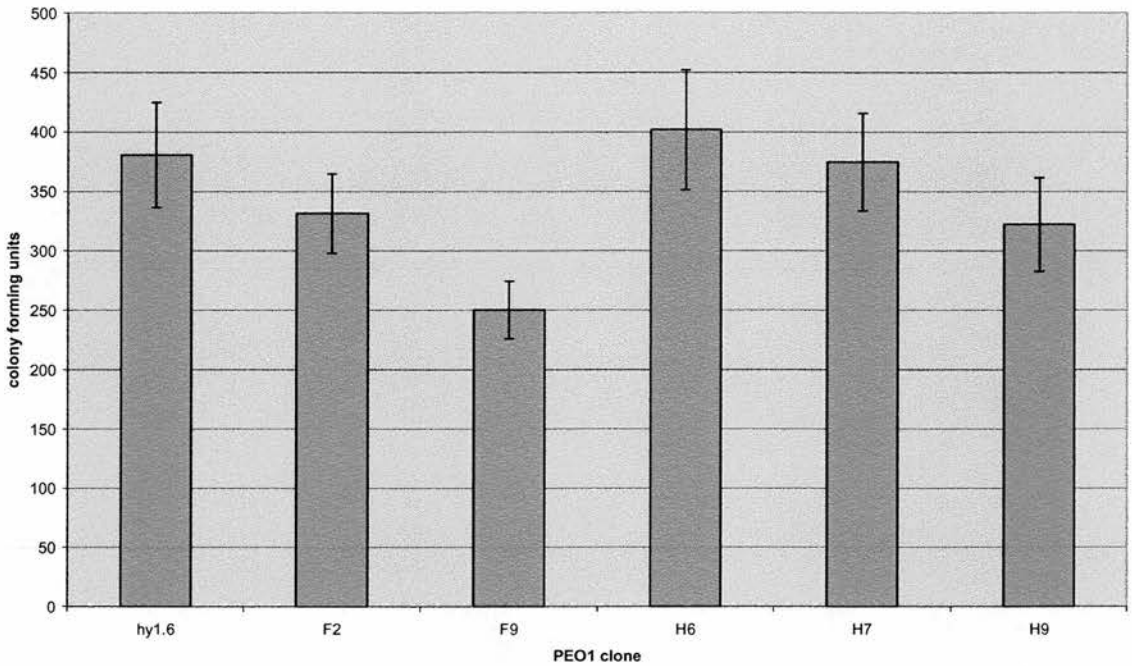

Colony-forming efficiency of the PEO1 parent line (hy 1.6), vector-only controls (F2 and F9) and sense transfectants (H6, H7 and H9). Log phase cells were harvested and syringed 10 times. Multiplicity was calculated to ensure it was <1.05. For each cell line 1000 cells were seeded onto a gridded Petri dish. The cells were then incubated at 37°C, 5% CO_2 for 21 days before being fixed with 2:1 acetone/methanol, stained with haematoxylin and counted. The experiment was repeated three times and the error bars represent the standard error of the mean.

Figure 8.12 Colony-forming efficiency of the PEO1 series following exposure to various doses of cisplatinum

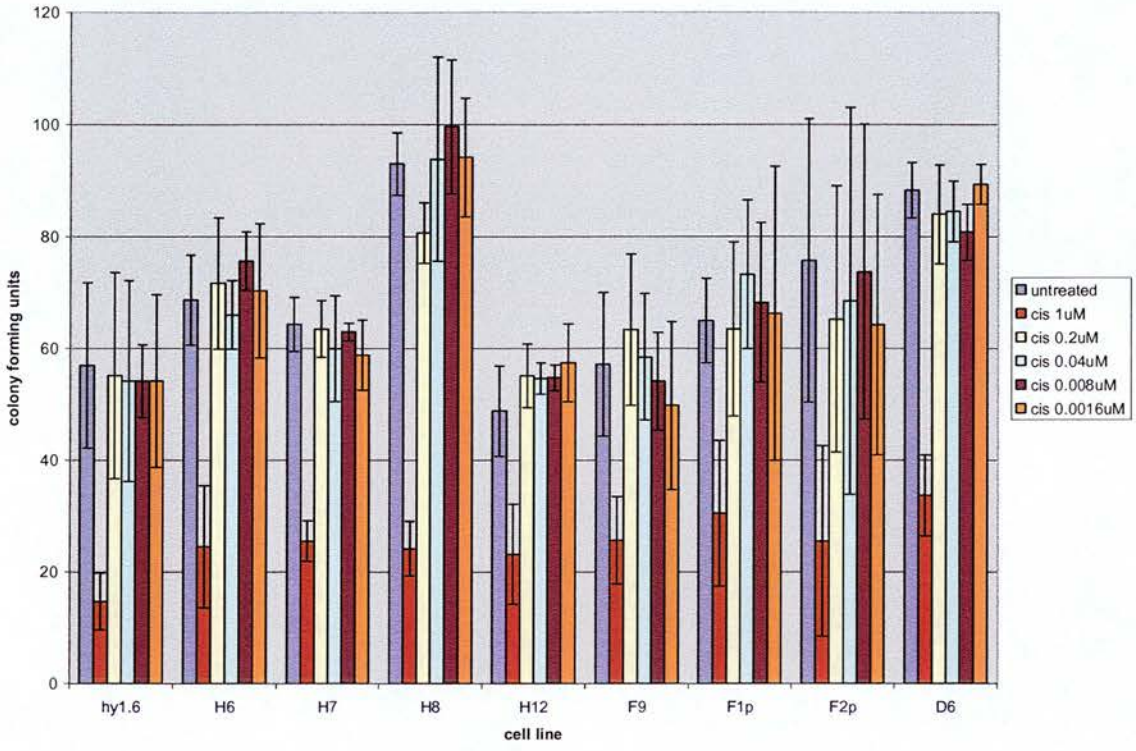

Colony-forming efficiency of the PEO1 parent line (hy 1.6), vector-only controls (F9, F1p and F2p) and sense transfectants (H6, H7, H8 and H12) following exposure to 0, 1μM, 0.04μM, 0.008μM and 0.0016μM cisplatinum. An antisense transfectant (D6) was also included in this analysis. Log phase cells were harvested and syringed 10 times. Multiplicity was calculated to ensure it was <1.05. For each cell line 200 cells were seeded onto a gridded Petri dish. The cells were then incubated at 37°C, 5% CO_2 at the appropriate drug concentration for 21 days before being fixed with 2:1 acetone/methanol, stained with haematoxylin and counted. The experiment was repeated three times and the error bars represent the standard error of the mean.

Figure 8.13 Colony-forming efficiency of the PEO1 series following exposure to 1μM cisplatinum

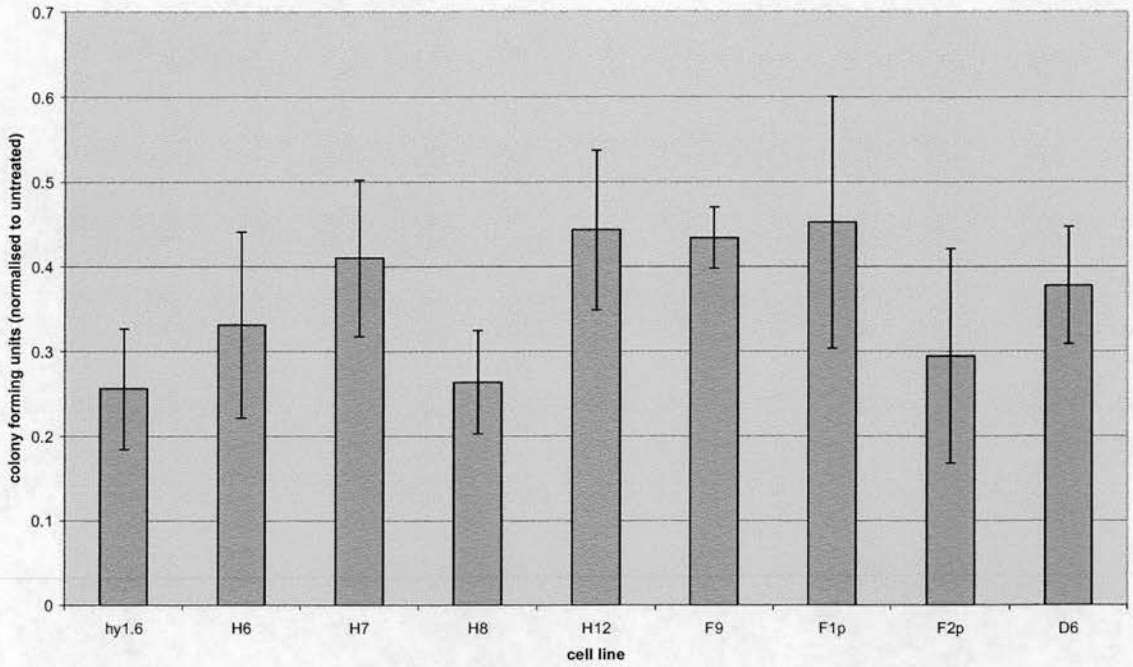

Colony-forming efficiency of the PEO1 parent line (hy 1.6), vector-only controls (F9, F1p and F2p) and sense transfectants (H6, H7, H8 and H12) following exposure to 1μM cisplatinum. An antisense transfectant (D6) was also included in this analysis. Log phase cells were harvested and syringed 10 times. Multiplicity was calculated to ensure it was <1.05. For each cell line 200 cells were seeded onto a gridded Petri dish. The cells were then incubated at 37°C, 5% CO_2 at the appropriate drug concentration for 21 days before being fixed with 2:1 acetone/methanol, stained with haematoxylin and counted. The experiment was repeated three times and the error bars represent the standard error of the mean.

8.5.4 Aggregation assays

Aggregation assays were performed on the PEO1 cells. The assay was difficult to reproduce consistently. Initial attempts suggested that *WWOX* transfected cells had a

decreased propensity to aggregate (figure 8.14a) but this did not prove to be reproducible in further experiments (figure 8.14b). As the results of the aggregation assay were inconsistent, it was not pursued any further.

Figure 8.14 Aggregation of PEO1 parent cells, vector-only controls and sense transfectants

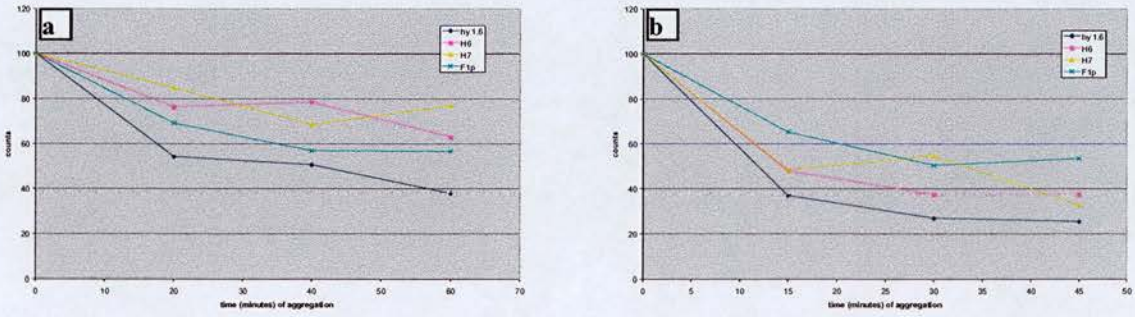

Aggregation of PEO1 parent cells (hy 1.6), vector-only control (F1p) and sense transfectants (H6 and H7). Log phase PEO1 parent, vector control and sense-transfected lines were trypsinised and recovered in serum-containing media. 1 x 10^6 cells were resuspended in 1ml of media and passed through a 21G needle to create a single-cell suspension. Cell suspensions were incubated at 37°C, 5% CO_2. At 0, 15, 30 and 60 minutes aliquots were removed using a wide bore pipette and the number of single cells was counted with a haemocytometer. All counts are normalised to the time zero count.

8.5.5 Invasion assays

Invasion assays were performed using matrigel invasion chambers (described in section 2.20). After 84 hours of invasion, the number of cells in the upper and lower

chambers was quantified using an MTT assay. The invasion was calculated as the OD570 for the lower chamber divided by the OD570 for the top chamber multiplied by 100. The MTT assay was performed 3 times for each well. Two wells were used for each cell line, the complete experiment was repeated three times and the mean taken. The number of cells in both the upper and lower chambers following 84 hours of invasion was reduced in the PEO1 sense transfectants compared with the parent line and vector-only controls (figure 8.15). The calculated invasion, however, was not significantly different between the cell lines (figure 8.16). A possible explanation for the decrease in cells in both chambers in the sense transfectants (despite equal numbers of cells being used for each line) may be that less of these cells are attaching to the matrigel of the upper chamber and are therefore available for invasion. It could also be that a lower number of the sense transfectants added to the upper chamber are surviving and therefore, again less are available for invasion. Matrigel attachment and apoptotic assays would potentially help to clarify this issue.

Figure 8.15 Number of PEO1 cells in upper (a) and lower (b) level of invasion chamber (A570 following MTT assay)

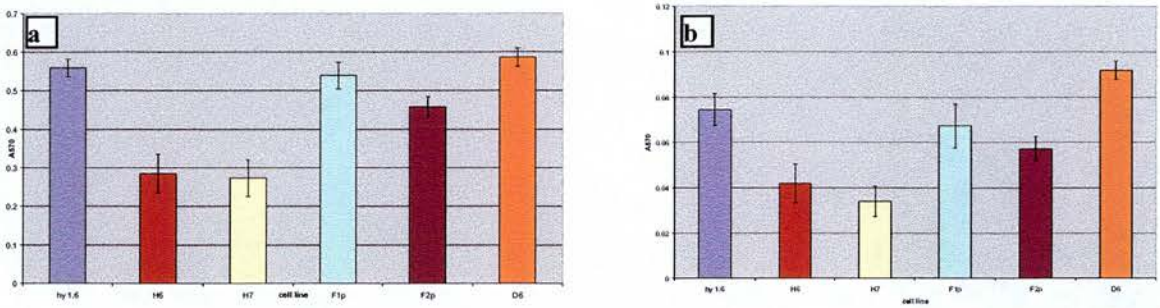

Number of PEO1 parent cells (hy1.6), sense transfectants (H6 and H7), vector-transfected controls (F1p and F2p) and antisense transfectants (D6) in the upper (a) and lower (b) levels of the invasion chamber (as measured by A570 following MTT assay) after 84 hours of the invasion assay. Invasion assays were conducted with media containing 10% acid-inactivated serum. 5 x 10^4 cells were loaded into the top of each invasion chamber. The cells were incubated at 37°C, 5% CO_2 for 84 hours then cells on either side of the insert were quantified by MTT assay. The MTT assay was performed 3 times for each well. Two wells were used for each cell line, the whole experiment was repeated three times and the mean taken. The error bars show the standard error of the mean.

Figure 8.16 Invasion of PEO1 parent cells, vector-only controls and sense transfectants

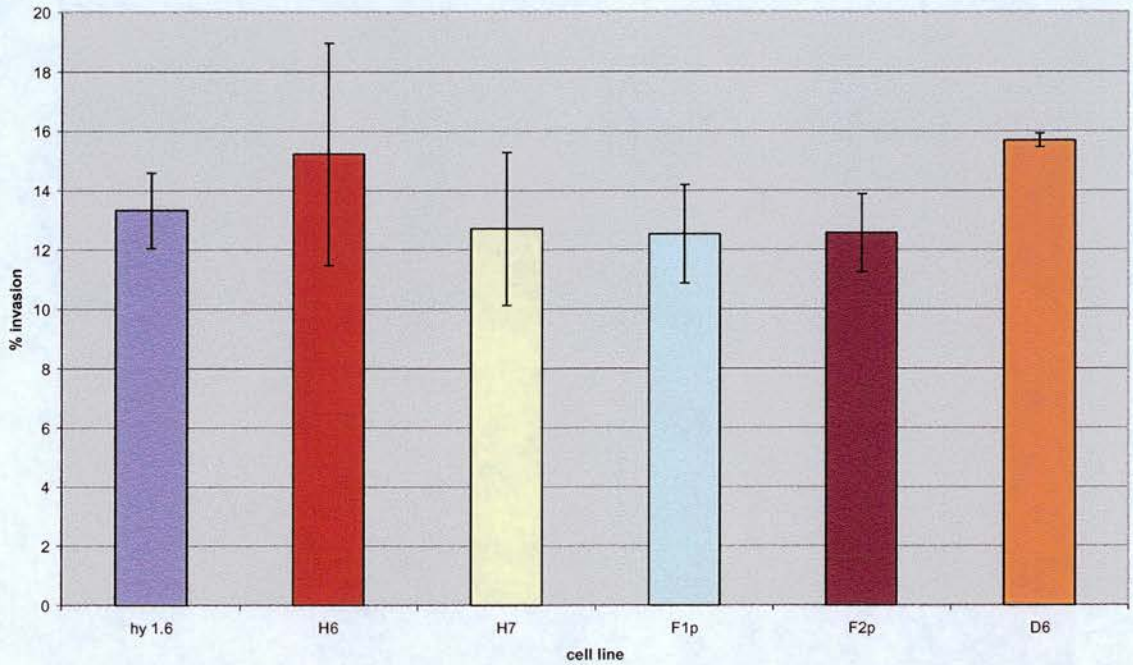

Invasion of PEO1 parent cells (hy1.6), sense transfectants (H6 and H7), vector-only controls (F1p and F2p) and an antisense transfectant (D6). Invasion assays were conducted with media containing 10% acid-inactivated serum. 5 x 10^4 cells were loaded into the top of each invasion chamber. The cells were incubated at 37°C, 5% CO_2 for 84 hours then cells on either side of the insert were quantified by MTT assay. The MTT assay was performed 3 times for each well. Two wells were used for each cell line, the whole experiment was repeated three times and the mean taken. The error bars show the standard error of the mean.

8.5.6 Migration assays

Migration assays were performed in transwells (as described in section 2.19). Transwells are similar to invasion chambers but are not coated with matrigel. Instead they contain pores (8μm in this case) and can by coated on their undersurface with extracellular matrix proteins. Again, an MTT assay was performed to quantify

the upper and lower chamber cells after 84 hours of migration. Migration was compared between cell lines of the PEO1 *WWOX*-transfected series as for the invasion assays. This assay showed that the PEO1 sense transfectants have a decreased ability to migrate towards fibronectin when compared to the parent line and a vector-only control (figure 8.17). Migration towards laminin was lower in the sense transfectants than in the parent line, but was the same as the vector-only control. These findings suggest that the exogenous expression of *WWOX* decrease the capacity of PEO1 cells to migrate towards fibronectin.

Figure 8.17 Migration of PEO1 parent cells, vector-only controls and sense transfectants towards bovine serum albumin, fibronectin and laminin

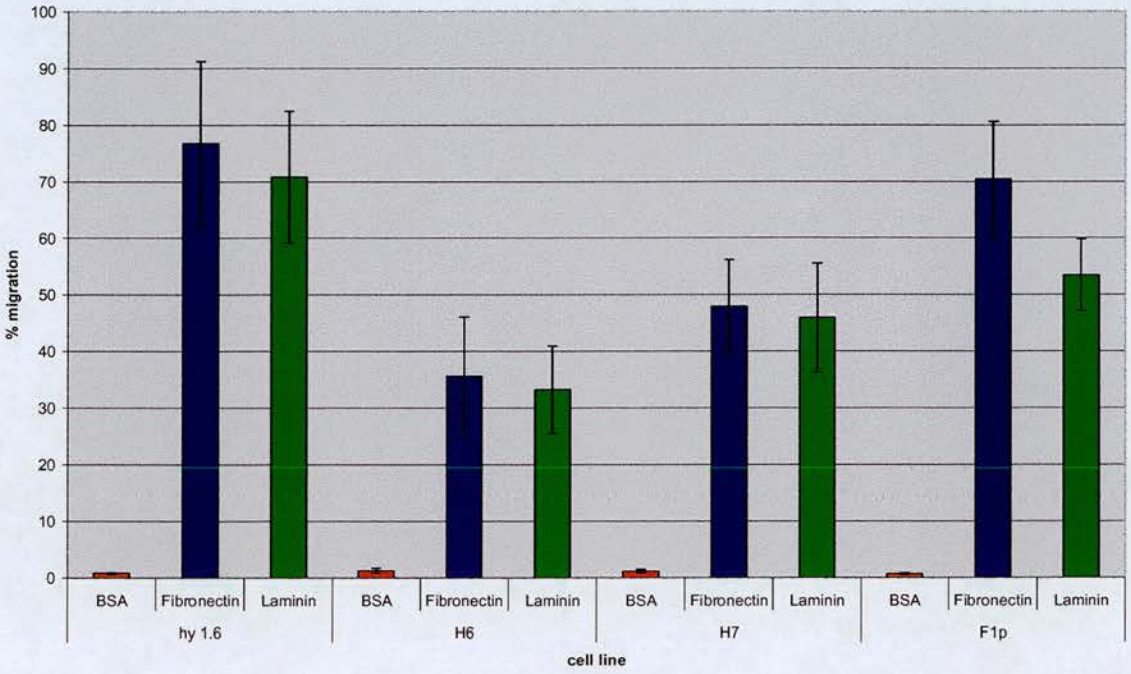

Migration of PEO1 parent cells (hy1.6), sense transfectants (H6 and H7) and a vector-only control (F1p) towards bovine serum albumin, fibronectin and laminin. Prior to the migration assay, the undersurface of each transwell was coated with a matrix component (fibronectin, laminin or BSA for the control wells), blocked with 0.1%BSA and then washed with PBS. 5×10^4 cells were aliquoted to each well and the cells were incubated at 37°C, 5% CO_2 for 84 hours. The number of cells on the upper and lower surface of the transwell was quantified by MTT assay. Migration was expressed as the ratio of the undersurface OD reading to the uppersurface OD reading. The experiment was repeated five times, the migration figures were averaged for the cell lines tested and the standard error of the mean was calculated (represented by the error bars). Migration towards BSA, fibronectin and laminin is represented by red, blue and green bars respectively.

8.5.7 Attachment assays

Attachment to matrigel and to plastic coated with fibronectin or laminin was investigated for the PEO1 cell line series. However, investigation of attachment to matrigel of the parent line was compromised due to a technical problem. The 3 vector-only control lines attached to matrigel following 1 hour of incubation, whereas there was no attachment of either the H6 or H7 *WWOX* sense transfectants (figure 8.18). This supported the suggestion from the invasion assays (section 8.5.5) that PEO1 sense transfectants may have a decreased capacity to attach to matrigel.

In a subsequent experiment, attachment to laminin and fibronectin following 30 minutes and 18 hours incubation was decreased when the PEO1 H7 sense transfectant was compared to the parent line (figure 8.19). When the assay was repeated using more cell lines, there was again evidence of decreased attachment of the sense transfectants (H6 and H7) to fibronectin compared to controls (figure 8.20). In this particular assay, however, little difference was observed in the attachment of the cells to laminin as compared with uncoated wells, presumably due to the supply of laminin having deteriorated.

These attachment assays suggest that *WWOX* reconstitution causes PEO1 cells to attach less well to matrigel, fibronectin and possibly also laminin. They were, however, not replicated a sufficient number of times to be considered definitive. However, the findings are interesting and were reproducible when the number of cell lines used at one time was kept to a minimum. Considerably more time would be required in order to fully characterise the attachment phenotype of these *WWOX* transfectants.

Figure 8.18 Attachment of PEO1 vector-only and sense transfectants to matrigel

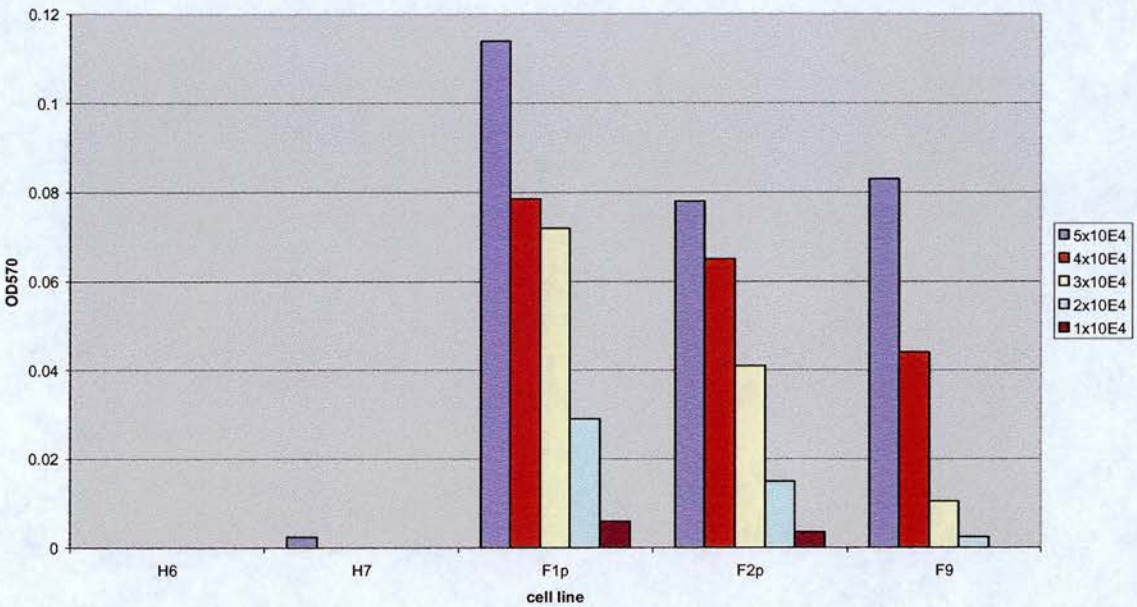

Attachment of vector-only controls (F1p, F2p and F9) and sense transfectants (H6 and H7) to matrigel 1 hour following the seeding of $5x10^4$ (blue bars), $4x10^4$ (red bars), $3x10^4$ (yellow bars), $2x10^4$ (green bars) and $1x10^4$ cells (purple bars). Cells were added to matrigel-coated 96 well trays obtained from Biocoat®. They were incubated for 1 hour at 37°C, 5% CO_2 and washed carefully. Following this, attached cells were quantified by MTT assay.

Figure 8.19 Attachment of PEO1 parent line and a sense transfectant to laminin and fibronectin

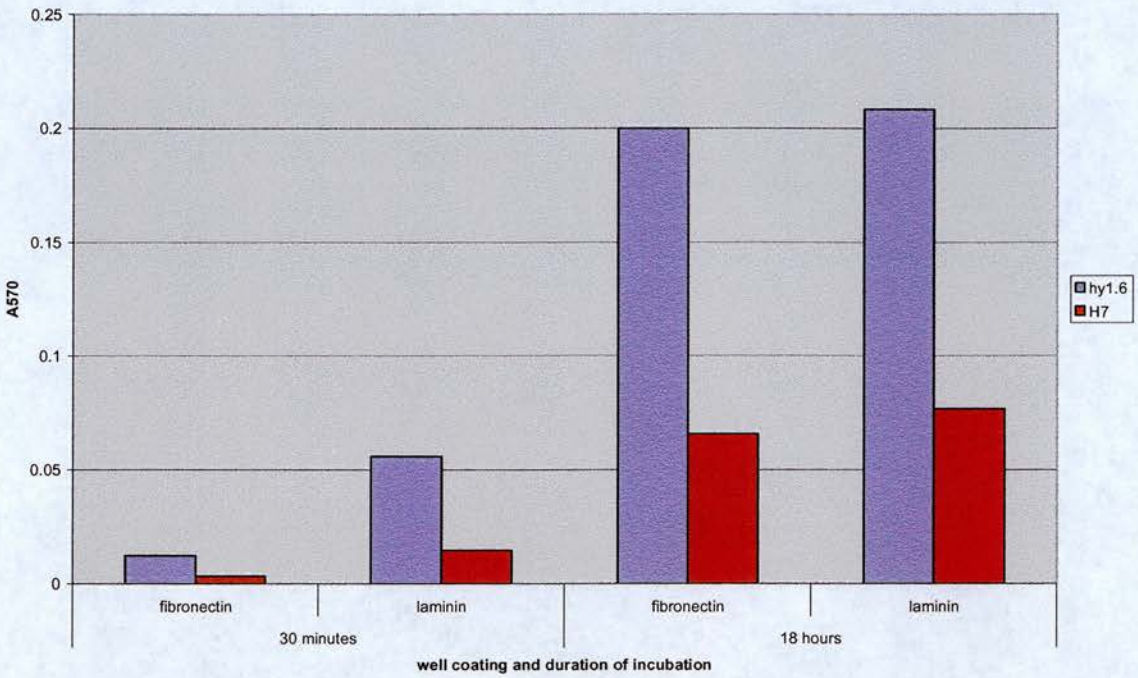

Attachment of the PEO1 parent line (hy1.6; blue bars) and a sense transfectants (H7; red bars) to fibronectin and laminin coated wells 30 minutes and 18 hours following the seeding of $5x10^4$ cells. Bacteriological-grade 96 well trays (Nunclon®) were prepared by the addition of 100µl of 10µg/ml of fibronectin or laminin to each well, followed by 60mins incubation at room temperature, careful washing with PBS, blocking with 200µl of 0.1% BSA, a further 1 hour incubation at room temperature and final washing with PBS. Then, $5x10^4$ PEO1 parent (hy1.6) or *WWOX*-transfected cells (H7) were added to each well. The cells were incubated for 30 minutes or 18 hours at 37°C, 5% CO_2 and then washed carefully. Following this, attached cells were quantified by MTT assay.

Figure 8.20 Attachment of PEO1 parent line, vector-only controls and sense transfectants to laminin and fibronectin

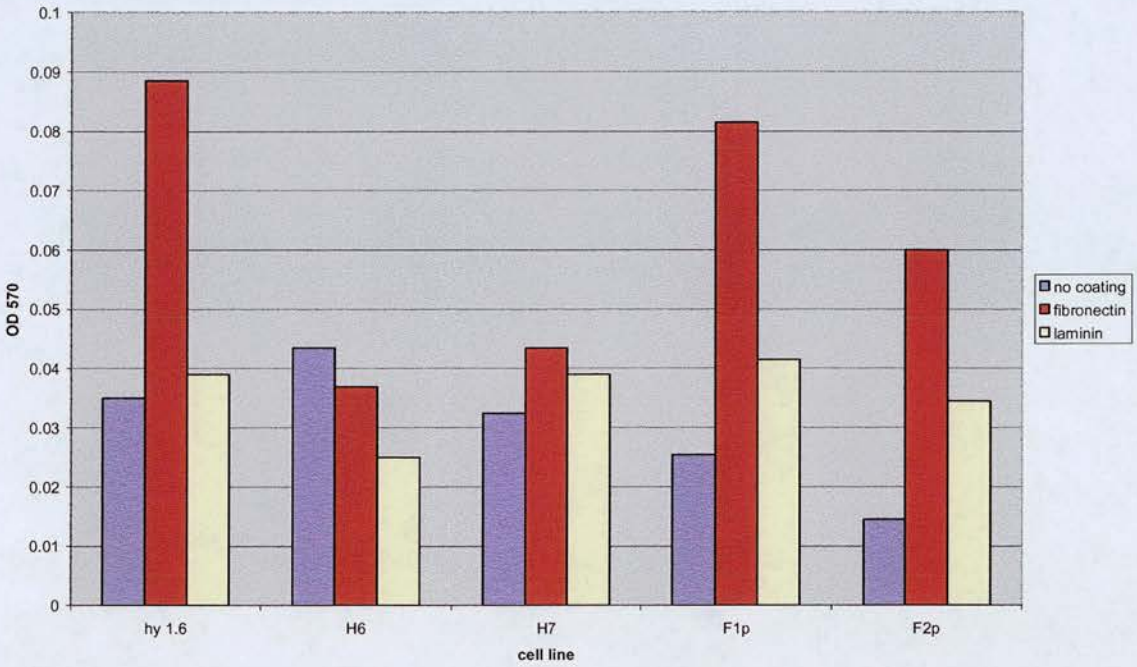

Attachment of the PEO1 parent line (hy1.6), 2 vector-only controls (F1p and F2p) and 2 sense transfectants (H6 and H7) to fibronectin and laminin coated wells 60 minutes following the seeding of $5x10^4$ cells. Bacteriological-grade 96 well trays (Nunclon®) were prepared by the addition of 100µl of 10µg/ml of fibronectin or laminin to each well, followed by 60mins incubation at room temperature, careful washing with PBS, blocking with 200µl of 0.1% BSA, a further 1 hour incubation at room temperature and final washing with PBS. Control wells had no coating applied but were still washed and blocked. Then, $5x10^4$ PEO1 parent (hy1.6), *WWOX*-transfected (H6, H7) or vector-transfected control cells were added to each well. The cells were incubated for 60 minutes at 37°C, 5% CO_2 and then washed carefully. Following this, attached cells were quantified by MTT assay. Attachment to uncoated, fibronectin-coated and laminin-coated wells is represented by the blue, red and yellow bars respectively.

8.6 Other work performed using this system

The PEO1 cell line system generated and characterised during this project was also used by Karen Taylor for microarray analysis, comparing the gene expression of the sense transfectants to controls. This generated a small number of candidate genes whose expression may be affected by *WWOX* upregulation, and this is being investigated further.

8.7 Evaluation of results

Expression of ectopic *WWOX* in PEO1 cells resulted in the abolition of tumourigenicity in nude mice. This is functional evidence that *WWOX* may operate as a tumour suppressor in ovarian cancer and therefore addresses the first aim of the study (to elucidate whether the *WWOX* gene functions as a tumour suppressor in epithelial ovarian cancer). This is an important result but certain caveats must be noted. Firstly, the result depends upon stable transfection of a cell line with constructs expressing exogenous *WWOX* or vector-only controls. Therefore the issue of clonal heterogeneity becomes a factor. That is, differences between the phenotype of transfected cell lines being due to changes in gene expression that have arisen during passage of cells since the transfection event rather than being due to the gene that has been transfected into the cells. I would strongly counter this argument here because the phenotype seen was either tumour growth (for the parent line, vector-only controls or antisense transfectants) or no tumour growth (for the sense transfectants) with no intermediate phenotype identified. There were a total of 5 cell lines in the former group (all of which produced tumours in nude mice) and a total of 4 cell lines in the latter group (none of which produced tumours in nude mice) so the

chance of this result occurring fortuitously as the result of clonal heterogeneity is infitessimally small. The second caveat is that these results have only been demonstrated for one ovarian cancer cell line. We could be more confident about the role of this gene as a suppressor of ovarian tumourigenesis in general (rather than in the PEO1 ovarian cancer cell line alone) if the *in vivo* phenotype could be replicated in another ovarian cancer system.

The fact that expression of ectopic *WWOX* in PEO1 cells resulted in the abolition of tumourigenicity in nude mice also implies that there is a functional *WWOX* pathway in the PEO1 cell line. Therefore a number of phenotypic assays were performed in an attempt to identify an *in vitro* phenotype for the gene. Expression of exogenous *WWOX* in PEO1 cells was found to have no effect on *in vitro* growth rate (on plastic or in agarose), clonogenicity (in the presence or absence of cytotoxic drugs), cellular aggregation or cellular invasion. *WWOX* expression in PEO1 cells was however shown to decrease the migration of PEO1 cells towards fibronectin and preliminary attachment assays also suggested that it may decrease the attachment of PEO1 cells to matrigel, fibronectin and other extracellular matrix components, such as laminin. Further work is required to clarify the role that *WWOX* plays in attachment to extracellular matrix components. However, the demonstration that exogenous expression of the *WWOX* gene in the PEO1 cell line system reproducibly decreases migration towards fibronectin and the suggestion that it decreases attachment to extracellular matrix components represents a significant step forward in the search for an *in vitro* phenotype for this gene. Once again, the possibility of these results being caused by clonal heterogeneity has to be considered. The best way to get around this is to use an inducible cell line system. Attempts to achieve this in the

present study using the Tet-On® system were unsuccessful due to high baseline (unstimulated) expression of transfected *WWOX* or 'leakiness' of the system. Once again, it would be easier to consider these phenotypic findings as generalisable to ovarian cancer if they were replicated in another ovarian cancer system.

These caveats aside, the findings in this chapter go some way towards the aim of ascribing a phenotype associated with expression of the *WWOX* gene.

9. DISCUSSION

9.1 Preamble

Unlike most epithelia, division of normal ovarian surface epithelial cells gives rise to two daughter cells with equal growth potential [49]. This means that mutated tumour suppressor genes can easily sustain a 'second-hit' and play a role in the development of ovarian cancer. Homozygous deletion [53], loss of heterozygosity [165,166] and loss of expression in malignant compared to non-malignant tissue [171] are all mechanisms of *WWOX* knockout or downregulation which have been identified. However, very few mutations have been found in the gene and no truncating point mutations have been identified. Also, there are no hereditary cancer syndromes known to result from defects in the *WWOX* gene. As such, it cannot be considered as a 'classic' tumour suppressor gene. The role of aberrant transcripts that were apparently specific for tumour tissue has been controversial.

Importantly, functional evidence does exist for a tumour suppressor role. Overexpression of *WWOX* in breast cancer cell lines inhibits tumourigenicity in nude mice and decreases the proliferation of breast cancer cells in soft agar [52]. Also, there is some evidence that murine Wox 1 is required for p53-mediated apoptosis of murine fibroblasts and that it enhances TNFα-mediated cytotoxicity. There is also a suggestion from coimmunoprecipitation and yeast two-hybrid analyses that murine Wox 1 may bind to the p53 polyproline region.

However, no firm phenotype has yet been ascribed to *WWOX*, the partners that bind to its WW domains are unknown, its natural intracellular substrate(s) in the cell are unknown and there is no evidence as yet that it interacts with p53 in the human cell.

The aims of the PhD were to

(i) Elucidate whether *WWOX* acts as a tumour suppressor gene in ovarian cancer.

(ii) Clarify the role of the *WWOX* gene (and its alternate transcripts) in ovarian carcinogenesis.

(iii) Ascribe a phenotype associated with expression of the *WWOX* gene and *WWOX* protein function.

In order to achieve these aims, two approaches were taken in parallel.

The first approach was to investigate the *WWOX* mRNA isoform expression profile of a panel of 71 human ovarian tumours, 13 normal ovaries and 37 human cancer cell lines. Full-length *WWOX* (isoform1) expression was found to be significantly lower in tumours than in normal ovaries ($p<0.0001$). Two tumours expressed no full-length *WWOX* mRNA. The *WWOX* Δ6-8 mRNA (isoform 4) was expressed at low levels, and was significantly associated with high grade ($p= 0.006$) and high stage ($p=0.012$) ovarian cancer but was also identified in non-malignant tissue. Three tumour cell lines (the CaOV3 ovarian line and the DU145 and PC3 prostate lines) were identified with extremely low levels of *WWOX* expression. 89% of the tumour cell lines were found to express *WWOX* isoform 4.

The second approach was to develop a cell line system with a functional *WWOX* pathway and by means of manipulation of the *WWOX* expression levels perform functional assays in the search for an *in vitro* phenotype. In addition, some preliminary experiments investigating pathways of *WWOX* induction in cell line systems were performed.

Three tumour cell lines (the HCT116 colorectal cancer cell line and PE01 and A2780 ovarian cancer cell line) were transfected with sense and antisense *WWOX* constructs and levels of *WWOX* expression were assessed by quantitative RT–PCR. On the basis of expression levels transfected clones were chosen for functional analysis. The reason for using a colorectal line in a mainly ovarian cancer–orientated project was the availability of well-characterised wild-type, p53-null, p21-null and Bax-null derivatives of the line. The most useful system was the PE01 cell line system. When *WWOX* was replaced in this cell line (its enzymatic domain is homozygously deleted in the PEO1 parent line) this resulted in complete abolition of tumourigenicity in nude mice. This suggested that there was a functional *WWOX* pathway in PEO1 cells so *in vitro* phenotypic analyses were conducted in this system. These in vitro analyses revealed that replacement of *WWOX* in PE01 cells had no effect upon growth (either in plastic or soft agar), clonogenicity (in the presence or absence of cytotoxic drugs) or on cell invasion. However it did result in decreased tumour cell migration towards fibronectin. There was also a suggestion that *WWOX* replacement resulted in decreased attachment to matrigel and fibronectin.

9.2 *WWOX* mRNA isoform expression in epithelial ovarian tumours, normal ovaries and cancer cell lines

In light of the paucity of mutations in *WWOX*, other mechanisms of *WWOX* dysregulation that may play a role in cancer, such as reduced expression or the production of aberrant isoforms, were investigated. At the time of this study, the

available antibodies directed against *WWOX* protein only recognised full-length *WWOX*, not any of the shorter alternate transcripts. However the sensitivity of the real-time PCR assay appeared to be superior to Western blotting as evidenced by PEO1 *WWOX* transfectants that expressed low levels of *WWOX* isoform 1 mRNA but apparently no protein (section 8.2). The expression of the alternate transcripts is generally orders of magnitude lower than that of *WWOX* isoform 1. These two facts together indicate that it is extremely unlikely that even if this antibody recognised the alternate transcripts that it would detect them.

9.2.1 Full-length *WWOX* (isoform 1) mRNA expression supports the role of the *WWOX* gene as a tumour suppressor

Full-length *WWOX* expression was found to be significantly lower in epithelial ovarian cancers compared to normal ovarian tissue ($p<0.0001$), which would support its role as a tumour suppressor gene or a negative regulator of cancer. In addition 2/71 tumours expressed no full-length *WWOX* (isoform 1). This frequency is consistent with previous reports describing the absence of isoform 1 in 1/36 oesophageal cancers [165], in 2/27 non-small cell lung cancers [166] and in 1/20 breast cancers [169]. The latter example, like our two cases, demonstrated no evidence of exonic homozygous deletion. Of these two non-expressors of *WWOX* isoform 1, one expressed a truncated transcript and the other tumour expressed no transcript at all. In neither case was homozygous deletion of exons identified in genomic DNA. The reasons for these findings are at present unclear. The tumour with a truncated transcript may have a mutation at a normal splice acceptor or donor

site resulting in altered mRNA processing. The tumour expressing no transcript may have undergone epigenetic silencing of the *WWOX* gene secondary to promoter methylation or histone deacetylation or may have acquired a large insertion into one of its exons, preventing PCR amplification of the transcript. However, previous studies [52] have demonstrated no evidence of somatic methylation as an inactivating mechanism for *WWOX*.

There was no association between *WWOX* isoform 1 expression levels and clinicopathological factors or patient survival. An ovarian cell line (CaOV3) and two prostate cancer cell lines (PC3 and DU145) expressed very low levels of *WWOX* isoform 1, again suggesting that this isoform may act as a tumour suppressor. These cell lines would be suitable for investigation of *WWOX* downregulatory mechanisms.

9.2.2 The role of the *WWOX* Δ6-8 (isoform 4) transcript in tumourigenesis is uncertain

The *WWOX* Δ6-8 (isoform 4) transcript was expressed at low levels in 63% of the ovarian tumour samples and in 16/17 (94%) of ovarian cancer cell lines. In addition, other alternate transcripts (possibly *WWOX* Δ7 and Δ7-8 on size criteria) were identified in 17% of ovarian tumours. This compares to a frequency of 5.5% in oesophageal squamous cell carcinoma [165] and 11.1% in non-small cell lung carcinoma [166], although a further 14.8% of these lung tumours expressed other alternate transcripts. The frequency of alternate transcript detection using a competitive PCR similar to that used in earlier studies was 57% suggesting that the discrepancy in expression frequency between the different tumour types was probably real rather than being method related.

The expression of *WWOX* isoform 4 mRNA was significantly associated with high tumour grade (p=0.006) and advanced stage ovarian cancer (p=0.012). There was a trend towards adverse survival in patients who expressed this isoform and significantly worse survival in robust isoform 1 expressers who also expressed isoform 4.

There are several possible explanations for the association of *WWOX* isoform 4 with adverse clinical parameters. *WWOX* isoform 4 could represent a surrogate marker of disruption at FRA16D or it could be a surrogate marker for a more general problem with the splicing machinery of the cancer cell. Alternatively, isoform 4 may imply an oncogenic gain of function characteristic. The fourth possibility is that isoform 4 (which has a disrupted oxidoreductase domain) may function as a dominant negative isoform, sequestering binding partners of *WWOX* isoform 1 and inhibiting its putative tumour suppressor role.

Low levels of *WWOX* isoform 4 expression were also identified in 69% of non-malignant ovarian tissues. Alternate transcripts have been noted in normal tissues previously but this has been somewhat understated [169,171]. This suggests that the isoform may be an infrequently produced splice form, even in normal cells. It has been estimated that in normal cells spliceosome errors occur in 2-3% of transcripts [195]. Under these circumstances, its presence in malignant tissue would not be surprising considering the size of the unprocessed *WWOX* transcript. Spliceosome errors have been estimated at 10-20% in cancer cells [196]. Indeed, alternative splicing isoforms are commonly associated with cancer. Cancer-associated splice variants have been reported for a number of genes including *EGFR*, *CD44*, and *NER* [197]. Wang et al [198] performed a genome-wide computational screen identifying

26258 alternative splicing isoforms, of which 845 were significantly associated with human cancer. Some of these alternate transcripts have the potential to play a role in tumourigenesis e.g. by inhibiting apoptosis (CD79 [199]) or by blocking tumour suppressor activity (BIN 1 [200]). It may be that the general increase in alternate transcript production in tumour tissue is because splicing fideltity is decreased by mutations or altered gene expression affecting the splicing apparatus.

In this regard it is interesting that in malignant tissue it is mainly alternative splicing rather than aberrant splicing of *WWOX* that is identified, although the latter was seen in the study by Ishii et al [171]. Alternative splicing uses inherent intron/exon splice sites of a single mRNA transcript to produce different mRNAs through differential splicing whereas aberrant splicing does not occur at de facto splice sites. This may suggest that in the case of *WWOX,* exon-skipping is not simply due to a loss of splicing specificity in tumours. Also, the fact that there is one main alternate isoform (isoform 4 or Δ6-8) that is frequently expressed rather than a large number of variant isoforms (the other forms are expressed at low frequency) raises the possibility that this phenomenon may not be due entirely to a random process of loss of splicing specificity.

An important question is whether these alternative transcripts are translated intact or not. At the time this project was conducted, no antibodies specific for isoform 4 had been identified. Two groups have recently generated antibodies that detect the *WWOX* alternate transcripts. One group [172] could only detect isoform 4 expression if the proteosome was blocked. They interpreted this as meaning that this transcript is targeted for destruction and is not translated. While this may be true, these data show that the level of alternate transcript expression in tumour tissue is at

a level at which expression of *WWOX* isoform 1 would not be detected (for which an antibody was available). Blocking the proteosome could result in the alternatively spliced proteins rising to a level that was detectable by Western blotting. The second group [171] did identify the presence of *WWOX* short form proteins in haematopoietic malignancies, although no indication of the specificity of the antibody was given.

Finally, when considering the question of whether the *WWOX* alternative transcripts may have a functional role in tumourigenicity, it is important to note that *WWOX* isoform 1 and *WWOX* isoform 4 have different intracellular locations. While *WWOX* isoform 1 is located largely in the cytoplasm (whether it be in the Golgi or in the mitochondrion), *WWOX* isoform 4 is located in the nucleus. This means that low levels of *WWOX* isoform 4 do not preclude it having a dominant negative effect on the function of *WWOX* isoform 1 as competition for binding partners may not be on an equal basis.

The role of *WWOX* isoform 4 is clearly speculative at this time. More definitive evidence regarding its role in ovarian cancer could be gained by transfecting it into immortalised human ovarian surface epithelial lines or by specific knockout of this isoform in cell lines expressing high levels of both *WWOX* isoform 1 and isoform 4, followed by analysis for any resulting phenotypic alteration. On the basis of the isoform expression in our cell line panel, MCF-7 (which was the highest expresser of both isoforms) would be ideal for this purpose.

9.3 *WWOX* appears to be upregulated by hyaluronidase and inducers of DNA damage

In a preliminary investigation of *WWOX* induction pathways, exposure of isogenic p53 normal and p53-null HCT116 colorectal cancer cells to hyaluronidase resulted in 150% upregulation of *WWOX* expression in the p53 normal cells but no upregulation of *WWOX* expression in the p53-null cells. This suggests that hyaluronidase-induced *WWOX* expression is p53-dependent (although an unknown mutation arising in a component of the *WWOX* induction pathway subsequent to the derivation of the p53-null line cannot be excluded). This conclusion was supported by the finding that *WWOX* was not induced in the PEO1 cell line (p53 mutant). This evidence, however, is a lot weaker as a vital component of the *WWOX* induction pathway may have been knocked out in the PEO1 cell line.

It is interesting and reassuring to note that the same degree of upregulation of murine *Wox1* (150%) was obtained by Chang et al [168] when they expressed L929 murine fibroblasts to the same dose of hyaluronidase (200units/ml) for a comparable duration of time (8-24 hours). This time course of *Wox1* induction fits with the time course for hyaluronidase to induce TNFα sensitivity in murine L929 fibroblasts (mouse *Wox1* was identified when Chang et al were exploring mechanisms whereby hyaluronidase enhanced TNFα cytotoxicity using differential display and cDNA library screening).

It may be that in the p53 wild-type non-malignant cell *WWOX*/*Wox1* is upregulated as part of the plethora of intracellular events that occur following exposure to hyaluronidase. *Wox1* transfection is known to enhance TNFα-mediated cytotoxicity in L929 mouse fibroblasts [168]. If however, *WWOX* is knocked out in a normal,

pre-malignant or malignant cell then presumably a state of increased resistance to TNFα-mediated cell death exists. It is important to establish that this induction pathway may also exist in human cancer cells.

The suggestion that p53 may be involved in *WWOX* induction led to the investigation of whether inducers of DNA damage (in the form of cytotoxic agents) induced *WWOX* expression in the same HCT116 cell line system. It was found that doxorubicin and oxaliplatin induced *WWOX* expression over the time course tested (48 hours) but 5-fluorouracil did not.

Doxorubicin was the only drug that increased *WWOX* expression in the wild-type HCT116 cells following 24 hours exposure and it maintained this effect at 48 hours. Oxaliplatin caused a more marked induction of *WWOX* but this was not evident until 48 hours.

In the p53-null cells the *WWOX* induction respone to doxorubicin and oxaliplatin exposure appeared blunted. In the doxorubicin-exposed cells after 24 hours there was only a 50% increase in *WWOX* expression (compared to 200% in the p53 normal cells). There was a 90% increase in *WWOX* expression after 48 hours which was again less than in the p53 normal cells. Also, the profile of induction was different. In the p53 wild-type cells, maximal *WWOX* induction occurred after 24 hours but in the p53-null cells, it occurred after 48 hours.

Similarly, the induction of *WWOX* in oxaliplatin-exposed p53-null cells was less than half of that in the p53 wild-type cells.

Although 5-fluorouracil did not appear to induce *WWOX* in this assay, other investigators have found that in some systems it takes 72 hours to demonstrate altered gene expression as a result of 5-fluorouracil exposure [194].

These findings suggest that *WWOX* mRNA induction may be partly dependent on p53 and is reduced or delayed in the absence of p53.

Since this work is preliminary, further confirmatory work is required to completely secure this data. Future work should extend the time course of the *WWOX* induction studies in response to cytotoxic agents and investigate, firstly, which component of the induction is a stress-related p53 response and, secondly, which component is secondary to induction of specific signal transduction pathways.

9.4 Discovery of *in vivo* and *in vitro* phenotypes for *WWOX* in an ovarian cell line system

Until now, the only functional data regarding the phenotype of the *WWOX* gene have been provided by Bednarek et al [52]. They showed that ectopic *WWOX* expression in breast cancer cell lines with low baseline levels of *WWOX* expression strongly inhibited anchorage-independent growth in soft agar and dramatically inhibited tumourigenicity *in vivo*.

The PEO1 parent cell line is homozygously deleted for *WWOX* exons 4-8 and expresses only small amounts of a *WWOX* Δ4-8 transcript. This cell line was stably transfected with constructs expressing the *WWOX* coding region. *WWOX* expression levels in the transfected clones were then determined using real-time PCR. A tight linear correlation between *WWOX* mRNA and protein levels was then demonstrated in this system.

9.4.1 *WWOX* reconstitution in PEO1 ovarian cancer cells suppresses tumourigenicity in nude mice

PEO1 parent cells and vector-only transfected control cells caused tumour growth when injected subcutaneously into the flanks of nude mice. Ectopic expression of *WWOX* in these cells caused complete abolition of tumourigenicity. This suggested that there was a functional downstream *WWOX* pathway in PEO1 cells. It also suggested that *WWOX* may function as a tumour suppressor in ovarian cancer. This is important of itself, but by replicating the findings of Bednarek et al [52] it adds credence to the hypothesis that *WWOX* acts as a tumour suppressor in human cancer.

9.4.2 *WWOX* reconstitution in PEO1 ovarian cancer cells results in decreased migration towards fibronectin *in vitro*

As there appeared to be a functional *WWOX* pathway in PEO1 cells, an *in vitro* phenotype for the gene was sought in this system. The PEO1 sense transfectants showed no difference in growth (either on plastic or soft agar), clonogenicity (in the presence or absence of cytotoxic drugs), cell aggregation or cell invasion compared to the parent line or vector-only controls but they did show significantly decreased tumour cell migration towards fibronectin. Preliminary work on the attachment characteristics of these PEO1 cells suggests that replacement of *WWOX* has an inhibitory effect on their attachment to matrigel as well as to laminin and fibronectin. These findings raise the possibility that *WWOX* may suppress the migration of ovarian cells and loss of *WWOX* may increase the migratory capacity of premalignant or malignant cells, facilitating local spread. Specifically, *WWOX* may

inhibit migration towards fibronectin. This along with the preliminary findings regarding the effect of *WWOX* reconstitution on the attachment of PEO1 cells to extracellular matrix components, suggests that this effect may be manifest through cell-surface proteins, such as integrins.

As cancer cells become metastatic, they develop an altered affinity for the extracellular matrix [201]. This change is mediated by alterations in cell-surface molecules, particularly integrins. Integrin types expressed on the surface of the malignant cell may be altered [202-204] compared to its non-malignant counterpart or there may be a change in affinity or avidity for a particular ligand. Ligand binding of integrins activates intracellular signalling that affects cellular migration, invasion, proliferation and survival. Migrating cells project lamellipodia that attach to extracellular matrix proteins (such as laminin, fibronectin and collagen) via integrins expressed on the cell surface. This allows the cell to pull itself forward. Therefore integrins would seem to be a likely candidate for the effector of the altered migration phenotype seen in *WWOX* transfected PEO1 cells.

Casey et al [205] found that OVCAR 5 ovarian carcinoma cells were able to form spheroids similar to multicellular aggregates isolated from patient ascitic fluid. This spheroid formation was increased by a β1 integrin-stimulating monoclonal antibody or exogenous fibronectin but was inhibited by blocking monoclonal antibodies against the α5 or β1-integrin subunits. These spheroids adhered to fibronectin, laminin and collagen type IV. This adhesion was partially inhibited by blocking antibodies against the α5, α6 and α2 integrin subunits respectively but a blocking antibody against the β1 integrin subunit completely inhibited adhesion to all three extracellular matrix components. These findings were interpreted as suggesting that

interactions between α5β1 integrin and fibronectin facilitate ovarian carcinoma spheroid formation and that multiple integrins are involved in adhesion to extracellular matrix proteins at the site of secondary tumour growth (the peritoneal mesothelium).

Integrins, however, are not the only molecule that could be effecting the phenotypic change seen in the *WWOX* transfected PEO1 cells. E-cadherin mediated cell-cell adhesion has been shown to inhibit anoikis in cancer cells [206]. This inhibition of anoikis is at least partly due to the maintenance of anti-apoptotic phosphatidylinositol 3-kinase signalling following E-cadherin binding[207]. It has been speculated that E-cadherin (which is not expressed in normal ovarian surface epithelial cells, becomes expressed in early ovarian cancer and is then lost again following progression to locoregionally disseminated disease) may facilitate the survival of tumour cells when they leave the ovary and spread throughout the peritoneum [208,209].

It may be that loss of *WWOX* expression in a malignant or pre-malignant cell alters integrin (or other cell surface molecule) expression profile, affinity or avidity in such a way that cell migration and attachment to extracellular matrix proteins at the site of secondary growth is promoted. This could have the effect of preventing the normal process of anoikis as the integrin (or other cell surface molecule) ligand interaction could promote cell survival.

In order to further elucidate the mechanism by which *WWOX* expression affects migration of ovarian cancer cells towards fibronectin, it will be necessary to characterise and compare the integrin expression on the surface of ovarian cancer cells expressing *WWOX* to those not expressing *WWOX*. The PEO1 cell line system

developed in this project would be ideal for this purpose. Characterisation of integrin expression would involve profiling the integrins expressed and assessing the affinity and avidity of each for their respective ligand. In order to further clarify the involvement of the migration/attachment phenotype in ovarian tumourigenesis, it would be useful to compare the gene expression of *WWOX* expressing and *WWOX* non-expressing PEO1 cells stimulated by fibronectin by microarray and proteomic analysis.

9.5 Future directions

The role of the *WWOX* alternate transcripts in tumourigenesis remains controversial and unproven. In order to directly test whether they were of functional significance, MCF-7 breast cancer cells could be transfected with constructs expressing RNA interference molecules targeting *WWOX* isoform 4 (this cell line expresses high levels of both *WWOX* isoform 1 and *WWOX* isoform 4). Functional analyses could then be performed in an attempt to identify an isoform-specific phenotype. Another strategy would be to transfect *WWOX* isoform 4 into human ovarian surface epithelial cells and investigate for a transformed phenotype.

The most important aspect of this project that requires further investigation is the effect that *WWOX* appears to have on the interaction of PEO1 ovarian cancer cells with extracellular matrix proteins. It would be desirable to fully characterise the ligands that are affected by *WWOX* expression and then identify which cell surface molecule is involved in these interactions. Cell attachment assays, however, are difficult to perform and reproduce but procedures to identify the cell surface integrin

expression by flow cytometry are now routine and this may be the simplest way to identify whether *WWOX* has an effect on this type of interaction. Flow cytometry can also be used to assess the affinity and avidity of integrins on the cell surface for their respective ligands.

As interactions between cell surface molecules and the extracellular matrix can affect cell survival and a role in apoptosis has been postulated for *Wox1* in the mouse, it would be important to assess the effect of *WWOX* on cell survival. Again, the PEO1 cell line system would be ideal for this purpose.

Since *WWOX* expression appears to affect cellular migration towards fibronectin, a microarray-based comparison of the gene expression of *WWOX* expressing and *WWOX* non-expressing PEO1 cells stimulated by fibronectin may shed light on intracellular signalling pathways that are affected by this interaction.

Ultimately, the most definitive evidence regarding whether *WWOX* functions as a tumour suppressor will come from the construction of the *WWOX* knockout mouse, which is currently being generated.

9.6 Summary of project and extent to which aims were achieved

Three aims were set out at the beginning of the project:

1) To elucidate whether the *WWOX* gene functions as a tumour suppressor in epithelial ovarian cancer.
2) To clarify the role of the *WWOX* gene (and its alternate transcripts) in ovarian carcinogenesis.

3) To ascribe a phenotype associated with expression of the *WWOX* gene and WWOX protein function.

These will be considered in turn and the extent to which the results achieve these aims will be discussed. This final summary of the project is summarised in the form of a schematic in figure 9.1.

a) Aim 1: To elucidate whether the *WWOX* gene functions as a tumour suppressor in epithelial ovarian cancer

The hypothesis was that the *WWOX* gene acts as a tumour suppressor in ovarian cancer.

WWOX isoform 1 expression was found to be absent in 2 out of 71 ovarian tumours and was down-regulated in ovarian tumours compared to normal ovaries ($p<0.001$). This provides supportive evidence that *WWOX* acts as a tumour suppressor gene in epithelial ovarian cancer. There are 2 caveats however: the choice of controls in this setting is difficult and normal ovarian tissue is not an ideal comparator (although nothing really is) and quantitation of expression at the protein level would have been superior if the antibody sensitivity had been satisfactory.

Up-regulation of *WWOX* in the PEO1 ovarian cancer cell line resulted in the abolition of tumourigenicity in nude mice. This provides strong evidence that *WWOX* acts as a suppressor of human ovarian tumourigenesis. The strength of this statement would be increased if this result could be replicated in a second ovarian cancer cell line.

b) To clarify the role of the *WWOX* gene (and its alternate transcripts) in ovarian carcinogenesis

The hypothesis being tested was that *WWOX* alternate transcripts act in a dominant negative fashion to facilitate ovarian tumourigenesis.

It was shown that *WWOX* isoform 4 was expressed at low levels in 63% of human ovarian tumour samples, at low levels in 69% of normal ovaries and at variable levels in 94% of ovarian cancer cell lines. This data does not help in the clarification of the role of *WWOX* alternate transcripts.

Expression of *WWOX* isoform 4 was significantly associated with high ovarian tumour grade ($p=0.006$) and advanced tumour stage ($p=0.012$). There was a trend towards adverse survival ($p=0.057$) in patients who expressed this isoform and significantly worse survival ($p=0.048$) in robust isoform 1 expressers who also expressed isoform 4. These findings help little in the clarification of a role (if one exists) for the *WWOX* alternate transcripts in ovarian tumourigenesis. They merely identify an association between isoform 4 expression and poor risk disease which could be due to a number of reasons (see earlier discussion).

c) To ascribe a phenotype associated with expression of the *WWOX* gene and WWOX protein function

The hypothesis being tested was that exogenous expression of the *WWOX* gene in an ovarian cell line defective for *WWOX* would result in a tumour-suppressing phenotypic change that could then be ascribed to the *WWOX* gene.

The first step in testing this hypothesis and then identifying a phenotype was to find a suitable cell line that was defective for *WWOX* but in which the rest of the *WWOX*

pathway remained intact. This was achieved when it was shown that expression of exogenous *WWOX* in the PEO1 cell line resulted in the abolition of tumourigenicity in nude mice. It was then demonstrated that this *WWOX* reconstitution in PEO1 cells resulted in significantly decreased tumour cell migration towards fibronectin. Preliminary work on the attachment characteristics of these PEO1 cells also suggested that exogenous *WWOX* expression inhibited cellular attachment to matrigel, fibronectin and laminin. These findings therefore identified a *WWOX*-specific phenotype (decreased tumour cell migration) and suggested that this phenotype extends to a role in inhibiting cancer cell binding to ECM components. The main caveats to this conclusion are that the work was only performed in one cell line (so generalisation requires caution) and that stable transfection was used in this system (hence clonal heterogeneity is a consideration). Despite this point, this data goes some way to achieving this aim (although further characterisation of this exciting phenotype would have been desirable if time allowed).

9.7 Conclusion

WWOX reconstitution in the PEO1 ovarian cancer cell line abolishes tumourigenicity in nude mice and decreases migration towards fibronectin *in vitro*. The former finding provides strong supportive evidence that *WWOX* acts as a tumour suppressor of human ovarian tumourigenesis and the latter finding provides a handle on an *in vitro* phenotype which until now has proved elusive.

Figure 9.1 Schematic diagram summarising findings and how they address initial aims of the project

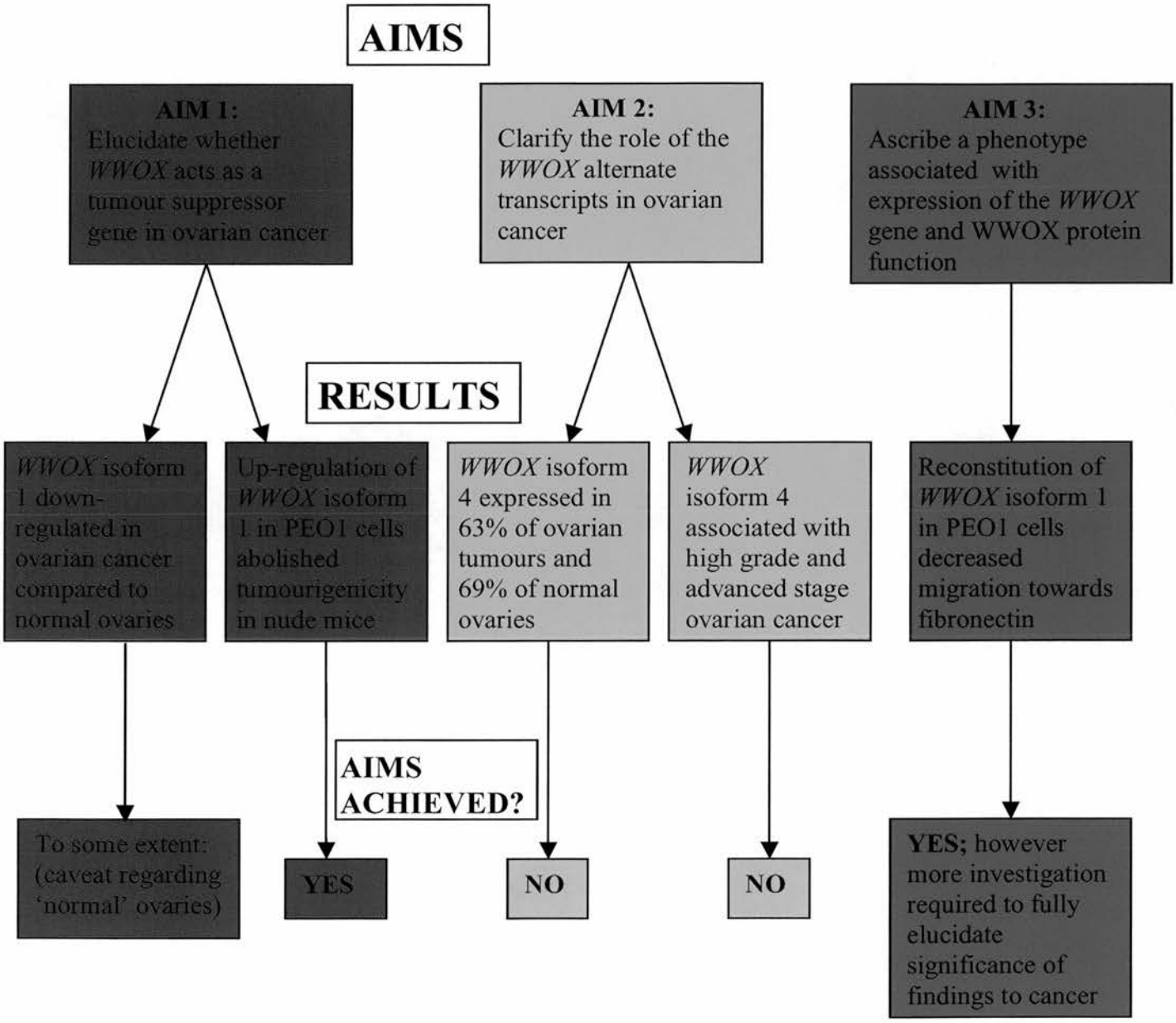

Schematic diagram summarising the main findings of the study and how and whether these address the initial aims of the project. Results pertaining to aims 1, 2 and 3 are shown in green, yellow and blue respectively.

References:

1. Harries, M. and Gore, M. (2002) Part I: chemotherapy for epithelial ovarian cancer-treatment at first diagnosis. *Lancet Oncol*, **3**, 529-36.
2. Greenlee, R.T., Hill-Harmon, M.B., Murray, T. and Thun, M. (2001) Cancer statistics, 2001. *CA Cancer J Clin*, **51**, 15-36.
3. CRC (2001) Cancer Research Campaign cancer stats. London: CRC, 2001.
4. Schuijer, M. and Berns, E.M. (2003) TP53 and ovarian cancer. *Hum Mutat*, **21**, 285-91.
5. Herrinton, L.J., Stanford, J.L., Schwartz, S.M. and Weiss, N.S. (1994) Ovarian cancer incidence among Asian migrants to the United States and their descendants. *J Natl Cancer Inst*, **86**, 1336-9.
6. Rao, B.R. and Slotman, B.J. (1991) Endocrine factors in common epithelial ovarian cancer. *Endocr Rev*, **12**, 14-26.
7. Risch, H.A. (1998) Hormonal etiology of epithelial ovarian cancer, with a hypothesis concerning the role of androgens and progesterone. *J Natl Cancer Inst*, **90**, 1774-86.
8. Venn, A., Watson, L., Bruinsma, F., Giles, G. and Healy, D. (1999) Risk of cancer after use of fertility drugs with in-vitro fertilisation. *Lancet*, **354**, 1586-90.
9. Garg, P.P., Kerlikowske, K., Subak, L. and Grady, D. (1998) Hormone replacement therapy and the risk of epithelial ovarian carcinoma: a meta-analysis. *Obstet Gynecol*, **92**, 472-9.
10. Risch, H.A., Marrett, L.D., Jain, M. and Howe, G.R. (1996) Differences in risk factors for epithelial ovarian cancer by histologic type. Results of a case-control study. *Am J Epidemiol*, **144**, 363-72.
11. Allen, D.G., Heintz, A.P. and Touw, F.W. (1995) A meta-analysis of residual disease and survival in stage III and IV carcinoma of the ovary. *Eur J Gynaecol Oncol*, **16**, 349-56.
12. Mutch, D.G. (2002) Surgical management of ovarian cancer. *Semin Oncol*, **29**, 3-8.
13. Agarwal, R. and Kaye, S.B. (2003) Ovarian cancer: strategies for overcoming resistance to chemotherapy. *Nat Rev Cancer*, **3**, 502-16.

14. Young, R.C., Walton, L.A., Ellenberg, S.S., Homesley, H.D., Wilbanks, G.D., Decker, D.G., Miller, A., Park, R. and Major, F., Jr. (1990) Adjuvant therapy in stage I and stage II epithelial ovarian cancer. Results of two prospective randomized trials. *N Engl J Med*, **322**, 1021-7.
15. Bolis, G., Colombo, N., Pecorelli, S., Torri, V., Marsoni, S., Bonazzi, C., Chiari, S., Favalli, G., Mangili, G., Presti, M. and et al. (1995) Adjuvant treatment for early epithelial ovarian cancer: results of two randomised clinical trials comparing cisplatin to no further treatment or chromic phosphate (32P). G.I.C.O.G.: Gruppo Interregionale Collaborativo in Ginecologia Oncologica. *Ann Oncol*, **6**, 887-93.
16. Trope, C., Kaern, J., Hogberg, T., Abeler, V., Hagen, B., Kristensen, G., Onsrud, M., Pettersen, E., Rosenberg, P., Sandvei, R., Sundfor, K. and Vergote, I. (2000) Randomized study on adjuvant chemotherapy in stage I high-risk ovarian cancer with evaluation of DNA-ploidy as prognostic instrument. *Ann Oncol*, **11**, 281-8.
17. Colombo, N., Guthrie, D., Chiari, S., Parmar, M., Qian, W., Swart, A.M., Torri, V., Williams, C., Lissoni, A. and Bonazzi, C. (2003) International Collaborative Ovarian Neoplasm trial 1: a randomized trial of adjuvant chemotherapy in women with early-stage ovarian cancer. *J Natl Cancer Inst*, **95**, 125-32.
18. Trimbos, J.B., Vergote, I., Bolis, G., Vermorken, J.B., Mangioni, C., Madronal, C., Franchi, M., Tateo, S., Zanetta, G., Scarfone, G., Giurgea, L., Timmers, P., Coens, C. and Pecorelli, S. (2003) Impact of adjuvant chemotherapy and surgical staging in early-stage ovarian carcinoma: European Organisation for Research and Treatment of Cancer-Adjuvant ChemoTherapy in Ovarian Neoplasm trial. *J Natl Cancer Inst*, **95**, 113-25.
19. Trimbos, J.B., Parmar, M., Vergote, I., Guthrie, D., Bolis, G., Colombo, N., Vermorken, J.B., Torri, V., Mangioni, C., Pecorelli, S., Lissoni, A. and Swart, A.M. (2003) International Collaborative Ovarian Neoplasm trial 1 and Adjuvant ChemoTherapy In Ovarian Neoplasm trial: two parallel randomized phase III trials of adjuvant chemotherapy in patients with early-stage ovarian carcinoma. *J Natl Cancer Inst*, **95**, 105-12.
20. Piver, M.S., Barlow, J.J. and Lele, S.B. (1978) Incidence of subclinical metastasis in stage I and II ovarian carcinoma. *Obstet Gynecol*, **52**, 100-4.

21. Piver, M.S. (1982) Optimal surgical therapy in stage I and II ovarian malignancies. *Int J Radiat Oncol Biol Phys*, **8**, 247-9.
22. Young, R.C., Decker, D.G., Wharton, J.T., Piver, M.S., Sindelar, W.F., Edwards, B.K. and Smith, J.P. (1983) Staging laparotomy in early ovarian cancer. *Jama*, **250**, 3072-6.
23. Aabo, K., Adams, M., Adnitt, P., Alberts, D.S., Athanazziou, A., Barley, V., Bell, D.R., Bianchi, U., Bolis, G., Brady, M.F., Brodovsky, H.S., Bruckner, H., Buyse, M., Canetta, R., Chylak, V., Cohen, C.J., Colombo, N., Conte, P.F., Crowther, D., Edmonson, J.H., Gennatas, C., Gilbey, E., Gore, M., Guthrie, D., Yeap, B.Y. and et al. (1998) Chemotherapy in advanced ovarian cancer: four systematic meta-analyses of individual patient data from 37 randomized trials. Advanced Ovarian Cancer Trialists' Group. *Br J Cancer*, **78**, 1479-87.
24. A'Hern, R.P. and Gore, M.E. (1995) Impact of doxorubicin on survival in advanced ovarian cancer. *J Clin Oncol*, **13**, 726-32.
25. (1991) Cyclophosphamide plus cisplatin versus cyclophosphamide, doxorubicin, and cisplatin chemotherapy of ovarian carcinoma: a meta-analysis. The Ovarian Cancer Meta-Analysis Project. *J Clin Oncol*, **9**, 1668-74.
26. McGuire, W.P., Hoskins, W.J., Brady, M.F., Kucera, P.R., Partridge, E.E., Look, K.Y., Clarke-Pearson, D.L. and Davidson, M. (1996) Cyclophosphamide and cisplatin compared with paclitaxel and cisplatin in patients with stage III and stage IV ovarian cancer. *N Engl J Med*, **334**, 1-6.
27. Muggia, F.M., Braly, P.S., Brady, M.F., Sutton, G., Niemann, T.H., Lentz, S.L., Alvarez, R.D., Kucera, P.R. and Small, J.M. (2000) Phase III randomized study of cisplatin versus paclitaxel versus cisplatin and paclitaxel in patients with suboptimal stage III or IV ovarian cancer: a gynecologic oncology group study. *J Clin Oncol*, **18**, 106-15.
28. Piccart, M.J., Bertelsen, K., James, K., Cassidy, J., Mangioni, C., Simonsen, E., Stuart, G., Kaye, S., Vergote, I., Blom, R., Grimshaw, R., Atkinson, R.J., Swenerton, K.D., Trope, C., Nardi, M., Kaern, J., Tumolo, S., Timmers, P., Roy, J.A., Lhoas, F., Lindvall, B., Bacon, M., Birt, A., Andersen, J.E., Zee, B., Paul, J., Baron, B. and Pecorelli, S. (2000) Randomized intergroup trial of cisplatin-paclitaxel versus cisplatin-cyclophosphamide in women with advanced epithelial ovarian cancer: three-year results. *J Natl Cancer Inst*, **92**, 699-708.

29. (2002) Paclitaxel plus carboplatin versus standard chemotherapy with either single-agent carboplatin or cyclophosphamide, doxorubicin, and cisplatin in women with ovarian cancer: the ICON3 randomised trial. *Lancet*, **360**, 505-15.
30. Sandercock, J., Parmar, M.K., Torri, V. and Qian, W. (2002) First-line treatment for advanced ovarian cancer: paclitaxel, platinum and the evidence. *Br J Cancer*, **87**, 815-24.
31. Neijt, J.P., Engelholm, S.A., Tuxen, M.K., Sorensen, P.G., Hansen, M., Sessa, C., de Swart, C.A., Hirsch, F.R., Lund, B. and van Houwelingen, H.C. (2000) Exploratory phase III study of paclitaxel and cisplatin versus paclitaxel and carboplatin in advanced ovarian cancer. *J Clin Oncol*, **18**, 3084-92.
32. Ozols, R., Bundy, B., Fowler, J., Clarke-Pearson, D., Mannel, R., Hartenbach, E. and Baergen, R. (1999) Randomized phase III study of cisplatin (CIS)/paclitaxel (PAC) versus carboplatin (CARBO)/PAC in optimal stage III epithelial ovarian cancer (OC): a Gynaecologic Oncology Group trial (GOG-158). *Proc Am Soc Clin Oncol*, **18**, 356a (abstract 1373).
33. du BOIS, A., Lueck, H., Meier, W., Moebus, V., Costa, S., Bauknecht, T., Richter, B., Warm, M., Schroeder, W., Olbricht, S., Nitz, U. and Jackisch, C. (1999) Cisplatin/paclitaxel vs carboplatin/paclitaxel in ovarian cancer: update of an Arbeitsgemeinschaft Gynaekologische Onkologie (AGO) Study Group trial. *Proc Am Soc Clin Oncol*, **18**, 356a (abstract 1374).
34. Armstrong, D.K. (2002) Relapsed ovarian cancer: challenges and management strategies for a chronic disease. *Oncologist*, **7 Suppl 5**, 20-8.
35. Risch, H.A., McLaughlin, J.R., Cole, D.E., Rosen, B., Bradley, L., Kwan, E., Jack, E., Vesprini, D.J., Kuperstein, G., Abrahamson, J.L., Fan, I., Wong, B. and Narod, S.A. (2001) Prevalence and penetrance of germline BRCA1 and BRCA2 mutations in a population series of 649 women with ovarian cancer. *Am J Hum Genet*, **68**, 700-10.
36. Thompson, D. and Easton, D.F. (2002) Cancer Incidence in BRCA1 mutation carriers. *J Natl Cancer Inst*, **94**, 1358-65.
37. Thompson, D. and Easton, D. (2001) Variation in cancer risks, by mutation position, in BRCA2 mutation carriers. *Am J Hum Genet*, **68**, 410-9.
38. Gayther, S.A., Warren, W., Mazoyer, S., Russell, P.A., Harrington, P.A., Chiano, M., Seal, S., Hamoudi, R., van Rensburg, E.J., Dunning, A.M. and et al. (1995) Germline

mutations of the BRCA1 gene in breast and ovarian cancer families provide evidence for a genotype-phenotype correlation. *Nat Genet*, **11**, 428-33.

39. Marcelis, C.L., van der Putten, H.W., Tops, C., Lutgens, L.C. and Moog, U. (2001) Chemotherapy resistant ovarian cancer in carriers of an hMSH2 mutation? *Fam Cancer*, **1**, 107-9.
40. Watson, P. and Lynch, H.T. (2001) Cancer risk in mismatch repair gene mutation carriers. *Fam Cancer*, **1**, 57-60.
41. Anthoney, D.A., McIlwrath, A.J., Gallagher, W.M., Edlin, A.R. and Brown, R. (1996) Microsatellite instability, apoptosis, and loss of p53 function in drug-resistant tumor cells. *Cancer Res*, **56**, 1374-81.
42. Brown, R., Hirst, G.L., Gallagher, W.M., McIlwrath, A.J., Margison, G.P., van der Zee, A.G. and Anthoney, D.A. (1997) hMLH1 expression and cellular responses of ovarian tumour cells to treatment with cytotoxic anticancer agents. *Oncogene*, **15**, 45-52.
43. Plumb, J.A., Strathdee, G., Sludden, J., Kaye, S.B. and Brown, R. (2000) Reversal of drug resistance in human tumor xenografts by 2'-deoxy-5-azacytidine-induced demethylation of the hMLH1 gene promoter. *Cancer Res*, **60**, 6039-44.
44. Strathdee, G., MacKean, M.J., Illand, M. and Brown, R. (1999) A role for methylation of the hMLH1 promoter in loss of hMLH1 expression and drug resistance in ovarian cancer. *Oncogene*, **18**, 2335-41.
45. McCoy, M.L., Mueller, C.R. and Roskelley, C.D. (2003) The role of the breast cancer susceptibility gene 1 (BRCA1) in sporadic epithelial ovarian cancer. *Reprod Biol Endocrinol*, **1**, 72.
46. De Vita, V., Hellman, S. and Rosenberg, S. (eds.) (2001) *Cancer. Principles and Practice of Oncology*. Lippincott, Williams and Wilkins, Philadelphia.
47. Zheng, J., Benedict, W.F., Xu, H.J., Hu, S.X., Kim, T.M., Velicescu, M., Wan, M., Cofer, K.F. and Dubeau, L. (1995) Genetic disparity between morphologically benign cysts contiguous to ovarian carcinomas and solitary cystadenomas. *J Natl Cancer Inst*, **87**, 1146-53.
48. Jiang, X., Morland, S.J., Hitchcock, A., Thomas, E.J. and Campbell, I.G. (1998) Allelotyping of endometriosis with adjacent ovarian carcinoma reveals evidence of a common lineage. *Cancer Res*, **58**, 1707-12.

49. Godwin, A.K., Testa, J.R. and Hamilton, T.C. (1993) The biology of ovarian cancer development. *Cancer*, **71**, 530-6.
50. Shelling, A.N., Cooke, I.E. and Ganesan, T.S. (1995) The genetic analysis of ovarian cancer. *Br J Cancer*, **72**, 521-7.
51. Sellar, G.C., Watt, K.P., Rabiasz, G.J., Stronach, E.A., Li, L., Miller, E.P., Massie, C.E., Miller, J., Contreras-Moreira, B., Scott, D., Brown, I., Williams, A.R., Bates, P.A., Smyth, J.F. and Gabra, H. (2003) OPCML at 11q25 is epigenetically inactivated and has tumor-suppressor function in epithelial ovarian cancer. *Nat Genet*, **34**, 337-43.
52. Bednarek, A.K., Keck-Waggoner, C.L., Daniel, R.L., Laflin, K.J., Bergsagel, P.L., Kiguchi, K., Brenner, A.J. and Aldaz, C.M. (2001) WWOX, the FRA16D gene, behaves as a suppressor of tumor growth. *Cancer Res*, **61**, 8068-73.
53. Paige, A.J., Taylor, K.J., Taylor, C., Hillier, S.G., Farrington, S., Scott, D., Porteous, D.J., Smyth, J.F., Gabra, H. and Watson, J.E. (2001) WWOX: a candidate tumor suppressor gene involved in multiple tumor types. *Proc Natl Acad Sci U S A*, **98**, 11417-22.
54. Tanaka, Y., Kobayashi, H., Suzuki, M., Kanayama, N. and Terao, T. (2004) Transforming growth factor-beta1-dependent urokinase up-regulation and promotion of invasion are involved in Src-MAPK-dependent signaling in human ovarian cancer cells. *J Biol Chem*, **279**, 8567-76.
55. Hongo, A., Kuramoto, H., Nakamura, Y., Hasegawa, K., Nakamura, K., Kodama, J. and Hiramatsu, Y. (2003) Antitumor effects of a soluble insulin-like growth factor I receptor in human ovarian cancer cells: advantage of recombinant protein administration in vivo. *Cancer Res*, **63**, 7834-9.
56. Sewell, J.M., Macleod, K.G., Ritchie, A., Smyth, J.F. and Langdon, S.P. (2002) Targeting the EGF receptor in ovarian cancer with the tyrosine kinase inhibitor ZD 1839 ("Iressa"). *Br J Cancer*, **86**, 456-62.
57. Miyamoto, S., Hirata, M., Yamazaki, A., Kageyama, T., Hasuwa, H., Mizushima, H., Tanaka, Y., Yagi, H., Sonoda, K., Kai, M., Kanoh, H., Nakano, H. and Mekada, E. (2004) Heparin-binding EGF-like growth factor is a promising target for ovarian cancer therapy. *Cancer Res*, **64**, 5720-7.
58. Matei, D., Chang, D.D. and Jeng, M.H. (2004) Imatinib mesylate (Gleevec) inhibits ovarian cancer cell growth through a mechanism dependent on platelet-derived growth factor receptor alpha and Akt inactivation. *Clin Cancer Res*, **10**, 681-90.

59. Kassim, S.K., El-Salahy, E.M., Fayed, S.T., Helal, S.A., Helal, T., Azzam Eel, D. and Khalifa, A. (2004) Vascular endothelial growth factor and interleukin-8 are associated with poor prognosis in epithelial ovarian cancer patients. *Clin Biochem*, **37**, 363-9.
60. Andrews, P.A., Mann, S.C., Huynh, H.H. and Albright, K.D. (1991) Role of the Na^+, $K(^+)$-adenosine triphosphatase in the accumulation of diamminedichloroplatinum(II) in human ovarian carcinoma cells. *Cancer Research*, **51**, 3677-81.
61. Jekunen, A.P., Hom, D.K., Alcaraz, J.E., Eastman, A. and Howell, S.B. (1994) Cellular pharmacology of dichloro(ethylenediamine)platinum(II) in cisplatin-sensitive and resistant human ovarian carcinoma cells. *Cancer Res*, **54**, 2680-7.
62. Katano, K., Kondo, A., Safaei, R., Holzer, A., Samimi, G., Mishima, M., Kuo, Y.M., Rochdi, M. and Howell, S.B. (2002) Acquisition of resistance to cisplatin is accompanied by changes in the cellular pharmacology of copper. *Cancer Res*, **62**, 6559-65.
63. Violini, S., D'Ascenzo, S., Bagnoli, M., Millimaggi, D., Miotti, S., Canevari, S., Pavan, A. and Dolo, V. (2004) Induction of a multifactorial resistance phenotype by high paclitaxel selective pressure in a human ovarian carcinoma cell line. *J Exp Clin Cancer Res*, **23**, 83-91.
64. Baekelandt, M.M., Holm, R., Nesland, J.M., Trope, C.G. and Kristensen, G.B. (2000) P-glycoprotein expression is a marker for chemotherapy resistance and prognosis in advanced ovarian cancer. *Anticancer Res*, **20**, 1061-7.
65. Brinkhuis, M., Izquierdo, M.A., Baak, J.P., van Diest, P.J., Kenemans, P., Scheffer, G.L. and Scheper, R.J. (2002) Expression of multidrug resistance-associated markers, their relation to quantitative pathologic tumour characteristics and prognosis in advanced ovarian cancer. *Anal Cell Pathol*, **24**, 17-23.
66. Goff, B.A., Ries, J.A., Els, L.P., Coltrera, M.D. and Gown, A.M. (1998) Immunophenotype of ovarian cancer as predictor of clinical outcome: evaluation at primary surgery and second-look procedure. *Gynecol Oncol*, **70**, 378-85.
67. Goff, B.A., Paley, P.J., Greer, B.E. and Gown, A.M. (2001) Evaluation of chemoresistance markers in women with epithelial ovarian carcinoma. *Gynecol Oncol*, **81**, 18-24.
68. Yokoyama, Y., Sato, S., Fukushi, Y., Sakamoto, T., Futagami, M. and Saito, Y. (1999) Significance of multi-drug-resistant proteins in predicting chemotherapy response and prognosis in epithelial ovarian cancer. *J Obstet Gynaecol Res*, **25**, 387-94.

69. Baekelandt, M., Lehne, G., Trope, C.G., Szanto, I., Pfeiffer, P., Gustavssson, B. and Kristensen, G.B. (2001) Phase I/II trial of the multidrug-resistance modulator valspodar combined with cisplatin and doxorubicin in refractory ovarian cancer. *J Clin Oncol*, **19**, 2983-93.
70. Fracasso, P.M., Brady, M.F., Moore, D.H., Walker, J.L., Rose, P.G., Letvak, L., Grogan, T.M. and McGuire, W.P. (2001) Phase II study of paclitaxel and valspodar (PSC 833) in refractory ovarian carcinoma: a gynecologic oncology group study. *J Clin Oncol*, **19**, 2975-82.
71. Giannakakou, P., Sackett, D.L., Kang, Y.K., Zhan, Z., Buters, J.T., Fojo, T. and Poruchynsky, M.S. (1997) Paclitaxel-resistant human ovarian cancer cells have mutant beta-tubulins that exhibit impaired paclitaxel-driven polymerization. *J Biol Chem*, **272**, 17118-25.
72. Giannakakou, P., Gussio, R., Nogales, E., Downing, K.H., Zaharevitz, D., Bollbuck, B., Poy, G., Sackett, D., Nicolaou, K.C. and Fojo, T. (2000) A common pharmacophore for epothilone and taxanes: molecular basis for drug resistance conferred by tubulin mutations in human cancer cells. *Proc Natl Acad Sci U S A*, **97**, 2904-9.
73. Cabral, F., Abraham, I. and Gottesman, M.M. (1981) Isolation of a taxol-resistant Chinese hamster ovary cell mutant that has an alteration in alpha-tubulin. *Proc Natl Acad Sci U S A*, **78**, 4388-91.
74. Gonzalez-Garay, M.L., Chang, L., Blade, K., Menick, D.R. and Cabral, F. (1999) A beta-tubulin leucine cluster involved in microtubule assembly and paclitaxel resistance. *J Biol Chem*, **274**, 23875-82.
75. Baird, R.D. and Kaye, S.B. (2003) Drug resistance reversal--are we getting closer? *Eur J Cancer*, **39**, 2450-61.
76. Schneiderman, D., Kim, J.M., Senterman, M. and Tsang, B.K. (1999) Sustained suppression of Fas ligand expression in cisplatin-resistant human ovarian surface epithelial cancer cells. *Apoptosis*, **4**, 271-81.
77. Li, J., Feng, Q., Kim, J.M., Schneiderman, D., Liston, P., Li, M., Vanderhyden, B., Faught, W., Fung, M.F., Senterman, M., Korneluk, R.G. and Tsang, B.K. (2001) Human ovarian cancer and cisplatin resistance: possible role of inhibitor of apoptosis proteins. *Endocrinology*, **142**, 370-80.
78. Righetti, S.C., Della Torre, G., Pilotti, S., Menard, S., Ottone, F., Colnaghi, M.I., Pierotti, M.A., Lavarino, C., Cornarotti, M.,

Oriana, S., Bohm, S., Bresciani, G.L., Spatti, G. and Zunino, F. (1996) A comparative study of p53 gene mutations, protein accumulation, and response to cisplatin-based chemotherapy in advanced ovarian carcinoma. *Cancer Res*, **56**, 689-93.

79. Lavarino, C., Delia, D., Di Palma, S., Zunino, F. and Pilotti, S. (1997) p53 in drug resistance in ovarian cancer. *Lancet*, **349**, 1556.
80. Sasaki, H., Sheng, Y., Kotsuji, F. and Tsang, B.K. (2000) Down-regulation of X-linked inhibitor of apoptosis protein induces apoptosis in chemoresistant human ovarian cancer cells. *Cancer Res*, **60**, 5659-66.
81. Sasaki, H., Kotsuji, F. and Tsang, B.K. (2002) Caspase 3-mediated focal adhesion kinase processing in human ovarian cancer cells: possible regulation by X-linked inhibitor of apoptosis protein. *Gynecol Oncol*, **85**, 339-50.
82. Yuan, Z.Q., Feldman, R.I., Sussman, G.E., Coppola, D., Nicosia, S.V. and Cheng, J.Q. (2003) AKT2 inhibition of cisplatin-induced JNK/p38 and Bax activation by phosphorylation of ASK1: implication of AKT2 in chemoresistance. *J Biol Chem*, **278**, 23432-40.
83. Fraser, M., Leung, B.M., Yan, X., Dan, H.C., Cheng, J.Q. and Tsang, B.K. (2003) p53 is a determinant of X-linked inhibitor of apoptosis protein/Akt-mediated chemoresistance in human ovarian cancer cells. *Cancer Res*, **63**, 7081-8.
84. Drummond, J.T., Anthoney, A., Brown, R. and Modrich, P. (1996) Cisplatin and adriamycin resistance are associated with MutLalpha and mismatch repair deficiency in an ovarian tumor cell line. *J Biol Chem*, **271**, 19645-8.
85. Duckett, D.R., Drummond, J.T., Murchie, A.I., Reardon, J.T., Sancar, A., Lilley, D.M. and Modrich, P. (1996) Human MutSalpha recognizes damaged DNA base pairs containing O6-methylguanine, O4-methylthymine, or the cisplatin-d(GpG) adduct. *Proc Natl Acad Sci U S A*, **93**, 6443-7.
86. Aebi, S., Kurdi-Haidar, B., Gordon, R., Cenni, B., Zheng, H., Fink, D., Christen, R.D., Boland, C.R., Koi, M., Fishel, R. and Howell, S.B. (1996) Loss of DNA mismatch repair in acquired resistance to cisplatin. *Cancer Res*, **56**, 3087-90.
87. Gifford, G., Paul, J., Vasey, P.A., Kaye, S.B. and Brown, R. (2004) The acquisition of hMLH1 methylation in plasma DNA after chemotherapy predicts poor survival for ovarian cancer patients. *Clin Cancer Res*, **10**, 4420-6.

88. Bali, A., O'Brien, P.M., Edwards, L.S., Sutherland, R.L., Hacker, N.F. and Henshall, S.M. (2004) Cyclin D1, p53, and p21Waf1/Cip1 expression is predictive of poor clinical outcome in serous epithelial ovarian cancer. *Clin Cancer Res*, **10**, 5168-77.
89. Sui, L., Dong, Y., Ohno, M., Goto, M., Inohara, T., Sugimoto, K., Tai, Y., Hando, T. and Tokuda, M. (2000) Inverse expression of Cdk4 and p16 in epithelial ovarian tumors. *Gynecol Oncol*, **79**, 230-7.
90. Lincet, H., Poulain, L., Remy, J.S., Deslandes, E., Duigou, F., Gauduchon, P. and Staedel, C. (2000) The p21(cip1/waf1) cyclin-dependent kinase inhibitor enhances the cytotoxic effect of cisplatin in human ovarian carcinoma cells. *Cancer Lett*, **161**, 17-26.
91. Waldman, T., Lengauer, C., Kinzler, K.W. and Vogelstein, B. (1996) Uncoupling of S phase and mitosis induced by anticancer agents in cells lacking p21. *Nature*, **381**, 713-6.
92. Gorospe, M., Cirielli, C., Wang, X., Seth, P., Capogrossi, M.C. and Holbrook, N.J. (1997) p21(Waf1/Cip1) protects against p53-mediated apoptosis of human melanoma cells. *Oncogene*, **14**, 929-35.
93. Gorospe, M., Wang, X., Guyton, K.Z. and Holbrook, N.J. (1996) Protective role of p21(Waf1/Cip1) against prostaglandin A2-mediated apoptosis of human colorectal carcinoma cells. *Mol Cell Biol*, **16**, 6654-60.
94. Polyak, K., Waldman, T., He, T.C., Kinzler, K.W. and Vogelstein, B. (1996) Genetic determinants of p53-induced apoptosis and growth arrest. *Genes Dev*, **10**, 1945-52.
95. Gardner, M.J., Jones, L.M., Catterall, J.B. and Turner, G.A. (1995) Expression of cell adhesion molecules on ovarian tumour cell lines and mesothelial cells, in relation to ovarian cancer metastasis. *Cancer Lett*, **91**, 229-34.
96. Cannistra, S.A., DeFranzo, B., Niloff, J. and Ottensmeir, C. (1995) Functional heterogeneity of CD44 molecules in ovarian cancer cell lines. *Clin Cancer Res*, **1**, 333-42.
97. Patel, I.S., Madan, P., Getsios, S., Bertrand, M.A. and MacCalman, C.D. (2003) Cadherin switching in ovarian cancer progression. *Int J Cancer*, **106**, 172-7.
98. Sundfeldt, K. (2003) Cell-cell adhesion in the normal ovary and ovarian tumors of epithelial origin; an exception to the rule. *Mol Cell Endocrinol*, **202**, 89-96.

99. Arboleda, M.J., Lyons, J.F., Kabbinavar, F.F., Bray, M.R., Snow, B.E., Ayala, R., Danino, M., Karlan, B.Y. and Slamon, D.J. (2003) Overexpression of AKT2/protein kinase Bbeta leads to up-regulation of beta1 integrins, increased invasion, and metastasis of human breast and ovarian cancer cells. *Cancer Res*, **63**, 196-206.
100. Kobayashi, H., Suzuki, M., Tanaka, Y., Hirashima, Y. and Terao, T. (2001) Suppression of urokinase expression and invasiveness by urinary trypsin inhibitor is mediated through inhibition of protein kinase C- and MEK/ERK/c-Jun-dependent signaling pathways. *J Biol Chem*, **276**, 2015-22.
101. Lin, S.W., Lee, M.T., Ke, F.C., Lee, P.P., Huang, C.J., Ip, M.M., Chen, L. and Hwang, J.J. (2000) TGFbeta1 stimulates the secretion of matrix metalloproteinase 2 (MMP2) and the invasive behavior in human ovarian cancer cells, which is suppressed by MMP inhibitor BB3103. *Clin Exp Metastasis*, **18**, 493-9.
102. Belotti, D., Paganoni, P., Manenti, L., Garofalo, A., Marchini, S., Taraboletti, G. and Giavazzi, R. (2003) Matrix metalloproteinases (MMP9 and MMP2) induce the release of vascular endothelial growth factor (VEGF) by ovarian carcinoma cells: implications for ascites formation. *Cancer Res*, **63**, 5224-9.
103. Lengyel, E., Schmalfeldt, B., Konik, E., Spathe, K., Harting, K., Fenn, A., Berger, U., Fridman, R., Schmitt, M., Prechtel, D. and Kuhn, W. (2001) Expression of latent matrix metalloproteinase 9 (MMP-9) predicts survival in advanced ovarian cancer. *Gynecol Oncol*, **82**, 291-8.
104. Sumigama, S., Ito, T., Kajiyama, H., Shibata, K., Tamakoshi, K., Kikkawa, F., Williams, T., Tainsky, M.A., Nomura, S. and Mizutani, S. (2004) Suppression of invasion and peritoneal carcinomatosis of ovarian cancer cells by overexpression of AP-2alpha. *Oncogene*, **23**, 5496-504.
105. Dong, W.G., Sun, X.M., Yu, B.P., Luo, H.S. and Yu, J.P. (2003) Role of VEGF and CD44v6 in differentiating benign from malignant ascites. *World J Gastroenterol*, **9**, 2596-600.
106. Sutherland, G.R., Baker, E. and Callen, D.F. (1988) A BrdU-enhanceable fragile site or viral modification site at 11q23.1 in lymphoblastoid cultures. *Cytogenet Cell Genet*, **47**, 201-3.
107. Richards, R.I. (2001) Fragile and unstable chromosomes in cancer: causes and consequences. *Trends Genet*, **17**, 339-45.
108. Jones, C., Slijepcevic, P., Marsh, S., Baker, E., Langdon, W.Y., Richards, R.I. and Tunnacliffe, A. (1994) Physical linkage of the

fragile site FRA11B and a Jacobsen syndrome chromosome deletion breakpoint in 11q23.3. *Hum Mol Genet*, **3**, 2123-30.
109. Yunis, J.J. and Soreng, A.L. (1984) Constitutive fragile sites and cancer. *Science*, **226**, 1199-204.
110. Limongi, M.Z., Pelliccia, F. and Rocchi, A. (2003) Characterization of the human common fragile site FRA2G. *Genomics*, **81**, 93-7.
111. Boldog, F., Gemmill, R.M., West, J., Robinson, M., Robinson, L., Li, E., Roche, J., Todd, S., Waggoner, B., Lundstrom, R., Jacobson, J., Mullokandov, M.R., Klinger, H. and Drabkin, H.A. (1997) Chromosome 3p14 homozygous deletions and sequence analysis of FRA3B. *Hum Mol Genet*, **6**, 193-203.
112. Inoue, H., Ishii, H., Alder, H., Snyder, E., Druck, T., Huebner, K. and Croce, C.M. (1997) Sequence of the FRA3B common fragile region: implications for the mechanism of FHIT deletion. *Proc Natl Acad Sci U S A*, **94**, 14584-9.
113. Becker, N.A., Thorland, E.C., Denison, S.R., Phillips, L.A. and Smith, D.I. (2002) Evidence that instability within the FRA3B region extends four megabases. *Oncogene*, **21**, 8713-22.
114. Paige, A.J., Taylor, K.J., Stewart, A., Sgouros, J.G., Gabra, H., Sellar, G.C., Smyth, J.F., Porteous, D.J. and Watson, J.E. (2000) A 700-kb physical map of a region of 16q23.2 homozygously deleted in multiple cancers and spanning the common fragile site FRA16D. *Cancer Res*, **60**, 1690-7.
115. Mangelsdorf, M., Ried, K., Woollatt, E., Dayan, S., Eyre, H., Finnis, M., Hobson, L., Nancarrow, J., Venter, D., Baker, E. and Richards, R.I. (2000) Chromosomal fragile site FRA16D and DNA instability in cancer. *Cancer Res*, **60**, 1683-9.
116. Krummel, K.A., Roberts, L.R., Kawakami, M., Glover, T.W. and Smith, D.I. (2000) The characterization of the common fragile site FRA16D and its involvement in multiple myeloma translocations. *Genomics*, **69**, 37-46.
117. Huang, H., Qian, C., Jenkins, R.B. and Smith, D.I. (1998) Fish mapping of YAC clones at human chromosomal band 7q31.2: identification of YACS spanning FRA7G within the common region of LOH in breast and prostate cancer. *Genes Chromosomes Cancer*, **21**, 152-9.
118. Mishmar, D., Rahat, A., Scherer, S.W., Nyakatura, G., Hinzmann, B., Kohwi, Y., Mandel-Gutfroind, Y., Lee, J.R., Drescher, B., Sas, D.E., Margalit, H., Platzer, M., Weiss, A., Tsui, L.C., Rosenthal, A. and Kerem, B. (1998) Molecular characterization of a common

fragile site (FRA7H) on human chromosome 7 by the cloning of a simian virus 40 integration site. *Proc Natl Acad Sci U S A*, **95**, 8141-6.

119. Cesari, R., Martin, E.S., Calin, G.A., Pentimalli, F., Bichi, R., McAdams, H., Trapasso, F., Drusco, A., Shimizu, M., Masciullo, V., D'Andrilli, G., Scambia, G., Picchio, M.C., Alder, H., Godwin, A.K. and Croce, C.M. (2003) Parkin, a gene implicated in autosomal recessive juvenile parkinsonism, is a candidate tumor suppressor gene on chromosome 6q25-q27. *Proc Natl Acad Sci U S A*, **28**, 28.
120. Morelli, C., Karayianni, E., Magnanini, C., Mungall, A.J., Thorland, E., Negrini, M., Smith, D.I. and Barbanti-Brodano, G. (2002) Cloning and characterization of the common fragile site FRA6F harboring a replicative senescence gene and frequently deleted in human tumors. *Oncogene*, **21**, 7266-76.
121. Callahan, G., Denison, S.R., Phillips, L.A., Shridhar, V. and Smith, D.I. (2003) Characterization of the common fragile site FRA9E and its potential role in ovarian cancer. *Oncogene*, **22**, 590-601.
122. Arlt, M.F., Miller, D.E., Beer, D.G. and Glover, T.W. (2002) Molecular characterization of FRAXB and comparative common fragile site instability in cancer cells. *Genes Chromosomes Cancer*, **33**, 82-92.
123. Sozzi, G., Veronese, M.L., Negrini, M., Baffa, R., Cotticelli, M.G., Inoue, H., Tornielli, S., Pilotti, S., De Gregorio, L., Pastorino, U., Pierotti, M.A., Ohta, M., Huebner, K. and Croce, C.M. (1996) The FHIT gene 3p14.2 is abnormal in lung cancer. *Cell*, **85**, 17-26.
124. Ahmadian, M., Wistuba, II, Fong, K.M., Behrens, C., Kodagoda, D.R., Saboorian, M.H., Shay, J., Tomlinson, G.E., Blum, J., Minna, J.D. and Gazdar, A.F. (1997) Analysis of the FHIT gene and FRA3B region in sporadic breast cancer, preneoplastic lesions, and familial breast cancer probands. *Cancer Res*, **57**, 3664-8.
125. Muller, C.Y., O'Boyle, J.D., Fong, K.M., Wistuba, II, Biesterveld, E., Ahmadian, M., Miller, D.S., Gazdar, A.F. and Minna, J.D. (1998) Abnormalities of fragile histidine triad genomic and complementary DNAs in cervical cancer: association with human papillomavirus type. *J Natl Cancer Inst*, **90**, 433-9.
126. Butler, D., Collins, C., Mabruk, M., Barry Walsh, C., Leader, M.B. and Kay, E.W. (2000) Deletion of the FHIT gene in

neoplastic and invasive cervical lesions is related to high-risk HPV infection but is independent of histopathological features. *J Pathol*, **192**, 502-10.

127. Luceri, C., Guglielmi, F., De Filippo, C., Caderni, G., Mini, E., Biggeri, A., Napoli, C., Tonelli, F., Cianchi, F. and Dolara, P. (2000) Clinicopathologic features and FHIT gene expression in sporadic colorectal adenocarcinomas. *Scand J Gastroenterol*, **35**, 637-41.
128. Menin, C., Santacatterina, M., Zambon, A., Montagna, M., Parenti, A., Ruol, A. and D'Andrea, E. (2000) Anomalous transcripts and allelic deletions of the FHIT gene in human esophageal cancer. *Cancer Genet Cytogenet*, **119**, 56-61.
129. Huiping, C., Kristjansdottir, S., Bergthorsson, J.T., Jonasson, J.G., Magnusson, J., Egilsson, V. and Ingvarsson, S. (2002) High frequency of LOH, MSI and abnormal expression of FHIT in gastric cancer. *Eur J Cancer*, **38**, 728-35.
130. Petursdottir, T.E., Hafsteinsdottir, S.H., Jonasson, J.G., Moller, P.H., Thorsteinsdottir, U., Huiping, C., Egilsson, V. and Ingvarsson, S. (2002) Loss of heterozygosity at the FHIT gene in different solid human tumours and its association with survival in colorectal cancer patients. *Anticancer Res*, **22**, 3205-12.
131. Yang, Q., Nakamura, M., Nakamura, Y., Yoshimura, G., Suzuma, T., Umemura, T., Shimizu, Y., Mori, I., Sakurai, T. and Kakudo, K. (2002) Two-hit inactivation of FHIT by loss of heterozygosity and hypermethylation in breast cancer. *Clin Cancer Res*, **8**, 2890-3.
132. Ohta, M., Inoue, H., Cotticelli, M.G., Kastury, K., Baffa, R., Palazzo, J., Siprashvili, Z., Mori, M., McCue, P., Druck, T. and et al. (1996) The FHIT gene, spanning the chromosome 3p14.2 fragile site and renal carcinoma-associated t(3;8) breakpoint, is abnormal in digestive tract cancers. *Cell*, **84**, 587-97.
133. Yanagisawa, K., Kondo, M., Osada, H., Uchida, K., Takagi, K., Masuda, A. and Takahashi, T. (1996) Molecular analysis of the FHIT gene at 3p14.2 in lung cancer cell lines. *Cancer Res*, **56**, 5579-82.
134. Greenspan, D.L., Connolly, D.C., Wu, R., Lei, R.Y., Vogelstein, J.T., Kim, Y.T., Mok, J.E., Munoz, N., Bosch, F.X., Shah, K. and Cho, K.R. (1997) Loss of FHIT expression in cervical carcinoma cell lines and primary tumors. *Cancer Res*, **57**, 4692-8.
135. Campiglio, M., Pekarsky, Y., Menard, S., Tagliabue, E., Pilotti, S. and Croce, C.M. (1999) FHIT loss of function in human primary

breast cancer correlates with advanced stage of the disease. *Cancer Res*, **59**, 3866-9.

136. Siprashvili, Z., Sozzi, G., Barnes, L.D., McCue, P., Robinson, A.K., Eryomin, V., Sard, L., Tagliabue, E., Greco, A., Fusetti, L., Schwartz, G., Pierotti, M.A., Croce, C.M. and Huebner, K. (1997) Replacement of Fhit in cancer cells suppresses tumorigenicity. *Proc Natl Acad Sci U S A*, **94**, 13771-6.
137. Pace, H.C., Garrison, P.N., Robinson, A.K., Barnes, L.D., Draganescu, A., Rosler, A., Blackburn, G.M., Siprashvili, Z., Croce, C.M., Huebner, K. and Brenner, C. (1998) Genetic, biochemical, and crystallographic characterization of Fhit-substrate complexes as the active signaling form of Fhit. *Proc Natl Acad Sci U S A*, **95**, 5484-9.
138. Brenner, C., Bieganowski, P., Pace, H.C. and Huebner, K. (1999) The histidine triad superfamily of nucleotide-binding proteins. *J Cell Physiol*, **181**, 179-87.
139. Fong, L.Y., Fidanza, V., Zanesi, N., Lock, L.F., Siracusa, L.D., Mancini, R., Siprashvili, Z., Ottey, M., Martin, S.E., Druck, T., McCue, P.A., Croce, C.M. and Huebner, K. (2000) Muir-Torre-like syndrome in Fhit-deficient mice. *Proc Natl Acad Sci U S A*, **97**, 4742-7.
140. Dumon, K.R., Ishii, H., Fong, L.Y., Zanesi, N., Fidanza, V., Mancini, R., Vecchione, A., Baffa, R., Trapasso, F., During, M.J., Huebner, K. and Croce, C.M. (2001) FHIT gene therapy prevents tumor development in Fhit-deficient mice. *Proc Natl Acad Sci U S A*, **98**, 3346-51.
141. Fouts, R.L., Sandusky, G.E., Zhang, S., Eckert, G.J., Koch, M.O., Ulbright, T.M., Eble, J.N. and Cheng, L. (2003) Down-regulation of fragile histidine triad expression in prostate carcinoma. *Cancer*, **97**, 1447-52.
142. Huang, H., Reed, C.P., Mordi, A., Lomberk, G., Wang, L., Shridhar, V., Hartmann, L., Jenkins, R. and Smith, D.I. (1999) Frequent deletions within FRA7G at 7q31.2 in invasive epithelial ovarian cancer. *Genes Chromosomes Cancer*, **24**, 48-55.
143. Capozza, F., Williams, T.M., Schubert, W., McClain, S., Bouzahzah, B., Sotgia, F. and Lisanti, M.P. (2003) Absence of caveolin-1 sensitizes mouse skin to carcinogen-induced epidermal hyperplasia and tumor formation. *Am J Pathol*, **162**, 2029-39.
144. Hellman, A., Zlotorynski, E., Scherer, S.W., Cheung, J., Vincent, J.B., Smith, D.I., Trakhtenbrot, L. and Kerem, B. (2002) A role for

common fragile site induction in amplification of human oncogenes. *Cancer Cell*, **1**, 89-97.
145. Hellman, A., Rahat, A., Scherer, S.W., Darvasi, A., Tsui, L.C. and Kerem, B. (2000) Replication delay along FRA7H, a common fragile site on human chromosome 7, leads to chromosomal instability. *Mol Cell Biol*, **20**, 4420-7.
146. Aldaz, C.M., Chen, T., Sahin, A., Cunningham, J. and Bondy, M. (1995) Comparative allelotype of in situ and invasive human breast cancer: high frequency of microsatellite instability in lobular breast carcinomas. *Cancer Res*, **55**, 3976-81.
147. Cleton-Jansen, A.M., Moerland, E.W., Kuipers-Dijkshoorn, N.J., Callen, D.F., Sutherland, G.R., Hansen, B., Devilee, P. and Cornelisse, C.J. (1994) At least two different regions are involved in allelic imbalance on chromosome arm 16q in breast cancer. *Genes Chromosomes Cancer*, **9**, 101-7.
148. Driouch, K., Dorion-Bonnet, F., Briffod, M., Champeme, M.H., Longy, M. and Lidereau, R. (1997) Loss of heterozygosity on chromosome arm 16q in breast cancer metastases. *Genes Chromosomes Cancer*, **19**, 185-91.
149. Iwabuchi, H., Sakamoto, M., Sakunaga, H., Ma, Y.Y., Carcangiu, M.L., Pinkel, D., Yang-Feng, T.L. and Gray, J.W. (1995) Genetic analysis of benign, low-grade, and high-grade ovarian tumors. *Cancer Res*, **55**, 6172-80.
150. Nishida, N., Fukuda, Y., Kokuryu, H., Sadamoto, T., Isowa, G., Honda, K., Yamaoka, Y., Ikenaga, M., Imura, H. and Ishizaki, K. (1992) Accumulation of allelic loss on arms of chromosomes 13q, 16q and 17p in the advanced stages of human hepatocellular carcinoma. *Int J Cancer*, **51**, 862-8.
151. Suzuki, H., Komiya, A., Emi, M., Kuramochi, H., Shiraishi, T., Yatani, R. and Shimazaki, J. (1996) Three distinct commonly deleted regions of chromosome arm 16q in human primary and metastatic prostate cancers. *Genes Chromosomes Cancer*, **17**, 225-33.
152. Chen, T., Sahin, A. and Aldaz, C.M. (1996) Deletion map of chromosome 16q in ductal carcinoma in situ of the breast: refining a putative tumor suppressor gene region. *Cancer Res*, **56**, 5605-9.
153. Latil, A., Cussenot, O., Fournier, G., Driouch, K. and Lidereau, R. (1997) Loss of heterozygosity at chromosome 16q in prostate adenocarcinoma: identification of three independent regions. *Cancer Res*, **57**, 1058-62.

154. Li, C., Berx, G., Larsson, C., Auer, G., Aspenblad, U., Pan, Y., Sundelin, B., Ekman, P., Nordenskjold, M., van Roy, F. and Bergerheim, U.S. (1999) Distinct deleted regions on chromosome segment 16q23-24 associated with metastases in prostate cancer. *Genes Chromosomes Cancer*, **24**, 175-82.
155. Paris, P.L., Witte, J.S., Kupelian, P.A., Levin, H., Klein, E.A., Catalona, W.J. and Casey, G. (2000) Identification and fine mapping of a region showing a high frequency of allelic imbalance on chromosome 16q23.2 that corresponds to a prostate cancer susceptibility locus. *Cancer Res*, **60**, 3645-9.
156. Bednarek, A.K., Laflin, K.J., Daniel, R.L., Liao, Q., Hawkins, K.A. and Aldaz, C.M. (2000) WWOX, a novel WW domain-containing protein mapping to human chromosome 16q23.3-24.1, a region frequently affected in breast cancer. *Cancer Res*, **60**, 2140-5.
157. Aldaz, C.M., Chen, T., Sahin, A., Cunningham, J. and Bondy, M. (1995) Comparative allelotype of in situ and invasive human breast cancer: high frequency of microsatellite instability in lobular breast carcinomas. *Cancer Res*, **55**, 3976-81.
158. Smith, D.I., Huang, H. and Wang, L. (1998) Common fragile sites and cancer (review). *Int J Oncol*, **12**, 187-96.
159. Ludes-Meyers, J.H., Bednarek, A.K., Popescu, N.C., Bedford, M. and Aldaz, C.M. (2003) WWOX, the common chromosomal fragile site, FRA16D, cancer gene. *Cytogenet Genome Res*, **100**, 101-10.
160. Chesi, M., Bergsagel, P.L., Shonukan, O.O., Martelli, M.L., Brents, L.A., Chen, T., Schrock, E., Ried, T. and Kuehl, W.M. (1998) Frequent dysregulation of the c-maf proto-oncogene at 16q23 by translocation to an Ig locus in multiple myeloma. *Blood*, **91**, 4457-63.
161. Kallberg, Y., Oppermann, U., Jornvall, H. and Persson, B. (2002) Short-chain dehydrogenase/reductase (SDR) relationships: a large family with eight clusters common to human, animal, and plant genomes. *Protein Sci*, **11**, 636-41.
162. Ried, K., Finnis, M., Hobson, L., Mangelsdorf, M., Dayan, S., Nancarrow, J.K., Woollatt, E., Kremmidiotis, G., Gardner, A., Venter, D., Baker, E. and Richards, R.I. (2000) Common chromosomal fragile site FRA16D sequence: identification of the FOR gene spanning FRA16D and homozygous deletions and translocation breakpoints in cancer cells. *Hum Mol Genet*, **9**, 1651-63.

163. Langdon, S.P., Lawrie, S.S., Hay, F.G., Hawkes, M.M., McDonald, A., Hayward, I.P., Schol, D.J., Hilgers, J., Leonard, R.C. and Smyth, J.F. (1988) Characterization and properties of nine human ovarian adenocarcinoma cell lines. *Cancer Res*, **48**, 6166-72.
164. Haber, D. and Harlow, E. (1997) Tumour-suppressor genes: evolving definitions in the genomic age. *Nat Genet*, **16**, 320-2.
165. Kuroki, T., Trapasso, F., Shiraishi, T., Alder, H., Mimori, K., Mori, M. and Croce, C.M. (2002) Genetic alterations of the tumor suppressor gene WWOX in esophageal squamous cell carcinoma. *Cancer Res*, **62**, 2258-60.
166. Yendamuri, S., Kuroki, T., Trapasso, F., Henry, A.C., Dumon, K.R., Huebner, K., Williams, N.N., Kaiser, L.R. and Croce, C.M. (2003) WW domain containing oxidoreductase gene expression is altered in non- small cell lung cancer. *Cancer Res*, **63**, 878-81.
167. Zanesi, N., Fidanza, V., Fong, L.Y., Mancini, R., Druck, T., Valtieri, M., Rudiger, T., McCue, P.A., Croce, C.M. and Huebner, K. (2001) The tumor spectrum in FHIT-deficient mice. *Proc Natl Acad Sci U S A*, **98**, 10250-5.
168. Chang, N.S., Pratt, N., Heath, J., Schultz, L., Sleve, D., Carey, G.B. and Zevotek, N. (2001) Hyaluronidase induction of a WW domain-containing oxidoreductase that enhances tumor necrosis factor cytotoxicity. *J Biol Chem*, **276**, 3361-70.
169. Driouch, K., Prydz, H., Monese, R., Johansen, H., Lidereau, R. and Frengen, E. (2002) Alternative transcripts of the candidate tumor suppressor gene, WWOX, are expressed at high levels in human breast tumors. *Oncogene*, **21**, 1832-40.
170. Mori, M., Mimori, K., Shiraishi, T., Alder, H., Inoue, H., Tanaka, Y., Sugimachi, K., Huebner, K. and Croce, C.M. (2000) Altered expression of Fhit in carcinoma and precarcinomatous lesions of the esophagus. *Cancer Res*, **60**, 1177-82.
171. Ishii, H., Vecchione, A., Furukawa, Y., Sutheesophon, K., Han, S.Y., Druck, T., Kuroki, T., Trapasso, F., Nishimura, M., Saito, Y., Ozawa, K., Croce, C.M. and Huebner, K. (2003) Expression of FRA16D/WWOX and FRA3B/FHIT genes in hematopoietic malignancies. *Mol Cancer Res*, **1**, 940-7.
172. Watanabe, A., Hippo, Y., Taniguchi, H., Iwanari, H., Yashiro, M., Hirakawa, K., Kodama, T. and Aburatani, H. (2003) An opposing view on WWOX protein function as a tumor suppressor. *Cancer Res*, **63**, 8629-33.

173. Poola, I. and Speirs, V. (2001) Expression of alternatively spliced estrogen receptor alpha mRNAs is increased in breast cancer tissues. *J Steroid Biochem Mol Biol*, **78**, 459-69.
174. Poola, I., Koduri, S., Chatra, S. and Clarke, R. (2000) Identification of twenty alternatively spliced estrogen receptor alpha mRNAs in breast cancer cell lines and tumors using splice targeted primer approach. *J Steroid Biochem Mol Biol*, **72**, 249-58.
175. Liu, D., Pearlman, E., Diaconu, E., Guo, K., Mori, H., Haqqi, T., Markowitz, S., Willson, J. and Sy, M.S. (1996) Expression of hyaluronidase by tumor cells induces angiogenesis in vivo. *Proc Natl Acad Sci U S A*, **93**, 7832-7.
176. Bertrand, P., Girard, N., Duval, C., d'Anjou, J., Chauzy, C., Menard, J.F. and Delpech, B. (1997) Increased hyaluronidase levels in breast tumor metastases. *Int J Cancer*, **73**, 327-31.
177. Tamakoshi, K., Kikkawa, F., Maeda, O., Suganuma, N., Yamagata, S., Yamagata, T. and Tomoda, Y. (1997) Hyaluronidase activity in gynaecological cancer tissues with different metastatic forms. *Br J Cancer*, **75**, 1807-11.
178. Lokeshwar, V.B., Soloway, M.S. and Block, N.L. (1998) Secretion of bladder tumor-derived hyaluronidase activity by invasive bladder tumor cells. *Cancer Lett*, **131**, 21-7.
179. Lokeshwar, V.B., Lokeshwar, B.L., Pham, H.T. and Block, N.L. (1996) Association of elevated levels of hyaluronidase, a matrix-degrading enzyme, with prostate cancer progression. *Cancer Res*, **56**, 651-7.
180. Croix, B.S., Rak, J.W., Kapitain, S., Sheehan, C., Graham, C.H. and Kerbel, R.S. (1996) Reversal by hyaluronidase of adhesion-dependent multicellular drug resistance in mammary carcinoma cells. *J Natl Cancer Inst*, **88**, 1285-96.
181. Chang, N.S. (1997) Hyaluronidase enhancement of TNF-mediated cell death is reversed by TGF-beta 1. *Am J Physiol*, **273**, C1987-94.
182. Susin, S.A., Lorenzo, H.K., Zamzami, N., Marzo, I., Snow, B.E., Brothers, G.M., Mangion, J., Jacotot, E., Costantini, P., Loeffler, M., Larochette, N., Goodlett, D.R., Aebersold, R., Siderovski, D.P., Penninger, J.M. and Kroemer, G. (1999) Molecular characterization of mitochondrial apoptosis-inducing factor. *Nature*, **397**, 441-6.
183. Whitman, S., Wang, X., Shalaby, R. and Shtivelman, E. (2000) Alternatively spliced products CC3 and TC3 have opposing effects on apoptosis. *Mol Cell Biol*, **20**, 583-93.

184. Zhu, J., Zhang, S., Jiang, J. and Chen, X. (2000) Definition of the p53 functional domains necessary for inducing apoptosis. *J Biol Chem*, **275**, 39927-34.
185. Krummel, K.A., Denison, S.R., Calhoun, E., Phillips, L.A. and Smith, D.I. (2002) The common fragile site FRA16D and its associated gene WWOX are highly conserved in the mouse at Fra8E1. *Genes Chromosomes Cancer*, **34**, 154-67.
186. Pekarsky, Y., Druck, T., Cotticelli, M.G., Ohta, M., Shou, J., Mendrola, J., Montgomery, J.C., Buchberg, A.M., Siracusa, L.D., Manenti, G., Fong, L.Y., Dragani, T.A., Croce, C.M. and Huebner, K. (1998) The murine Fhit locus: isolation, characterization, and expression in normal and tumor cells. *Cancer Res*, **58**, 3401-8.
187. Glover, T.W., Hoge, A.W., Miller, D.E., Ascara-Wilke, J.E., Adam, A.N., Dagenais, S.L., Wilke, C.M., Dierick, H.A. and Beer, D.G. (1998) The murine Fhit gene is highly similar to its human orthologue and maps to a common fragile site region. *Cancer Res*, **58**, 3409-14.
188. Brattain, M.G., Fine, W.D., Khaled, F.M., Thompson, J. and Brattain, D.E. (1981) Heterogeneity of malignant cells from a human colonic carcinoma. *Cancer Res*, **41**, 1751-6.
189. Behrens, B.C., Hamilton, T.C., Masuda, H., Grotzinger, K.R., Whang-Peng, J., Louie, K.G., Knutsen, T., McKoy, W.M., Young, R.C. and Ozols, R.F. (1987) Characterization of a cis-diamminedichloroplatinum(II)-resistant human ovarian cancer cell line and its use in evaluation of platinum analogues. *Cancer Res*, **47**, 414-8.
190. Louie, K.G., Behrens, B.C., Kinsella, T.J., Hamilton, T.C., Grotzinger, K.R., McKoy, W.M., Winker, M.A. and Ozols, R.F. (1985) Radiation survival parameters of antineoplastic drug-sensitive and -resistant human ovarian cancer cell lines and their modification by buthionine sulfoximine. *Cancer Res*, **45**, 2110-5.
191. Redmond, A., Moran, E. and Clynes, M. (1993) Multiple drug resistance in the human ovarian carcinoma cell line OAW42-A. *Eur J Cancer*, **29A**, 1078-81.
192. (1998) United Kingdom Co-ordinating Committee on Cancer Research (UKCCCR) Guidelines for the Welfare of Animals in Experimental Neoplasia (Second Edition). *Br J Cancer*, **77**, 1-10.
193. Liem, A.A., Appleyard, M.V., O'Neill, M.A., Hupp, T.R., Chamberlain, M.P. and Thompson, A.M. (2003) Doxorubicin and vinorelbine act independently via p53 expression and p38

activation respectively in breast cancer cell lines. *Br J Cancer*, **88**, 1281-4.
194. Maxwell, P.J., Longley, D.B., Latif, T., Boyer, J., Allen, W., Lynch, M., McDermott, U., Harkin, D.P., Allegra, C.J. and Johnston, P.G. (2003) Identification of 5-fluorouracil-inducible target genes using cDNA microarray profiling. *Cancer Res*, **63**, 4602-6.
195. Skandalis, A., Ninniss, P.J., McCormac, D. and Newton, L. (2002) Spontaneous frequency of exon skipping in the human HPRT gene. *Mutat Res*, **501**, 37-44.
196. LeHir, H., Charlet-Berguerand, N., de Franciscis, V. and Thermes, C. (2002) 5'-End RET splicing: absence of variants in normal tissues and intron retention in phaeochromocytomas. *Oncology*, **63**, 84-91.
197. Xu, Q. and Lee, C. (2003) Discovery of novel splice forms and functional analysis of cancer-specific alternative splicing in human expressed sequences. *Nucleic Acids Res*, **31**, 5635-43.
198. Wang, Z., Lo, H.S., Yang, H., Gere, S., Hu, Y., Buetow, K.H. and Lee, M.P. (2003) Computational analysis and experimental validation of tumor-associated alternative RNA splicing in human cancer. *Cancer Res*, **63**, 655-7.
199. Cragg, M.S., Chan, H.T., Fox, M.D., Tutt, A., Smith, A., Oscier, D.G., Hamblin, T.J. and Glennie, M.J. (2002) The alternative transcript of CD79b is overexpressed in B-CLL and inhibits signaling for apoptosis. *Blood*, **100**, 3068-76.
200. Ge, K., DuHadaway, J., Du, W., Herlyn, M., Rodeck, U. and Prendergast, G.C. (1999) Mechanism for elimination of a tumor suppressor: aberrant splicing of a brain-specific exon causes loss of function of Bin1 in melanoma. *Proc Natl Acad Sci U S A*, **96**, 9689-94.
201. Hood, J.D. and Cheresh, D.A. (2002) Role of integrins in cell invasion and migration. *Nat Rev Cancer*, **2**, 91-100.
202. Mizejewski, G.J. (1999) Role of integrins in cancer: survey of expression patterns. *Proc Soc Exp Biol Med*, **222**, 124-38.
203. Serini, G., Trusolino, L., Saggiorato, E., Cremona, O., De Rossi, M., Angeli, A., Orlandi, F. and Marchisio, P.C. (1996) Changes in integrin and E-cadherin expression in neoplastic versus normal thyroid tissue. *J Natl Cancer Inst*, **88**, 442-9.
204. Filardo, E.J., Brooks, P.C., Deming, S.L., Damsky, C. and Cheresh, D.A. (1995) Requirement of the NPXY motif in the

integrin beta 3 subunit cytoplasmic tail for melanoma cell migration in vitro and in vivo. *J Cell Biol*, **130**, 441-50.
205. Casey, R.C., Burleson, K.M., Skubitz, K.M., Pambuccian, S.E., Oegema, T.R., Jr., Ruff, L.E. and Skubitz, A.P. (2001) Beta 1-integrins regulate the formation and adhesion of ovarian carcinoma multicellular spheroids. *Am J Pathol*, **159**, 2071-80.
206. Kantak, S.S. and Kramer, R.H. (1998) E-cadherin regulates anchorage-independent growth and survival in oral squamous cell carcinoma cells. *J Biol Chem*, **273**, 16953-61.
207. Pece, S., Chiariello, M., Murga, C. and Gutkind, J.S. (1999) Activation of the protein kinase Akt/PKB by the formation of E-cadherin-mediated cell-cell junctions. Evidence for the association of phosphatidylinositol 3-kinase with the E-cadherin adhesion complex. *J Biol Chem*, **274**, 19347-51.
208. Roskelley, C.D. and Bissell, M.J. (2002) The dominance of the microenvironment in breast and ovarian cancer. *Semin Cancer Biol*, **12**, 97-104.
209. Davidson, B., Berner, A., Nesland, J.M., Risberg, B., Berner, H.S., Trope, C.G., Kristensen, G.B., Bryne, M. and Ann Florenes, V. (2000) E-cadherin and alpha-, beta-, and gamma-catenin protein expression is up-regulated in ovarian carcinoma cells in serous effusions. *J Pathol*, **192**, 460-9.